Acoustic Monitoring of Temporal and Spatial Abundance of Birds Near Outer Continental Shelf Structures

Synthesis Report

U.S. Department of the Interior
Bureau of Ocean Energy Management
Office of Renewable Energy Programs
www.boem.gov

BOEM
BUREAU OF OCEAN ENERGY MANAGEMENT

Acoustic Monitoring of Temporal and Spatial Abundance of Birds Near Outer Continental Shelf Structures

Synthesis Report

Authors

Julia Robinson Willmott
Greg Forcey

DISCLAIMER

This report was prepared under contract between the Bureau of Ocean Energy Management (BOEM) and Normandeau Associates, Inc. This report has been technically reviewed by BOEM, and it has been approved for publication. Approval does not signify that the contents necessarily reflect the view and policies of BOEM, nor does mention of trade names or commercial products constitute endorsement or recommendation for use. It is, however, exempt from review and compliance with BOEM editorial standards.

REPORT AVAILABILITY

CITATION

ABOUT THE COVER

Preface and Acknowledgments

The objective of this study, as stated in Section C.2 of the contract, was "to field test and operate acoustic/thermographic detectors on offshore structures to detect bird species." To accomplish this objective, Normandeau has developed the Acoustic/Thermographic Offshore Monitoring (ATOM) system as well as associated processes for analyzing collected data. ATOM is designed to gather acoustic, thermographic, and other data streams that will provide species-specific data on vocalizing birds and bats flying in offshore environments on a long-term, continuous basis together with data on flight altitude, abundance, and meteorological data. To comply with the Endangered Species Act and other U.S. environmental protection laws, the ATOM system and associated data analysis can provide pre- and postconstruction data for bird and bat risk/impact studies for commercial offshore wind energy development projects and other large-scale offshore developments.

Work on this project was performed by a large, multifaceted team of Normandeau staff and subcontractors. The table below lists all project personnel, their institutional affiliations, and project role.

All project personnel contributed to the information contained within this report with the primary contributions of original text, graphics, and data coming from the technical project personnel listed below.

Institutional affiliations and project roles of all personnel associated with the project

Person	Project Role
Normandeau Associates, Inc.	
Christian Newman	Project Director
Julia Robinson Willmott	Project Manager (Apr 2013–Jan 2014), Data Management and Reporting, Principal Report Author
Caleb Gordon	Project Manager (Oct 2010–Apr 2013)
Ian Baldwin	ATOM Technical Development Manager (Oct 2010–Jun 2011)
Charles Grandgent	ATOM Technical Development Manager (Jun 2011–current), System Characterization Testing, Report Author
Christopher Ribe	ATOM System Chief Designer and Developer (Oct 2010–Dec 2012)
Jeff DePree	ATOM Software Developer
Robin Smith	Analyst Workbench Software Developer and Detection Software Developer, system Characterization Testing, Report Author
Michelle Vukovich	Thermographic Video Analyst, Report Author
Lauren Hooton	Bat Call Analysis, Report Author
Allison Costello	Bat Call Analysis

Person	Project Role
Martin Costello	ATOM Deployment Manager, System Characterization Testing, Report Author
Adam Kent	System Characterization Testing, Report Author
Greg Forcey	ATOM Data Analyses, Principal Report Author
Chris Stoney	ATOM Component Testing
David Hampton	ATOM Prototype Construction
Miles McAllister	ATOM Construction and Development
Peter Colverson	ATOM Circuit Board Construction; Test Deployment Assistance
Jenny Carter	Project Administration and Report Preparation
Renèe Zenaida	Document Preparation
Alexis Hampton	Project Coordination and Administration
Innovative Automation Technologies, LLC	
Donald MacArthur	ATOM audible acoustic subsystem design, development, report author (project year 1 only)
Erica MacArthur	ATOM audible acoustic subsystem design, development, report author (project year 1 only)
Applied Engineering, Inc.	
Roy Harrell	ATOM component fabrication
Rhinosys, Inc.	
John Carter	ATOM software development
Cornell Lab of Ornithology	
Ron Rohrbaugh	Acoustic bird identification project manager, co-PI and Report Author
Andrew Farnsworth	Acoustic bird identification co-PI and Report Author
Harold Cheyne	Acoustic bird identification co-PI
Kenneth Rosenberg	Acoustic bird identification co-PI
Michael Powers	Technical Contributor and Report Author
Anne Klingensmith	Technical Contributor and Report Author
Jesse Ross	Technical Contributor and Report Author
Sara Keen	Technical Contributor
Lynette Rayle	Technical Contributor
Peter Dugan	Technical Contributor
Chris Tessaglia-Hymes	Technical Contributor

Person	Project Role
Michael Pitzrick	Technical Contributor
Janelle Morano	Technical Contributor
University of Florida, Department of Mechanical and Aerospace Engineering	
Louis Cattafesta III	ATOM audible acoustic subsystem sound engineering analysis
University of Florida, Department of Electrical and Computer Engineering	
Jian Li	ATOM audible acoustic subsystem sound engineering analysis
Bureau of Safety and Environmental Enforcement	
Lisa Algarin	Contracting Officer
Bureau of Ocean Energy Management	
James Woehr	Contracting Officer's Representative

Contents

List of Figures

List of Tables

Abbreviations and Acronyms

ABPDN	Average bat passes per detector-night
ADA	Acoustic Data Accelerator
AE	Adaptive Equipment, Inc.
AIC	Akaike Information Criterion
AIF	Audio Interchange File
AMP	Acoustic Monitoring Program
ANOVA	Analysis of Variance
AOCS	Atlantic Outer Continental Shelf
ATOM	Acoustic Thermographic Offshore Monitoring system
AW	Analyst Workbench
BARN	Bio-Acoustic Resource Network
BOEM	Bureau of Ocean Energy Management
BRP	Bioacoustics Research Program
CAF	Core Audio Format
CLO	Cornell Lab of Ornithology
cRIO	National Instruments CompactRIO audio computer
dB	decibels
dBA	Weighted decibel
DBMS	Data Base Management System
DTD	Data Template Detectors
FFT	Fast Fourier Transform
FLIR	Forward Looking Infrared
FP	False Positives
FPR	False Positive Rate
FPSLT	Frying Pan Shoals Light Tower
GB	Gigabyte
GPS	Global Positioning System
HPC	High Performance Computing
Hz	Hertz; a unit of frequency equivalent to cycles per second that is used to describe a sine wave
IATech	Innovative Automation Technologies, LLC
IR	Infrared
kHz	kilohertz, 103 Hz
m	meters

mph	miles per hour
ms	milliseconds
MW	Megawatt
NEPA	National Environmental Policy Act
NFC	Nocturnal Flight Calls
NIST	National Institute of Standards and Technology
OCS	Outer Continental Shelf
OOP	Object Oriented Programming
RF	Random Forest (model)
ReBAT	Remote Bat Acoustic Technology
RMS	Root mean square
ROC	Receiver Operator Characteristics
SM2	SongMeter Device
SNR	Signal to Noise
SPL	Sound Pressure Level
SR	Sound Retrieval
TB	Terabyte
TPR	True Positive Rate
UD Lewes	University of Delaware at Lewes
UF	University of Florida
UV	Ultraviolet

Executive Summary

Normandeau was tasked to design and test a system combining thermal imagery and acoustic and ultrasound sensors to survey bird and bat species potentially affected by offshore developments. Monitoring birds offshore has been limited worldwide due to difficulty of access and high cost. Boat-transect surveys and "ships of opportunity" are subject to potentially large sampling error and are too limited in scope to provide sufficient information. Traditional visual aerial surveys are expensive and also subject to substantial sampling error. An effective and economical way to monitor bird presence offshore would be to use specially designed, strategically positioned and remotely operated acoustic microphones and thermographic cameras attached to offshore structures such as meteorological towers, oil and gas platforms, or wind turbines. Acoustic microphones and thermographic cameras could monitor vocalizations of birds both day and night at all seasons of the year and in any weather conditions including periods of low visibility that would prevent effective visual monitoring. This report describes the initial development of the system and the results from test deployments.

The Acoustic Thermographic Offshore Monitoring (ATOM) system is designed to gather data through all weather conditions both day and night. Deployment at the remote Frying Pan Shoals Light Tower (FPSLT), 29 mi offshore (Figure ES1), provided a challenging work arena with costly and limited access to the system for installation, maintenance, repairs, and retrieval. The restricted ability to access the system increased system down-time, delaying repairs and increasing the cost of deploying and maintaining the system. These factors forced subsequent improvements and modifications to both hardware and software to create a more robust unit that was able to withstand harsh offshore conditions.

A number of seabird species, including gulls, terns and frigatebirds, were expected to occur during the offshore deployment and were identified as expected by ATOM. The dataset of land bird species identified by ATOM is a significant contribution to filling gaps in knowledge about these migrants, and includes herons, bitterns, and many passerines. The data show a clear pattern of migrant occurrence in the offshore environment, with April and October showing peak density, using combined acoustic and thermographic data. Peak in fall density of migrating birds occurred during periods of north to northwest winds (i.e., with a tail wind). Flight bearing in passerines showed seasonal differences but similar trends were not evident with non-passerines. Passerines showed strong tendencies to fly to the south and southeast during the fall and to the northwest during the spring. Mean flight direction during Apr was 286º (NW) and in Oct was 151º (SSE).

Most birds appear to fly higher in the evenings with an estimated 1.8 times increase in flight height between 8 PM and 12 AM than at all other times. Flight altitude seems unaffected by wind speed. Instead, from both acoustic and thermographic data, there is more bird activity during wind speeds of less than 10 km/hr with no discernable alteration in altitude. Flight direction is affected by wind speed and direction with data showing birds inclining to fly into head wind. Flight speed data are consistent throughout the year as well as throughout the day with an average speed of 23 km/hr.
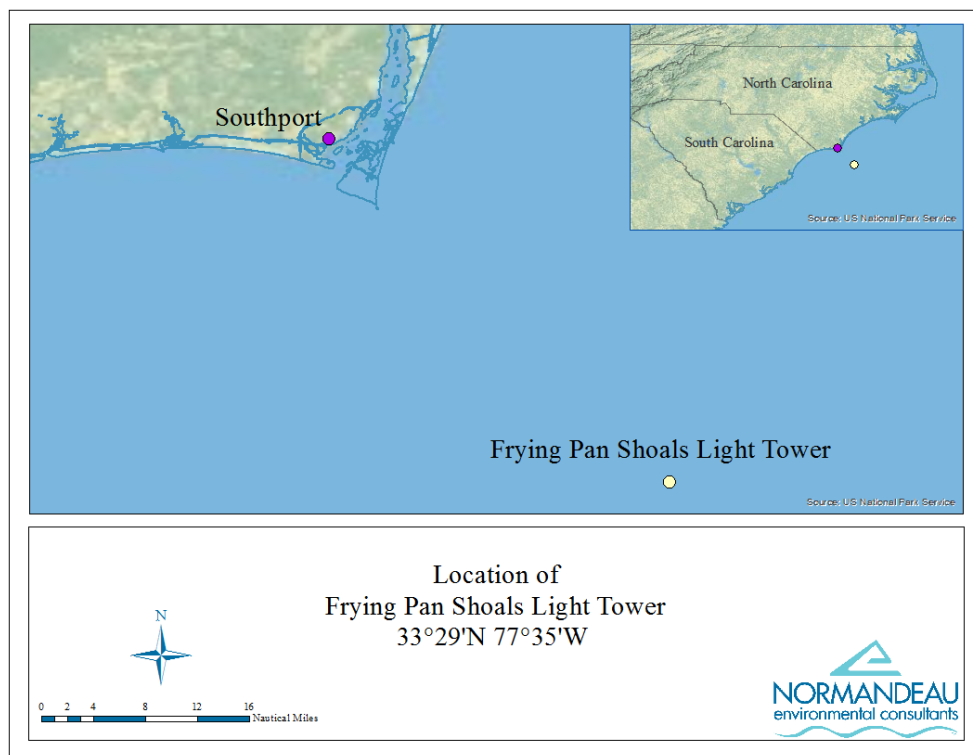
Figure ES1.   Location of Frying Pan Shoals Light Tower.

Bats were not recorded at FPSLT. Although there were large data gaps in the ultrasonic data, no bats were seen in the thermographic data either. Bats have been encountered this far offshore and away from any terrestrial habitat; however, it is unlikely that they occur at remote stations like FPSLT with any regularity.

The system is designed to survey birds and bats within the rotor swept area of a turbine, and consequently most flight altitude data are within this detection area. Acoustic data also fill information gaps on small birds flying higher than 150 m that might otherwise be missed by thermographic methods due to the decay in detection over distance for small birds. Information from these two detection methods provides new data on peak migration times for both vocal and silent species.

Although an original goal was that ATOM would give species-specific information on flight altitude, velocity, and bearing, sufficient data were not collected that would match many species level identifications with all detectors. Increased system reliability should augment the amount of data that could be matched, and longer deployment would gather more data from all sensors. However, species-specific data collected show Yellow-rumped Warbler with flight altitudes of 103.9 m and 46.3 m (n=2), and Laridae with flight altitudes ranging from 49.1 m to 193.9 m, mean 87.43 m (n=35).

The results presented in this report are evidence of progress in the use of acoustic and thermographic monitoring to understand the ecology of large-scale migrations and apply that knowledge to conservation planning. Particularly novel is the dataset itself, the first of its kind from the offshore environment in the western Atlantic Ocean.

1 Introduction

The proliferation of artificial structures associated with energy development, both on land and offshore on the continental shelf, potentially pose a real, but poorly understood, risk to migratory birds. Because significant portions of bird and bat migration occur at night, directly monitoring the timing and magnitude of migration is very difficult, confounding the ability to assess the risk that accompanies hazards such as structures. Though recent advances in technologies such as radar and thermal imaging allow quantification of some aspects of bird migration, only the recording and subsequent analysis of distinctive vocalizations made by birds while in active migratory flight can provide species-specific information at a specific place and time. Therefore, a multi-modal sensor system that includes a sophisticated acoustic recording and analysis component is necessary to more accurately assess the risk to migratory birds from offshore and other energy development.

Normandeau was tasked by BOEM to design and test a system that combined thermal imagery and acoustic and ultrasound sensors to survey bird and bat species potentially affected by offshore developments. Monitoring birds offshore has been limited worldwide due to difficulty of access and high cost. Boat-transect surveys and "ships of opportunity" are subject to potentially large sampling error and are too limited in scope to provide sufficient information. Traditional visual aerial surveys are expensive and also subject to substantial sampling error. An effective and economical way to monitor bird presence offshore would be to use specially designed, strategically positioned and remotely operated acoustic microphones and thermographic cameras attached to offshore structures such as meteorological towers, oil and gas platforms, or wind turbines. Acoustic microphones and thermographic cameras could monitor vocalizations of birds both day and night at all seasons of the year and in any weather conditions, including periods of low visibility that would prevent effective visual monitoring. In collaboration with Cornell Laboratory of Ornithology (CLO), a system has been created for analyzing thermographic, ultrasound, and audio recordings of nocturnally migrating birds and bats. This was achieved by applying technology that minimizes time-consuming human review through advanced analysis software to manage, detect, and classify thermographic images and bird and bat sounds. This software allows improved monitoring of nocturnally migrating birds and bats, leading to a better understanding of migration ecology as a whole and allowing for the assessment of potential risks that structures, such as wind turbines, may pose to migrating birds and bats.

The Acoustic Thermographic Offshore Monitoring (ATOM) system can be deployed on a variety of structures associated with wind energy development on the Atlantic Outer Continental Shelf (AOCS) and, in particular, structures associated with offshore wind energy development.

This report presents a description of the development of the ATOM system and its component parts and the development of the software and reports on the data collected during test deployments.

1.1 Study Context, Objectives, and Basic Approach

BOEM has identified impacts to birds from alternative energy development as a primary biological concern. Due to the lack of information on the biological impacts of offshore wind energy technology, BOEM has sought to analyze existing information sources on bird use of Outer Continental Shelf (OCS) areas and identify needs for further study to develop material useful in assessing potential impacts to birds under the National Environmental Policy Act (NEPA) and other statutes. Interest in development of wind energy in the OCS has increased significantly in recent years with the publication of the BOEM Framework for Renewable Energy Development on the Outer Continental Shelf.

Traditionally, offshore monitoring of birds has been limited due to a variety of factors. Boat and airplane surveys offshore are both costly, limited by weather constraints, and subject to potentially large sampling error. Depending on weather conditions, birds fly at different altitudes (e.g., lower in windy conditions) and call at different rates (e.g., higher in foggy conditions) and not all bird species call at equal rates (e.g., vireos tend to call less frequently at night than most warblers).

The objective of this study was to field test and operate acoustic and thermographic detectors on offshore structures to detect bird species by call and to estimate bird numbers based on a combination of call rates and thermographic video. An additional goal of this study was to assess similar information for bats using ultrasound recordings and thermographic video.

The system for thermographic and acoustic monitoring of nocturnal migrants and their flight calls developed for this study includes a combination of deployable thermographic sensors and acoustic sensors that can either record data autonomously or transmit data to a central site for recording. Associated system software tools include algorithms and protocols for the management and analysis of the large volumes of data recorded by the sensor network. By recording these data at strategically placed stations, a researcher can determine the species composition, timing, and relative magnitude of movement of vocal species and monitor flight direction, altitude, and speed using thermographic data. These measures of migration activity illuminate spatial and temporal variability. Further, when combined with covariates such as environmental conditions, these data provide valuable information about the influences of these conditions on migration.

In addition to movements of migratory landbirds, activity of pelagic species is an increasingly important component for understanding the ecology of a marine system. Although surveys and datasets that describe the diversity and abundance of pelagic species in pelagic environments have increased rather dramatically over the last decade, there are still large gaps in knowledge about the distribution and occurrence. In addition to monitoring for passerines and other primarily terrestrial species offshore, studying patterns of presence of seabirds provides a critical set of data points for assessing their levels of activity in the offshore environment.

1.2 Project Team and Task Structure

The table "Institutional affiliations and project roles of all personnel associated with the project" in Preface and Acknowledgements provides a complete list of all personnel involved with this

project. Normandeau Associates, Inc. (Normandeau) led teams for developing all components of the system. Several collaborators contributed to different components of the project. Collaborators are experts in their fields and in some cases world authorities in the subject.

Development of the hardware components of the system was done in collaboration with Innovative Automation Technologies (IATech) in the first project year and with Applied Engineering (AE) and with CLO for the duration of the project.

Software development for acoustic data analyses and reporting was done in collaboration with the University of Florida (UF) and CLO. CLO will use information gained during this project to inform automated bird call recognition software and is committed to making this software publically available. Thermographic software development was done in collaboration with RhinoSys Inc., a software development company based in Florida. Ultrasound software development was completed by Normandeau prior to the start of the project through the development of the ReBAT® system. This was a large cost saving for the project and allowed the inclusion of bats in the analysis.

Normandeau conducted analysis and interpretation for all data including thermographic imagery and for ultrasound recordings, while CLO conducted analysis of bird acoustic data. CLO is a world leader in using acoustic technologies to provide information on both pelagic and terrestrial birds that might use the aerosphere of a particular region.

2 System Construction and Pretesting

As part of the contract, key project personnel traveled to BOEM headquarters in Herndon, Virginia, for a kickoff meeting. At the meeting, personnel discussed project plans, time frames, technical approach, and any other issues or questions that could arise during review of the entire structure and planning of the project. Subsequent to the kickoff meeting, Normandeau staff researched possible coastal wind turbine deployment locations and initiated communication with multiple stakeholders at each site with requests for physical specifications. A deployment proposal was submitted in late winter 2011 to the University of Delaware at Lewes (UD Lewes) to use their coastal wind turbine. This proposal was approved in the spring 2011 and the ATOM system was deployed there on 18 Jul 2011.

A Gantt chart (Figure 1) shows ATOM project milestones. During the first milestone (the test deployment at UD Lewes in late summer of 2011), the system was placed on a 2 MW Gamesa wind turbine to simulate actual deployment conditions on land. This test deployment demonstrated that the system was capable of operating autonomously while continuously recording thermographic and audio data (audible and ultrasound), that the software for automatically detecting likely bird events was functional, and that detection algorithms for the other sensors could function effectively at an operational wind turbine. It also helped to determine the optimal number and position of sensors for deployment at different locations.

In the fall of 2011, the system was again deployed in a test situation to gather animal-rich data for system development, this time from ground level in Gainesville, Florida. Finally, in Dec 2011, the system was deployed at Frying Pan Shoals Light Tower (FPSLT) to test system

function in an offshore environment. FPSLT is 29 mi offshore, southeast of Southport, North
Carolina (Figure 2).

In May 2013, all equipment for the ATOM system was removed from FPSLT and brought back
to Gainesville. Final data analysis was conducted by CLO and Normandeau from May 2013 to
Nov 2013.
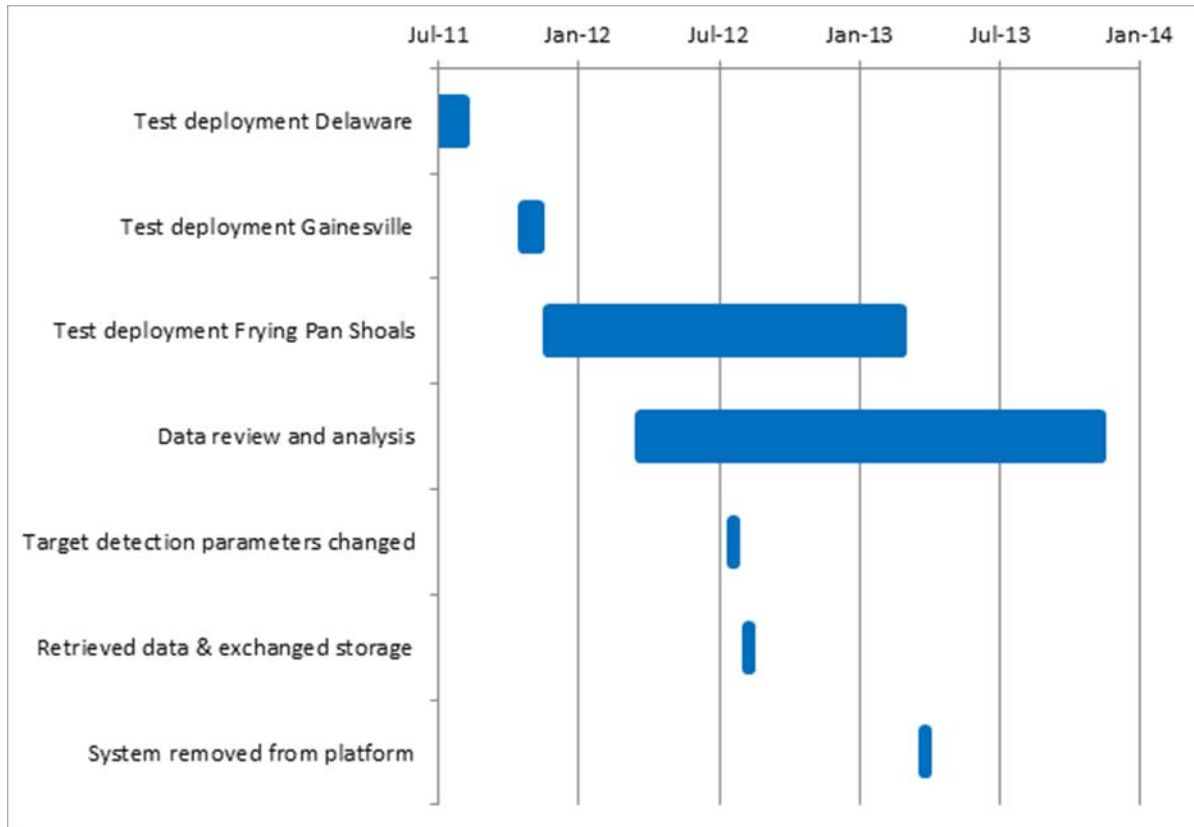
Figure 1.   Timeline for ATOM system milestones.
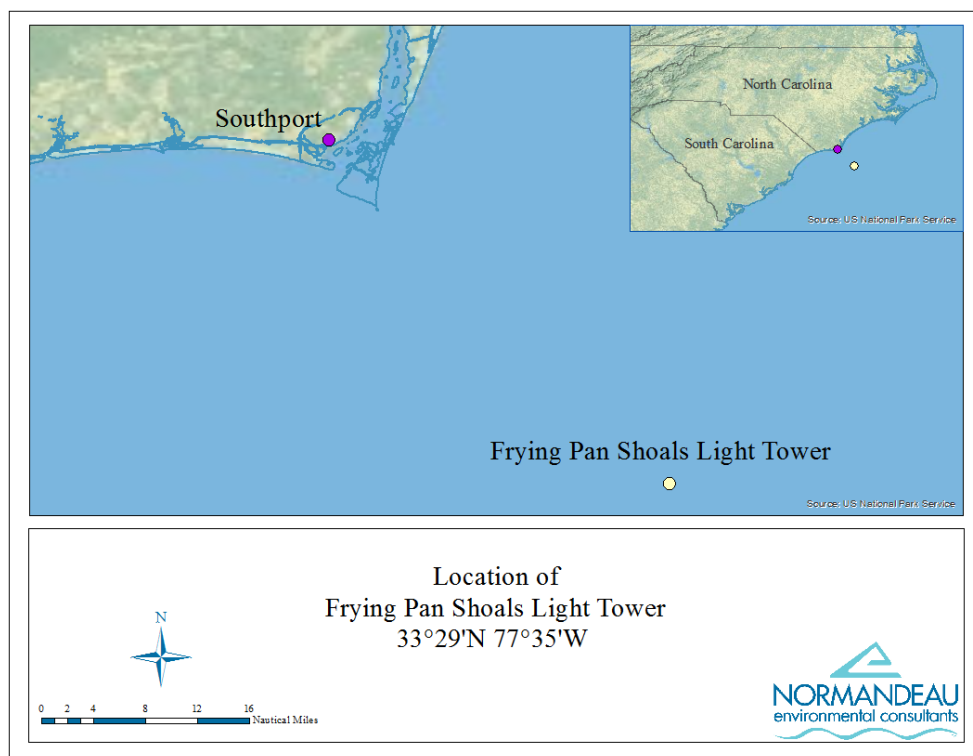
Figure 2.   Location of Frying Pan Shoals Light Tower.

One of the tasks within this project was to ensure that the ATOM system could be deployed on a variety of structures associated with offshore energy development, including wind turbines and meteorological towers, and to determine the optimal number and position of the acoustic and thermographic detectors on various offshore structures.

Originally, oil or gas extraction platforms in the Gulf of Mexico were included, but this was removed from the scope of this project through a contract modification soon after the kickoff meeting.

Different offshore structures have different physical attributes and background noise levels, and, as such, the sensor arrays and signal processing systems may need to be adapted to and optimized for operation on each of these types of structures individually. Our basic approach to this task was to conduct a test deployment at a coastal wind turbine during the summer of 2011 (Figure 3). This test deployment was preceded by planning, experimental design, and preparation and followed by analysis of the results and optimization of sensor configurations for each type of offshore structure. The system was installed beneath the wind turbine at UD Lewes on 18 Jul 2011. For the period 18 Jul–9 Aug 2011, the system collected 0.88 terabytes (TB) of audio data, 13.2 TB of thermographic data, and 6 gigabytes (GB) of ultrasound data.

Figure 3.   The complete ATOM system set up at the base of the UD Lewes wind turbine tower (7/19/2011, Lewes, DE).

At that time, the system had both Verizon cellular and Hughes satellite modems connected to different computers; two FLIR Tau 320 (Forward Looking Infrared) cameras and an integrated custom-built wiper system (Figure 4); eight acoustic microphones; one AR-125 ultrasonic microphone (Binary Acoustic Technology, Tucson); an integrated meteorological system recording visibility, temperature, wind, and humidity (Columbia Weather Systems MicroServer); and a power monitoring system (Power Control Hub) with built in satellite communication. The audible sound subsystem had bidirectional communication between the nodes and the host module and used a LAN-based Ethernet connection. All sensor data were received by the control computer. The five separate computers that comprised the central core of the ATOM system were housed in two, custom-fabricated weatherproof containers: one for the storage computer, including the 32 storage drives (30 × 2 TB, 2 × 3 TB), and one for all of the others (Figure 5). The latter also included the two thermographic cameras (Figure 6). See Appendix 1 for a full list of component parts of the ATOM system.

The system's two thermal cameras look up from the main control computer box through thermally transparent germanium windows covering the holes on each end of the metal bar above. The windows on the upper surface of the bar were covered by movable metal covers with rubber O-rings that cleaned the windows as needed by mechanisms that applied fluid to the upper surface of the windows and then moved the O-rings across the surface to remove debris (see Figure 4).

The power monitoring system reported voltage draw of each component; operating state; input and output voltages; input and output currents of the solar charge controller; input voltages to the power control board; the temperature of numerous system components including the control computer, solar charge controller, power control board, storage computer box, and hard drives; the internal relative humidity of the control and storage boxes; and ambient weather conditions including temperature, humidity, wind speed, wind direction, rain rate, solar radiation, and visibility. It also reported the number of system restarts for various system computers, the amount of hard drive space available and used on the storage and control computers, and the network bandwidth used (Figure 7). The reporting of these data assists in identifying causes of any malfunction and indicates where any system weakness may be for targeted maintenance.

The entire system typically ran on approximately 70 watts, suggesting the system would be able to run continuously even if persistent overcast conditions prevented solar power charging of the system for up to one week. To put this in context, S or X band radar systems typically draw over 1000 watts.

Prior to deployment, high-temperature and low-temperature performance tests of the main control computer and data storage computer housings were conducted. Low-temperature tests were performed to test cold start and data writing in cold environments. Tests showed successful function of these components in environments as warm as 60°C and as cold as -20°C.
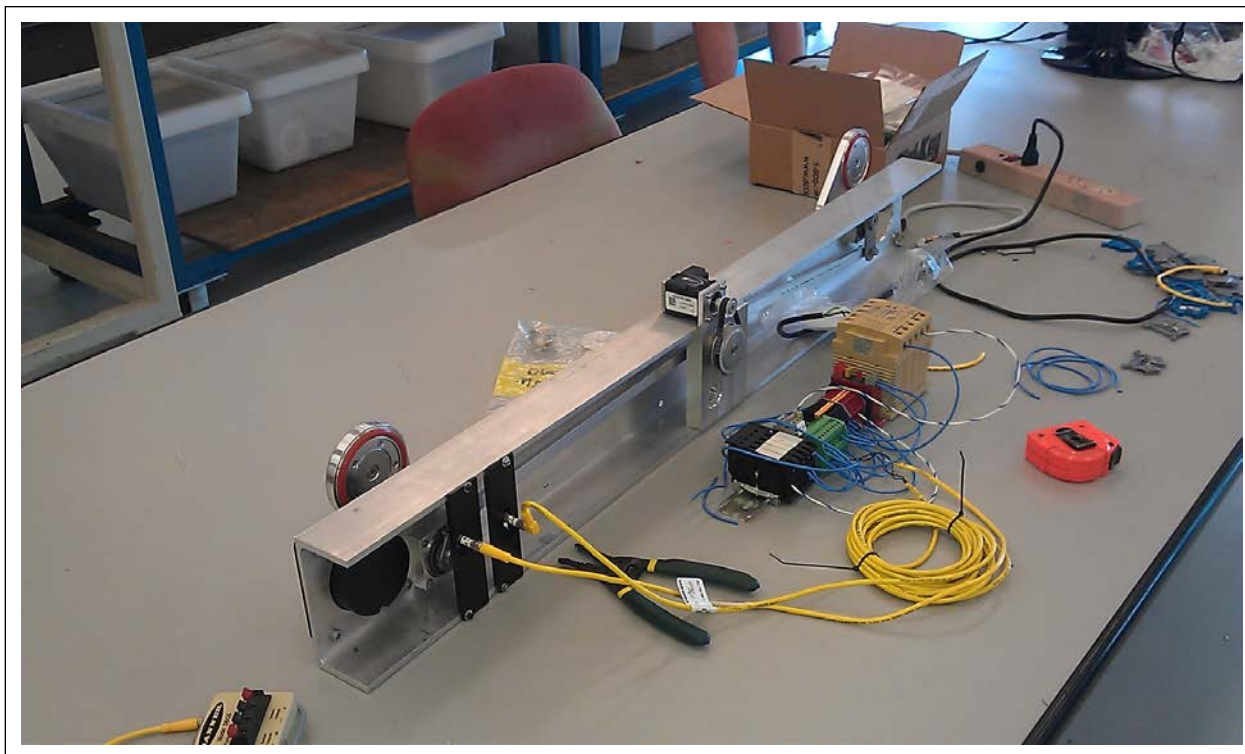
Figure 4.   Automatic lens wiping mechanism prototype of the ATOM system.

Figure 5.   ATOM data storage subsystem.
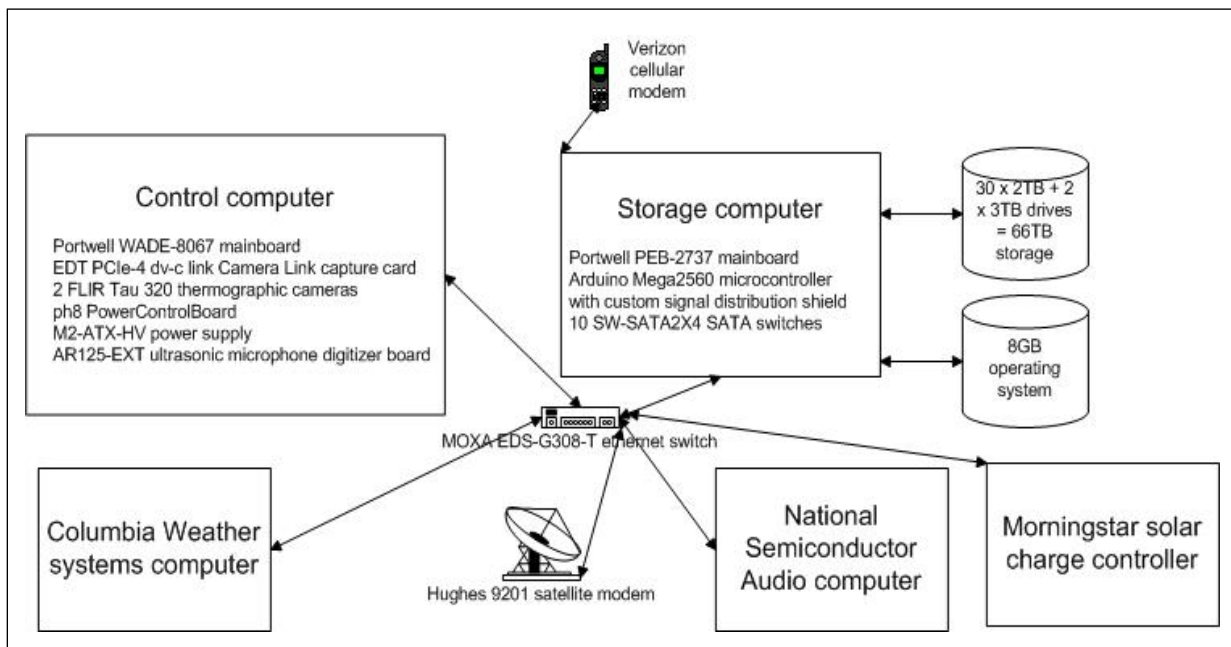
Figure 6.   Final composition of the central system control and communication elements of the
fully integrated ATOM system for the UD Lewes deployment.
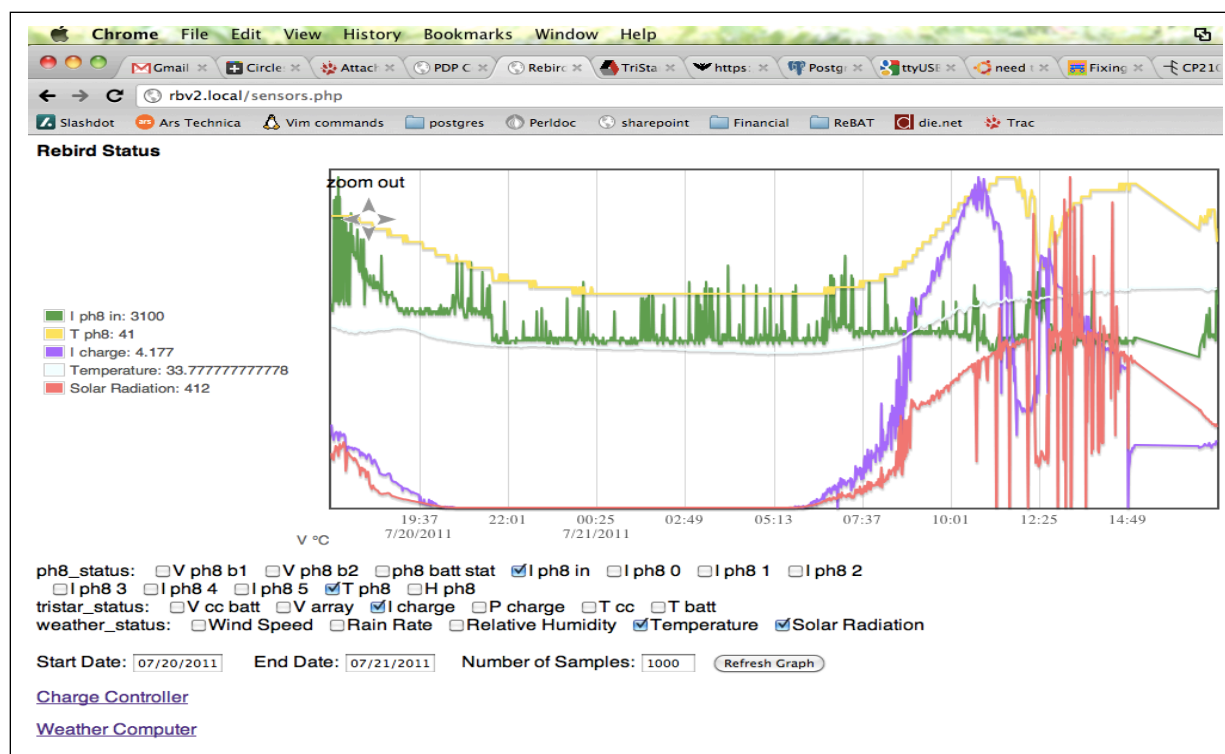
Figure 7. A screen capture of the system health web interface showing 24 hours of data collected by ATOM during the UD Lewes test deployment (a plot of selected operational parameters vs. time).

2.1 Audible Sound Subsystem

The audible sound subsystem of ATOM as deployed at UD Lewes consisted of two subarrays of four weatherproofed audible sound microphones arranged in a linear configuration. This configuration was selected based on consideration of the desired objectives of bird detection, location, and flight height calculation within rotor swept altitudes in an offshore environment. These objectives were used to inform development of an ATOM system microphone array analysis conducted by IATech in conjunction with UF sound engineers. These tests were conducted in spring 2011 and comprised a series of laboratory and outdoor tests of the ATOM audible sound subsystem to help refine, calibrate, and evaluate the success of the beam forming and ranging algorithms that were used to calculate the position and flight heights of birds passing above the microphone array during ATOM system deployments. The beam forming algorithm calculated the angle from which the sound source emanated relative to the sound array by combining input on signal strengths at various angles from all eight microphones. The ranging algorithm used the signal strength data from the eight microphones, as well as positional features of the recorded sound, to calculate the distance of the sound source from the microphone array. For all of these tests, a sample recording of Red Knot flight calls was used (provided by project collaborators at CLO; Figure 8). The most likely sound pressure levels were identified in collaboration with CLO. The control experiment was set to have parameters of 80–90 dBA sound pressure level at a distance of 1 m, simulating the natural strength of Red Knot vocalizations in the wild.

The tests were conducted in four separate stages: control calibration experiments (indoor), preliminary beam forming and ranging experiments (indoor), weather balloon beam forming and ranging experiments (outdoor), and radio-controlled aircraft beam forming and ranging experiments (outdoor).

Control Calibration Experiments: Output level of the speaker was adjusted until the recommended sound pressure level (SPL) at this distance was achieved. This provided a baseline sound output level that was used in all successive experimental stages.
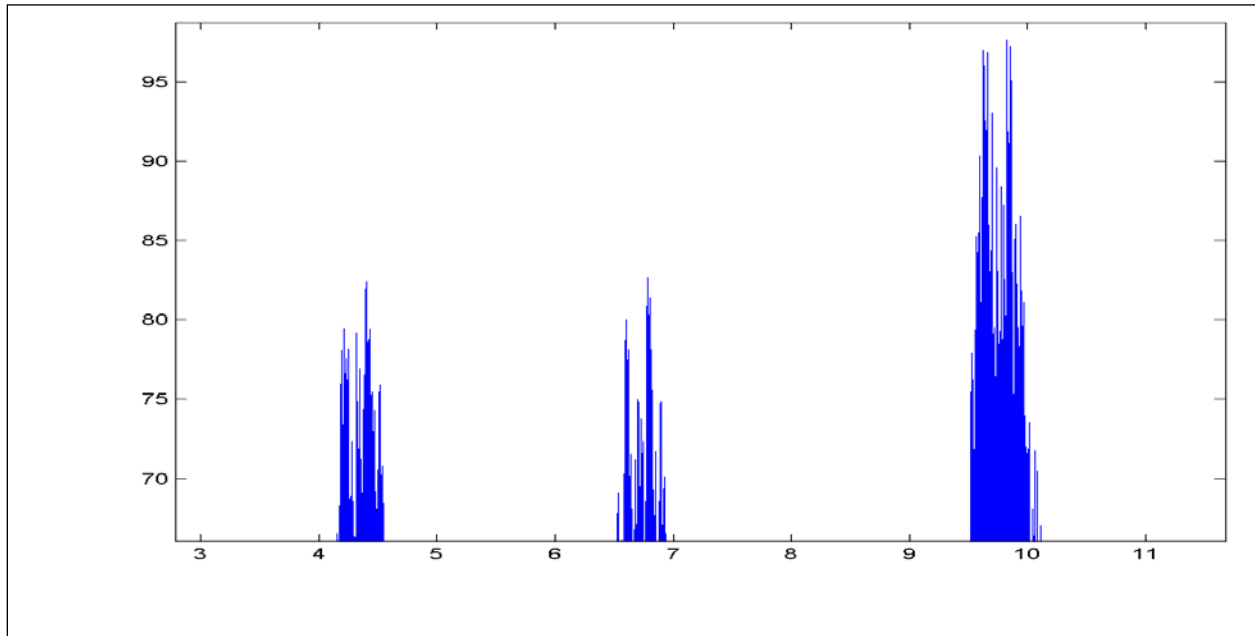
Figure 8.   Example of a Red Knot vocalization (three double-note calls are visible over a period of roughly six seconds).

Preliminary Beam Forming Experiments: Controlled laboratory experiments were conducted in a sound laboratory environment in Gainesville, Florida, during spring 2011. Three different source locations were tested. All tests were conducted at a perpendicular distance of 8 m from the array, simulating the above-ground level of the bird. While the distance used is lower than the flight heights of birds that the ATOM system is designed to detect in marine environments, the relationship between the flight heights to node spacing was similar. The first test was conducted with the acoustic source perpendicularly aligned with the center of the left node. The second test was conducted with the acoustic source perpendicularly aligned with the midpoint of the left and right nodes. The third test was conducted with the acoustic source perpendicularly aligned with the center of the right node.

Although the tests were conducted in an enclosed test area, this did not prevent the beam-forming and ranging algorithm from performing properly. Figure 9 through Figure 14 illustrate the testing configuration and beam steering response from the left and right nodes. The black ovals represent the individual microphones in the two nodes. Within each node, the microphones are linearly configured and spaced at 1-ft intervals.
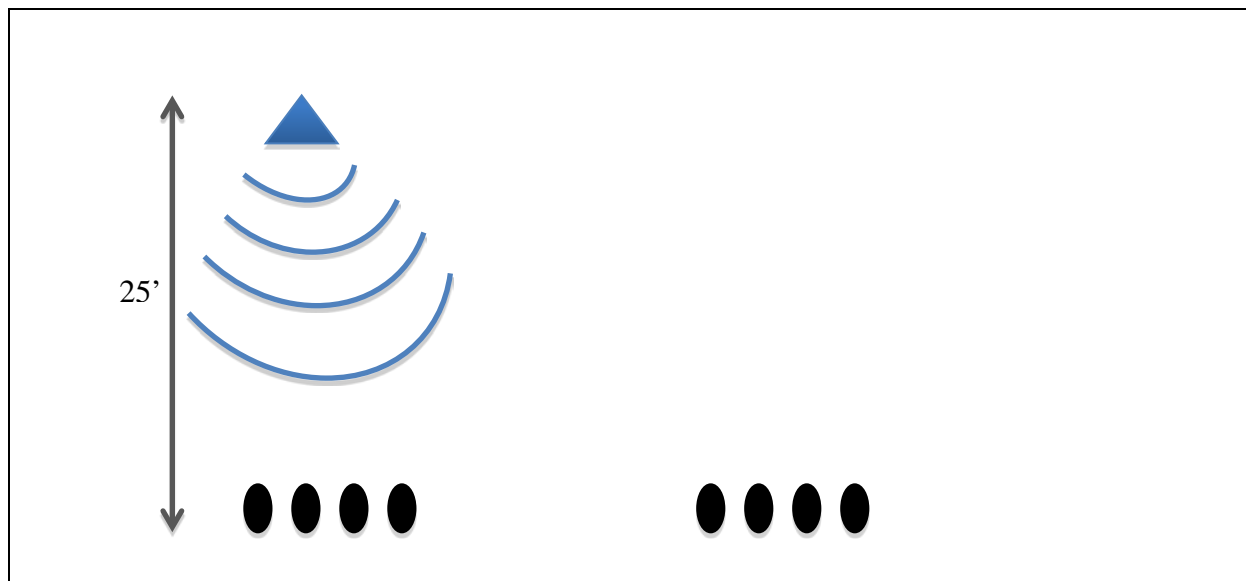
Figure 9.   Preliminary beam forming laboratory testing at 25 ft from the left microphone or node.

Figure 10 shows the strength of the audible sound signal as a function of the angle of incidence of the sound; therefore, the highest peak represents the angle of the sound source relative to the microphone node. The top graph shows the left node, and the bottom graph shows the right node. The configuration for this output is presented in Figure 9. During this trial, the microphone was centered directly over the left microphone node; hence, that node recorded the strongest peak at 0° angle (directly in front), whereas the right node recorded the strongest peak at an angle of approximately 12° displaced to the left.
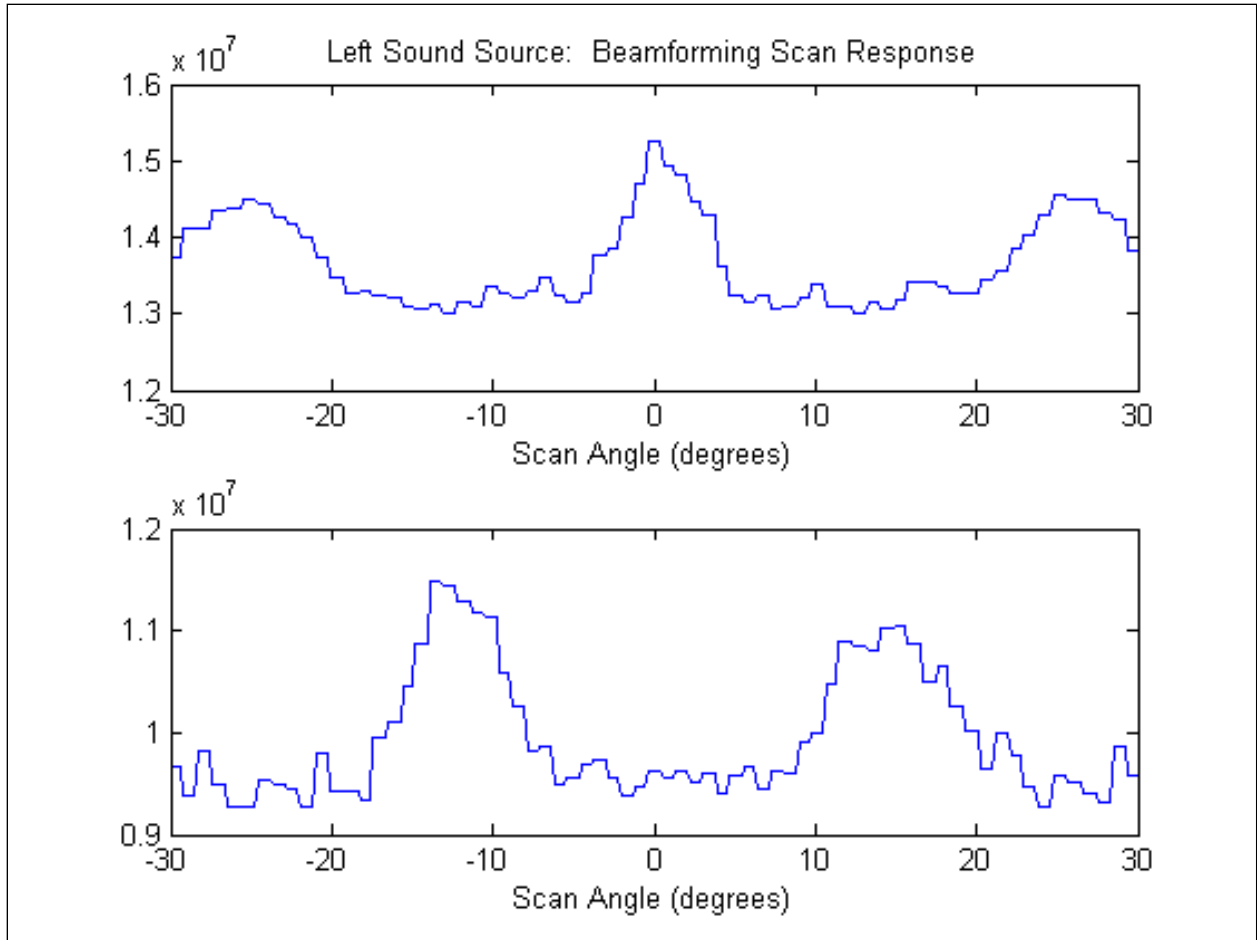
Figure 10. Beam forming response output from the left positional test (as depicted in Figure 9).
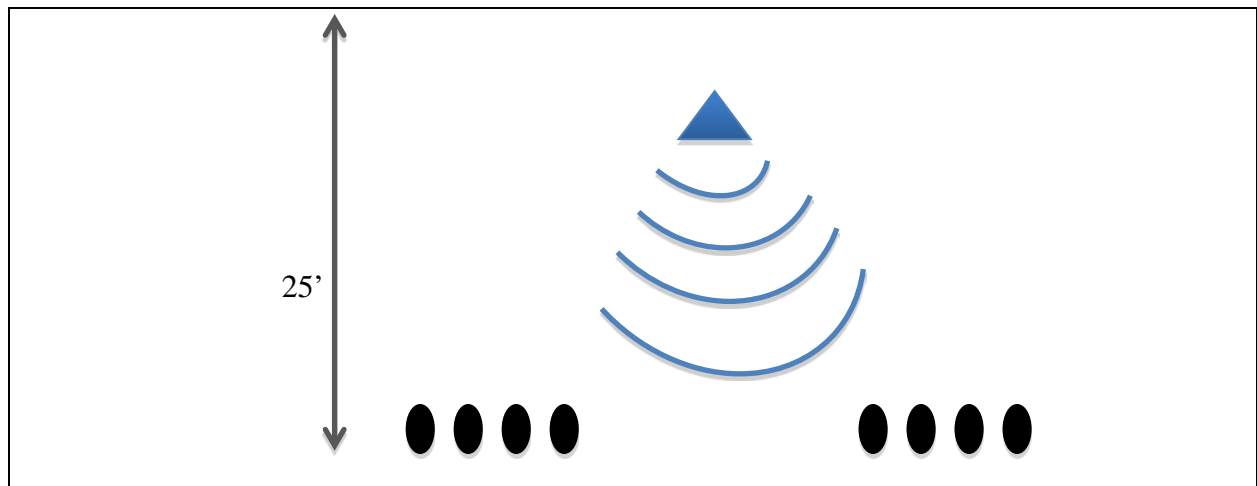
Figure 11. Preliminary beam forming laboratory testing spatial configuration at the midpoint of the left and right microphone nodes, displaced 25 ft forward.

Figure 12 shows the strength of the audible sound signal as a function of the angle of incidence of the sound; therefore, the highest peak represents the angle of the sound source relative to the microphone node in the configuration presented in Figure 11. The top graph shows the left node, and the bottom graph shows the right node. During this trial, the microphone was centered directly in between the left and right microphone node; hence, each node recorded the strongest peak at approximately a 7° angle displaced toward the center.
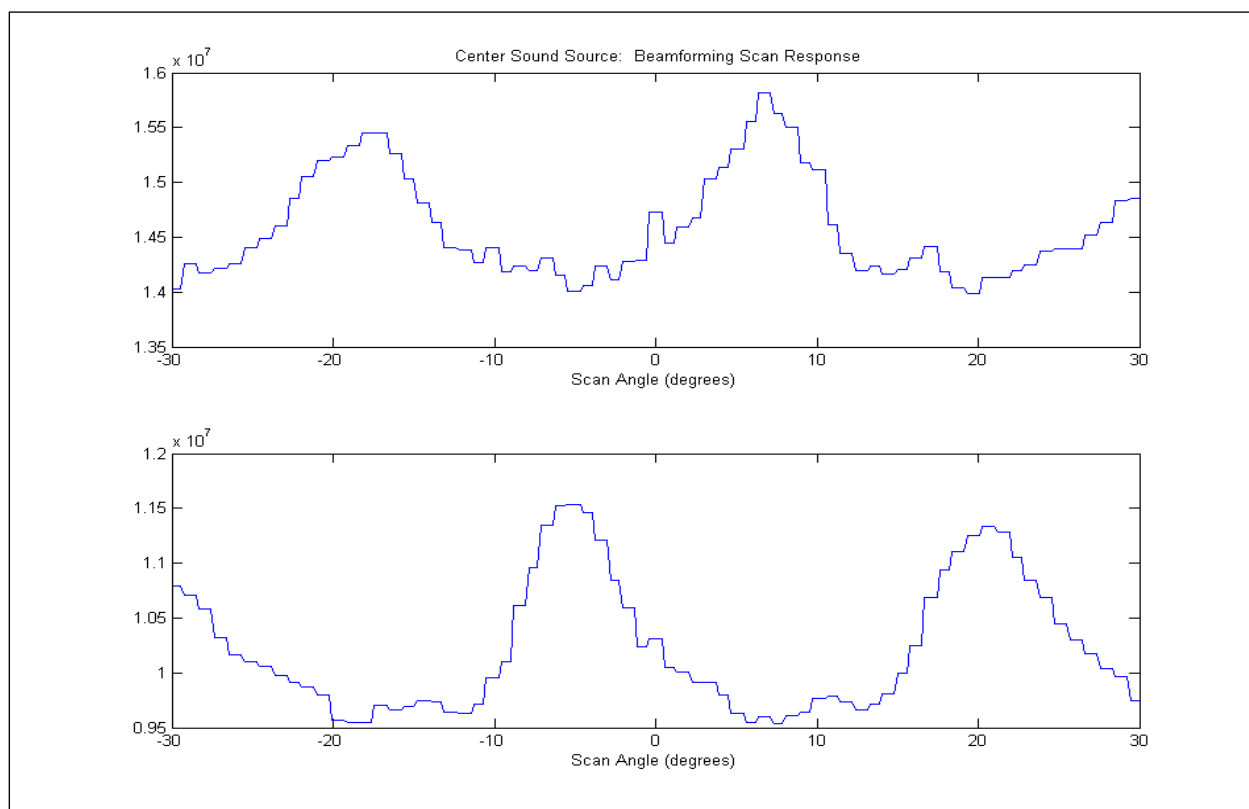
Figure 12. Beam forming response output from the center positional test as depicted in Figure 11.
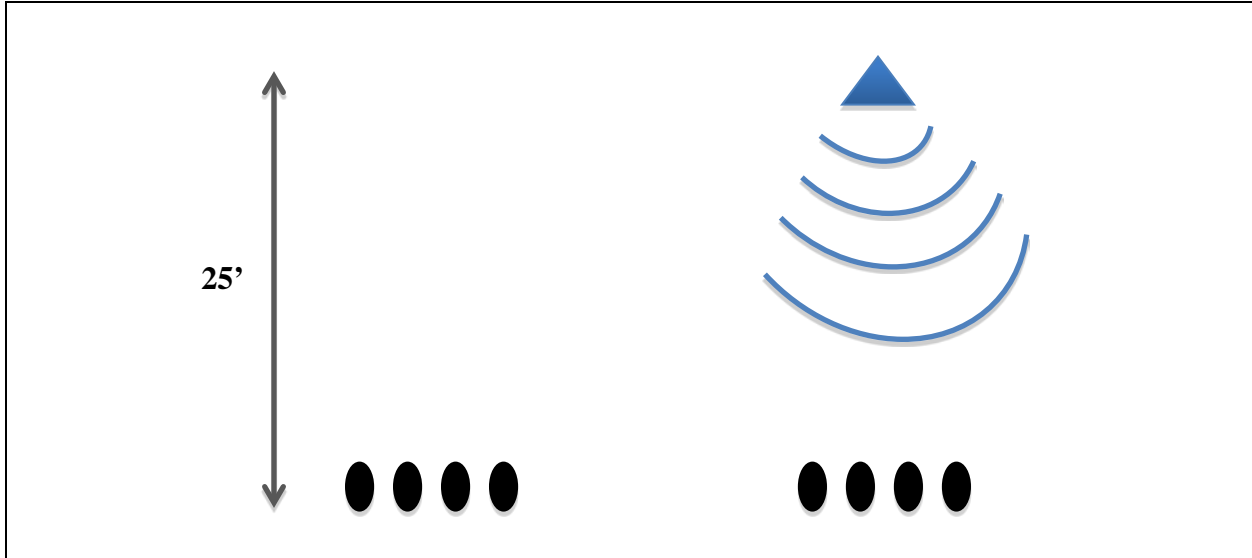
Figure 13. Preliminary beam forming laboratory testing spatial configuration at 25 ft from the right microphone node.

In Figure 14, each graph shows the strength of the audible sound signal as a function of the angle of incidence of the sound; therefore, the highest peak represents the angle of the sound source relative to the microphone node. The top graph shows the left node, and the bottom graph shows the right node. During this trial, the microphone was centered directly over the right microphone node; hence, that node recorded the strongest peak at a 0° angle (directly in front), whereas the left node recorded the strongest peak at an angle of approximately 12° displaced to the right.

The ranging algorithm used sound inputs from all of the microphones in the array to calculate the distance of the sound source from the node. Distance (range) calculations from this algorithm from the laboratory tests are depicted in Table 1. In all cases, the actual distance or range of the sound source from the microphone arrays was 300 in.
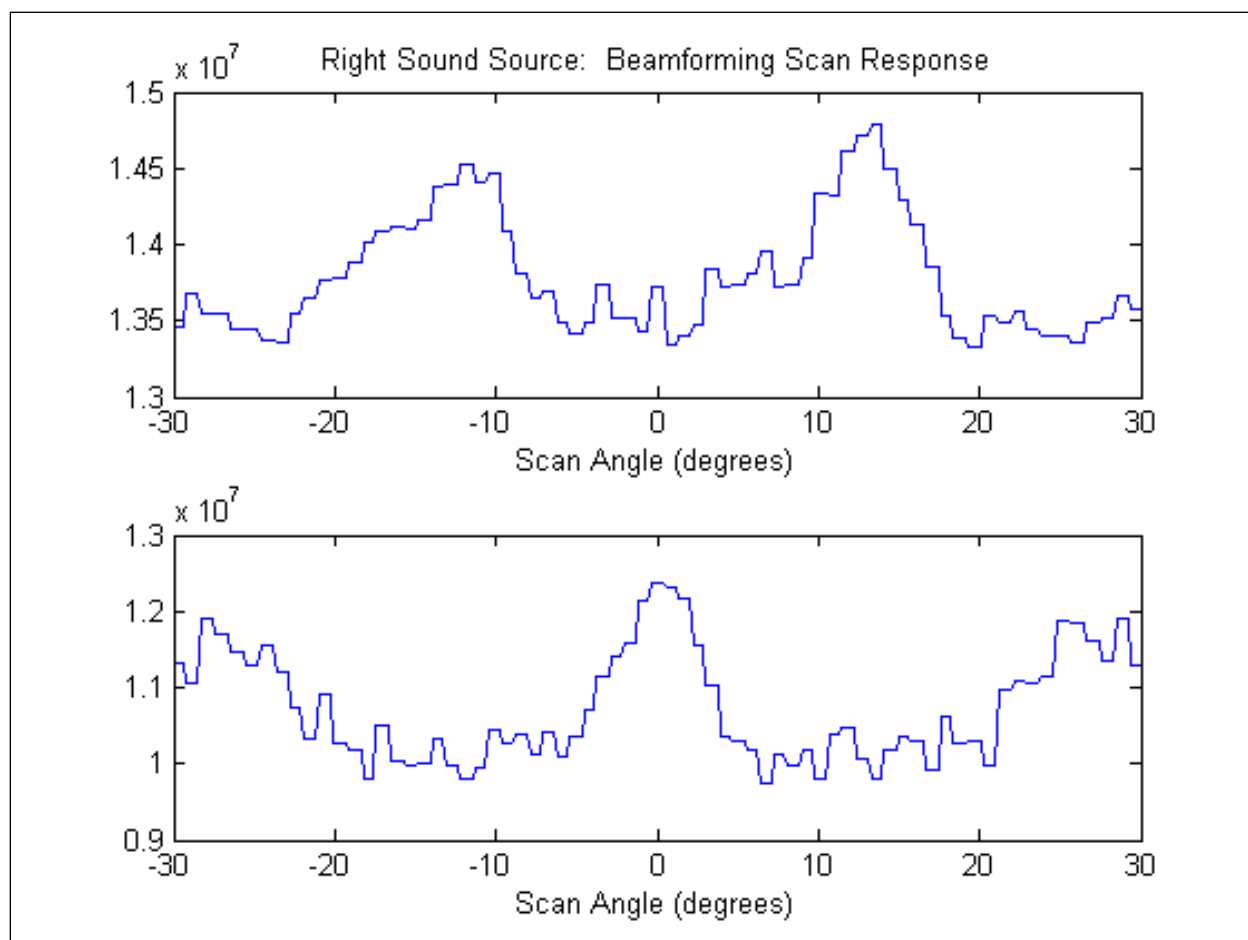
Figure 14. Beam forming response output from the right positional test as depicted in Figure 13.

Table 1.

Estimated ranges and error (%) from range calculations conducted during preliminary laboratory testing.

Test Configuration	Estimated Range (in.)	Error (%)
Left	301.89	0.63
Center	352.75	17.5
Right	301.89	0.63

Weather Balloon-Based Beam Forming and Ranging Experiments: A set of experiments was conducted using a weather balloon (Figure 15) to test the performance of the ATOM audible sound system in an outdoor environment with sound emanating from above the microphone arrays at larger distances from the microphones. These experiments were conducted in

Gainesville, Florida, during Jun 2011 using the same Red Knot calls projected at the same volume as in the preliminary laboratory experiments described above.

The weather balloon experiments were performed with all eight microphones in a linear configuration. The inter-microphone spacing was set to 1 ft and the spacing between the microphone nodes was 25 ft. The results shown below are for the experiment with the weather balloon at an approximate elevation of 50 ft (17 m) above the ground.

The acoustic signal was broadcast from altitudes of 8 m and 17 m above the ground, and the Red Knot call was then broadcast at lifelike volume from the two different heights and recorded by the microphone array below. This experiment was performed directly outside the Gainesville, Florida, office of IATech where there is significant ambient noise.
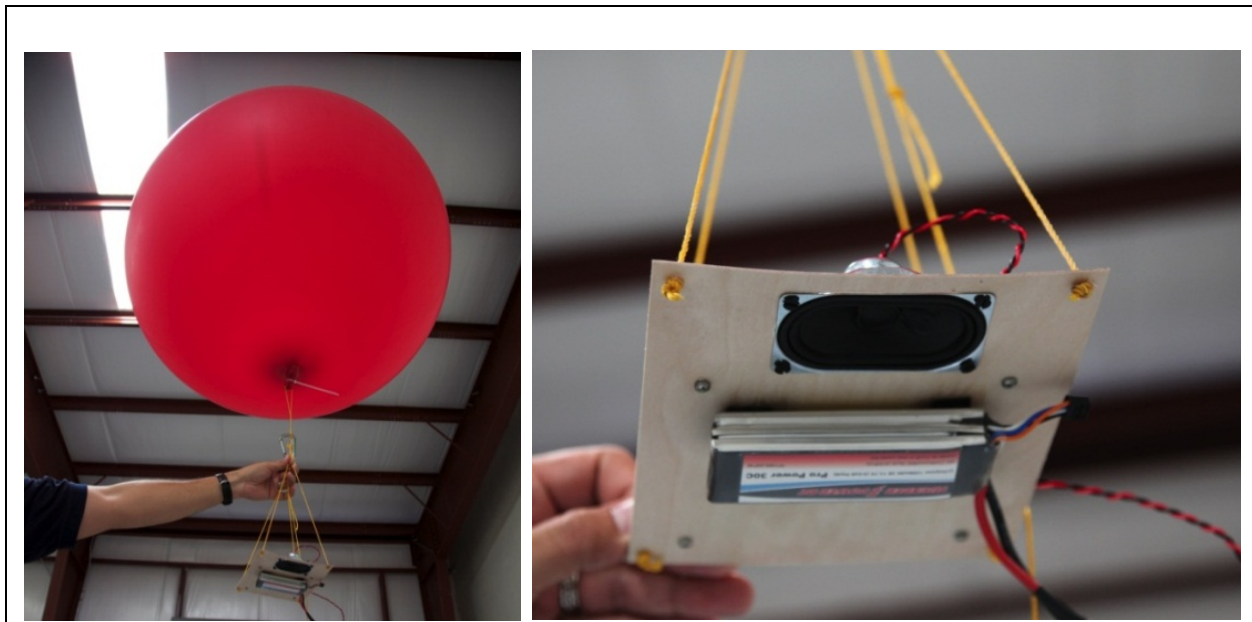
Figure 15. Weather balloon (left) and sound driver hardware with speaker (right).

Raw analog data are shown below in Figure 16 and Figure 17. The separate plots in the figure represent the acoustic data collected for each individual channel of the array. Four Red Knot calls are contained in this sequence, though only the second is easily visible on this graph (just after t = 3 seconds) because of ambient noise. The double-note quality of the Red Knot flight call is observable.
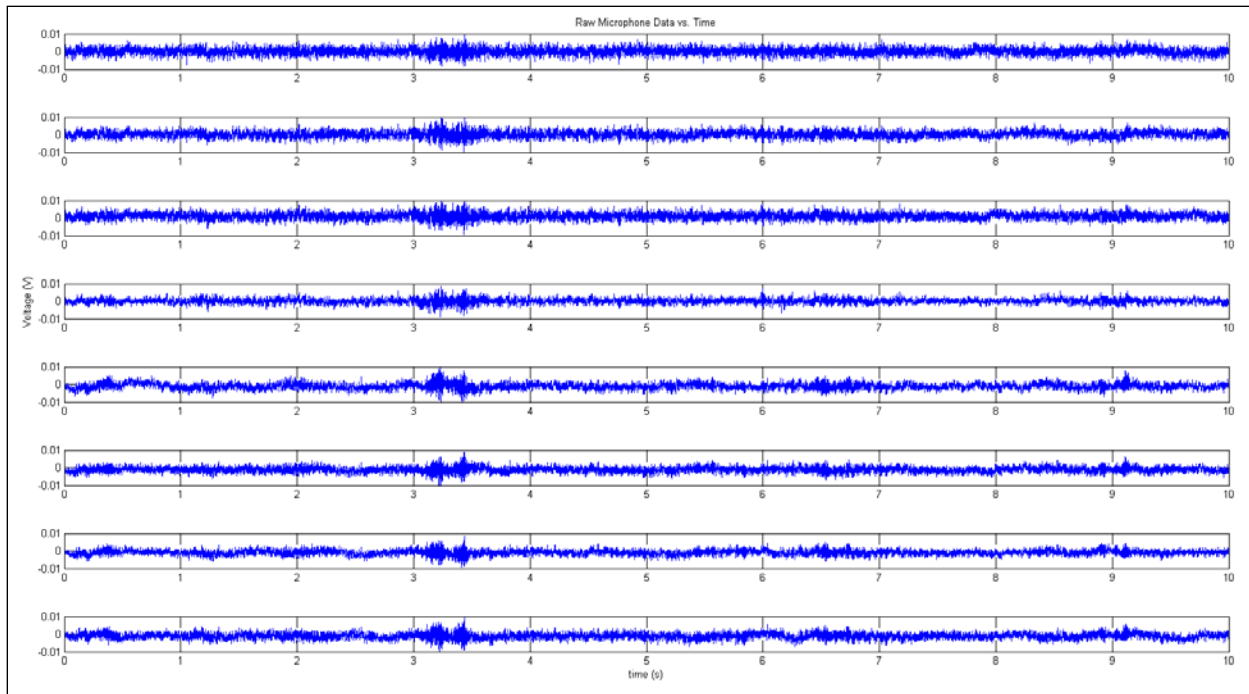
Figure 16. Raw microphone data (sound pressure level, or signal strength).
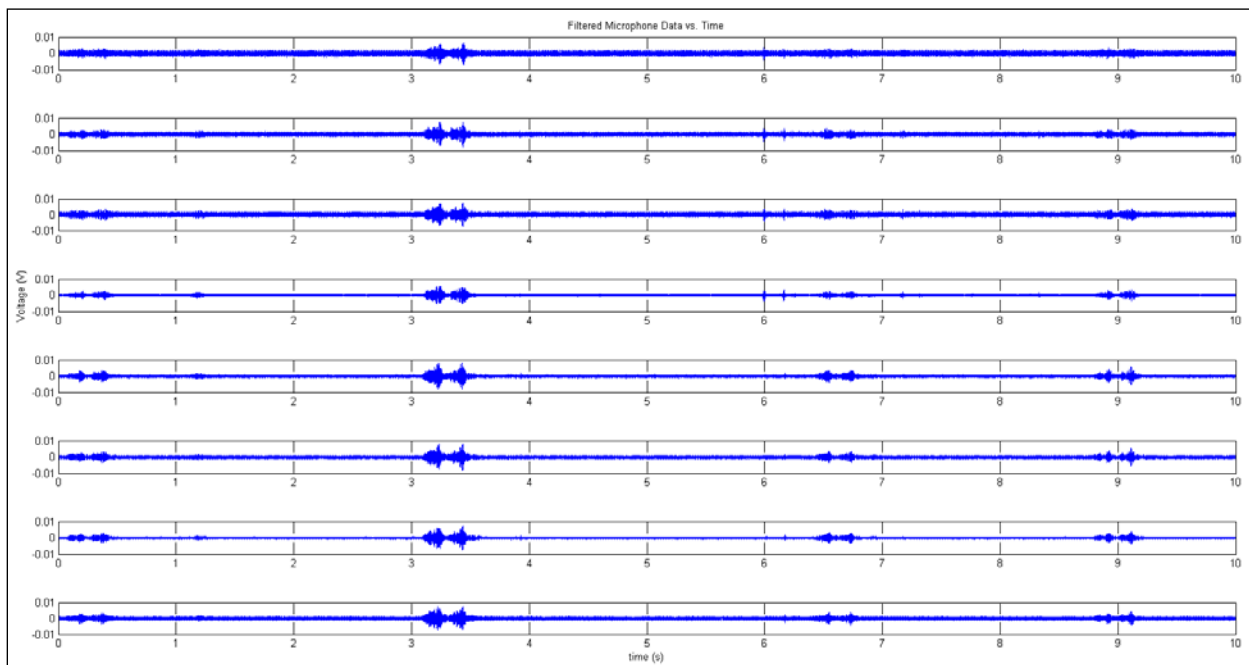
Figure 17. Filtered microphone data (sound pressure level, or signal strength).

In an attempt to remove some of the noise that can be seen in Figure 16, a bandpass filter was applied to the signals in the frequencies of 2 kHz–10 kHz. All sequences are now easily observable. These results are illustrated in Figure 17.The bandpass filter significantly attenuated out of band frequencies in the acoustic measurements while maintaining the integrity of the original signal.

Radio-Controlled-Aircraft-Based Beam Forming and Ranging Experiments: To test the beam forming and ranging performance of the ATOM audible acoustic subsystem at higher altitudes, corresponding to the altitudes of interest for offshore wind bird risk studies, and also with moving targets, a series of tests were conducted in which the Red Knot vocalizations described previously were broadcast at lifelike sound output levels from a speaker attached underneath a radio controlled aircraft (Figure 18). The aircraft was flown over the ATOM audible acoustic subsystem microphone array in an outdoor, open field environment in Gainesville, Florida, at a variety of measured flight altitudes up to 100 m above ground level (Figure 19).

Figure 18. Radio-controlled aircraft with speaker mounted to underside of airframe.

Figure 19. Radio-controlled aircraft test of the ATOM audible acoustic subsystem showing the two microphone nodes.

Plots of the aircraft flight paths relative to the microphone array are shown in Figure 20 (2D, 3D plots). During these experiments, the 3D flight trajectory of the aircraft was recorded by a GPS unit as it flew over the microphone array. The upper plot is two dimensional, showing the x and y dimensions of the flight path relative to the microphone array, whereas the lower plot is three dimensional, also indicating the flight altitude of the aircraft as it circled around, making passes over the microphone array at various altitudes corresponding to altitudes of interest for bird-offshore wind risk studies.

The results of the radio-controlled aircraft flyover tests indicate successful detection of lifelike broadcasts of Red Knot flight calls from as high as 82 m, which was the highest altitude tested (Figure 21). Altitudes shown are 38 m (top), 65 m (middle), and 82 m (bottom). In all cases, a significant amount of ambient noise can be seen, but the double note Red Knot vocalization is also detectable. It is also clearly audible in the sound files produced in these flight tests at all three of these altitudes (see Figure 21).
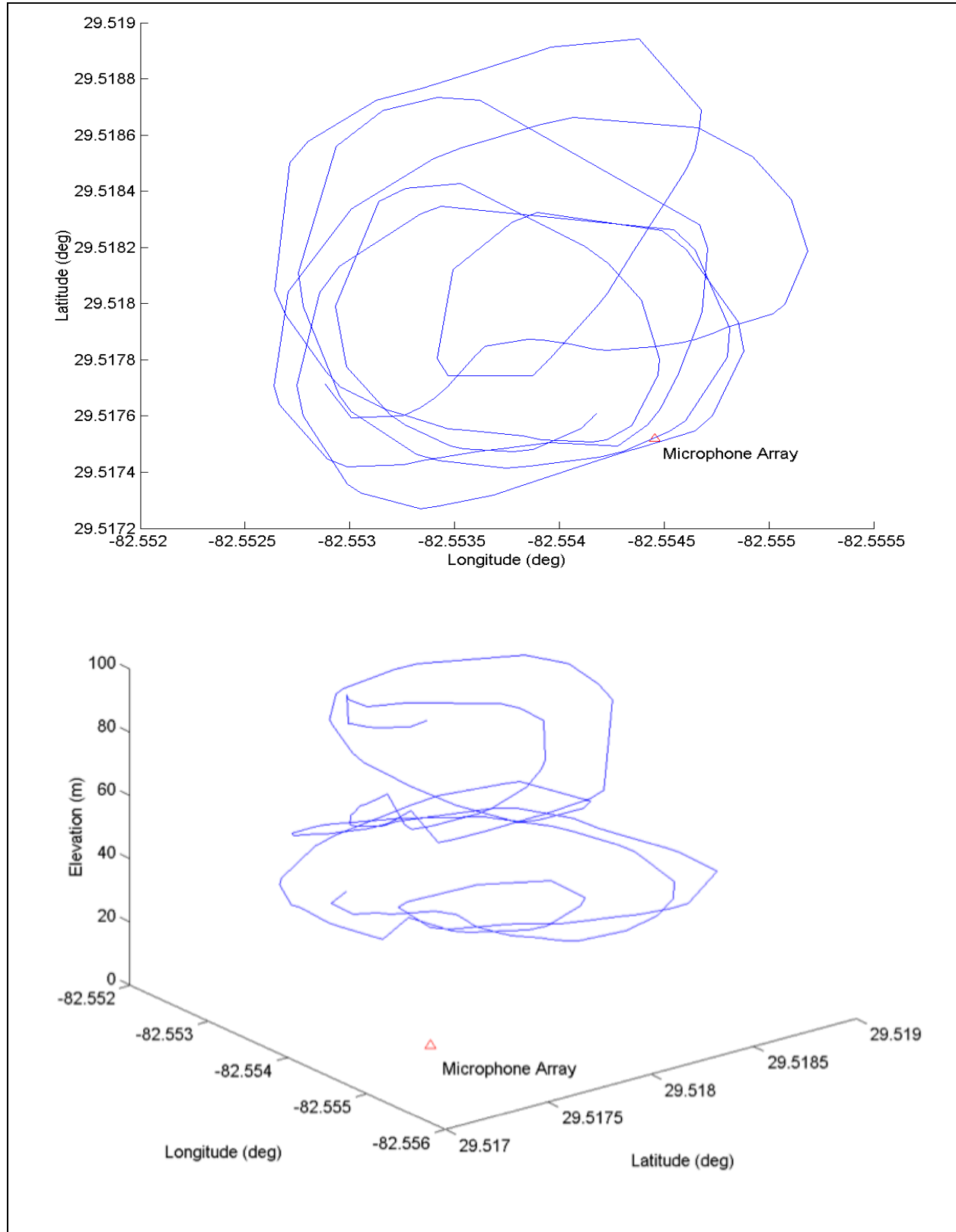
Figure 20. Flight trajectory of radio-controlled aircraft.
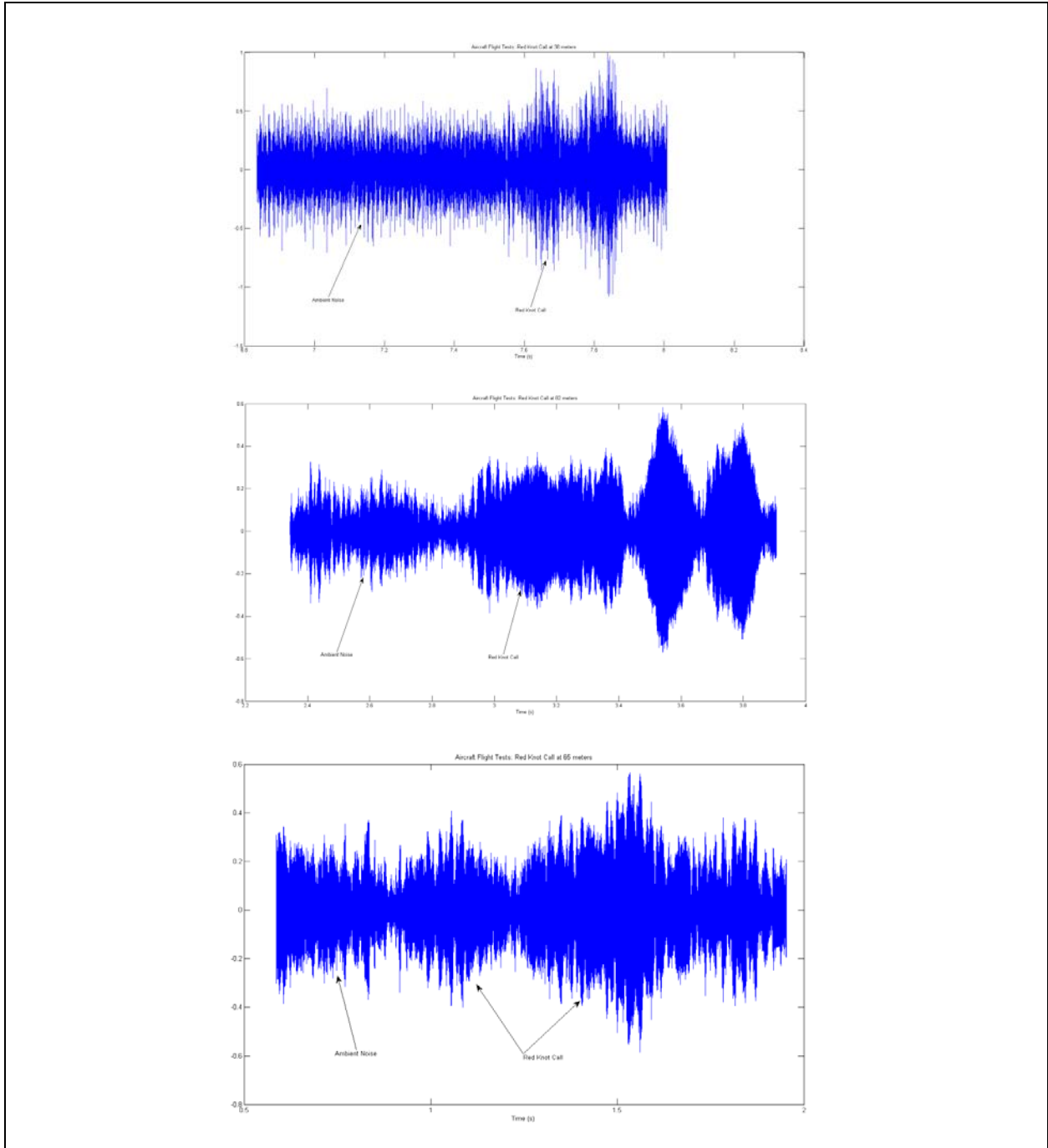
Figure 21. Sound pressure level (signal strength) diagrams from radio-controlled aircraft flyover testing.

2.2 Analyses Software Development

2.2.1 Thermographic Software

"Analyst Workbench" (AW) is the original software developed for the ATOM system, which provides the basic infrastructure and tools for analysts to visualize, analyze, and interpret the data for biological risk assessment. The basic AW structure is composed of two parts: (1) the analyst server, a Linux-based program that resides on Normandeau's in-house Linux server; and (2) the analyst client, a Windows-based desktop application that resides on each analyst's (client) computer.

The analyst server runs on a Linux system at Normandeau premises. This system has direct/fast access to the hard disks that contain the recorded infrared (IR) video and audio from ATOM systems in the field. This system also has direct access to the database server that contains the metadata for the recorded IR video and audio. The desktop application connects to the server and the server provides all video, audio, and track data needed by AW. The server supports simultaneous network connections from multiple AW client applications. It is capable of streaming video data at up to 1.5× real time. The video and data supplied by the server are described below.

The analyst client communicates with the analyst server application to retrieve video data from the ATOM server and stream it to the analyst. Analysts can select video data sequences in which moving objects have been detected by the automated target detection algorithm. The moving objects themselves are referred to as "tracks" and extend across multiple frames of video. Multiple tracks may occur in the same sets of video frames, for example, representing multiple birds in a flock. Tracks are manually screened to identify those potentially containing bird and/or bat targets. These targets have additional data allocated by the AW software. These data include approximate altitude, direction, and velocity of all identified tracks.

Analyst client can play video based on a track or the full video file. During this project, a full video file could only be played if it was on a directory accessible to the computer. A track defines a few seconds of video from a file that may or may not contain a target of interest. The tracks are solely created by SwisTrack. SwisTrack is software that uses algorithms to identify objects from recorded video based on a set of parameters. The parameters can be refined to reduce the number of false positives (i.e., moving clouds).

There are several options for selecting tracks for review or viewing. The first step is to select the year, month, and day from the calendar. Days that have no tracks have an "X" covering the day. The next step is to select the time frame. The system defaults to the entire day. Finally, the tracks can be filtered by those that have been analyzed or not analyzed or display all tracks. The "Get Tracks" button is clicked to return the list of tracks for the chosen criteria.

The track selection process continues when the list of tracks are displayed (Figure 22). The analyst has the option to select one, multiple, or all the tracks listed. When "Open" is selected the first track in the list is displayed.
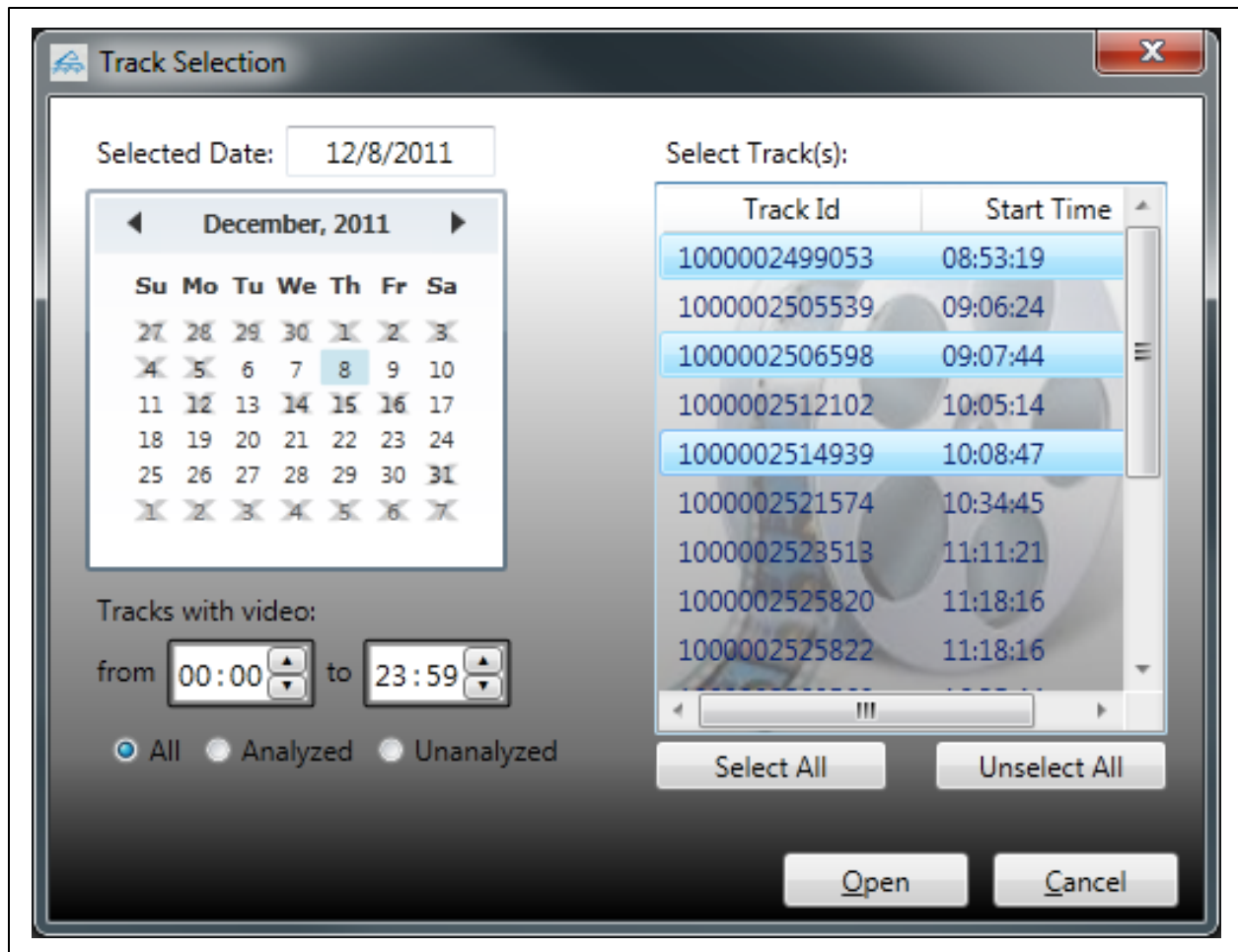
Figure 22. One of two track selection screens in the analyst client application.

The stereo camera view streams the video from both cameras for the time code specified by the track. The status bar at the bottom on the viewing screen contains some useful information (see Figure 23). From left to right, showing is the current user, current track being displayed, and position of the current track with the list of tracks selected for play. To the far right is an indicator of the play setting (Track or File).
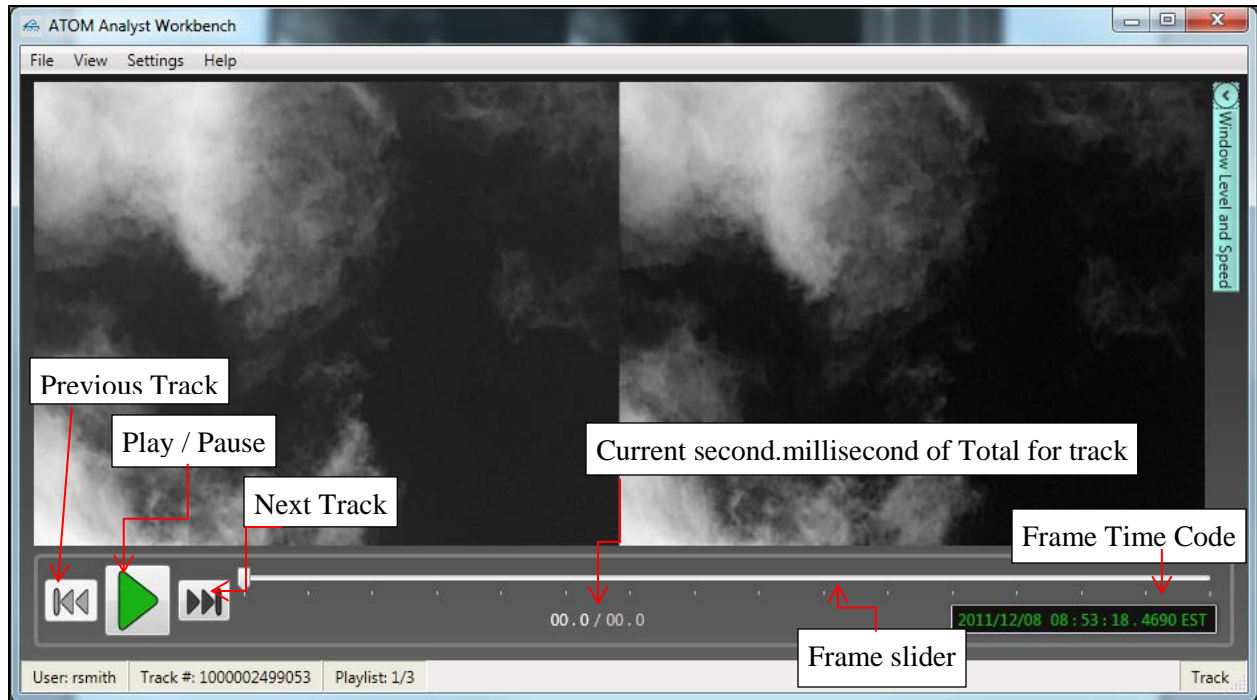
Figure 23. Stereo camera view in the analyst client application with various user tools labeled.

The Track Information dialog is where the track details are shown. The analysis tab collects the type of target contained in the track (Figure 24).
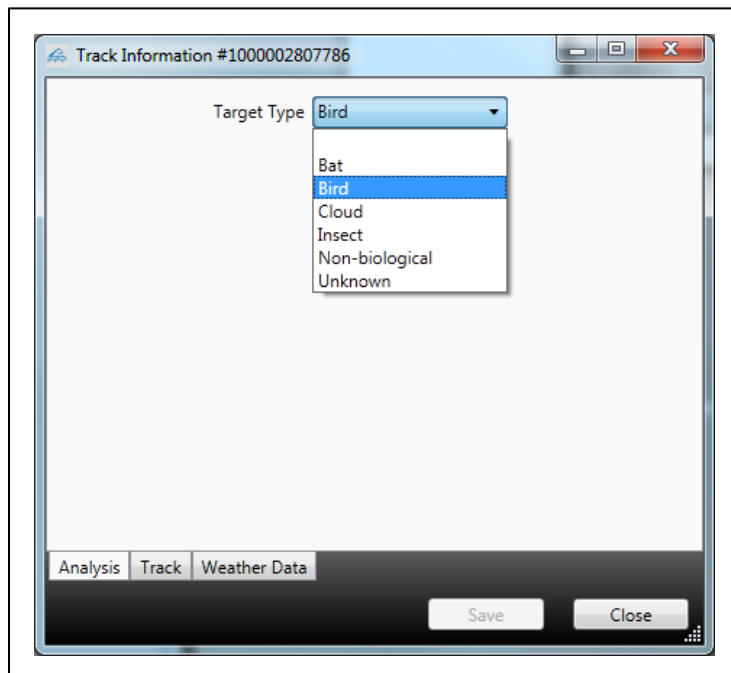
Figure 24. Track information—analysis tab in the analyst client software.

The track tab (Figure 25) contains information calculated using points from both the right and left video to estimate distance from the camera and velocity and includes bearing based on the direction of travel. The distance from the camera is a median based on the number of points in common between the right and left camera. The Show Details section gives the particulars about the generation of that median (see Figure 24). The primary length, wingspan, and body length are for the analyst to save any measurement that can be gleaned from the video image. The accuracy and error of the calculations were characterized with field tests (see System Characterization, page 57).
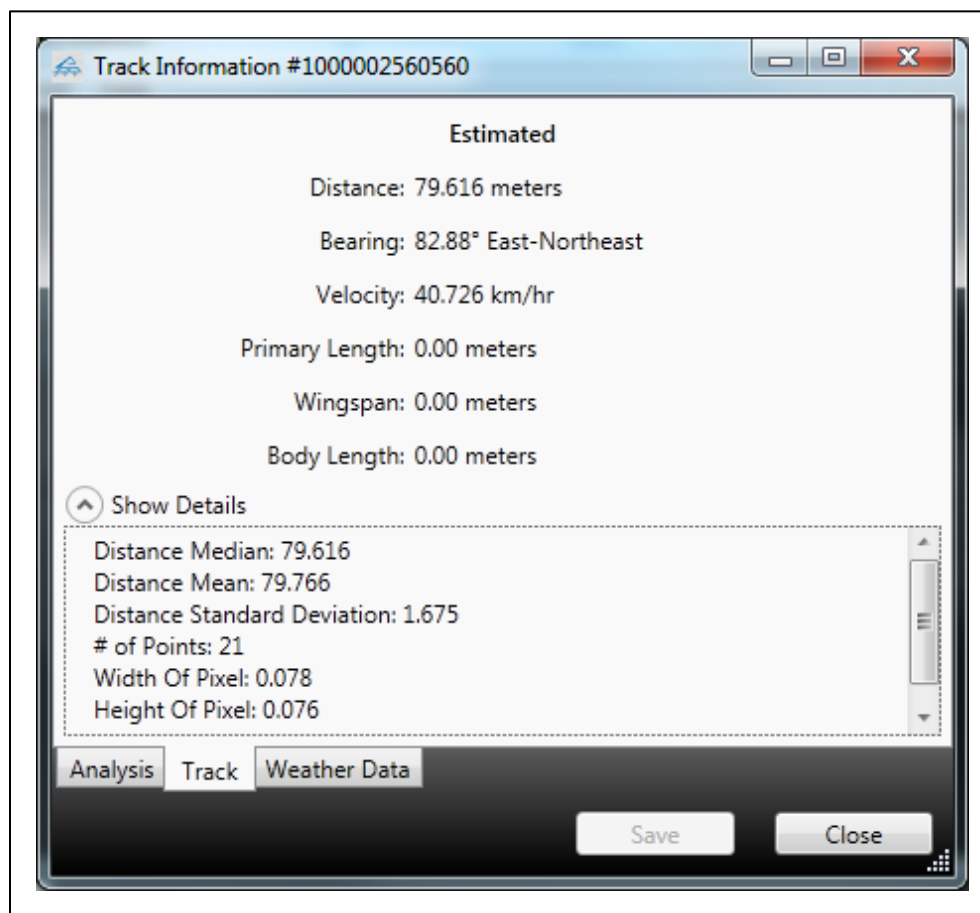
Figure 25. Track information—track tab in the analyst client software.

A track represents the movement of a single target. There could be multiple tracks for a same segment of video that contains multiple targets (birds). When reviewing segments of video with multiple targets, the analyst can display the flight path over the video image to identify the target for the given track (see Figure 26).

Figure 26. Screenshot of analyst client software showing target flight path
feature on a set of bird tracks from Frying Pan Shoals Dec
2011 thermographic data.

The single camera view includes a zoom feature. The fill button (see Figure 27) will adjust the
size of the image so that the entire image will fill the current size of the single camera view
window. The analyst can play the track and the image in the single camera view, which matches
what is being viewed in the dual camera view.

Figure 27. Single camera view in analyst client
software with a bird from the Dec 2011
Frying Pan Shoals data shown.

When the distance from the camera can be calculated, it is also possible to get estimates about size depending on the view of the target. The analyst creates a line over the video using the left button on the mouse to initiate the measurement. This can be done over the single camera view or the default dual camera view. When the line is complete (when the analyst lifts up on the left mouse button) a window will appear so the measurement can be assigned to the correct item (Figure 28). The tracking information window (Figure 25) must be open for the measurement type window to appear. Once the type is selected, the measurement is placed in the appropriate location on the track tab.
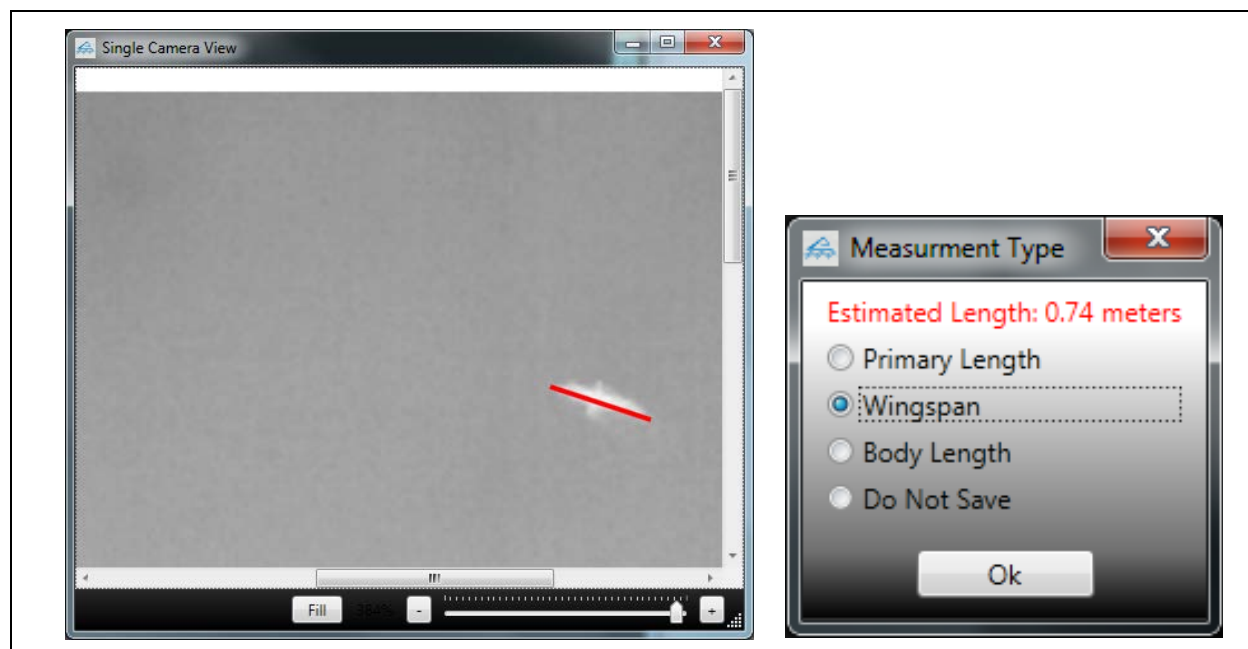
Figure 28. Screenshot of bird from previous figure showing the measurements feature of the analyst client software and measurement type selection dialogue box. Wingspan measurement is shown.

The file event log allows the analyst to review the full video file rather than just the track segment. This can be used to verify that all targets have been identified by SwisTrack. It creates a simple text file with the same name as the video file but with the extension of .txt in a location selected by the analyst. The analyst need only click the add event time button (Figure 29) to add the time code of the frame currently being displayed on the screen.
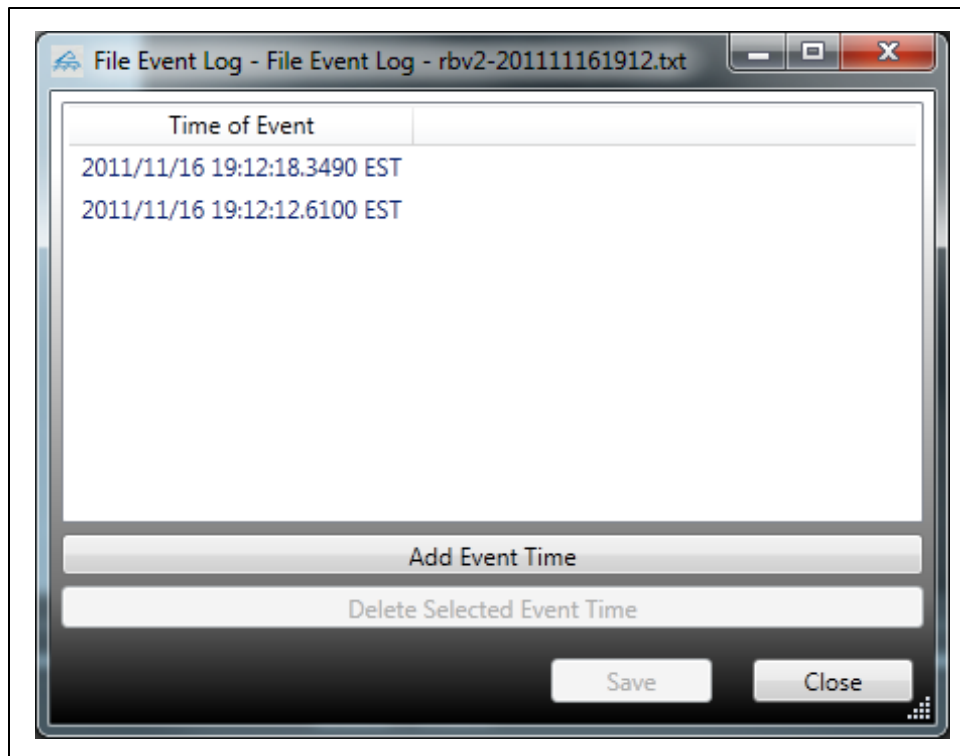
Figure 29. Analyst client screenshot illustrating file event log

2.2.2 Acoustic Software

CLO focused specifically on the development of algorithms that can scan a recorded sound stream to detect signals that match a series of user-specified characteristics and classify those signals to a single species. Previous CLO projects, such as Evans and Rosenberg (2000), Mills (2000), Charif et al. (2005), Fitzpatrick et al. (2005), and Farnsworth and Russell (2007), among others, have shown the power of acoustic monitoring for both nocturnal and diurnal monitoring of migratory birds. CLO has been, and continues to be, uniquely positioned within the scientific community to implement a bioacoustic research and development initiative, possessing the necessary infrastructure and software platform to acoustically monitor target species. Through more than a decade of engineering and software development, CLO has developed methodologies that, in part, mitigate data processing problems by automating event detection in a way that is repeatable and provides some basic performance metrics. These innovations permit us to capitalize on the unique information that acoustic monitoring provides in sampling nocturnally migrating birds because a large percentage of migrant passerine species migrate at night and give stereotypical calls that can be identified to species by ear or by viewing spectrographic images of recorded calls (Evans and O'Brien 2002; Farnsworth 2005).

Designing the Acoustic Monitoring Program (AMP): To transform the state of ecologically relevant acoustic science, as part of the Normandeau/BOEM project, CLO developed a whole new set of mechanisms for gathering, processing, and managing acoustic data on spatial and temporal scales commensurate with today's unprecedented environmental challenges. This overarching infrastructure and engineered system is referred to as the Acoustic Monitoring

Program (AMP) with the main motivation being to enable scientists to answer major research and conservation questions at ecologically meaningful scales.

The primary technical objective of AMP was to design, engineer, and implement a system to acquire, process, and manage very large amounts of acoustic data at defined levels of efficiency and reliability. This was accomplished by combining modern acoustic technologies with high-performance computing. The four goals of the project were to engineer and implement (1) a low cost and efficient technology for collecting sound recordings; (2) an efficient, high-performance acoustic detection-classification-localization software tool system; (3) a high-performance data management system; and (4) a suite of software based tools that permit end users to produce meaningful results through data analysis and visualization. Funds from this project were used to achieve goals two and four above.

AMP System Design: New hardware was purchased and installed, and existing programs (such as BARN, http://barn.xbat.org) were modified. Improvements were made to the original detection and classification algorithms, and new algorithms were developed for additional species. This was very time consuming and CLO recognized that there were immediate and impending data processing needs related to the BOEM project. Therefore, a phased work plan that allowed a functioning workflow was established that gradually improved over time as various AMP technologies became available.

The concept of operations for this system used a high-performance computing platform called the Acoustic Data Accelerator (ADA). The ADA processor performs a variety of computational tasks including detection and classification, localization and tracking, and acoustic modeling. The ADA computer uses 12 CPUs with 48 GB of memory running a parallel processing 64-bit MATLAB program, which is scalable to run on multiple computers. SEDNA, a set of tools that combine MATLAB based routines (Mathworks 2011) and standard functionality found in XBAT (Figueroa 2005), runs on this platform providing parallel processing capabilities. An additional ADA computer was added and server software distributed to the High Performance Computing (HPC) unit. SEDNA was expanded from supporting 8 processors to 16 processors, increasing noise analysis and detection capabilities. The ADA infrastructure uses scheduling software to scale and balance workloads. Focus was initially on algorithm development and on the design and testing of "deep learning" modules and on localization algorithms for various call types. These algorithms run on the ADA computer, providing research level testing and performance evaluation. These approaches were tested against existing technologies (see Erbe and King 2008; Mellinger and Clark 2000; Parks et al. 2009; Ramaswamy et al. 2001; Urazghildiiev et al. 2008; Urazghildiiev and Clark 2007a; Urazghildiiev and Clark 2007b; Dugan et al. 2010a; Dugan et al. 2010b).

A scalable disk farm was directly attached to the ADA computers that access a series of acoustic data sets. Funds from this project were used to purchase this disk farm. First, focus was on building the requirements for constructing a database to accommodate the various processing jobs outlined on the ADA. Processing jobs includes detection and classification, localization and tracking, noise analysis, and acoustic modeling. Data requirements and table structure necessary for efficiently storing the data as they run from the ADA machine were developed. User applications were also studied and refined. A number of data products, analysis tools, and visual

displays existed to accommodate the various research needs of scientists internal and external to CLO. Also incorporated into this were elements of existing software products (e.g., RAVEN, BARN, and MATLAB applications) to build a flexible database interface to be used by both the developers and end-users.

Data Base Management System (DBMS): A combination of standard detection algorithms and "deep learning" modules are used to populate the Data Base Management System (DBMS). "Deep learning" is a set of algorithms that use neural networks to look for pattern recognition. Algorithm development also included building necessary tools for creating detection-classification modules using data-template and "deep learning" recognition engines, together with a library of classifiers already developed through previously funded work.

The AMP system has dual ADA computers and runs a distributed server application with high-speed connection to Tier II and Tier III disk storage (see Figure 30). The Tier II storage unit offers high-speed communication between the ADA computers connected through several high-speed fiber optic channels. The various software applications to the DBMS were directly interfaced. Existing software was combined with new software that operated through the local area network to access data on the AMP system. RAVEN, a java based application, serves as an end-user tool for accessing data. Various MATLAB applications (e.g., SEDNA and XBAT) serve as developer tools for scientists to gain access for specific research goals. High performance computing applications were also further developed for use on the ADA platform. These applications included auto detection, localization, acoustic modeling, and noise analysis.
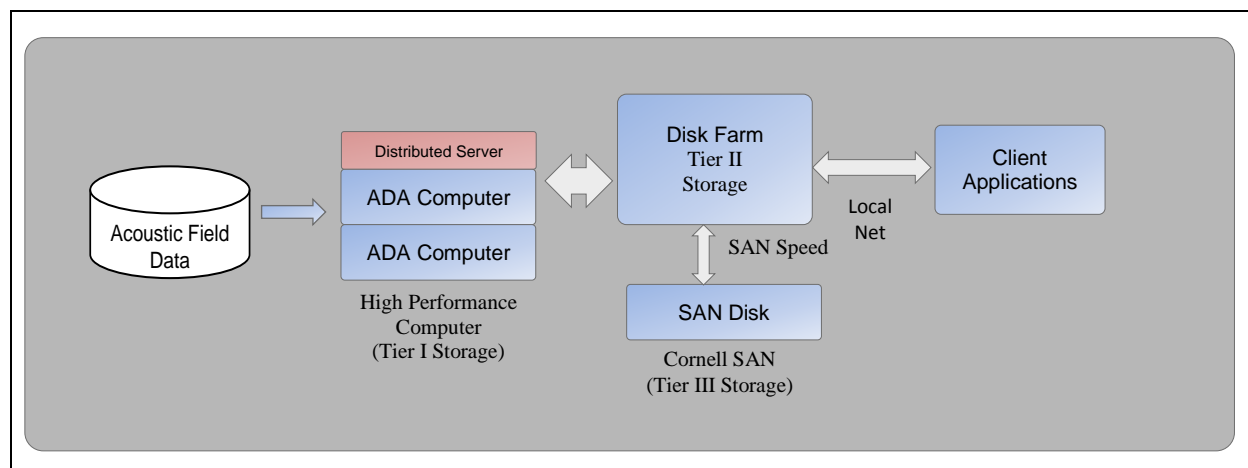
Figure 30. AMP data processing system. The architecture includes a LaCia (Tier II) high-speed disk farm.

Automated Detection and Classification of Acoustic Signals: Successful analysis and interpretation of acoustic data requires a deep and broad library of species vocalizations. These vocalizations are critically important for learning and teaching species identification, producing exemplars for training automated detection algorithms, comparing individual and species-level variation, and learning to ameliorate the negative effects of unwanted noise in long-term field recordings. Although CLO has the world's largest archive of natural sounds in its Macaulay

Library, this collection is almost devoid of the species-specific flight calls needed for studying and monitoring nocturnally migrating birds.

Approximately 80,000 hours of flight-call recordings have been accumulated through small-scale acoustic monitoring during the past 15 years, and through analysis of approximately 10,000 hours of these recordings (e.g., for Department of Defense Legacy Program and other projects), dozens of species have been identified. That leaves most of the 400 species of migratory birds occurring in the U.S. underrepresented or absent from CLO's current archive, including many species of high conservation priority (e.g., Swainson's Warbler) and species occurring in offshore environments. Moreover, the archive does not yet reflect the full variation that exists among individuals, age classes, sexes, or across geographic areas. In short, a high priority for the Normandeau/BOEM project has been to build a much larger library of relevant reference vocalizations to serve as a training dataset for automated detection and classification algorithms.

During the project, CLO has been filling in species level gaps in their flight-call library and bolstering sample sizes for other species by using existing data processing tools and workflows to explore the remaining 70,000 hours of recordings. This work continued throughout the project. The process accelerated as more efficient AMP processes and tools came online (see Appendix 2. Descriptions of Bird Call Samples Used by Cornell Lab of Ornithology in Testing of Preliminary Acoustic Monitoring Program (AMP) System). Nocturnal flight calls are the only source of information for directly identifying passing nocturnal migrants to species (Evans and O'Brien 2002; Farnsworth 2005). In the recent past, the primary method for extracting flight call data from tens of thousands of hours of recordings was automated by using band-limited energy filters that search for signals of specified duration, signal-to-noise ratio, or occupancy in a defined frequency band. This process often produced unworkably large datasets, and classification of the datasets required expensive and time-consuming expert effort. CLO's first approaches built on the challenges of using band-limited energy filters, using template detectors to streamline portions of the process. Matched filter detectors have been under investigation at CLO for several years, but the approaches pursued made several grand improvements on past attempts. Perhaps most important was the ability to scale template detection and evaluate the challenges of going to scale in ways not previously possible. A process was developed for building matched filters, developing a suitable operating point, creating performance measures, and developing an understanding of how the detectors/classifiers work in varying noise environments. Specific goals were to (1) establish baseline detection capabilities for six species of nocturnally migrating birds using matched filter detection methodology, (2) develop baseline performance metrics for the automatic detection algorithms, (3) integrate these algorithms into a platform to automatically look for acoustic events in large scale acoustic data, and (4) develop visualization techniques for inspecting the data and understanding the migratory trends over large temporal/spatial scales. Spectrogram correlation was used for auto detection, as this technique allows development of several types of detection algorithms that facilitates the creation of a multi-species detection engine. In this analysis, relatively small amounts of data were used to understand performance parameters to be applied to larger datasets, allowing an estimate of important diagnostics, such as processing time and expected false detection rates.

Matched filtering is a common technique developed for many detection applications, including signal and image processing. From the literature, it's clear that authors have used a variety of

approaches to develop both time-series and time-frequency methods. As pointed out by Duda et al. (2001) and Ballard and Brown (1982), alternative forms for image-based template matching exist, such as the Hough transform, and are commonly used in pattern recognition problems. Here, CLO uses an image processing approach for creating a matched filter, also referred to as a template. The basic relationship is taken from Porat (1997).

$$y_{T_i(t,f)} = \int_{t1}^{t2} T_i(t - \tau, f)\, x(\tau, f)\, d\tau \qquad \text{(Eq. 1)}$$

The relationship in (Eq. 1) is a time-frequency representation of a standard convolutional relationship. The equation fixes frequency and assumes time as the variable quantity. The time-frequency domain is shown as $x(\tau, f)$. One downside of match filtering is dealing with the amount of variability among objects (Zimmer 2011). Therefore, this analysis uses a series of templates to derive energy values, described by the ith value noted in $T_i(t, f)$, and the template is described in time-frequency as $T(t, f)$. In general, a greater number of templates captures more signal variability and results in tighter detector performance. Too many templates, however, require additional processing and can cause the detection capability to reduce the ability to generalize. The process outlined in (Eq. 1) requires acoustic analysts to select a series of templates (calls). The acoustical features of these templates become the matching criterion for (Eq. 1) for finding and classifying target events in a long-term recording. A convolution result provides a match strength $y_{T_i(t,f)}$, which can be viewed as a correlation value that ranges from zero to one. A template with the maximum value is selected as shown in (Eq. 2).

$$\rho = arg\max_{T_i}[y_{T_i(t,f)}] \qquad \text{(Eq. 2)}$$

In this sample study, the performance of templates developed for six species was tested. Introducing several different species permits possible detection between templates, (Eq. 2) can be indexed to determine the template label, or class.

$$\rho_j = arg\max_{T_{ij}}[y_{T_{ij}(t,f)}] \qquad \text{(Eq. 3)}$$

Figure 31 shows the basic framework for using a matched filter detection approach when trying to identify species-specific targets in a long-term passive acoustic recording. It shows the series of templates to represent the signal of interest and the engine performing various pre-processing steps such as time-frequency normalization and sample rate adjustments. Sounds are convolved with the spectrogram and a decision circuit is used to derive a maximum likelihood threshold value. Output is represented as signal and noise reports.
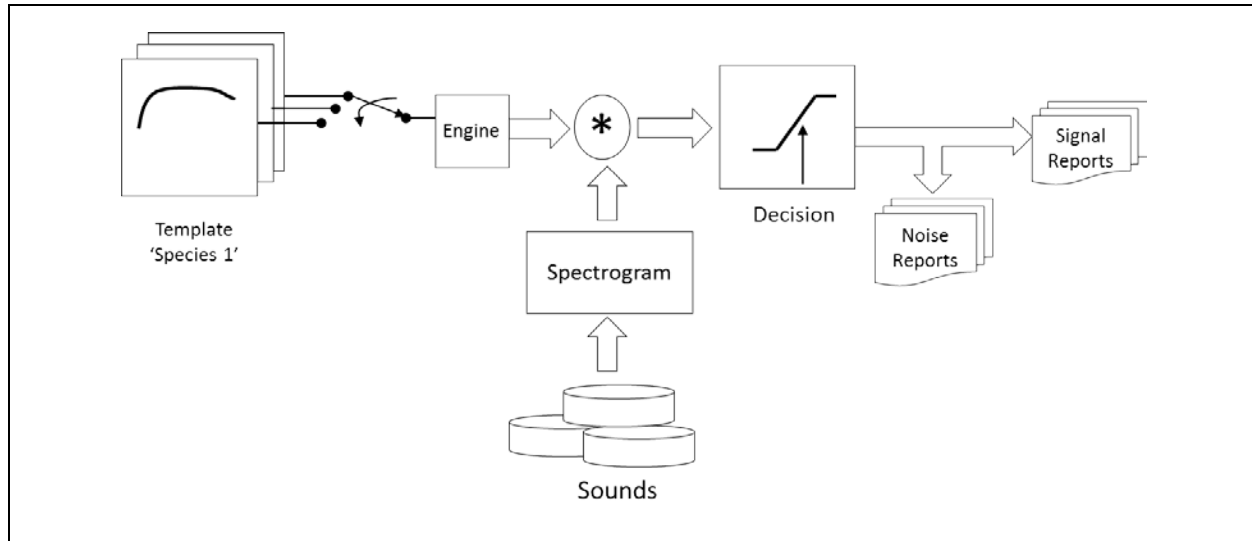
Figure 31. Basic processing for spectrogram match filtering, or template detection.
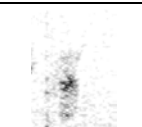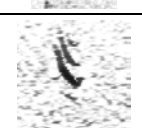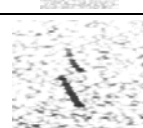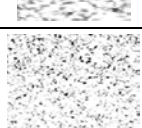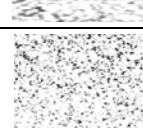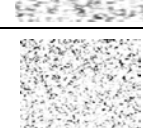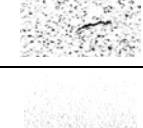
Spectrogram correlation identifies signals of interest. Optimized detector performance will result in minimal errors because the development and refinement of the templates are driven by false negative errors (missed detections) and false positives (false alarms). From this perspective, one would typically design the detection elements (i.e., templates) to match the appropriate application. For example, the end-user might be a human operator who could be bogged down by a high false positive rate or a downstream machine learning processor that could actually learn from high false positives.

Two separate acoustic datasets were used to develop and test templates. First, from the CLO library of known calls (exemplars), candidates were selected that would match the largest number in the entire pool of calls by testing them against one another. Next, their effectiveness was tested by examining their performance on a test dataset known not to have signals of interest. Their effectiveness was also ascertained by examining their performance on a test dataset with a known number of target signals.

Templates are often developed based on different signal to noise (SNR) characteristics. This process uses numerical measurements where the ambient noise levels are calculated and used when selecting templates based on an automatic criterion, minimizing errors across the samples. For this analysis, visual inspection selected representative sounds from a training dataset, building detectors for each species by selecting templates that performed best when tested against a pool of known calls. Table 2 shows sample spectrographs (time-frequency representation) of the type that were used to develop the species-specific templates.

Table 2.

Sample spectrograms and key parameters of flight call exemplars for template development.

Species	Parameters				High	Medium	Low
	Window Size	Window Type	Advance % samples	FFT Size			
American Redstart	256	Hann	0.01	512			
Canada Warbler	256	Hann	0.01	512			
Common Yellowthroat	256	Hann	0.01	512			
Savannah Sparrow	256	Hann	0.01	512			
Swainson's Thrush	256	Hann	0.01	512			
Gray-cheeked Thrush	256	Hann	0.01	512			

Templates for American Redstart, Canada Warbler, Common Yellowthroat, and Savannah Sparrow were created from field recordings collected in Danby, Tompkins Co., New York, between Jul and Oct 2009. Templates for Gray-cheeked Thrush and Swainson's Thrush were created from field recordings collected at the Powdermill Nature Reserve (Powdermill Avian Research Center; associated with publication of Lanzone et al. 2009) and areas surrounding Ligonier and Erie, Pennsylvania, from 2004 to 2009 and Youngstown, Ohio, in 1998.

Table 3 describes the acoustical characteristics of species level events that were detected in the test datasets.

Table 3.

Acoustical characteristics of individual species' calls in datasets used for testing the template detectors.

Template	Number of Calls	Mean Bandwidth (Hz)	Mean Center Frequency (Hz)	Standard Deviation Center Frequency (Hz)	Mean Duration (ms)	Standard Deviation Duration (ms)
American Redstart	2076	NA	NA	NA	NA	NA
Canada Warbler	16	1266	6779	369.8	24	6.2
Common Yellowthroat	317	1700	5704	978.9	29	10.5
Savannah Sparrow	7	1018	7688	329.2	32	24.4
Swainson's Thrush	948	449	2593	169.0	90	27.6
Gray-cheeked Thrush	5	913	3325	406.7	88	17.6

Auto detection performance is measured by comparing templates taken from training data to exemplars in a test set. Training and test samples should be independent, meaning that exemplars should be taken from different acoustic recordings. Measuring performance begins with templates run using a series of thresholds. This approach results in receiver operators' characteristic (ROC) curves (shown in Figure 32). The ROC curves provide a pictorial view of how the probability of detection varies with false alarm probability over a series of thresholds.
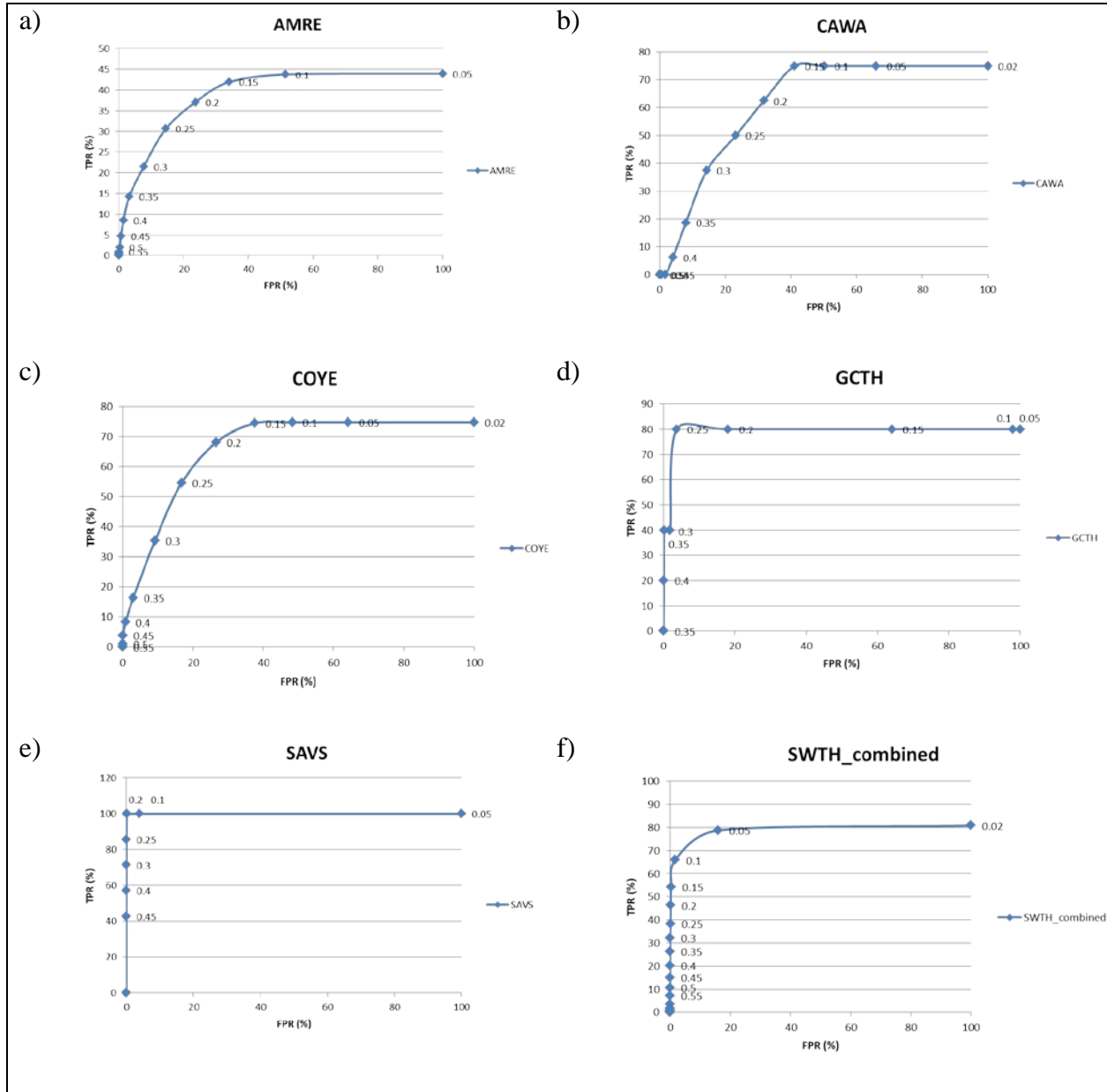
Figure 32. Receiver operator characteristic (ROC) curves.

A high false positive rate might be the single most important measure limiting human operators' ability to browse initial results from an automated detector run. Therefore, a measure of temporal capacity, such as the false positive rate, may be a better indicator and a more realistic view of false positive error. The false alarm rate, given by $\llbracket FA \rrbracket\_rate$, is measured by comparing the detector false alarms over 20-min sections of sound libraries. The $\llbracket FA \rrbracket\_rate$ is calculated by dividing N_fa by the time interval. Three different datasets were selected to measure the false positive performance (Table 4). The three data sets have a combination of ambient sounds, specifically selected as they contain environmental sounds often encountered when monitoring nocturnal migration.

Table 4.

Noise datasets used to test false positive rates.

Ambient Noise Set	Set Name	Description
NorthPeak_Clean	NorthPeak_SWTH	Recorded on Santa Barbara Island, CA; 20 minutes of clean sound recordings, no obvious contamination from biological, environmental or mechanical sources. Sounds clipped from same recording as test file NORTHPK_20101017_174500-02_113300.
Northeast_Insects_Rain	ColumbiaDanbyFHNC	Sound clips recorded from three different locations (Que-Valencia, Columbia; Danby, NY; and Johnson City, NY) to provide heavy insect sounds and light to moderate rain. Recorded with the Wildlife Acoustics NFC package. Sound files: 6.7 minutes from QUE-VALENCIA_2010092_180900, 6.9 minutes from ROSE_20100829_191400, 6.4 minutes from FHNC-PLL-PRR_20101001_002758.
NorthPeak_Birds	SignalPeak	Recorded on Santa Barbara Island, with NFC package, 1 channel recording. Sound file used SIGNALPK_20100816_190700-01 20 minutes of moderate to intense noise from sea birds.

Results of the analysis are presented in graphs that represent false alarm rates versus threshold value (Figure 33). The image shows: (a) SignalPeak recordings with ocean noise and gulls in the background; (b) NorthPeak_SWTH recordings without ocean noise; and (c) ColumbiaDanbyFHNC recordings with high levels of insect and rain noise.
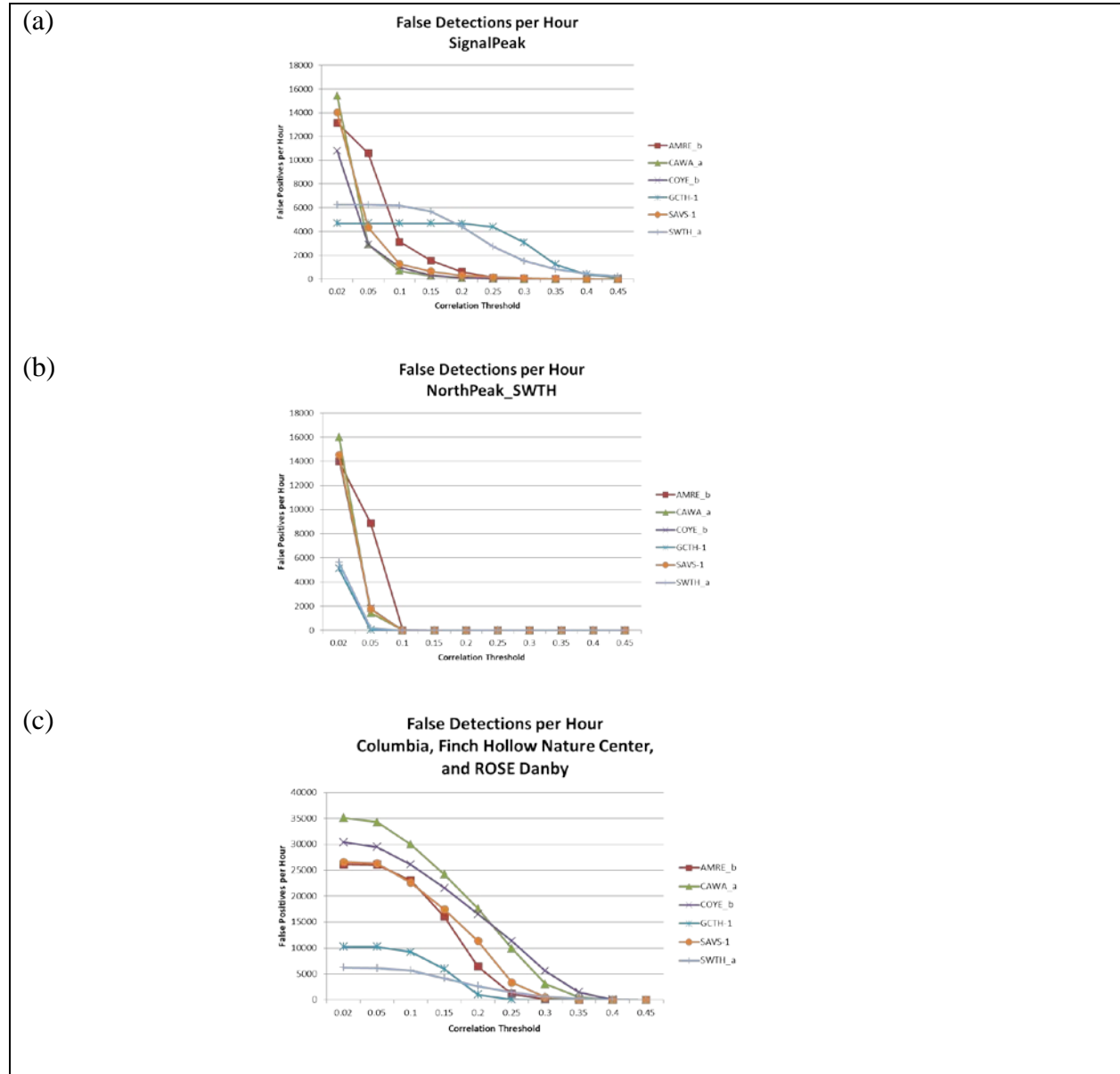
Figure 33. False alarm rates for three ambient sound recordings plotted against data templates
        for six species.

False alarm rates were measured against the detection threshold using three different noise sets.
To understand what a human operator would experience by using a data template for the six
species, a threshold (TH) was selected to be TH = 0.30. With a TH = 0.30, most of the false
alarm rates drop below 5,000 events per hour. Although this is still a significant number of
alarms, this implies that the detection probability would be no lower than 0.20 (AMRE) and
around 0.35 for SWTH and COYE.

Running long-term detections with those thresholds, detection performance and error rates are
summarized in Table 5 through Table 7. The detection probability *P(D)* is determined by

comparing the number of samples successfully identified by the templates N_{det} divided by the total that were labeled by human operators N_{Pos}, also called total positives. The percent missed, or false negatives *M(D)*, is the total number missed N_{miss} divided by the total positives N_{Pos}.

Table 5.

Species-specific template performance showing the number of possible targets (N$_{Pos}$), threshold settings, detection probability (P(D)), and false negative rate (M(D)).

Template	N_{Pos}	Threshold	P(D)	M(D)
American Redstart	2076	0.3	0.215	0.785
Canada Warbler	16	0.3	0.375	0.625
Common Yellowthroat	317	0.3	0.353	0.647
Savannah Sparrow	7	0.3	0.714	0.286
Swainson's Thrush	948	0.3	0.322	0.678
Gray-cheeked Thrush	5	0.3	0.400	0.600

A signal detector's ability to reject noise depends on many factors (Urick 1996); moreover, noise rejection can be measured in many ways (Urazghildiiev and Clark 2007b; Lampert and O'Keefe 2011). For this study, events tagged by the detector, but not hand labeled, were considered false alarm reports, or false positives. Therefore, the false positives are those events that are not successfully identified by the detector, and the total false positives are N_fa. The percentage of false positives is assigned FA(D) and calculated by N_fa divided by the total number of negatives N_Neg. The results are shown in Table 6.

Table 6.

Species-specific template performance showing threshold settings, total false negatives (N$_{Neg}$), and percentage of false positives (FA(D)).

Template	Threshold	N_{Neg}	FA(D)
American Redstart	0.3	3343	0.0769
Canada Warbler	0.3	5778	0.1440
Common Yellowthroat	0.3	4592	0.0919
Savannah Sparrow	0.3	4705	0.0002
Swainson's Thrush	0.3	948	0.0000
Gray-cheeked Thrush	0.3	815	0.0184

In Table 6, the total number of negatives N_{Neg} is determined by allowing the detector to output the total observed number of events at the lowest possible threshold. Hourly rates for false positives are given in Table 7.

Table 7.

Species-specific template performance showing false positive rate for three sound recordings with varying ambient noise.

Template	Data Set FA_{rate} (calls per hour)		
	NorthPeak_Clean	Northeast_Insects_Rain	NorthPeak_Birds
American Redstart	0	435	27
Canada Warbler	0	3183	12
Common Yellowthroat	0	5605	0
Savannah Sparrow	0	524	75
Swainson's Thrush	0	5149	1512
Gray-cheeked Thrush	0	213	3078

Multiclass problems would require running all the templates, whereby the classification performance is measured using a confusion matrix as described in Duda et al. (2001). Diagonal elements of the matrix correspond to template selection where the actual class does not match the estimated one,

$$P(\omega_k|x_j) \ where \ k \neq j. \qquad (Eq. \ 4)$$

Equation (4) represents elements on the off-diagonal of the confusion matrix, perfect classification elements are zero. The diagonal values are determined by (Eq. 5),

$$P(\omega_k|x_j) \ where \ k = j. \qquad (Eq. \ 5)$$

Equation (5) states that the diagonal elements are exact matches to the template class $T_i(t, f)$.

To demonstrate the benefits of parallel computing technology, auto-detection-classification and noise analyses were run using the SEDNA toolbox. Results were compared using a series of processing environments that included a single desktop computer, a 12-node computer running serial (non-parallel) MATLAB software, and a 12-node computer running parallel MATLAB.

Generally speaking, the algorithm developers create non-optimized software modules. The first step is to have an experienced consultant optimize the software. Once optimized, the code executes faster and more efficiently. Optimized versions were used on the high performance server (HPC 12 Node Machine). To measure the performance improvement by HPC enhancements to the SEDNA code, benchmarking code was built into the system. The code was

used to measure the time to process the files and the size of the files used as output. In addition, advantage was taken of MATLAB's profiler code, which allows the programmer to see which parts of the code are the bottlenecks in the process. Sound files are generally stored as multi-channel data files. This is good from a data organization perspective and is also useful for other software that uses multi-channel data (e.g., to geo-locate sound sources using time-delay information across the sensors). For storing the output, it becomes better to store the data as single sensor files of a day's duration, as this is the most practical period for running analysis and visualization tools. The splitting of sound by channels allows for the parallelizing of the process by distributing the computing task across channels to take advantage of multi-core processing and parallel solutions by splitting the process across servers/computer clusters. The parallel processing for SEDNA is shown in Figure 34.
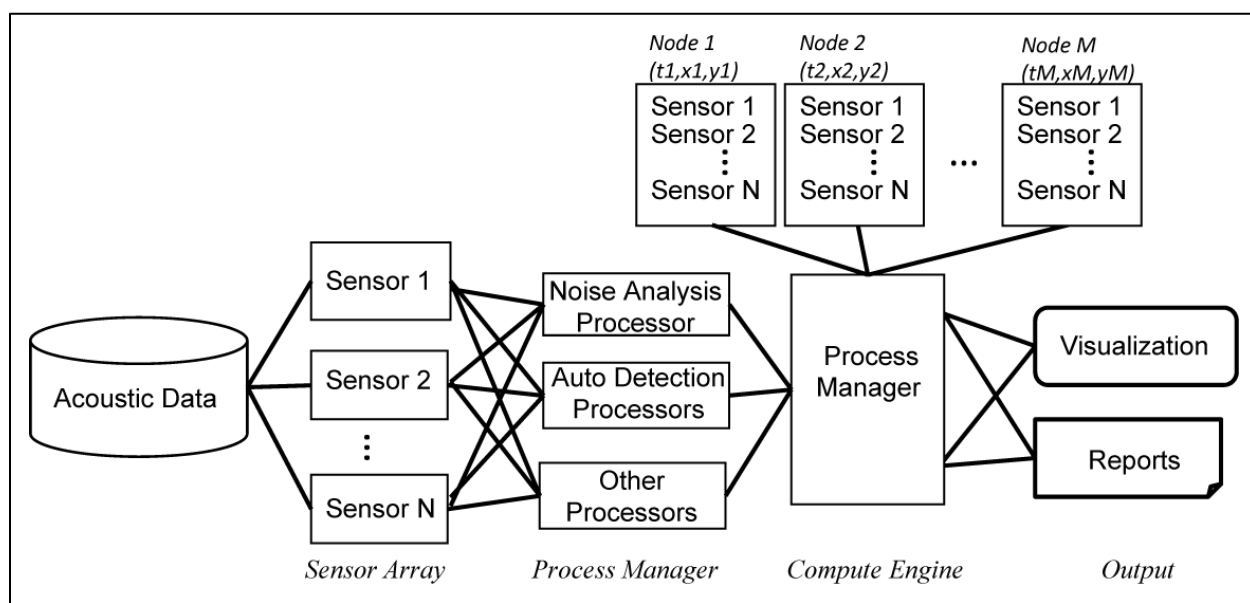
Figure 34. Computing architecture diagram showing high level processing for data taken from acoustic arrays and processed using parallel processing engine. The process manager uses high performance methods for optimizing processing time.

The SEDNA noise analyzer processes small sections of data; these are shown as Nodes in Figure 35. If each chunk were read separately from disk, the overhead for disk I/O would limit the throughput of the analyzer. To avoid this, data files are mapped into RAM so that reading each successive data chunk after reading the first essentially becomes a memory access task.

To efficiently inspect acoustic events, a technique called "Montage" has been adopted in the SEDNA tool set. Montage technology was first widely used in MRI imaging (Atlas 2011; Mathworks 2011). The basic view of the montage tool is shown in Figure 35. A human operator can scroll through the events using the bottom slider and change the labels at the bottom of each exemplar. The tool was developed in MATLAB, which makes it easy to incorporate custom utilities, such as sound exporting and feature views.
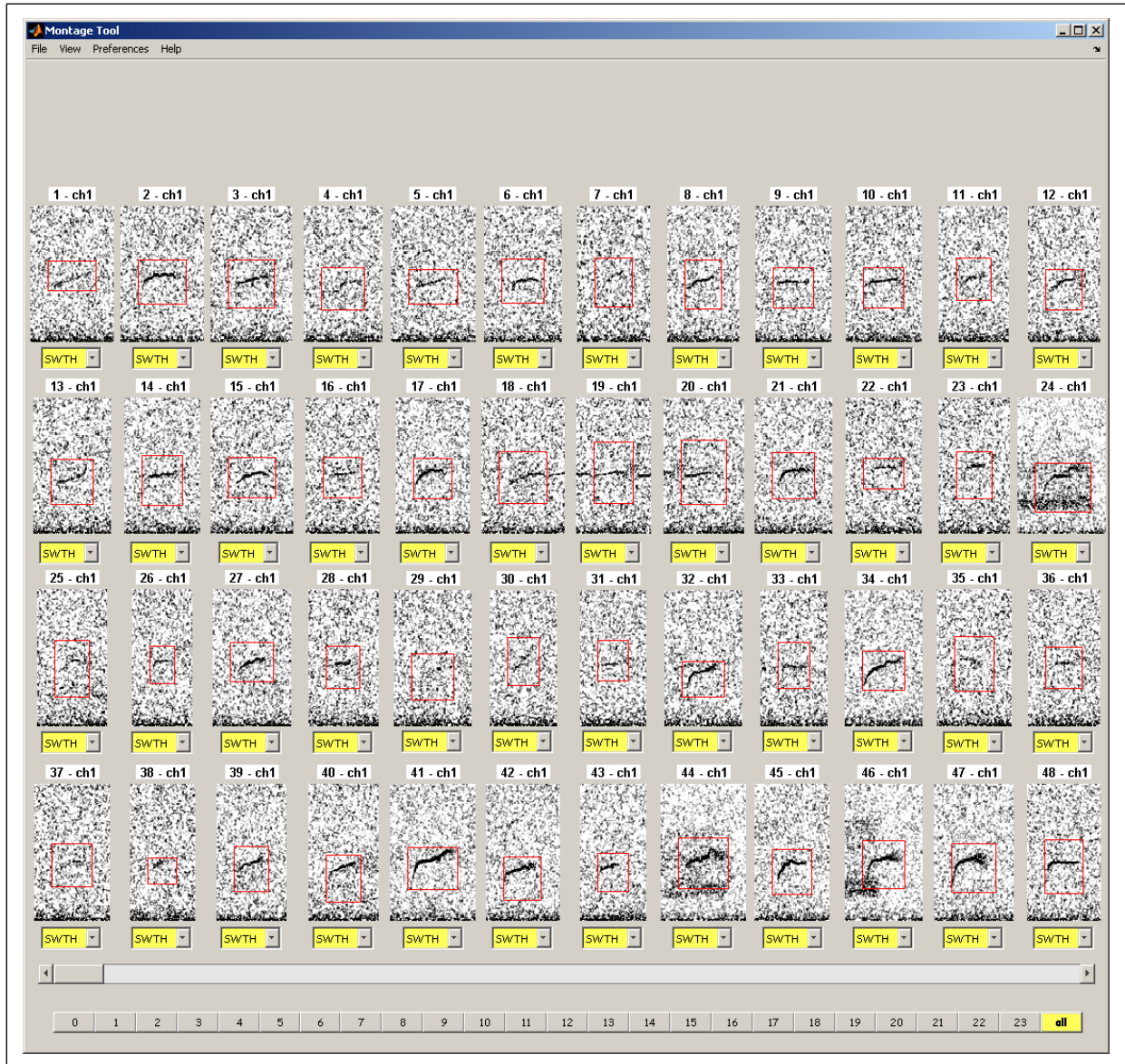
Figure 35. The SEDNA Montage viewer.

The figure shows several compact versions of Swainson's Thrush calls. Beneath each call, a label field provides a location to allow the human operator to change the call label. In environments that cause higher than normal detection errors, many noisy events would be presented as positive call types. The goal for a tool like montage is to allow the human operator to visualize many signals at one time, making browsing more efficient.

The flight calls of six different species of nocturnally migrating birds were examined and a data template detector was applied to each species. The results were mixed, showing high levels of false positives for moderate to high detection thresholds. Realistic false positive rates should exhibit approximately 100 detections/hour; however, the rates reported here were 1,000/hour and higher with some rates of 20,000/hour. This type of result is not unexpected for two reasons:

first, data template construction was done using a relatively small number of samples; second, this was the first phase of an iterative and lengthy process. It is clear that the data template provides for a fast and efficient algorithm when considering high throughput applications, and as an initial test for the detection-classification system it performed within expectations.

The SEDNA toolset was also applied. SEDNA, based on MATLAB tools, serves as a toolbox for creating applications that can run using high performance computing environments. SEDNA uses the fast prototyping environment that MATLAB offers, allowing the research program to customize tools quickly and efficiently to meet the needs of the project, including noise analysis.

2.2.3 Ultrasound Software

Due to the large amount of bat acoustic monitoring that Normandeau conducts, all the necessary tools were already in place for analysis of ultrasonic data with the ATOM system. Since 2008, Normandeau has collected more than 52,000 hrs of bat acoustic data, which includes over 124 million bat calls. Our analysts have identified over 2.8 million calls using a combination of a custom interface (ReBAT.com) and SonoBat™ (SonoBat 3.0, Arcata, CA) acoustic analysis software. The ReBAT.com data management interface allows for the automated, unsupervised ingestion of this data stream (>124 million files to date) as well as maintenance of the data. The data are ingested into a SQL database that stores the records as well as the results of the data analysis. Once ingested, all ultrasonic sound files are run through SCAN'R© (Binary Acoustic Technology, Tucson, AZ) filtering software to remove noise files. Additionally, ReBAT.com provides initial classification of calls as "bat" or "not bat." This eliminates over 80% of the remaining noise (not bat) files while discarding <1% of the bat files.

ReBAT.com organizes sound files by day of recording and allows analysts to view the spectrograms of each individual file (Figure 36). The spectrograms on ReBAT.com also include "crosshairs" that can be moved over each call to gain information when classifying calls to species; namely, minimum frequency. Bat passes (files) are then assigned to a species or species group based on comparison to reference libraries of species-specific bat calls. When more information is needed to make a classification decision, files are viewed within SonoBat. SonoBat provides a variety of parameters that can be used for manual call identification and can also perform automated call identification analysis (Figure 37). Once a file has been identified as a particular species or species group, the result is stored on ReBAT.com and all analysis information can be downloaded to a spreadsheet.
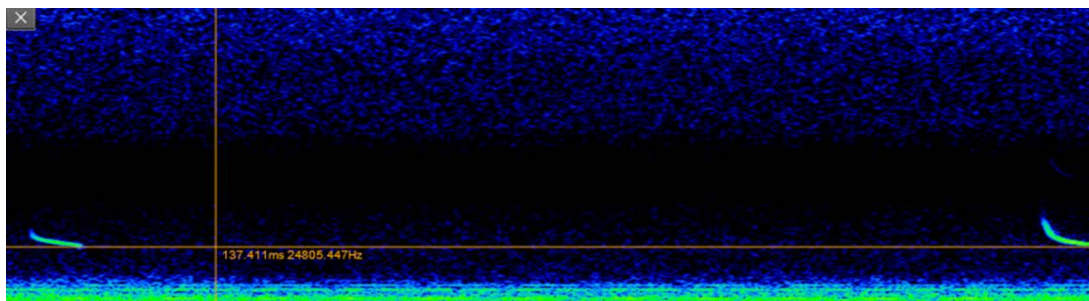
Figure 36. Part of a spectrogram of bat calls displayed in ReBAT.com. Notice the crosshairs that indicate the number of milliseconds since the beginning of the file as well as the minimum frequency (kHz).
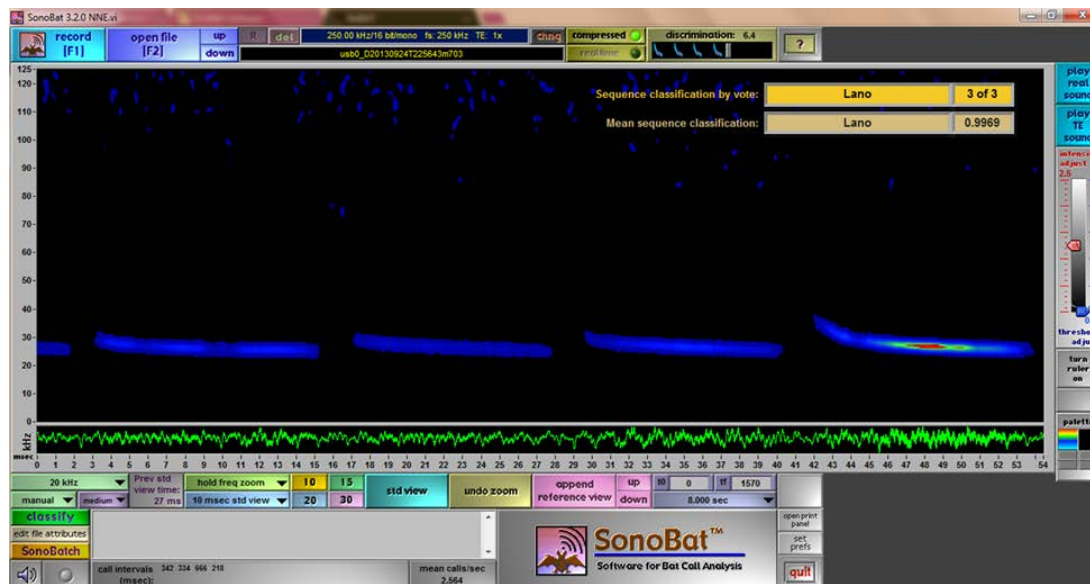
Figure 37. Example SonoBat display of a bat pass with the automated species
classification displayed.

3 Results from the UD Lewes Deployment

3.1 Thermographic

Thermographic data were collected on 30 days during the ATOM system test deployment at the
UD Lewes' coastal wind turbine during Jul and Aug 2011. ATOM's thermographic subsystem
recorded two channels of thermographic video, gathering 410.9 hours of data.

The software for thermographic data analysis, referred to as AW (see Thermographic Software),
was installed on two ATOM-dedicated main computers in Normandeau's image analysis
laboratory during summer 2012. These were used to analyze all thermographic data collected
during ATOM deployments beginning with the UD Lewes deployment data. Tracks with targets
identified to the extent possible were reported with associated date, time, altitude, direction, and
velocity metadata.

Bat tracks were identified as such by analysis of flight patterns in AW review. Flight trajectories
of foraging bats deviate rapidly and unpredictably from a straight line, whereas the flight paths of
birds tend to be straighter (Kunz et al. 2007). It has also been suggested that some bats may use
relatively straight flight trajectories while migrating, and other bats may have overall tendencies
toward straighter flight trajectories (Ghose et al. 2006; Kunz et al. 2007); therefore, straight
flight tracks were classified as bird/bat if no other evidence was available for distinguishing birds
from bats. In some cases with low flying animals, the shape of the animal was distinctive enough
to confidently identify whether it was a bird or a bat (see Figure 38). The four tracks classified as
"unknown" were small moving spots that may have been meteors, satellites, or very high flying
animals. The movement of clouds produced tracks during the four days of video processed by the
automated target detector and were manually reviewed.

Figure 38. Thermographic image of a bat (species identity unknown) recorded during the ATOM system test deployment at UD Lewes (Jul–Aug 2011). This image shows an example in which the distinction between birds and bats can be made confidently based on the animal's shape in the image.

Of the 15 thermographic bat detections discovered in the Delaware analysis to date, two occurred at the same moment as ultrasonic bat detections reported in the previous section and are considered matches (i.e., same individual bat recorded on both ultrasound and thermographic sensors). The identity of these bats can be unambiguously determined from the ultrasound recordings as Eastern Red Bat (*Lasiurus borealis;* LABO) and Big Brown Bat (*Eptesicus fuscus;* EPFU). A thermographic image of one of these bats along with tracklines showing their flight trajectories is shown in Figure 39.
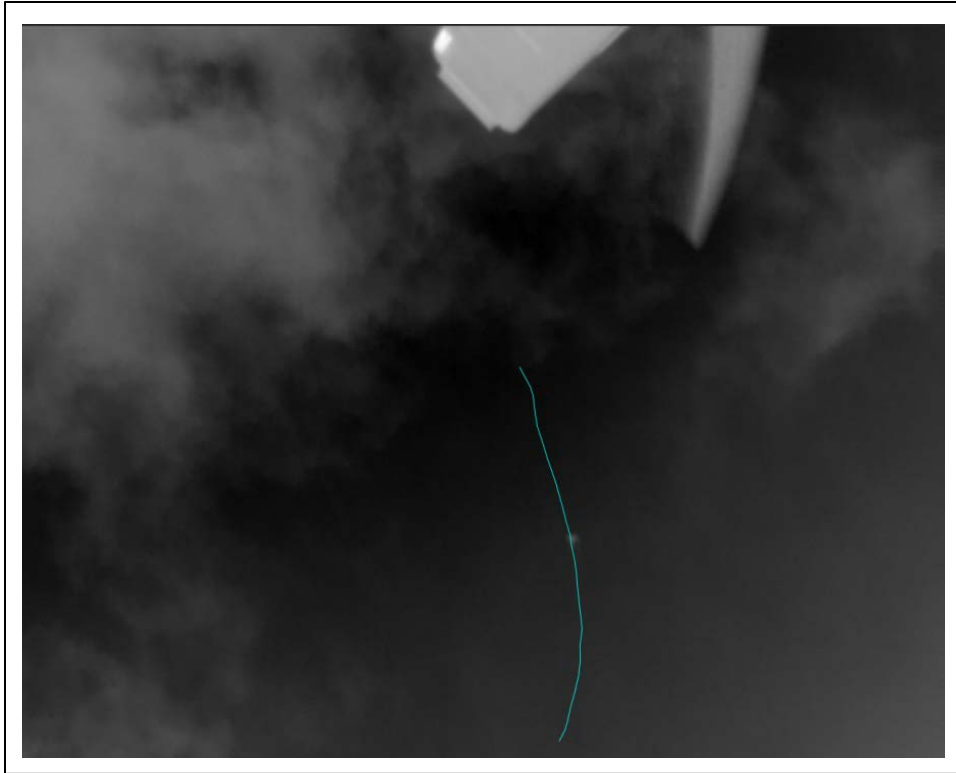
Figure 39. Eastern Red Bat (*Lasiurus borealis* [LABO]) recorded 14 Aug
2011 at 20:56:51 during the ATOM test deployment at UD
Lewes.

In the ultrasound-thermographic match for LABO, the thermographic target was recorded at a
distance of 42.35 m from the camera and a mean bearing (flight direction) of 6.73 NNE. The UD
Lewes camera was deployed 1 m from the ground, giving a total altitude for this individual of
43.35m.

In the ultrasound-thermographic match for EPFU, the thermographic target was recorded at a
distance of 40.87 m from the camera (an altitude of 41.87 m); a mean bearing (flight direction)
of 12.02 NNE and a velocity of 23.075 km per hour.

A full review of flying vertebrate thermographic detections to date with their associated flight
altitudes, bearing, and velocity are contained in Table 8 (bird/bats) and Table 9 (bats). Some
calculations (e.g., flight altitude, velocity) for some of these animals are not available because
animals were not recorded sufficiently in both cameras or because of software functionality
limitations at that time. Flight altitudes were calculated by adding 1 m to the distance from
camera measurement to account for the detector's position off the ground. Distance from camera
is calculated by the ATOM computer by triangulating the signals from the two cameras for each
target.

Table 8.

Complete data on flying vertebrate (either bird or bat) passes recorded on four days by the thermographic video cameras during the ATOM test deployment at UD Lewes (Jul and Aug 2011).

Date (YYYY-MM-DD)	Start Time	Flight Altitude (m)	Mean Bearing	Velocity (km/hr)
2011-08-13	05:26:51.891	Data Not Available	25.07 NNE	Data Not Available
2011-08-13	10:09:42.561	Data Not Available	12.61 NNE	Data Not Available
2011-08-13	10:46:12.198	Data Not Available	14.23 NNE	Data Not Available
2011-08-13	11:07:19.495	Data Not Available	44.66 NNE	Data Not Available
2011-08-13	19:42:51.759	7.857	13.18 NNE	3.762
2011-08-13	21:36:32.363	Data Not Available	86.71 ENE	Data Not Available
2011-08-13	21:56:22.792	Data Not Available	23.55 NNE	Data Not Available
2011-08-13	22:17:30.924	49.511	35.79 NNE	33.104
2011-08-14	01:53:35.495	49.106	57.13 ENE	26.978
2011-08-14	20:53:41.165	Data Not Available	41.39 NNE	Data Not Available
2011-08-14	22:43:09.132	Data Not Available	71.09 ENE	Data Not Available
2011-08-15	01:49:25.429	Data Not Available	17.94 NNE	Data Not Available

Table 9.

Complete data on bat passes recorded on four days by the thermographic video cameras during the ATOM test deployment at UD Lewes (Jul and Aug 2011).

Date (YYYY-MM-DD)	Start Time	Flight Altitude (m)	Mean Bearing	Velocity (km/hr)
2011-08-13	20:59:28.066	Data Not Available	52.79 ENE	Data Not Available
2011-08-13	21:01:04.561	41.87	12.02 NNE	23.075
2011-08-13	21:11:51.759	54.365	18.26 NNE	29.149
2011-08-13	21:56:31.198	Data Not Available	79.17 ENE	Data Not Available
2011-08-13	22:14:19.231	Data Not Available	40.48 NNE	Data Not Available
2011-08-13	23:04:53.330	17.951	40.78 NNE	11.684
2011-08-13	23:57:31.330	44.021	19.95 NNE	24.411
2011-08-14	01:53:39.792	Data Not Available	37.19 NNE	Data Not Available

Date (YYYY-MM-DD)	Start Time	Flight Altitude (m)	Mean Bearing	Velocity (km/hr)
2011-08-14	01:53:41.231	Data Not Available	9.41 NNE	Data Not Available
2011-08-14	01:53:51.429	44.207	1.74 NNE	25.246
2011-08-14	20:56:51.429	43.351	6.73 NNE	19.622
2011-08-15	01:20:09.330	73.297	5.36 NNE	27.619
2011-08-15	02:09:30.561	Data Not Available	6.32 NNE	Data Not Available
2011-08-15	02:31:32.363	Data Not Available	40.32 NNE	Data Not Available
2011-08-15	02:59:31.759	Data Not Available	40.32 NNE	Data Not Available

Thermographic signal from wind turbines is not likely to significantly impact the detection and classification of bird and bat thermal images. Although turbine rotors move, resulting in a potential source of false positives in thermographic tracking algorithms intended to detect flying animals, the movements are stereotyped in such a way as to enable the development of simple algorithmic signal filtration mechanisms to distinguish the thermographic signal of spinning blades from that of flying wildlife. The automated target detection algorithm currently being used in the ATOM system already possesses this functionality, as it did not register the movement of wind turbine rotor blades as potential animal flight tracks during the UD Lewes deployment.

3.2 Ultrasound

Bat ultrasound acoustic data were collected on 10 nights during the ATOM system test deployment at UD Lewes' coastal wind turbine (19–22 Jul 2011; 24–25 Jul 2011; 13–15 Aug 2011). The ultrasonic bat detector was installed on a tripod approximately 1.2 m above ground level. Analysis of recorded echolocation calls was performed on all operational detector nights using SCAN'R™ (Binary Acoustic Technology, Tucson, AZ) filtering software to remove noise files. Call files (duration = 1.7 seconds) were used to describe a bat pass. Call files classified as bat were further analyzed using SonoBat™ (SonoBat 2.2, Arcata, CA) acoustic analysis software and were assigned to a species or species group based on comparison to reference libraries of species-specific bat calls. Calls are stored, viewed, and analyzed in an internal relational database referred to as ReBAT.com.

Bat activity at wind facilities is typically detected using only ultrasound sensors and is reported as average bat passes per detector-night (ABPDN). Bat passes, rather than number of individual bats, are reported because a single bat may produce more than one recorded bat pass during a night or over a period of nights. Thus bat passes are used as an indicator of activity. The ultimate goal of the ATOM system, with respect to bat analysis, is to combine information from thermographic and ultrasound sensors to produce more realistic estimates of actual numbers of bats passing through rotor swept altitudes, rather than simply relying on ABPDN as an indicator of bat activity. As a first step, data from the ultrasound detector were analyzed alone as would be done in a conventional analysis of bat activity.

Previous studies (Fiedler 2004; Kerns et al. 2005; Arnett et al. 2006; Barclay et al. 2007) have indicated that bat activity and/or bat mortality may be correlated with atmospheric conditions. If these relationships are robust, they may provide an avenue for managing bat mortality at operational wind facilities.

To understand how atmospheric variables can affect bat activity and potential risk of collisions with wind turbines, the number of bat passes from Eastern Red Bats, Silver-haired Bats, and bat passes identified as belonging to the Big Brown Bat/Silver-haired Bat species group collected from the ultrasonic detector was modeled as a function of five atmospheric variables (Table 10). This approach allowed for determination of the atmospheric variables that were most associated with bat activity detected during the pilot study. An information-theoretic approach to model building was used, which involves constructing models *a priori* based on known biological information and before any data analysis is done (Burnham and Anderson 2002). Constructing models using this approach reduces the occurrence of spurious results from models that are biologically supported.

A Poisson regression was used to model the number of bat passes as a function of atmospheric variables. This type of regression is useful when modeling count data because count data (e.g., bat passes) are often Poisson-distributed (Dalgaard 2008). The response variable was the number of bat passes of each species totaled for a given night during 2011. Five atmospheric variables were chosen based on their likely influence on bat activity (Table 10). Variables were chosen based on known relationships from the literature and expert opinion. All variables were standardized using Z-scores prior to analysis to a mean of 0 and a standard deviation of 1. In addition to modeling atmospheric variables, a null model for each species was run, which only included the detector variable and assumes that atmospheric conditions have no influence. The null model served as a baseline so that the differences in likelihood of the other models that include atmospheric variables could be examined. Poisson regression was performed in R using the General Linear Model function (R Development Core Team 2012).

Table 10.

Variables used in modeling approach examining bat activity in relation to atmospheric patterns from ATOM system test deployment at UD Lewes (Jul–Aug 2011).

Variable Abbreviation	Description
Wind Speed	Average Daily Wind Speed
AverageTemp	Average Daily Temperature
Pressure	Average Daily Barometric Pressure
MaxWind	Maximum Daily Wind Speed
Precipitation	Total precipitation from a 24-hr period

Models were evaluated by comparing the Akaike Information Criterion (AIC) values and Akaike weights among the other models in each candidate set. These metrics assess the likelihood of the model relative to other models in the candidate set. Comparisons of AIC values and model

weights are only valid within a given suite of models for a specific season and species. Comparisons cannot be done across seasons or species (Burnham and Anderson 2002). Models with lower AIC values (those closer to 0) indicate a model that provides the most parsimonious explanation.

From the 10 nights of data collected during the pilot study, 641 bat passes were detected and identified for an ABPDN index of 64.1. Eight species or species groups were identified from the acoustic data (Table 12). Eastern Red Bats (LABO) were detected most often during acoustic surveys, followed by bats belonging to the Big Brown Bat/Silver-haired Bat species group (EPFU_LANO) (Figure 40). Overall bat activity was highest within the first two hours following sunset, after which activity declined and was low and variable for the remainder of the night (Figure 41). During the 10 nights of monitoring, Big Brown Bat and Eastern Red Bat activity was highest on 24 Jul 2011, with Eastern Red Bat activity remaining high during the three nights of monitoring in Aug (Figure 42).

Results from the atmospheric data indicated different species were influenced by different atmospheric conditions. For Eastern Red Bats, barometric pressure alone was the best predictor of activity, with activity increasing with increasing barometric pressure. The model that best predicted Silver-haired Bat activity was Temperature + Maximum wind speed. Silver-haired Bat activity decreased with increasing temperature and increased with increasing wind speed. Bat activity identified as belonging to the Big Brown Bat/Silver-haired Bat species group was most influenced by the Temperature + Wind Speed model, with activity decreasing with increasing temperature, and increasing with increasing wind speed. For reference, the range of values for each weather variable under which these models were developed can be seen in Table 11.

Table 11.

Range of values for each weather variable.

	Wind Speed (m/s)	Maximum Wind Speed (m/s)	Temperature (^{o}C)	Adjusted Pressure (mmHg)	Precipitation (mm)
Range	0.5–2.1	2–4.2	21.9–30.4	753.11–762.51	0.0–6.1

Table 12.

Bat species* detected during ATOM system test deployment at UD Lewes (Jul–Aug 2011).

Common Name	Scientific Name	Abbreviation
Big Brown Bat	*Eptesicus fuscus*	EPFU
Big Brown Bat/Silver-haired Bat	*Eptesicus fuscus_Lasionycteris noctivagans* species group	EPFU_LANO
Eastern Red Bat	*Lasiurus borealis*	LABO
Eastern Red Bat/Tri-colored Bat	*Lasiurus borealis_Perimyotis subflavus* species group	LABO_PESU
Hoary Bat	*Lasiurus cinereus*	LACI
Hoary Bat/Silver-haired Bat	*Lasiurus cinereus_Lasionycteris noctivagans* species group	LACI_LANO

Common Name	Scientific Name	Abbreviation
Silver-haired Bat	*Lasionycteris noctivagans*	LANO
Tri-colored Bat	*Perimyotis subflavus*	PESU
Unknown	Unable to identify to species or species group	UNKN

* Two species are listed together as a "species group" when their calls could not be confidently distinguished.
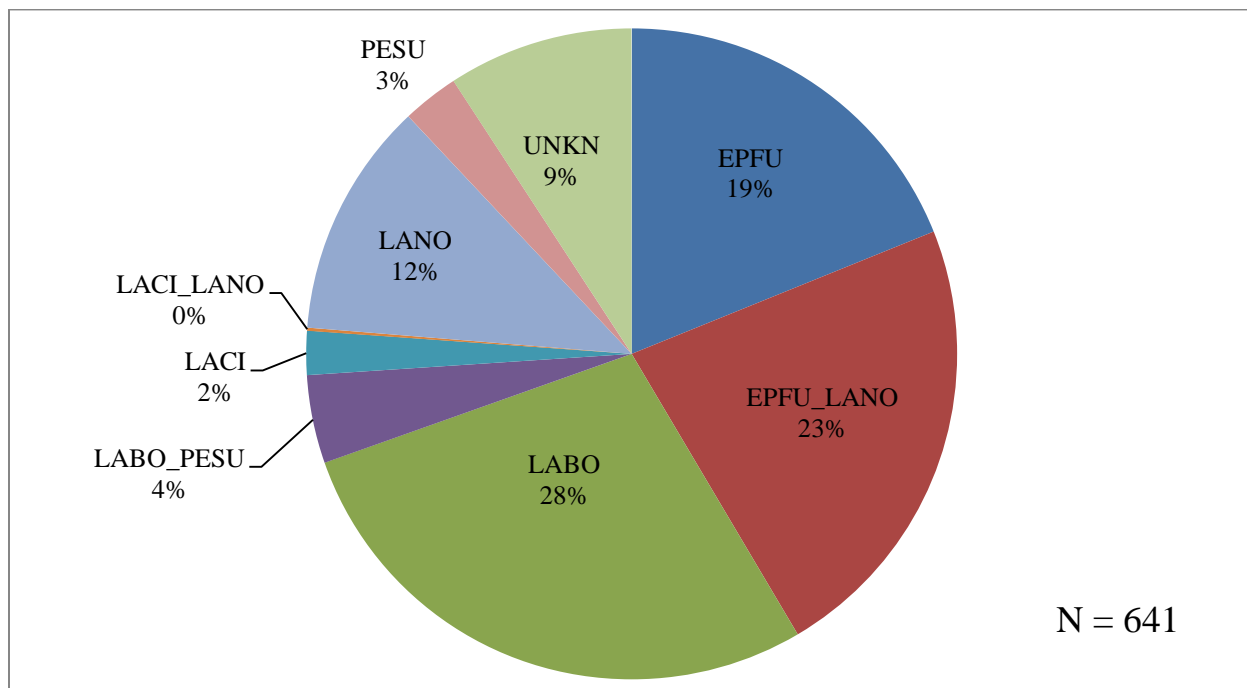
Figure 40. Bat species detected during ATOM system test deployment at UD Lewes (Jul–Aug 2011). See Table 12 for abbreviations of bat taxa.
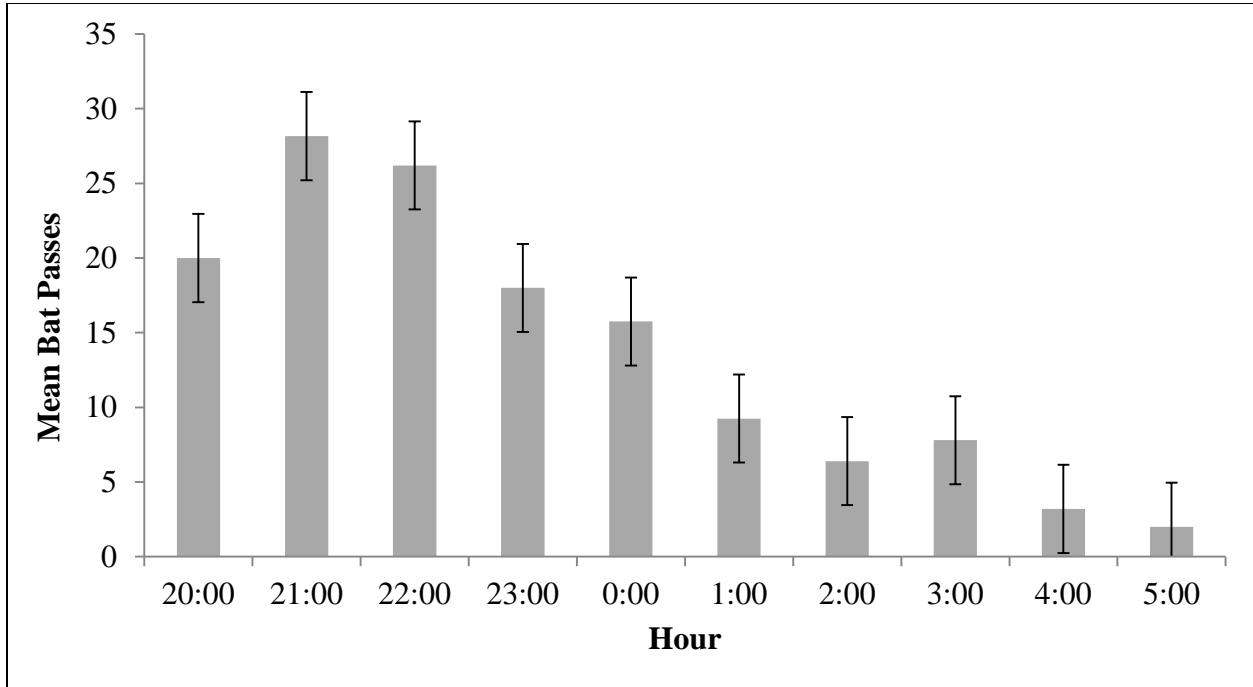
Figure 41. Mean bat passes (± standard error) per hour recorded during ATOM system test deployment at UD Lewes (Jul–Aug 2011). All bat species and all detector nights are lumped.
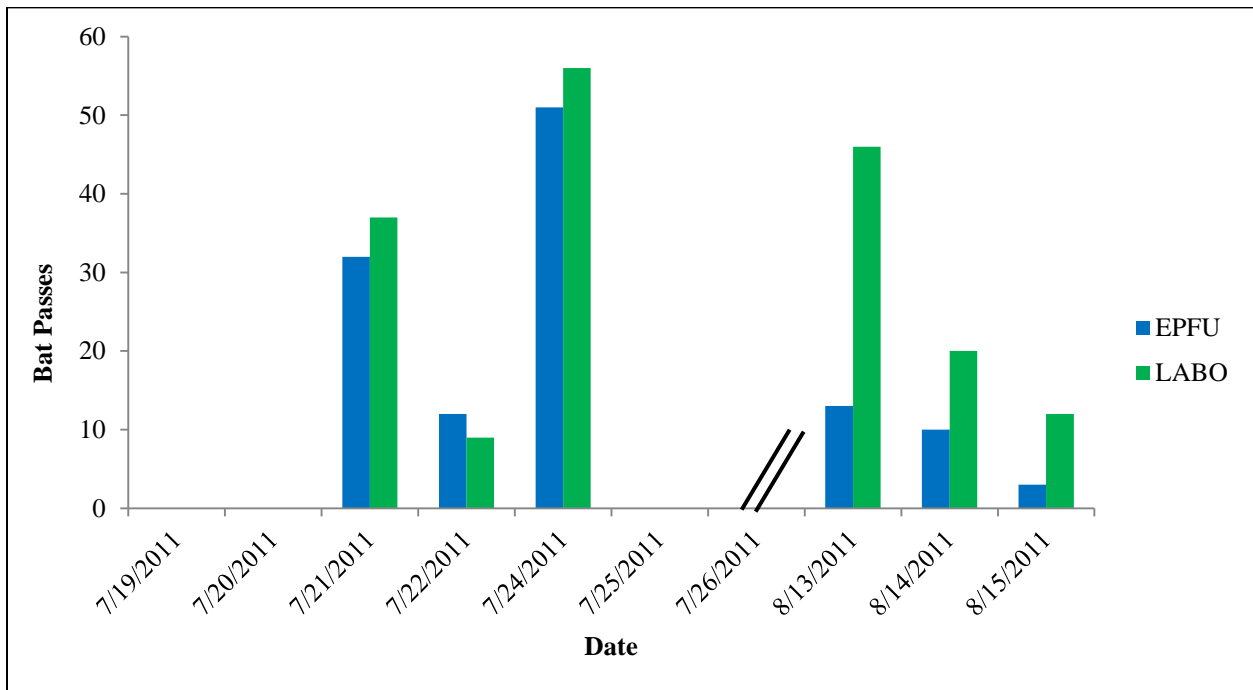
Figure 42. Bat passes per hour of the two most abundant bat species, Big Brown Bat (EPFU) and Eastern Red Bat (LABO), recorded during each night of the ATOM system test deployment at UD Lewes (Jul–Aug 2011).

The ultrasonic microphone on the ATOM system was able to successfully record bat echolocation calls over multiple nights and in various weather conditions and did not appear to be significantly hindered by the noise of the turbine.

ATOM should be able to integrate conventional ultrasound analysis with thermographic analysis to convert ABPDN data into more realistic estimates of the numbers of bats passing through rotor swept altitudes per night. Such translation will use data on the directionality and position of bat passes over the thermographic sensors to infer the extent to which the observed numbers of ultrasound acoustic bat passes are likely to have been caused by smaller numbers of bats making repeated passes or by single continuous streams of bats, generally making one acoustic bat "pass" per bat.

Using sound samples gathered during the UD Lewes deployment, background noise sources and bird call signals within audible and near-audible frequencies were analyzed. The frequency with the loudest noise signal came from the turbine rotor and was in the infrasound range, 0.56 Hz. Bird or bat calls are at a far lower frequency and so rotor noise can be easily filtered. Figure 43 shows a strong light blue horizontal line above the middle of the image which represents turbine noise. The strong green vertical lines represent electrical "pops" that are probably caused by wind blowing across the microphone. These noise sources require ATOM system software to filter.
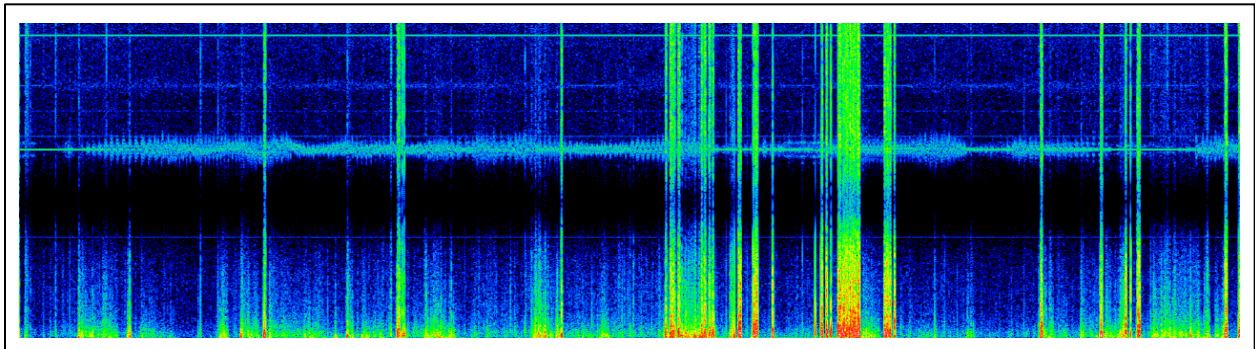
Figure 43. An ultrasound spectrogram from a microphone deployed on the nacelle of the UD Lewes wind turbine (Jul 2011).

3.3 Acoustic

The UD Lewes deployment revealed that the audible acoustic sensor and control system developed by IATech for ATOM was not likely to effectively serve the purpose of marine *in situ* deployments at wind turbines or other marine structures, primarily because of insufficient reliability, robustness, and inappropriate microphone array configuration (spacing too wide, arranged linearly). Acoustic data gathered during the UD Lewes deployment was not otherwise analyzed as the detection and identification software was under development by CLO.

4 Changes to System

It was determined that a complete redesign of the audible acoustic sensor system was necessary, entailing the development of a new audible acoustic sensor array and new control software for the audible acoustic subsystem of ATOM.

4.1 Audio System Changes

The sonic audio system underwent significant configuration changes following the initial system deployment. The Brüel & Kjaer 4198 Outdoor weatherproof microphones (B&K 4198) used for the initial deployment were replaced with arrays of Bolide Technology Group BT-MP8087 microphones. This change was made because the preferred array configuration required inter-microphone spacing of 2 cm or less. The size and shape of the B&K 4198 microphones made this spacing impossible to achieve. The BT-MP8087 microphones were selected for their compact form and integrated preamplifiers, which simplified integration with the existing National Instruments CompactRIO audio computer (cRIO). Figure 44 shows two of the three-microphone arrays that were deployed with the FPSLT ATOM system. The pen in the left image helps demonstrate the size of the new array.

The microphone change also allowed us to remove the large preamplifier boxes that interfaced with the B&K 4198 microphones. These preamplifier boxes had been housed along with a power supply and the cRIO inside of a separate stainless steel enclosure. This reduction in parts allowed repackaging of the cRIO inside the main control box and elimination of the separate external box for the audio system.

A Wildlife Acoustics SongMeter device (SM2) was also initially deployed. However, this was not robust enough to withstand the conditions on FPSLT and was removed once it had ceased to function.

To accommodate the new audible acoustic sensors and eliminate 5 sec/min recording gaps that had been incorporated into the initial acoustic system control software, a redesign of the acoustic system control software was initiated, which entailed completely rewriting the software.

The control computer software that interfaces with the cRIO was updated to automatically convert audio files to the preferred CAF format before storing them on the control computer and to add file records to the system database. The system database schema was updated to allow tracking of all types of media files in use on the system. The audio and video recording processes were updated to detect available storage space and to pause recording when available storage space ran low. This change was made to ensure a smooth recovery process and resumption of recording when the storage system failed or filled up.

Figure 44. Images of the revised microphone array for the FPSLT deployment.

4.2 Control Box Changes

While the system was deployed at UD Lewes, work progressed on a camera lens shutter and wiper system fitted to a second control box. When this system was completed in Sep 2011, the internal components from the original control box were transferred to the new control box. In addition to the shutter/wiper system, the internal layout of the control box was modified to accommodate the cRIO and a set of audio connectors were added to the exterior of the control box (Figure 45). A pair of small 5V power supplies was also added to allow the power control board to be fully powered independently of the control computer power supply. This change was made in conjunction with some software changes to prevent a problem discovered during the UD Lewes deployment wherein the system could be powered down remotely but could not be powered back up without a site visit.
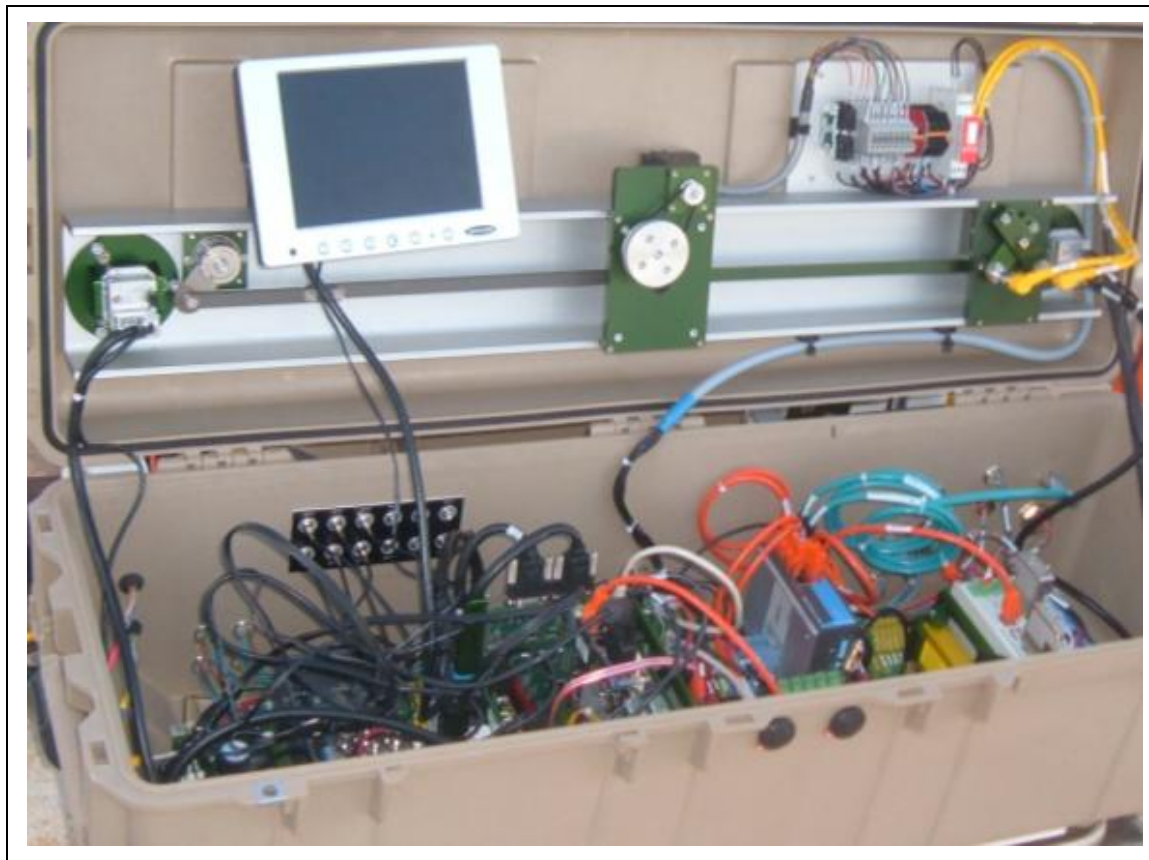
Figure 45. An image of the second control box showing audio connectors.

4.3 System Mounting Frame

A mounting frame was designed and fabricated that allowed most of the system components to be bolted to a common steel structure (Figure 46). This mounting frame was designed to simplify the deployment of the system by reducing the amount of onsite assembly required. It was designed with handles so it could be carried by 2–4 people and could also be used to securely tie the system down to a flat surface. The dimensions of the mounting frame were constrained to allow it to be transported in the bed of a pickup truck. It was equipped with wheels to allow it to be more easily moved. For deployment at FPSLT, the wheels were replaced with mounting brackets that were welded to the deck of the tower.

The mounting frame can accommodate the control box, the storage computer, a 5-gal washer fluid reservoir for the lens wiping system, the satellite modem box, the ultrasonic microphone housing (which is mounted directly to the control box), and the weather instrument cluster. The sonic microphone arrays are mounted separately away from the mounting frame to maximize the distance between them. The battery box and power system were kept separate from the mounting frame to maintain a reasonable size.

Figure 46. The mounting frame designed to streamline deployment and decommissioning.

4.4 Data Management Processes

After the initial data set was returned from the UD Lewes deployment, development began on a set of software programs for managing data collected by the system. These programs included a data offload process, which is a server program that detects an ATOM storage computer on the local network and transfers files off of the storage computer, and a data archive process, which is a server process that locates ATOM data files stored on the server and copies them to a pair of archive hard drives. A storage cleanup process was also developed, which is a storage computer process that queries the server database to determine which files have been archived and can be deleted from the storage computer. A data load process was also developed. This is a server process that takes a list of files or range of dates and prompts the user to insert archive hard drives into the server as necessary to bring those files online for analysis.

5 System Characterization

ATOM system characterization tests were designed to assess the system's performance limits and to verify calculations for thermal video imaging and ultrasound functions. Although acoustic audio was collected during the field test, it was not evaluated for performance characterization. The thermal video and ultrasonic data have a limited area of detection, which is not a factor in the acoustic data. Tests by CLO also indicate that calls from live birds can be detected at greater distances. Therefore the acoustic data from the actual installed site are a more accurate indicator of the performance limits. Thermal imaging field tests were conducted on 8 Jul 2013 in an open

field in north-central Florida. A helium balloon was used for the thermal testing (Figure 47). The size of the balloon could be easily measured for size, and the height could be manipulated by a string of a known length. The balloon would also support the weight of an iPhone used for the acoustic data. Ultrasound tests of the ReBAT® system were conducted independent of acoustic and thermal tests in Mar 2012.

Results indicated acoustic detection above the microphone at close to 200 m or more for actual calls from live birds. Thermal imaging worked well to capture sufficient video to verify the height calculations of the AW software. The known limitation of the thermal image is the narrow field of view and possibly the image resolution. Small birds at high altitudes could be difficult to identify because they can become a small dot on an image. However, higher resolution images would require significantly higher amounts of hard drive storage. Ultrasound tests indicated that in an open field context, the ReBAT® system worked at between 40 and 50 m when a bat was calling in front of the system. Thermal imaging could detect targets as far as 200 m or more from the camera, while bird sounds could be detected at potentially 300 m or more depending on the intensity of the call and noise interference.
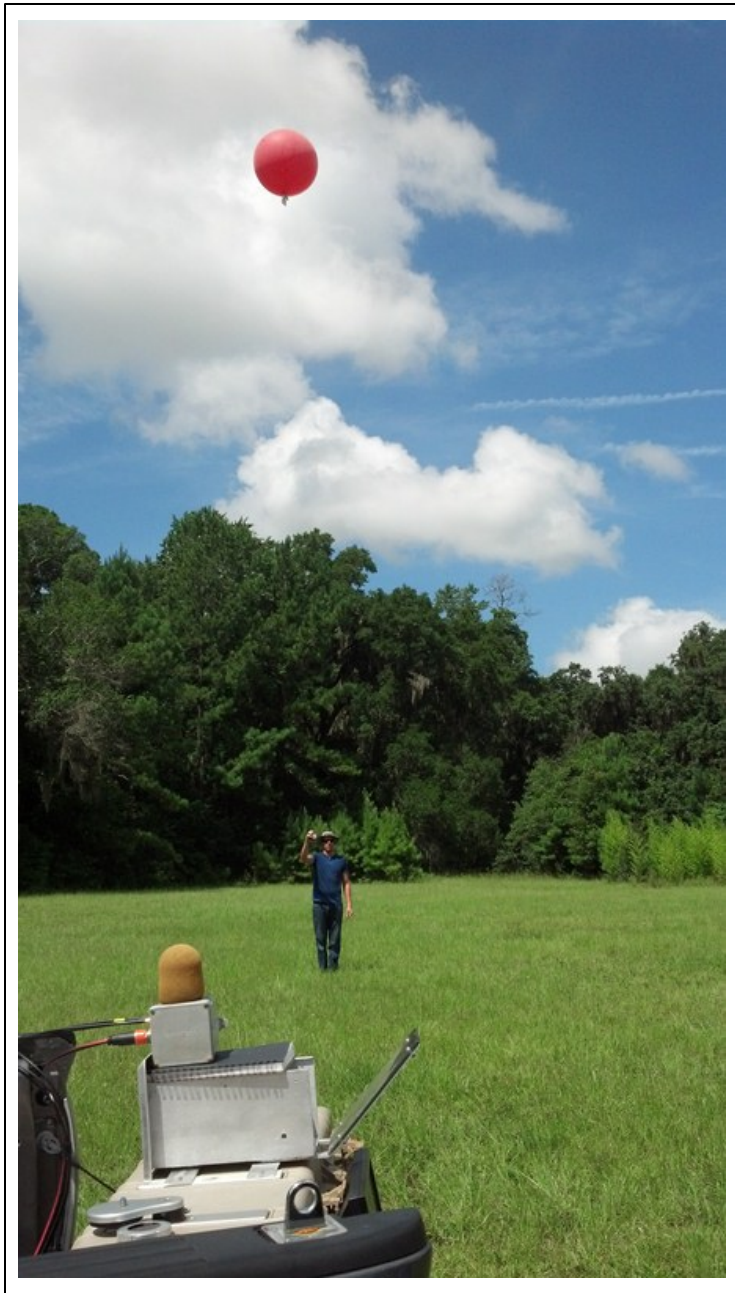
Figure 47. ATOM test system showing acoustic micro-
phone and weather balloon.

5.1 Acoustic

Controlled environment experiments were conducted for acoustic testing of equipment. Prior to field testing, iPhone sound outputs were tested in an anechoic chamber to estimate correction distances for iPhone outputs versus live bird sound outputs.

5.1.1 Anechoic Chamber Tests

Anechoic chamber tests indicate that sounds from a live bird are audible at a much farther distance than sounds from an iPhone based on differences in base volume. For example, the apparent volume of an iPhone at 4 m is roughly equivalent to a real bird at 32 m, while the sound produced from an iPhone at 64 m might be heard from a bird as far as 500 m away (Table 13). Under field conditions as compared within an anechoic chamber, sound would be expected to travel shorter distances in general due to such factors as humidity and competing sounds (e.g., wind, water, insects, traffic).

Table 13.

Approximate conversion distance for iPhone used during
anechoic chamber test versus the distance from which a live
bird could be heard.

ATOM Test Distance	Equivalent Bird Distance (m) for a 79dB SPL call
1	8
2	16
4	32
8	64
16	128
32	256
64	512

Source: Harold Cheyne, CLO, email, 28 May 2013

5.1.2 Field Tests

Acoustic field tests occurred concurrently with thermal imaging tests between 11:23 AM and noon when weather was relatively calm so that wind interference did not negatively affect the tests. Temperature during testing ranged from 86° to 87°F. Relative humidity was between approximately 66% and 62%. Wind was approximately 6.5 to 7 mph from the east, northeast.

The recordings from this test were not used to evaluate the system performance limits. Data from the installation site is the best indicator of the performance. The ability of the system to detect the sounds projected from the iPhone diminished with distance from the speaker. Sounds produced by live birds are expected to be detectable at a greater distance based on results on anechoic chamber tests described above (see Section 8.3).

Between two and five audio files were recorded for each elevation in 5-m intervals from 5 to 50 m above the microphone (Table 14).

Table 14.

Audio and video files collected by elevation and time.

Height (meters)	Time	Audio File Name	Video File Name
5	11:25:07 AM	rbv3-20130708T102507.caf	rbv3-201307081123.psir
	11:25:42 AM	rbv3-20130708T102542.caf	
	11:26:17 AM	rbv3-20130708T102617.caf	
	11:26:52 AM	rbv3-20130708T102652.caf	
	11:27:28 AM	rbv3-20130708T102728.caf	
10	11:29:13 AM	rbv3-20130708T102913.caf	rbv3-201307081128.psir
	11:29:48 AM	rbv3-20130708T102948.caf	
	11:30:23 AM	rbv3-20130708T103023.caf	
	11:30:59 AM	rbv3-20130708T103059.caf	
	11:31:34 AM	rbv3-20130708T103134.caf	
15	11:32:44 AM	rbv3-20130708T103244.caf	rbv3-201307081133.psir
	11:33:19 AM	rbv3-20130708T103319.caf	
	11:33:55 AM	rbv3-20130708T103355.caf	
20	11:35:05 AM	rbv3-20130708T103505.caf	rbv3-201307081133.psir
	11:35:40 AM	rbv3-20130708T103540.caf	
	11:36:15 AM	rbv3-20130708T103615.caf	
	11:36:51 AM	rbv3-20130708T103651.caf	
	11:38:36 AM	rbv3-20130708T103836.caf	
25	11:41:32 AM	rbv3-20130708T104132.caf	rbv3-201307081143.psir
	11:42:43 AM	rbv3-20130708T104243.caf	
	11:44:28 AM	rbv3-20130708T104428.caf	
30	11:46:14 AM	rbv3-20130708T104614.caf	
	11:46:49 AM	rbv3-20130708T104649.caf	
	11:47:24 AM	rbv3-20130708T104724.caf	
35	11:48:35 AM	rbv3-20130708T104835.caf	
	11:49:10 AM	rbv3-20130708T104910.caf	
	11:49:45 AM	rbv3-20130708T104945.caf	
40	11:51:31 AM	rbv3-20130708T105131.caf	
	11:52:06 AM	rbv3-20130708T105206.caf	

Height (meters)	Time	Audio File Name	Video File Name
45	11:56:48 AM	rbv3-20130708T105648.caf	
	11:57:23 AM	rbv3-20130708T105723.caf	
	11:57:58 AM	rbv3-20130708T105758.caf	
50	11:59:44 AM	rbv3-20130708T105944.caf	
	12:00:10 AM	rbv3-20130708T110019.caf	
	12:00:54 AM	rbv3-20130708T110054.caf	

5.2 Thermal Video Imaging

Unlike acoustic and ultrasound detections, thermal images have "hard sides," meaning the field of detection is clearly defined. At lower heights, the field of detection for thermal images was narrower, but as height increased, the area captured by the thermal image increased (Table 15, Figure 48).

The purpose of the thermal video image testing was to verify the height estimation used by the software. Once the height is established, it is possible to calculate other information such as velocity and size. Bearing is the only item that does not rely on the height measurement. An object at a known height and size visible in the field of view of both cameras was used to validate the height calculation.

A thermal video image is a two dimensional representation of a three dimensional space and is made up of a series of dots or, in computer terms, pixels. Each pixel is filled with one color; thermal images consist of shades of gray. There, a grid of 256 high × 324 wide pixels is used to create each rectangular thermal image. This is considered a low resolution (using the total number of pixels = height × width) in the world of megapixel images. To compare, 256 × 324 produces a 0.08 megapixel image and another camera may create a pixel image of 1280 × 960, which equates to a 1.2 megapixel image. The cameras are saving images at a rate of 30 frames/sec and in 1 min each camera creates 1800 images that need to be stored. The advantage of a higher resolution camera would be the ability to identify a smaller target at a higher altitude, but that would require significantly more storage to save the images.

Table 15 shows the size of a pixel for a target at a specific distance above the camera. The ability to see and identify a target at a particular height varies with the size of object. A small target at a high altitude will fill fewer pixels and therefore have a larger margin of error for calculating the size as well as not being able to see any distinguishing features.

For example, a warbler species that is 12.7 cm in body length and is flying horizontally/straight at 10 m above the camera's field of view would fill 13 pixels in the thermal image. At that height the width of a pixel is 0.9777 cm; so the bird's body length divided by that pixel width equals 12.98 cm (approximately 13 cm). The same bird flying 130 m above the camera would only fill 1 pixel. Larger birds, such as a Brown Pelican with a wingspan of more than 2 m, would be visible at a much higher altitude.

Table 15.

Thermal camera field of view (all measurements in meters).

Distance above Camera	Image Height	Image Width	Pixel Height	Pixel Width
0	0.00	0.00		
5	1.23	1.58	0.004796	0.004888
10	2.48	3.17	0.009593	0.009777
15	3.68	4.75	0.014389	0.014665
20	4.91	6.34	0.019185	0.019554
25	6.14	7.92	0.023981	0.024442
30	7.37	9.50	0.028778	0.02933
35	8.59	11.09	0.033574	0.034219
40	9.82	12.67	0.03837	0.039107
45	11.05	14.25	0.043166	0.043996
50	12.28	15.84	0.047963	0.048884
55	13.51	17.42	0.052759	0.053772
60	14.73	19.01	0.057555	0.058661
65	15.96	20.59	0.062352	0.063549
70	17.19	22.17	0.067148	0.068438
75	18.42	23.76	0.071944	0.073326
80	19.65	25.34	0.07674	0.078215
85	20.87	26.93	0.081537	0.083103
90	22.10	28.51	0.086333	0.087991
95	23.33	30.09	0.091129	0.09288
100	24.56	31.68	0.095925	0.097768
105	25.78	33.26	0.100722	0.102657
110	27.01	34.84	0.105518	0.107545
115	28.24	36.43	0.110314	0.112433
120	29.47	38.01	0.115111	0.117322
125	30.70	39.60	0.119907	0.12221
130	31.92	41.18	0.124703	0.127099
135	33.15	42.76	0.129499	0.131987
140	34.38	44.35	0.134296	0.136875
145	35.61	45.93	0.139092	0.141764
150	36.84	47.52	0.143888	0.146652
155	38.06	49.10	0.148684	0.151541

Distance above Camera	Image Height	Image Width	Pixel Height	Pixel Width
160	39.29	50.68	0.153481	0.156429
165	40.52	52.27	0.158277	0.161317
170	41.75	53.85	0.163073	0.166206
175	42.97	55.43	0.16787	0.171094
180	44.20	57.02	0.172666	0.175983
185	45.43	58.60	0.177462	0.180871
190	46.66	60.19	0.182258	0.18576
195	47.89	61.77	0.187055	0.190648
200	49.11	63.35	0.191851	0.195536
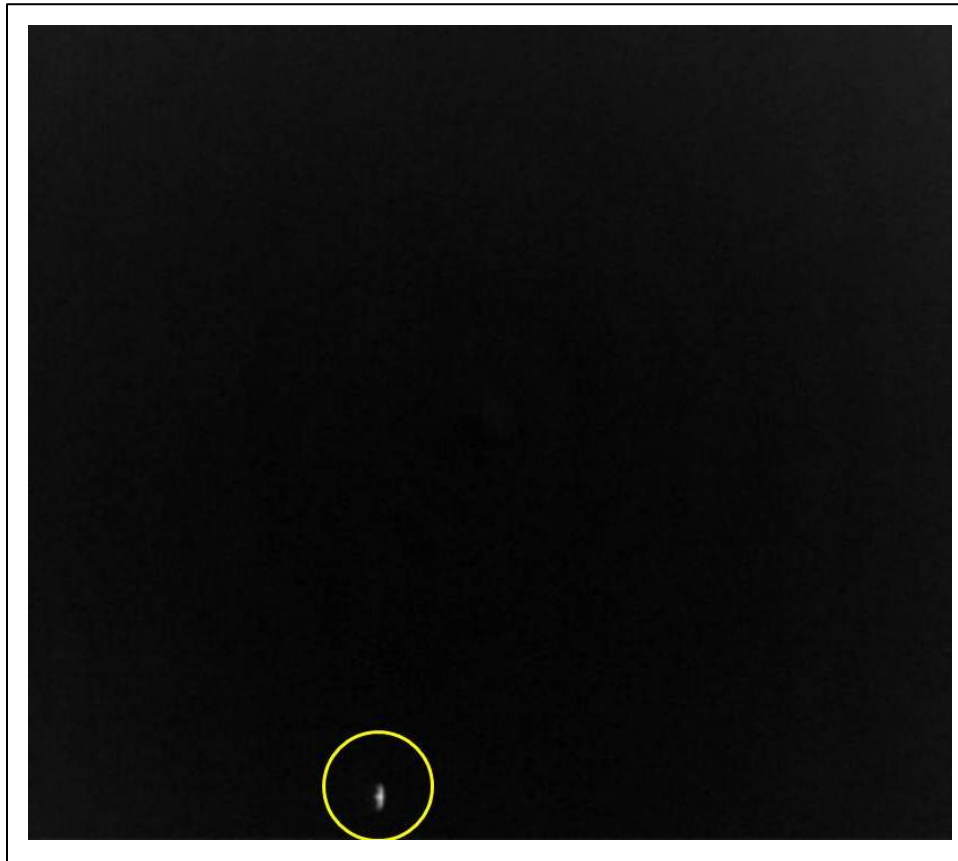
Figure 48. Thermal image of a bird (likely a tern) approximately 35.5 cm
long and 100 m above the camera at FPSLT.

An ATOM system has two thermal cameras 93 cm apart. Figure 49 is a graphical representation of the field of view for each camera. The red lines represent the left camera and the blue lines the right. The figure also establishes the area viewable to both cameras that is the stereo view. This

stereo view is what allows us to calculate distance above the camera. There is 0.5 m on the right of the right camera image and 0.5 m on the left of the left camera image that is only visible to that respective camera. Should the object appear in that 0.5 m space, no calculations can be performed because of the lack of a stereo view.
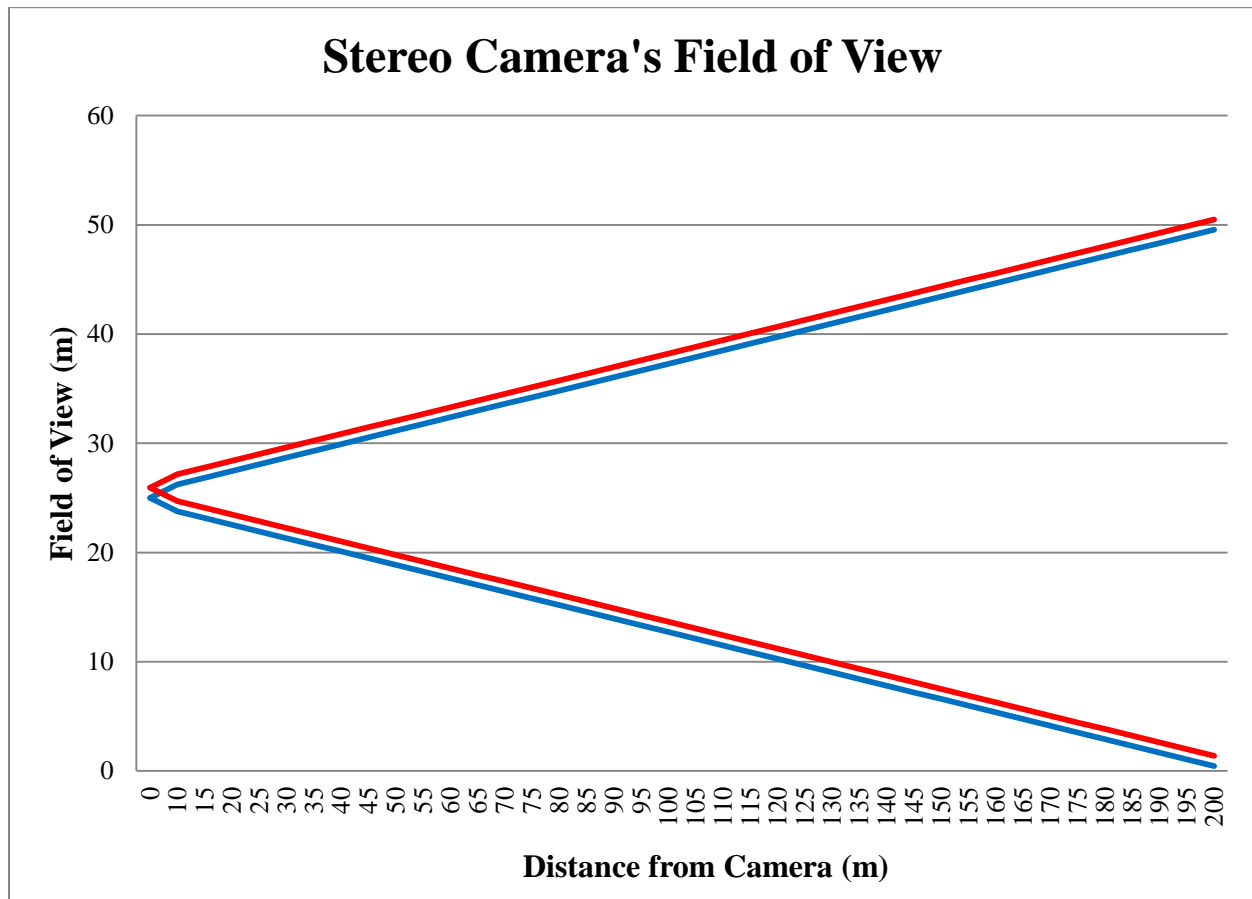
Figure 49. Field of view of thermographic camera at 0 to 200 m from camera. Different color lines represent the two cameras.

Other calculations that rely on the height value, such as line length and velocity, are tested using a software test environment. The PC software is written within Microsoft Visual Studio using Object Oriented Programming (OOP) technics. The Visual Studio code project includes modules that perform tests using the same code a user will invoke during the execution of the AW software. A test environment is established with specific inputs and expected results. Each software method/function is run with the test parameters. Any method failing to return the expected result was identified so that errors due to logic and/or code modification could be easily identified and corrected. The intent of these tests was to maintain the integrity of the output of the software.

The acoustic and thermal video field tests were performed between 11:23 AM and noon when weather was relatively calm to avoid strong wind interference. Temperature during testing

ranged from 86° to 87°F. Relative humidity was between approximately 66% and 62%. Wind was approximately 6.5 to 7 mph from the east, north east.

The balloon was visible in the recorded video up to 25 m and there was enough video to validate the height calculation. The balloon was out of the stereo field of view for tests above 25 m. The slight wind made it difficult to control the balloon's position at the higher altitudes.

To validate the height, the video is played in the AW software and paused on a frame or image with the balloon visible in both cameras as shown in Figure 50. A line is drawn to establish two points, one in the right camera image and one in the left camera image. The points should have the same y axis value (42.5 in the example shown). The intent is to identify the same point in both images. The bottom of the balloon appears to have an 'X' on the image and the center of that 'X' is being used as the common point. The result was a distance of 15.1 m from the software using a video image of when the balloon was at a known height of 15 m. Height calculations from 5, 10, 15, 20, and 25 m were all within 0.5 m of the known height.
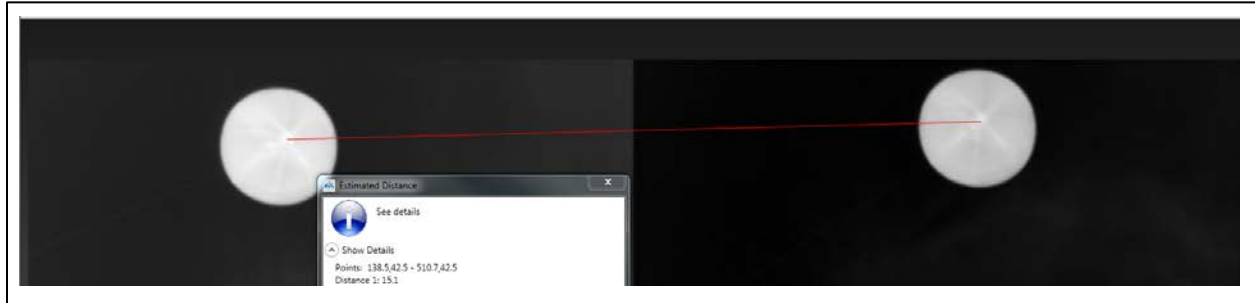
Figure 50. Thermal images of weather balloon at 15 m from the two cameras.

As the balloon moved farther from the camera, the proportional decrease in image size was clearly visible. For example, in Figure 51, the image on the left (10 m) is 2.5 times the size of the image on the right (25 m).
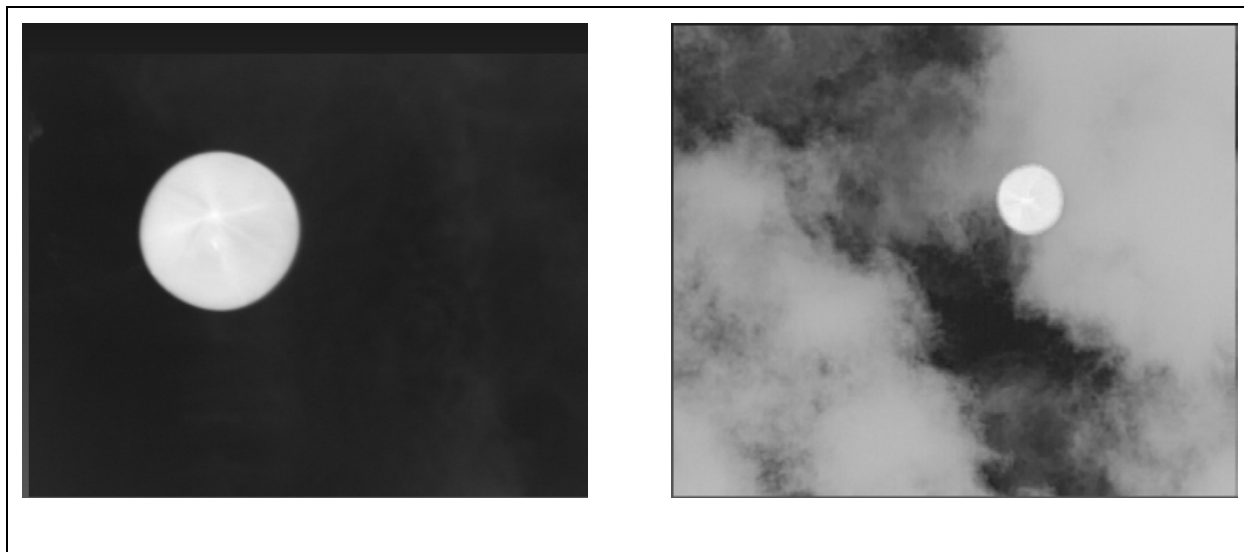
Figure 51. Thermal image of weather balloon at 10 m above the camera (left) and 25 m above the camera (right).

The stereographic distance calculation was derived from Tjandranegara (2005).

Specifications for the Camera Tau 324:
http://www.flir.com/cvs/cores/view/?id=54717&collectionid=612&col=54726

5.3 Ultrasound

Ultrasound tests were previously conducted by Normandeau during development of the ReBAT® system. The ultrasonic component of the ATOM system consists of an AR-125 microphone (Binary Acoustic Technology, Tucson, AZ) contained within a ReBAT® housing that protects the microphone from precipitation. The AR-125 microphone is a directional, wide bandwidth ultrasonic receiver that is sensitive to frequencies between 1 kHz and 125 kHz, and with a dynamic range of greater than 90 dB. The ReBAT® housing was developed by Normandeau to allow extended, remote deployment of ReBAT® systems in all weather conditions. The aluminum casing provides protection from the elements, while the size and 45° angle positioning of the plastic reflector plate (Figure 52) allows for bat call detection. The microphone is positioned pointing downwards towards the center of the reflector plate for maximum call detection potential. The purpose of this experiment was to investigate (a) the detection field for the ultrasonic microphone, and (b) the influence of the weatherproof housing on the detection field.

Normandeau conducted controlled field tests of the AR-125 microphone and the weatherproof housing (Figure 52) on three days in Mar 2012 (forward and perpendicular orientations) and one day in Apr 2012 (backward orientation). These days were selected for similar weather (temperature, humidity, and wind speed) to control for the effect of varying weather conditions on acoustic detection.

Figure 52. View of underside of the ReBAT® housing with the AR-125 microphone visible inside pointing down at the reflector plate.

Each housing type (bare microphone and microphone within housing) was tested separately (Table 16) and at three different orientations: forward, 90°, and backward. Each of these treatments was tested with recorded echolocation calls being emitted from an ultrasonic speaker at various distances up to a maximum distance of either 40 m or 80 m. Due to *a priori* knowledge of the directional capabilities of the AR-125 microphone, the forward-facing treatments were tested up to a greater maximum distance than the perpendicular and backward-facing treatments. We varied the time of day at which each treatment was tested to ensure that each treatment was tested within a range of temperature and humidity levels.

Table 16.

Six treatments (housing type and direction) used for testing the range of ultrasonic detection for the ATOM system and maximum distance of the speaker from the microphone for each treatment.

Housing type	Orientation	Maximum distance (m)
Bare AR-125	Forward	80
Bare AR-125	Perpendicular*	40
Bare AR-125	Backwards	40
ReBAT® housing	Forward	80
ReBAT® housing	Perpendicular*	40
ReBAT® housing	Backwards	40

*the same 90° orientation was used each time.

Both the bare microphone and the housing were mounted on a pole at 1.5 m above the ground (measured from the center of the microphone and the center of the reflector plate, respectively) and oriented due north. An Avisoft (Berlin, Germany) UltraSoundGate Player BL Light (speaker) was mounted on a PVC tube (Figure 53) and raised to 1 m above the middle of (a) the bare AR-125 microphone and (b) the reflector plate on the ReBAT® housing (Figure 54). The AR-125 microphone, in combination with SPECT'R© recording software (Binary Acoustic Technology), is triggered to begin recording when ultrasonic noise above a certain decibel threshold is detected. It will record files up to 1.7 sec in duration. A playlist (1 min, 52 sec including 1 sec delay between files) of recorded echolocation calls of four bat species (*Eptesicus fuscus*, *Lasiurus borealis*, *L. cinereus*, and *Perimyotis subflavus*) and 1 bat species group (Eastern *Myotis* spp.) was played from the Avisoft speaker. The playlist was played once for each treatment and distance.

Figure 53. The Avisoft speaker attached to
a PVC tube.

Figure 54. The ReBAT® system facing the Avisoft speaker at a distance of 5 m.

The range of detection for each treatment was measured in two main ways:

1. Counting the total number of calls (high and low frequency together and high frequency alone) detected for each treatment at each distance

2. Determining the maximum distance at which calls (high and low frequency together and high frequency alone) could be detected for each treatment

Preliminary studies suggest that bat detection range and sensitivity vary widely among different detector brands (Adams et al. 2011). We considered high frequency calls (for these purposes, higher than 32 kHz) separately from total calls because high frequency sound attenuates rapidly in air. As such, the ability to detect high frequency calls is a good indicator of microphone sensitivity and distance capabilities.

R statistical software (R Development Core Team 2012) was used to perform ANOVAs to determine total number of calls detected (all calls and high frequency calls) and maximum distance of detection (all calls and high frequency calls) for each treatment group.

For both the number of calls and the maximum distance of detection tests, there was a significant interaction between housing type and orientation. In other words, the number of calls recorded and the distance of detection differed depending on the combination of housing type and direction.

For low and high frequency calls combined (Figure 55), there was an interaction between housing type and orientation (F = 112.8, df = 2, p < 0.001). The combination of using the housing in the forward direction recorded more calls (average = 466.7) than any other treatment. The bare microphone in the forward orientation recorded more calls (average = 81.7) than all treatments except the ReBAT® housing in the forward orientation.

Similarly, when just considering the total number of high frequency calls recorded, there was an interaction between housing type and orientation (F = 24.6, df = 2, p < 0.001; Figure 56). Additionally, the ReBAT® housing in the forward orientation recorded more calls (average = 38.7) than any other treatment.
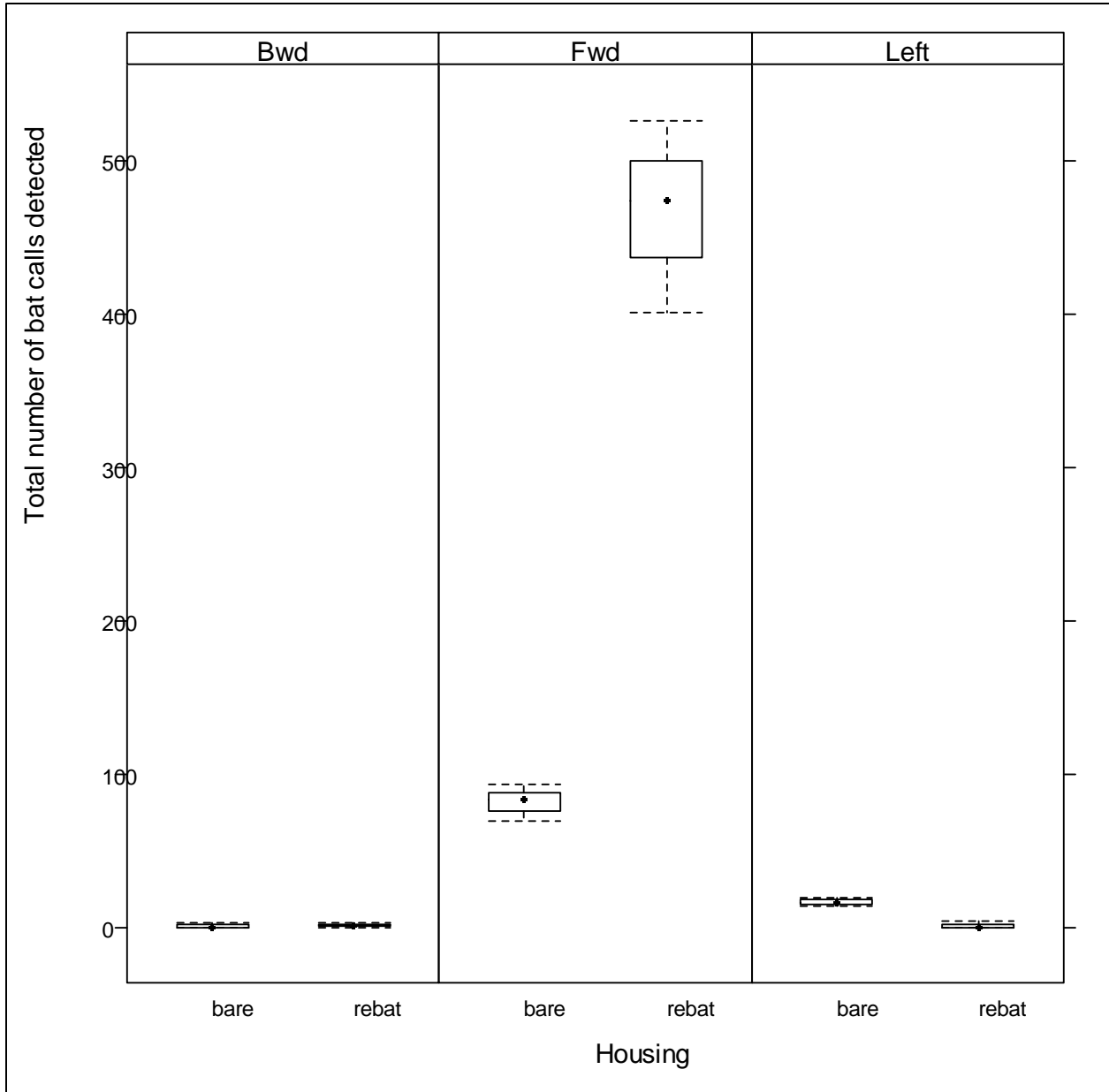
Figure 55. Conditional boxplot of the total number of calls detected for each housing and
orientation combination.
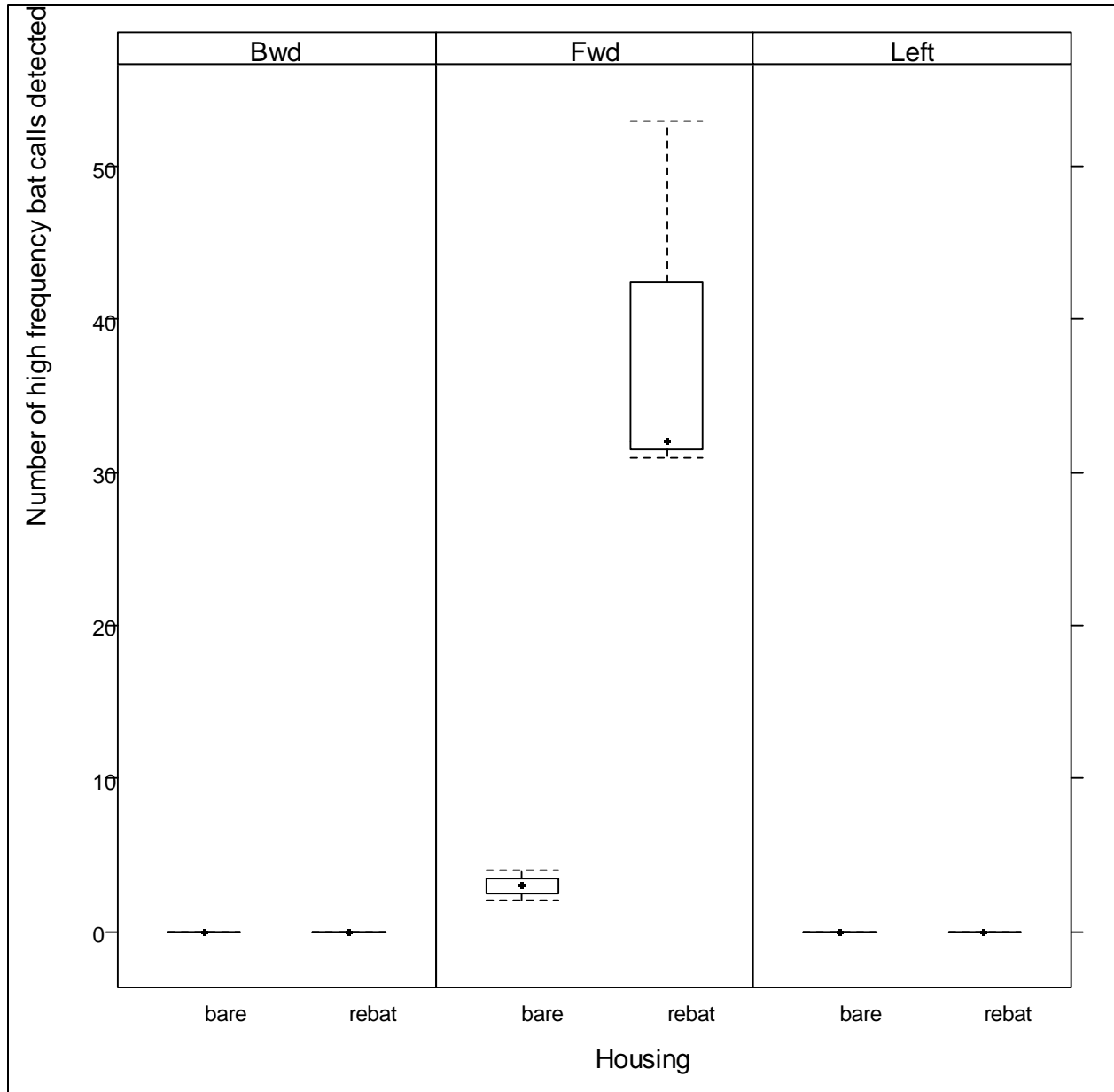
Figure 56. Conditional boxplot of the total number of high frequency calls detected for each housing and orientation combination.

For low and high frequency calls combined, there was a significant interaction between housing type and orientation (F = 50.1, df = 2, p < 0.001). Same as with the total number of calls recorded, the ReBAT® housing in the forward orientation recorded calls at a greater distance (range 40–50 m) than any other treatment (Figure 57). The bare microphone in the forward orientation recorded at a greater distance (range 15–20 m) than any treatments except the ReBAT® housing in the forward orientation. Likewise, there was an interaction between housing

type and orientation (F = 72.0, df = 2, p < 0.001; Figure 58) for the maximum distance of detection of high frequency calls. The ReBAT® housing in the forward orientation recorded high frequency calls at a greater distance (range 25–30 m) than any other treatment, and the bare microphone in the forward orientation recorded high frequency calls at a greater distance (range 5–10 m) than any treatment except the ReBAT® housing in the forward orientation.
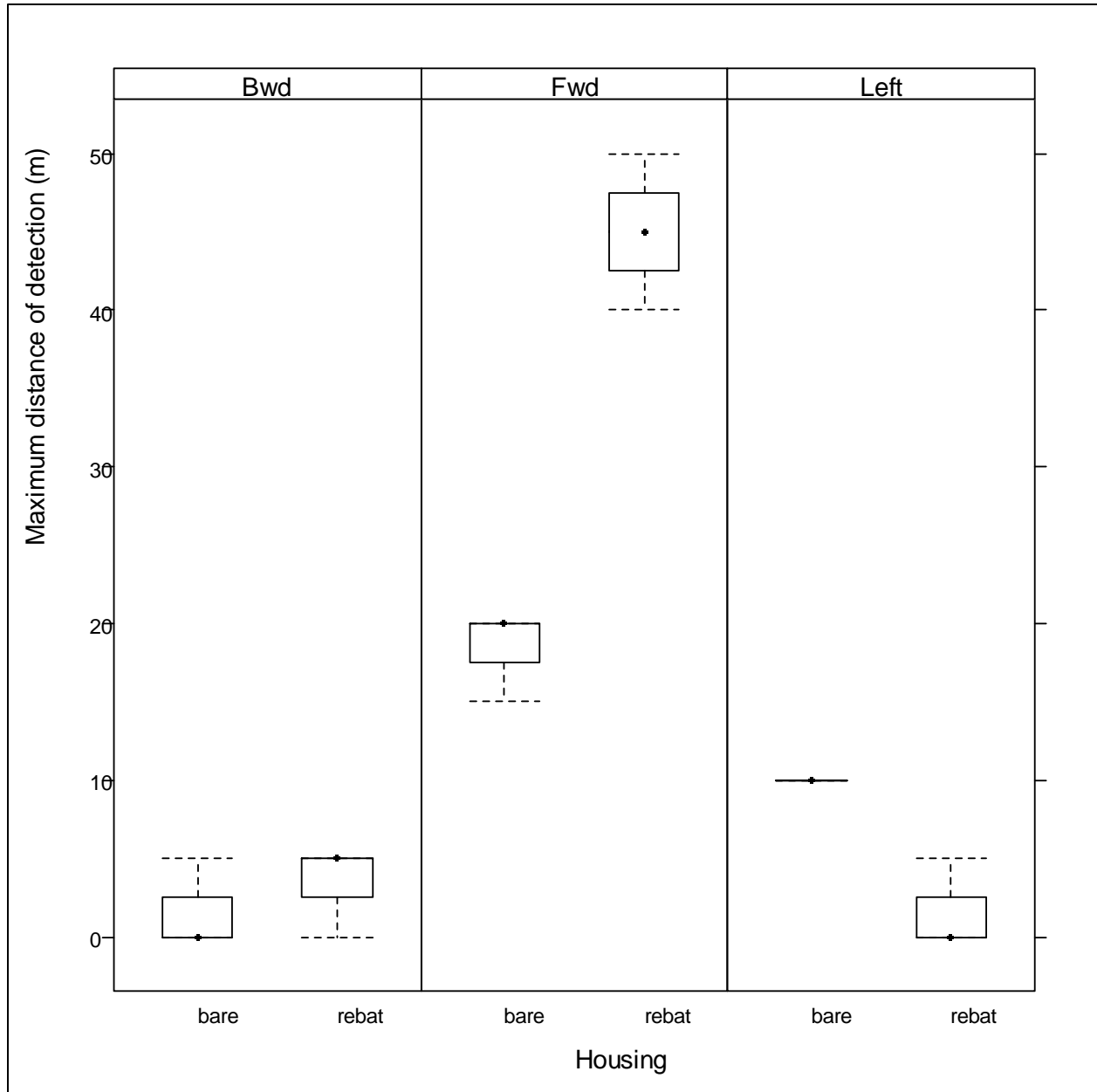
Figure 57. Conditional boxplot showing the maximum distance of detection of bat calls for each housing and orientation combination.
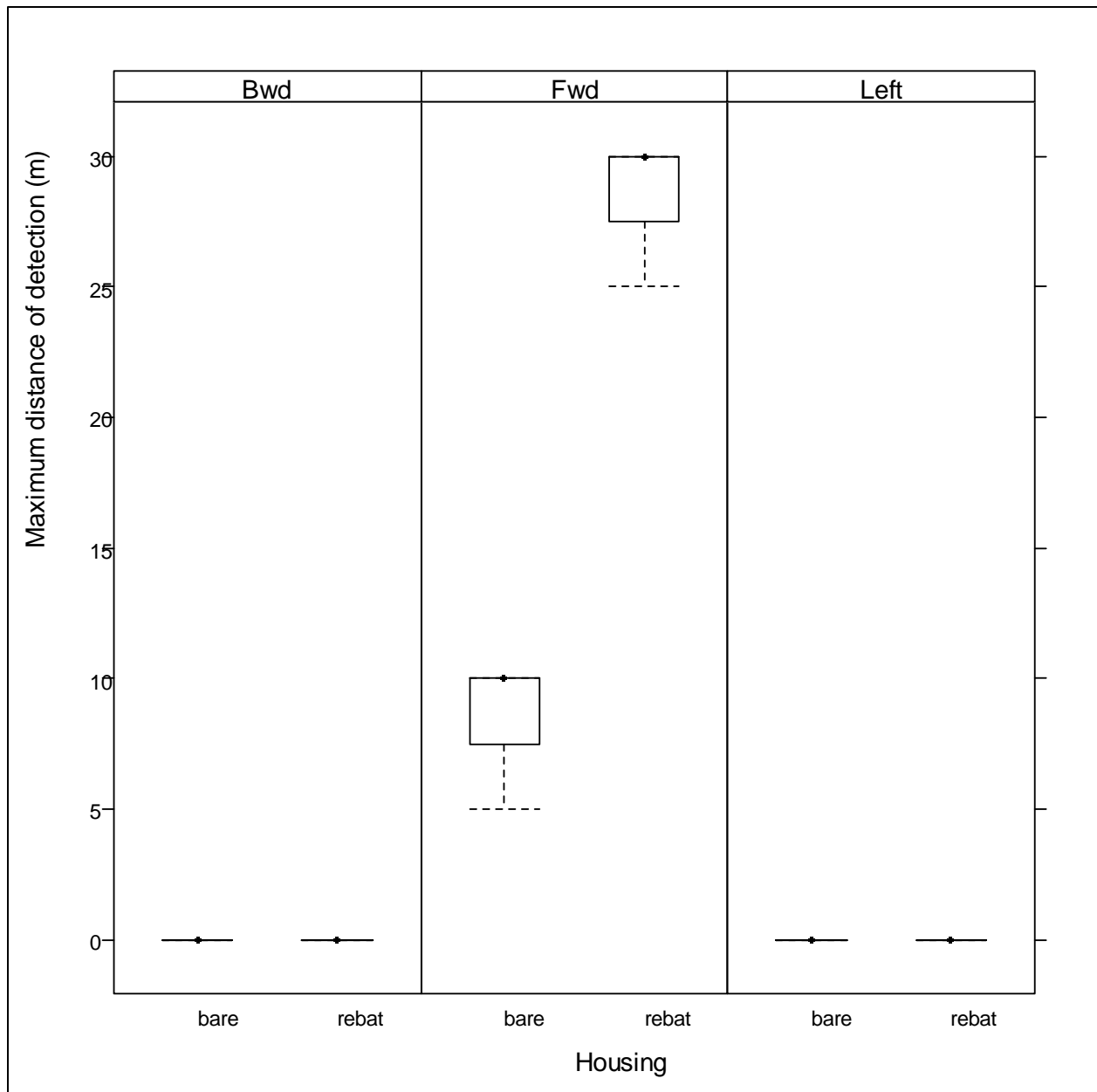
Figure 58. Conditional boxplot showing the maximum distance of detection of high frequency bat calls for each housing and orientation combination.

Based on results of field testing of the ReBAT® system, the estimated area of detection for ultrasound is an ellipse approximately 55 m long and about 5 to 15 m wide, extending from 40 to 50 m in front of the ReBAT® detector to about 5 m behind the detector (Figure 59).

Figure 59. Minimum (gray) and maximum (green) range of detection of the ultrasonic microphone within the ReBAT® housing.

In general, the microphone records best in the forward orientation because the microphone is highly directional. The ultrasonic microphone within the ReBAT® housing recorded more calls and at a greater distance compared to the bare microphone. This indicates that the ReBAT® housing is not hindering the ability of the AR-125 microphone to detect bat calls. Although good at detecting bats if they are in front of the microphone, the range of detection is limited when bats are at 90° and 180° orientations from the receiver.

5.4 Results

System characterization testing provided information useful for calculating maximum detection distances for each of three different functions: acoustic, thermal imaging, and ultrasound (Figure 60). Anechoic chamber tests informed field testing of the system's acoustic detection abilities. Based on a correction factor derived from anechoic chamber tests, field testing indicates bird sounds could be detected at 300 m or more depending on the intensity of the call and noise interference. Thermal image tests verified that the distance calculations are good and that the size of the bird determines the maximum detection distance. Ultrasound tests indicate the ReBAT® system best detects bats flying in front of the microphone at 40 to 50 m.
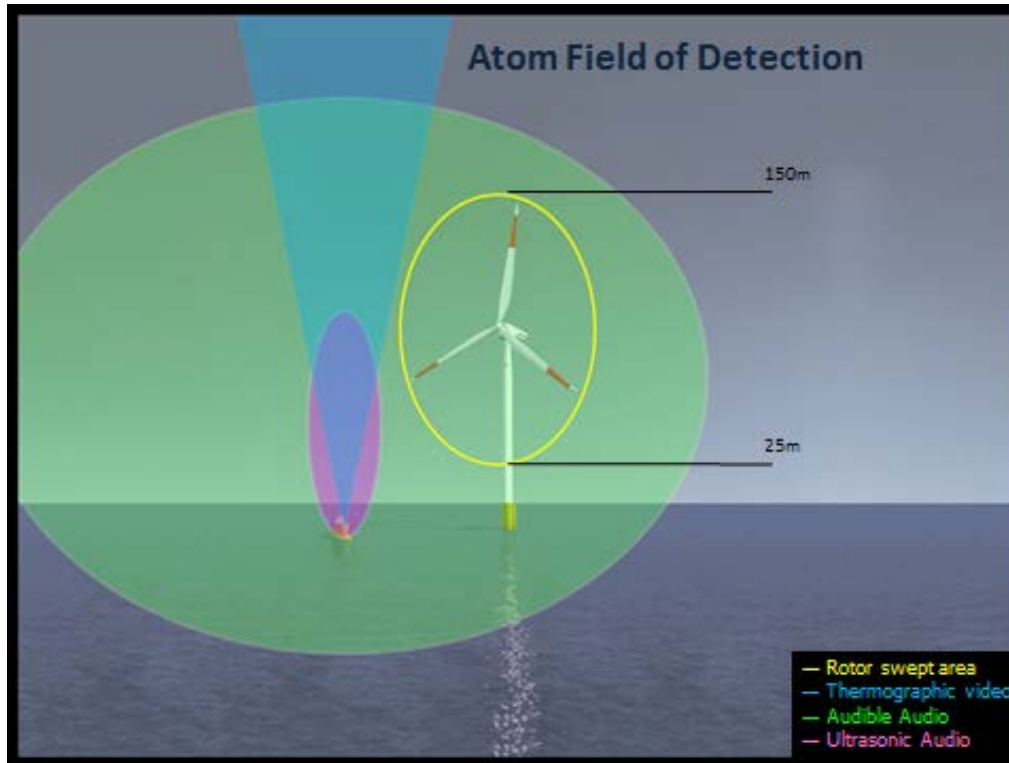
Figure 60. ATOM fields of detection for acoustic, ultrasound, and thermal.

6 FPSLT Offshore Deployment

After months of discussions with a variety of organizations regarding a number of potential deployment locations, the FPSLT was selected as an AOCS deployment platform because it was the only location available to house the system (Figure 61).

FPSLT is located 29 mi offshore, southeast of Southport, North Carolina (coordinates 33°29′N 77°35′W) (Figure 62). The 80-ft platform was constructed in 1966 and sold by the government in 2010 to the current private owner, Richard Neal. This platform was ideally suited for deploying an ATOM system to gather *in situ* data on spatio-temporal patterns of bird and bat occurrence at a location on the U.S. AOCS but the remoteness of the tower was a significant challenge throughout the project given the fact that this was the first time the ATOM system was being deployed offshore. The original intent for this project was to deploy ATOM at a location 3 to 10 mi offshore, but no such locations were available at the time. Because the location was 29 mi offshore, it changed the assumptions and costs of transportation to and from the tower. Helicopters rather than boats became the main method to get to the tower because of the very narrow time windows with suitable conditions for safely visiting the tower. Boat trips also necessitated staff to extend deployment times. Even visiting the tower via a helicopter required specific weather conditions. All these factors caused delays in servicing the equipment. The distance also made it impossible to send data back via a cellular network to check quality and to begin analyses. The system was connected via satellite but the bandwidth only allowed for remote checks to see if the system was recording and to make minor software changes.
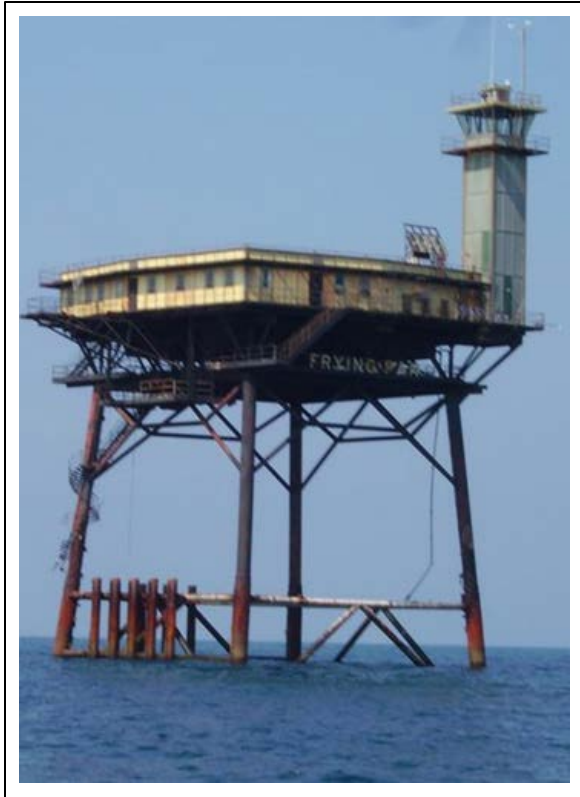
Figure 61. Frying Pan Shoals Light Tower.
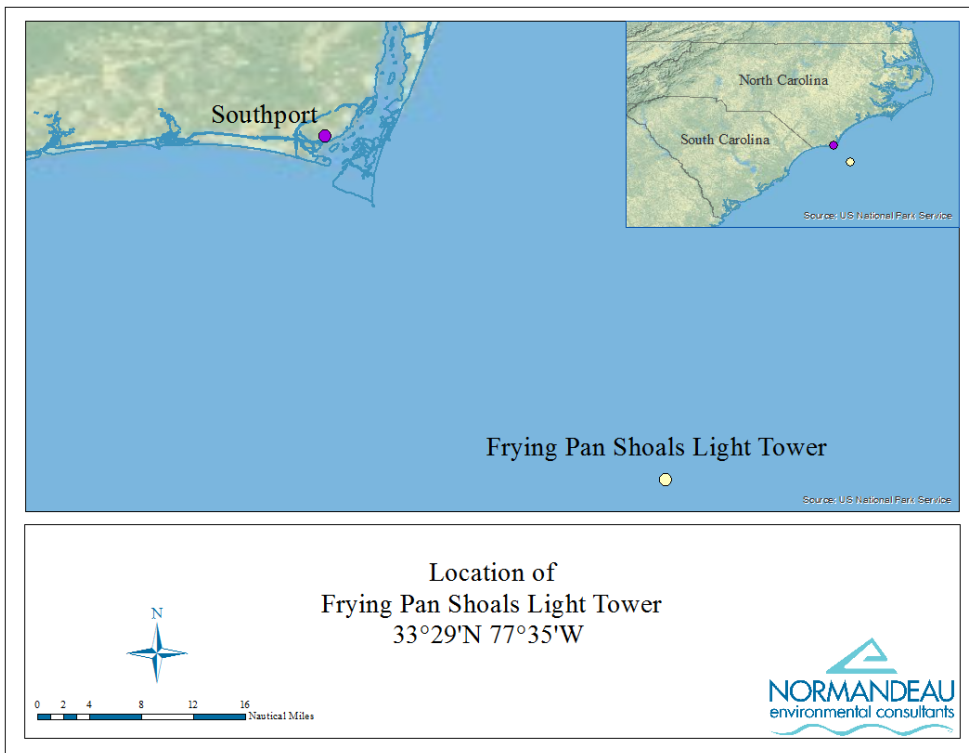
Figure 62. Location of Frying Pan Shoals Light Tower.

The logistical challenges were highlighted on the initial deployment. Deployment of the ATOM system at FPSLT occurred in Dec 2011 (see Figure 63, Figure 64). It took eight (8) helicopter trips over 2 days to transport the necessary equipment and personnel to the tower. While all personnel made it safely to the tower, the solar panels and framing materials were lost. The helicopter pilot mistakenly pressed the "drop" button mid-flight and the solar panels and brackets were dropped into the ocean from where they were unrecoverable.

This was an initial setback to the start of data collection but a solution was implemented using the existing power at the tower. There were old (approximately 20 yrs old) solar panels at the tower but they produced only 20–25% of the power needed to run the ATOM system full-time. Software modifications were completed to address the reduced power available. Before the installation was completed, modifications were made to the power control board firmware and the control computer software that allowed the system to conserve power by operating at a reduced duty cycle. This software operated by periodically shutting down the control computer and setting the power control board to power it back up after a set amount of time. During the winter period of the deployment, the system was set to operate for 45 min and sleep for 3 hrs, resulting in a 20% duty cycle and an 80% decrease in the power demands of the system. This solution worked until the end of Jan 2012, when the existing solar panels could not fully charge the batteries. The systems were not able to power up until the tower was visited on 31 Mar and 1 Apr 2012 and the power was fixed. The following outlines subsequent visits.

- Jun 2012: Maintenance visit to replace malfunctioning data storage computer
- Aug 2012: Maintenance visit to replace malfunctioning data storage computer
- Nov 2012: Maintenance visit to replace solar panels damaged from Hurricane Sandy
- Apr 2013: Decommission the system

Figure 63. ATOM system deployed on the flight deck of FPSLT.
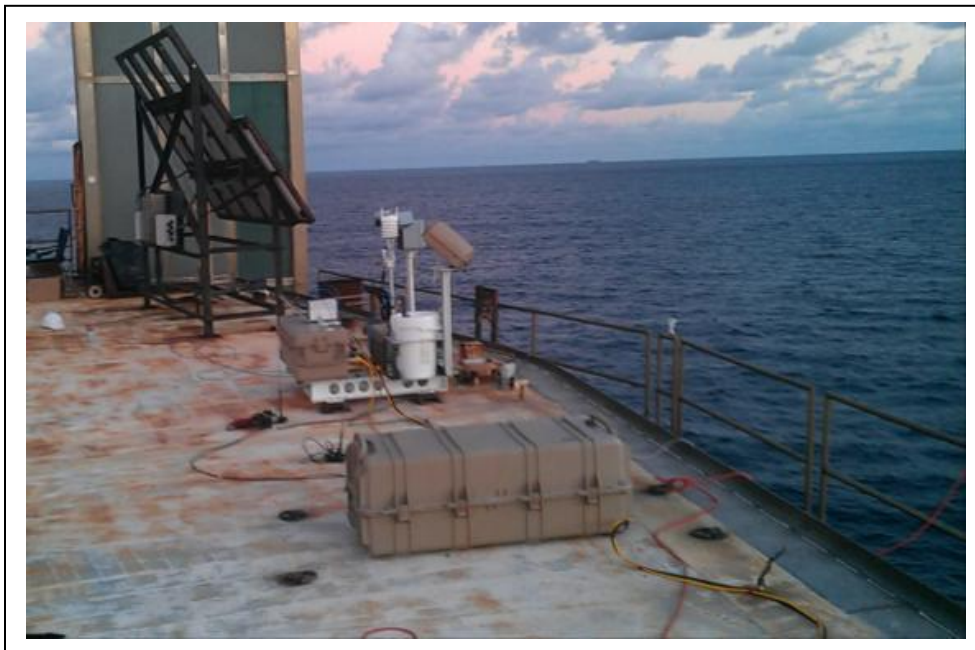
Figure 64. The ATOM system at FPSLT (Dec 2011).

7 Analyses from FPSLT

7.1 Introduction

Birds observed over or on the ocean can be grouped into two broad groups, seabirds and land birds. In general, seabirds are birds that can land on the water while land birds cannot. While these categories hold true in most cases, there are exceptions. For example, frigatebirds are considered seabirds, although they cannot land on water. Shorebirds are generally considered land birds, although Red and Red-necked phalaropes spend most of their lives, apart from the breeding season, on the ocean and are usually considered seabirds. All raptors, herons, doves, and songbirds are considered land birds, while tubenoses and all waterfowl can be considered seabirds. Pelagic birds are seabirds that spend the majority of their non-breeding lifetime offshore and rarely use inland waters. While seabirds have been the subject of systematic surveys, especially in recent years, very little systematic research has been conducted on land birds over the open ocean.

7.1.1 Seabirds Expected

The earliest reports of seabirds in the North Atlantic were based mainly on observations from cruises, but these were not repeated in a quantifiable manner (Gordon 1955; Helmuth 1920; Venables 1938, 1939; Wiley 1959; others). For example, Nichols (1913) kept notes on birds sighted on several voyages in the western North Atlantic between 1900 and 1913, although this information was not summarized in a quantitative format. Baker (1947) kept notes on birds seen on six North Atlantic cruises between 1943 and 1944, although ships followed slightly different routes on each trip. Other examples of somewhat systematic surveys include Grayce (1950), who counted birds on a stretch of the North Atlantic between Newfoundland and England from late Aug to late Nov 1948.

Some of the earliest systematic seabird surveys by the Woods Hole Oceanographic Institution began in 1931 and continued irregularly through 1949, from about 44° north latitude (off the coast of Maine) south to the West Indies, although due to the variability in sampling effort during these voyages, the data were reduced to numbers of birds per day (Scholander 1955; Moore 1951). The Handbook of North American Birds: Volume 1 (Palmer 1962) was one of the first books to attempt to create distribution maps for pelagic birds in North America. These maps were often based on nonquantifiable data and sometimes had large gaps where distribution was unknown.

In 1978 and 1979, U.S. Fish and Wildlife Service observers surveyed for birds from National Marine Fisheries Service and U.S. Coast Guard vessels (Paton et al. 2010). These surveys used transects recorded in 10-min periods for a total of 42 days of survey effort off Rhode Island. Seabirds and a few land birds were observed in these surveys. Between 1980 and 1988, the Northeast Fisheries Science Center of the National Marine Fisheries Service ran the Cetacean and Seabird Assessment Program with observers from Manomet Bird Observatory (Payne et al. 1984; Paton et al. 2010).

Powers et al. (1980) conducted a review of seabird surveys conducted by Manomet Bird Observatory between Cape Hatteras, North Carolina, and the Bay of Fundy, Canada, between

Jan 1978 and Apr 1980. These surveys used fixed-area zone counts collected in 10-min intervals. The authors created species diversity indices by region and season for shelf and shelf-break water in the western North Atlantic.

Between Oct 2010 and Jul 2012, in the longest-running, airplane-based systematic survey of marine birds in eastern North American, bird surveys were conducted off Rhode Island by airplanes flying at a fixed altitude of 76 m above sea level (Winiarski et al. 2012).

Two other detailed reports have recently compiled data on seabird and shorebird use of waters in the AOCS (O'Connell et al. 2009, 2011). The authors of these two reports state that they believe they "have identified all of the existing datasets of seabird occurrence known for the northwestern Atlantic." Data used in these reports originated from dozens of data sets including government agencies, academic scientists, non-government organizations, and private individuals and was estimated by the authors to contain more than 85% of the seabird occurrence data for the U.S. Atlantic known to exist. The data covers a broad area of the western North Atlantic, although the density of data is much greater from the Carolinas north to Maine. Some of these datasets overlap with data reviewed in Paton et al. (2010). These data represent about half a million observation records, including the Programme Integre Recherches sur les Oiseaux Pelagiques dataset for Canada, one of the largest seabird datasets available with more than 200,000 records. Data collection methods varied among data sources, so results are not all comparable.

A compilation of information on the common seabird species to be expected in the AOCS and in the vicinity of the ATOM deployment location is presented in Table 17. This list shows seabird species most frequently reported in the cited references. It is impossible to quantify the most frequently encountered species across the entire AOCS because no single reference exists for the entire AOCS area and surveys were not conducted in such as manner as to produce comparable results.

Table 17.

Seabird species frequently encountered in the AOCS, presented in alphabetical order.

Common Name	Scientific Name	References
Atlantic Puffin	*Fratercula arctica*	O'Connell et al. 2009
Audubon's Shearwater	*Puffinus lherminieri*	South FL Birding 2013
Band-rumped Storm-Petrel	*Oceanodroma castro*	South FL Birding 2013
Black Scoter	*Melanitta americana*	O'Connell et al. 2009
Black-capped Petrel	*Pterodroma hasitata*	South FL Birding 2013
Black-legged Kittiwake	*Rissa tridactyla*	Payne et al. 1984
Bridled Tern	*Onychoprion anaethetus*	South FL Birding 2013
Brown Booby	*Sula leucogaster*	South FL Birding 2013

Common Name	Scientific Name	References
Brown Noddy	*Anous stolidus*	South FL Birding 2013
Common Eider	*Somateria mollissima*	O'Connell et al. 2009
Common Loon	*Gavia immer*	O'Connell et al. 2009
Common Murre	*Uria aalge*	O'Connell et al. 2009
Cory's Shearwater	*Calonectris diomedea*	Payne et al. 1984; South FL Birding 2013
Dovekie	*Alle alle*	O'Connell et al. 2009; Payne et al. 1984
Great Black-backed Gull	*Larus marinus*	O'Connell et al. 2009; Payne et al. 1984
Great Shearwater	*Puffinus gravis*	Payne et al. 1984; South FL Birding 2013
Herring Gull	*Larus argentatus*	O'Connell et al. 2009; Payne et al. 1984
Laughing Gull	*Leucophaeus atricilla*	Payne et al. 1984
Leach's Storm-Petrel	*Oceanodroma leucorhoa*	Payne et al. 1984; South FL Birding 2013
Magnificent Frigatebird	*Fregata magnificens*	South FL Birding 2013
Masked Booby	*Sula dactylatra*	South FL Birding 2013
Northern Fulmar	*Fulmarus glacialis*	Payne et al. 1984
Northern Gannet	*Morus bassanus*	O'Connell et al. 2009; Payne et al. 1984
Pomarine Jaeger	*Stercorarius pomarinus*	South FL Birding 2013
Razorbill	*Alca torda*	O'Connell et al. 2009; Payne et al. 1984
Red Phalarope	*Phalaropus fulicarius*	Payne et al. 1984; South FL Birding 2013
Red-necked Phalarope	*Phalaropus lobatus*	Payne et al. 1984; South FL Birding 2013
Red-throated Loon	*Gavia stellata*	O'Connell et al. 2009
Sooty Shearwater	*Puffinus griseus*	Payne et al. 1984
Sooty Tern	*Onychoprion fuscatus*	South FL Birding 2013
Surf Scoter	*Melanitta perspicillata*	O'Connell et al. 2009
White-winged Scoter	*Melanitta fusca*	O'Connell et al. 2009
Wilson's Storm-Petrel	*Oceanites oceanicus*	Payne et al. 1984; South FL Birding 2013

7.1.2 Land Birds Expected

A recent compendium of offshore distribution of shorebirds (O'Connell et al. 2011) lists several species as migrating primarily over the Atlantic Ocean during at least one leg of their migratory journey. This information is based on expert opinion and not on surveys. Actual occurrence of shorebirds within the AOCS at elevations within a few hundred meters of sea level would be

expected to be highly variable based on the typical high flight of shorebirds during migration (Lincoln et al. 1998).

Most modern and systematic offshore surveys in the North Atlantic have produced few or no data on land birds. The earliest reports of land birds over the Atlantic were based solely on visual observations and were thus limited in scope to the lowest flying birds. Migration of songbirds over the Atlantic Ocean has been discussed in the ornithological literature since the early 1900s (Cooke 1904; Lincoln 1935; Baird and Nisbet 1960; others) and notes of land birds observed flying over the Atlantic have also been reported (Brown 1896; Baker 1947; Murphy 1915; Butler 1926; Penard 1926; others). Systematic but irregular expeditions from Woods Hole Oceanographic Institution from the 1930s through the 1940s documented land birds as well as seabirds in the North Atlantic from about 44° north latitude south to the West Indies (Scholander 1955). Many of these land birds were documented more than 200 mi offshore. Table 18 gives an example of some shorebird and passerine species reported in the literature mentioned above. Even more so than with seabirds, it is impossible to quantify the most frequently encountered land bird species across the entire AOCS because most sightings were incidental and for many species there are very few published records.

Table 18.

Shorebird and passerine species observed migrating over the Atlantic Ocean, presented in alphabetical order.

Common Name	Scientific Name	References
American Golden-Plover	*Pluvialis dominica*	O'Connell et al. 2011
American Redstart	*Setophaga ruticilla*	Scholander 1955
American Robin	*Turdus migratorius*	Scholander 1955
Baltimore Oriole	*Icterus galbula*	Scholander 1955
Bank Swallow	*Riparia riparia*	Paton et al. 2010; Scholander 1955
Barn Swallow	*Hirundo rustica*	Scholander 1955
Belted Kingfisher	*Megaceryle alcyon*	Scholander 1955
Black-and-white Warbler	*Mniotilta varia*	Scholander 1955
Black-bellied Plover	*Pluvialis squatarola*	O'Connell et al. 2011
Blackpoll Warbler	*Setophaga striata*	Paton et al. 2010
Black-throated Blue Warbler	*Setophaga caerulescens*	Scholander 1955
Buff-breasted Sandpiper	*Calidris subruficollis*	O'Connell et al. 2011
Cedar Waxwing	*Bombycilla cedrorum*	Scholander 1955
Common Yellowthroat	*Geothlypis trichas*	Scholander 1955
Dark-eyed Junco	*Junco hyemalis*	Paton et al. 2010
Dickcissel	*Spiza americana*	Scholander 1955
Eastern Meadowlark	*Sturnella magna*	Scholander 1955

Common Name	Scientific Name	References
European Starling	*Sturnus vulgaris*	Scholander 1955
Golden-crowned Sparrow	*Zonotrichia atricapilla*	Scholander 1955
Great Blue Heron	*Ardea herodias*	Scholander 1955
Hudsonian Godwit	*Limosa haemastica*	O'Connell et al. 2011
Least Flycatcher	*Empidonax minimus*	Scholander 1955
Least Sandpiper	*Calidris minutilla*	O'Connell et al. 2011
Marbled Godwit	*Limosa fedoa*	O'Connell et al. 2011
Mourning Dove	*Zenaida macroura*	Paton et al. 2010
Nashville Warbler	*Oreothlypis ruficapilla*	Scholander 1955
Northern Flicker	*Colaptes auratus*	Scholander 1955
Ovenbird	*Seiurus aurocapilla*	Scholander 1955
Prairie Warbler	*Setophaga discolor*	Scholander 1955
Red Crossbill	*Loxia curvirostra*	Scholander 1955
Red Knot	*Calidris canutus*	O'Connell et al. 2011
Rock Pigeon	*Columba livia*	Scholander 1955
Ruddy Turnstone	*Arenaria interpres*	O'Connell et al. 2011
Sanderling	*Calidris alba*	O'Connell et al. 2011
Savannah Sparrow	*Passerculus sandwichensis*	Paton et al. 2010; Scholander 1955
Semipalmated Plover	*Charadrius semipalmatus*	O'Connell et al. 2011
Semipalmated Sandpiper	*Calidris pusilla*	O'Connell et al. 2011; Scholander 1955
Slate-colored Junco	*Myadestes unicolor*	Scholander 1955
Snow Bunting	*Plectrophenax nivalis*	Paton et al. 2010; Scholander 1955
Solitary Sandpiper	*Tringa solitaria*	O'Connell et al. 2011
Spotted Sandpiper	*Actitis macularius*	O'Connell et al. 2011
Tree Swallow	*Tachycineta bicolor*	Paton et al. 2010
Whimbrel	*Numenius phaeopus*	O'Connell et al. 2011
White-crowned Sparrow	*Zonotrichia leucophrys*	Scholander 1955
White-rumped Sandpiper	*Calidris fuscicollis*	O'Connell et al. 2011
Willet	*Tringa semipalmata*	O'Connell et al. 2011
Yellow-breasted Chat	*Icteria virens*	Scholander 1955
Yellow-rumped Warbler	*Setophaga coronata*	Paton et al. 2010

7.1.3 Bat Species Expected

Much less is known about offshore bats than offshore birds. The three main long-distance migrant bat species in North America (Eastern Red Bat, Hoary Bat and Silver-haired Bat) are the species most often found off the east coast of North America. A recent synthesis of bat literature indicates that migratory bat species are as equally likely to be recorded offshore and at coastal or inland sites (Pelletier et al. 2013). While levels of observed activity offshore were comparable between migratory and non-migratory species, non-migratory species were less likely to be recorded offshore relative to the coastal or inland sites (Pelletier et al. 2013). Some studies indicate that Eastern Red Bats are perhaps the most active offshore (e.g., Pelletier and Peterson 2013; Carter 1950). Eastern Red Bats and Silver-haired Bats have been found on ships off the coast of New England (e.g., Carter 1950; Mackiewicz and Backus 1956). Silver-haired Bats, Eastern Red Bats, Hoary Bats, and Seminole Bats periodically occur in Bermuda (Van Gelder and Wingate 1961). More recently, Johnson et al. (2011) monitored activity on Assateague Island off the coast of Maryland and found that Eastern Red Bats made up 60% of all bat activity, followed by Big Brown Bats, Hoary Bats, Tri-colored Bats, and Silver-haired Bats. Activity was highest during the fall migration period (Johnson et al. 2011). Currently, Stantec Consulting is conducting a detailed study on bat activity over a wide range of sites off the coast of New England (Pelletier and Peterson 2013). Their 27 monitoring sites include islands, lighthouses, buoys, and ships, and the species composition was highly variable among sites. Eastern Red Bats had highest overall activity and were present at all sites, while Hoary Bats and Silver-haired Bats were present at fewer sites. Species of the genus *Myotis* were recorded at all but 3 of the 27 sites. Again, activity was highest during fall migration (Pelletier and Peterson 2013). See Table 19 for a list of reported species of bats found in the U.S. Atlantic Region.

Table 19.

North American bat species known to be active
offshore in the U.S. Atlantic Region.

Common Name	Scientific Name
Eastern Red Bat	*Lasiurus borealis*
Hoary Bat	*Lasiurus cinereus*
Silver-haired Bat	*Lasionycteris noctivagans*
Big Brown Bat	*Eptesicus fuscus*
Seminole Bat	*Lasiurus seminolus*
Tri-colored Bat	*Perimyotis subflavus*

7.2 Outline of Data Gathered by ATOM

Deployment of the ATOM system at the FPSLT was initiated on 6 Dec 2011. The system gathered thermographic, audible acoustic, and ultrasound acoustic data on the AOCS to facilitate assessment of risk to birds and bats from offshore wind energy development at the deployment location. Although data were gathered through all weather patterns and during the day and night,

data collection was not continuous during that time as a number of issues caused system malfunctions of various types, causing periods when one or more sensors did not gather data Table 20 reflects the data gathered and analyzed from the FPSLT deployment by each sensor, the results of which are presented here.

Data ingestion occurred at Normandeau's Gainesville, Florida, office and consisted of data upload to the ATOM-dedicated Linux server from the ATOM data storage system retrieved from the field. Drives containing copies of acoustic data were then forwarded to CLO for analysis. All other analyses occurred within the Gainesville office.

Table 20.

Total recording hours reviewed by month and ATOM system component showing nocturnal and diurnal composition.

Month	Thermographic Recording Hours			Acoustic Recording Hours			Ultrasonic Recording Hours		
	Total	Diurnal	Nocturnal	Total	Diurnal	Nocturnal	Total	Diurnal	Nocturnal
Dec 2011	126.74	53.63	73.11	153.49	66.53	86.96	518.45	251.15	267.3
Jan 2012	11.92	3.00	8.92	30.64	13.16	17.48	570.02	297.6	272.42
Feb 2012									
Mar 2012							336.75	201.28	135.47
Apr 2012	490.41	254.59	235.83	660.78	341.37	319.41	689.37	369.78	319.59
May 2012	284.83	164.87	119.96	493.95	285.85	208.10	538.63	309.4	229.23
Jun 2012	583.29	350.72	232.57	584.79	351.77	233.02			
Jul 2012	147.89	90.22	57.67	154.29	87.62	66.67			
Aug 2012	171.17	106.51	64.66						
Sep 2012	558.28	304.63	253.65	405.95	224.71	181.24			
Oct 2012	442.33	220.35	221.98	474.19	240.85	233.34			
Nov 2012				356.12	177.60	178.52			
Dec 2012				95.59	40.55	55.04			

7.2.1 Acoustic Analysis

Sound files were delivered to CLO five times during the study. Upon receiving each retrieval, the recordings were evaluated, processed, and copied to a central server for analysis. The sounds that were included in each delivery were grouped together for analysis in what is referred to as a Sound Retrieval (SR), a code to describe the dates included in an analysis. Analysis of SR-01

(recordings beginning 16 Nov 2011 and retrieved 03 Apr 2012) are discussed below. Date ranges represented by each SR along with information about recording effort are presented in Table 21.

Table 21.

Date range, total number of files, and total hours of recording effort captured in each of the sound retrieval periods.

Sound Retrieval Period	Date Range		Recording Effort	
	Begin Date	End Date	Total Files	Hours Recorded
SR-01	16 Nov 2011	3 Apr 2012	35	199.5
SR-02	03 Apr 2012	10 Jun 2012	133,952	1190.684
SR-03	10 Jun 2012	08 Jul 2012	54,022	480.1956
SR-04	08 Jul 2012	28 Oct 2012	60,148	534.6489
SR-05	28 Oct 2012	12 Dec 2012	62,200	552.8889
Grand Total	**16 Nov 2011**	**12 Dec 2012**	**310,322**	**2758.418**

Two analyses are focused on for the purposes of this report: (1) describe the passage of migrant songbirds during the recording period and (2) explore patterns of avian activity at the recording site.

As an initial test of the ability to process and analyze acoustic data collected from 06 Dec 2011 to 6 Jan 2012 and 1–3 Apr 2012 by the ATOM system was completed. This section of the report (a) provides an evaluation of data quality, identifies specific issues, and makes recommendations to resolve problems for future analyses; and (b) describes methods and results for two analysis techniques that were used to extract biological signals from the dataset.

Time was initially spent reviewing and spot-checking long-term spectrograms for potential problems. It became clear that high levels of noise at FPSLT, especially during some days, would likely impair the ability to locate biological signals either by automated detector or by analyst review. Also, it seemed likely that some of the environmental noise would potentially be an important source of false detections by automated detectors. Potentially problematic ambient sounds included:

1. **Low frequency sound**: Intense low frequency sound is prevalent. Frequently noise of this type is so powerful as to render frequencies below 2.5 kHz difficult to read (Figure 65). Noise is unevenly distributed among channels, which makes reading the spectrograms inconvenient using tools like XBAT, Raven, and Montage Tool, which apply global brightness and contrast settings. Channels 1 and 2 usually had the most intense low frequency sounds, while other channels have variable low frequency sound intensity. On low-intensity channels, spectrograms appear degraded with very few gradations in sound level represented in the color map. This phenomenon renders

spectrogram data difficult to interpret by a human analyst. Sound recorders commonly used by CLO employ high pass filters, which reduce the intensity of low frequency sound.

The amplitude of this low frequency sound varies considerably over time. Figure 66 and Figure 67 plot the Root Mean Square (RMS) amplitude for two 32-sec sound files each day, the one nearest midnight and the one nearest noon, as calculated using Raven. Sound is represented as a wave. The RMS is the square root of the mean distance over time, between the high peak and the lowest trough of the sound wave.

2. **Clipping**: Intense ambient noise distorts the audio waveform, making it difficult to evaluate. The waveform is a visual representation of the sound, and intense ambient noise sometimes results in clipping. Clipping makes spectrograms difficult to read and sounds difficult to interpret during playback (Figure 68).

3. **Broad-band Pulse**: Broad-band pulses, possibly caused by loose rope line or cable blowing in wind, are prevalent and a cause of false detections when using automated data template detectors (DTDs). Securing equipment that can generate noise when blown in the wind is essential for the effective use of automated sound detectors (Figure 69).
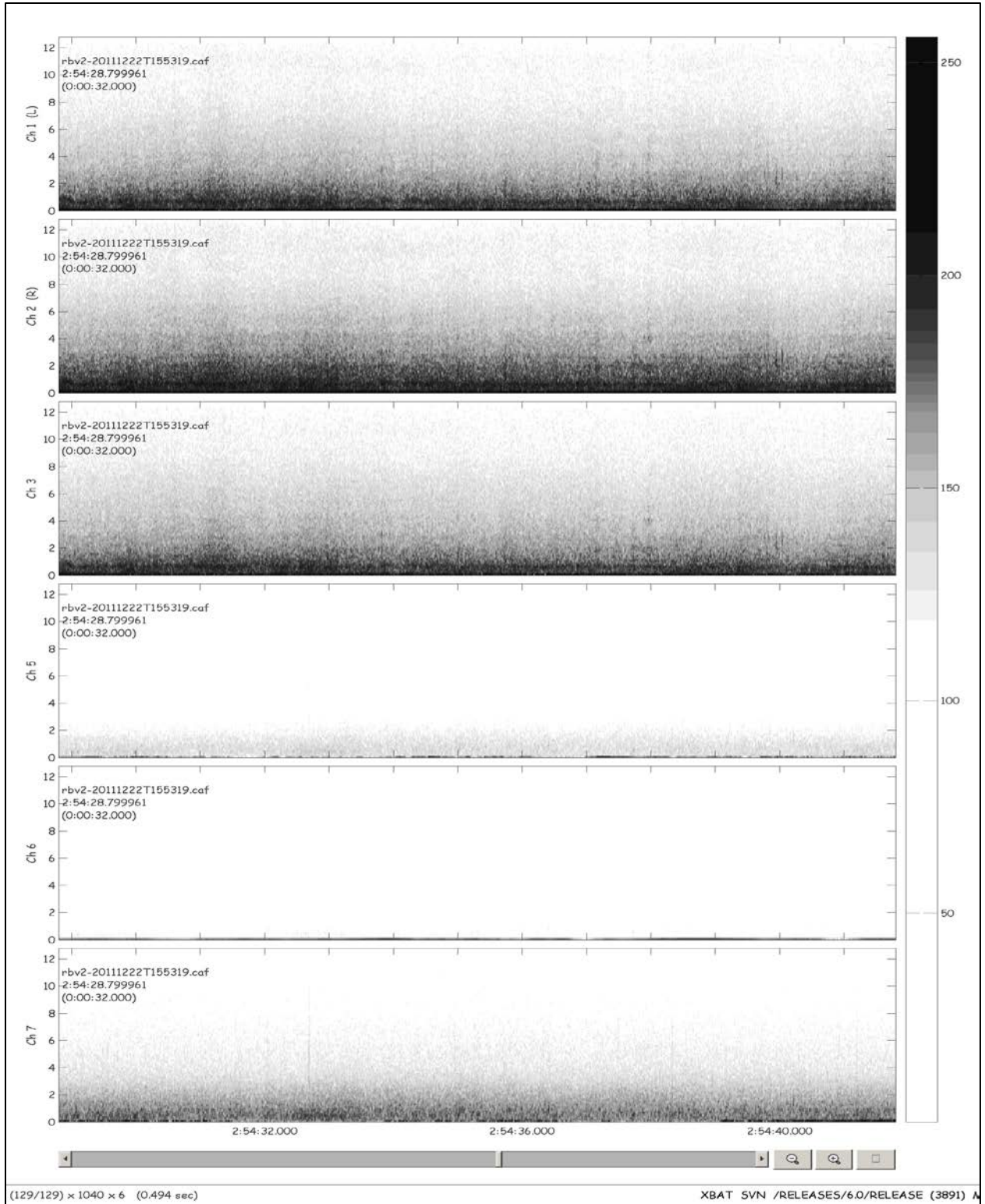
Figure 65. Spectrogram showing powerful low frequency sound with unequal distribution of sound intensity across channels.
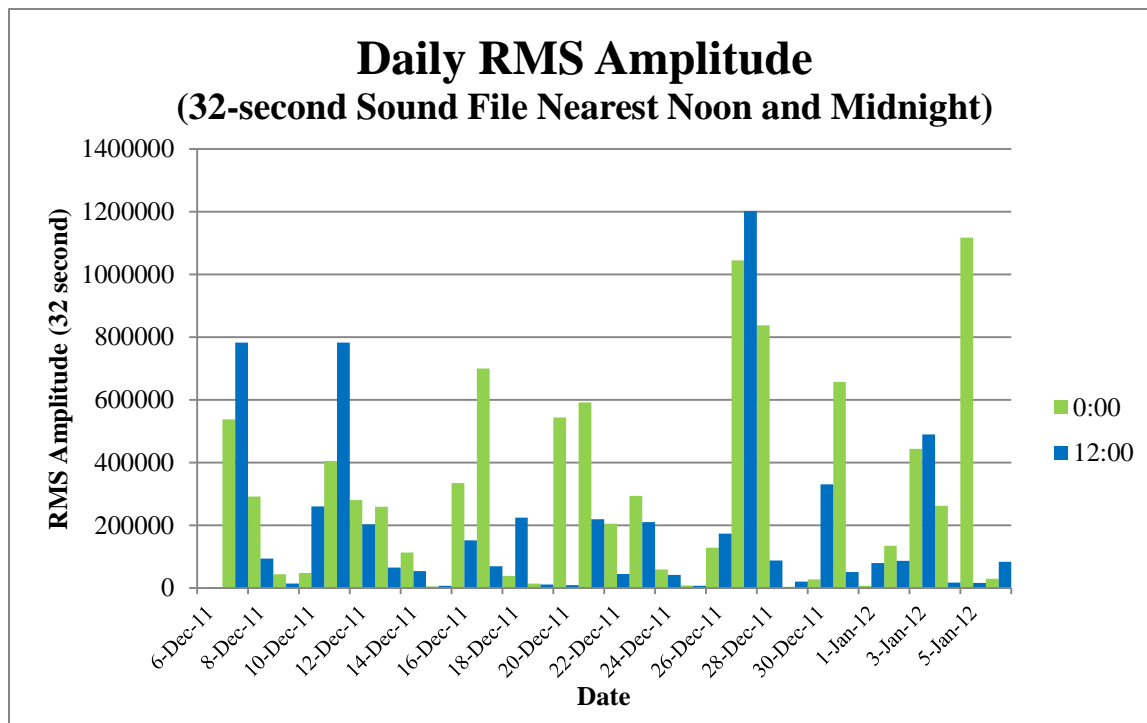
Figure 66. RMS amplitude for 32-second sound files nearest noon and midnight (6 Dec 2011–6 Jan 2012).
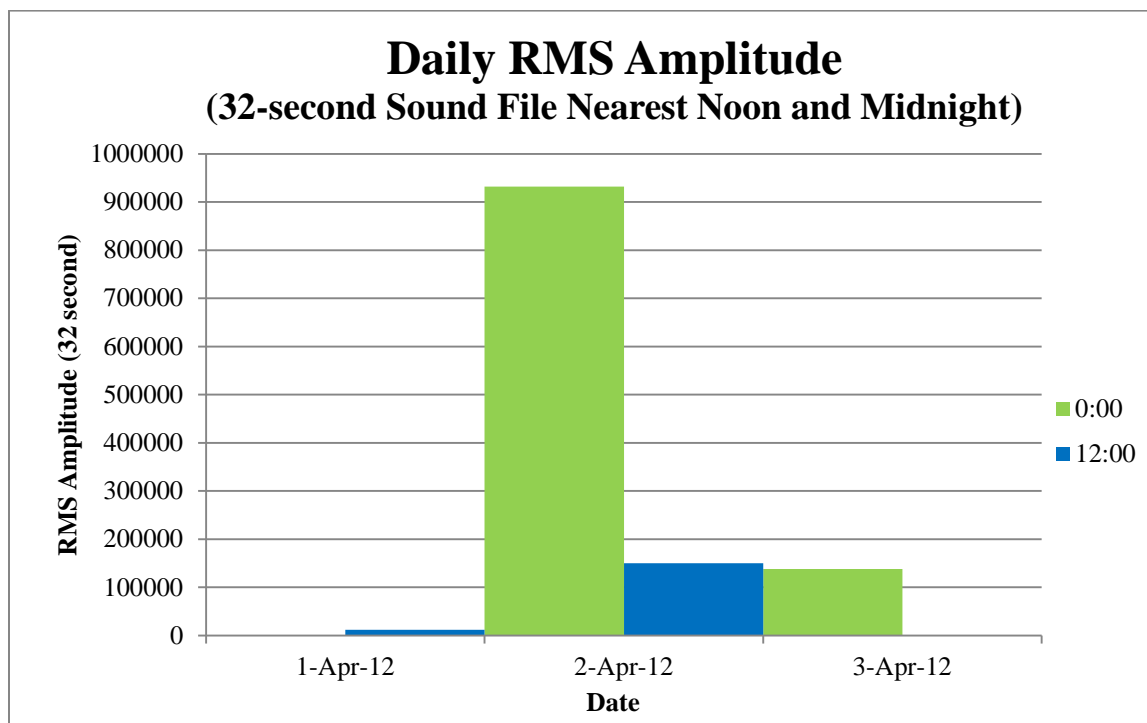
Figure 67. RMS amplitude for 32-second sound files nearest noon and midnight (1–3 Apr 2012).
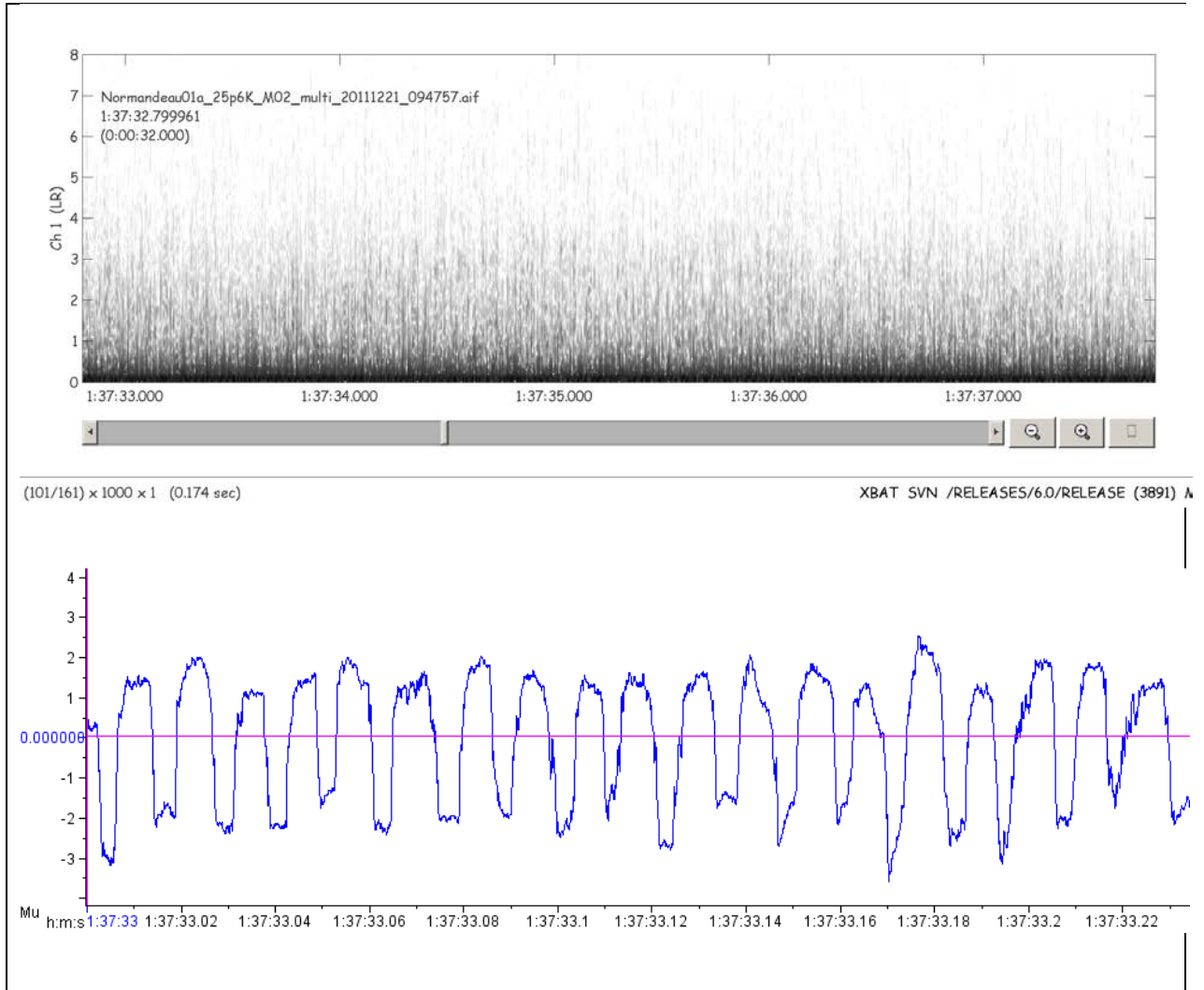
Figure 68. Graphical representation of clipping as a result of ambient noise.
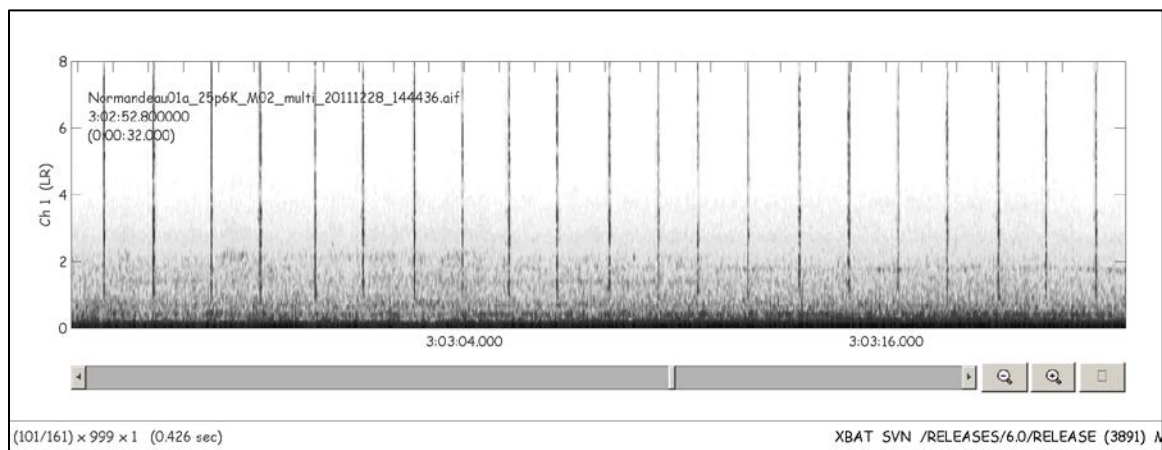
Figure 69. Broad-band pulses likely generated by loose rope line or cable blowing in the
            wind.

XBAT software was not immediately able to read files recorded by ATOM for several reasons. Below is a list of incompatibilities and software improvements that proved beneficial in future handling and analysis of ATOM data.

Three incompatibility issues (HTML files, damaged sound files, and the ability to read multi-channel CAF sound files) were found during the analysis of the FPSLT dataset and are detailed below.

1. **HTML file names**: The first drive sent by Normandeau was mounted in a Windows 7 system, but Windows Desktop was unable to copy files due to the presence of html files with names not compatible with Windows, for example "index.html?C=M;O=A.html." Files were copied using Windows Command Line.

   Windows cleared the problem the second time the drive was mounted by running CHKDSK without prompting the user, which renamed and moved the html files.

2. **Damaged sound files**: Fifteen CAF format sound files were unreadable by XBAT, causing MATLAB to hang without revealing the name of the problem files.

3. **CAF multi-channel read functionality**: Recordings from ATOM were delivered as 24-bit CAF files. All original sound files had a sampling rate of 25.6 kHz and eight channels. Because Raven, the sound analysis software used for browsing recordings, cannot read CAF files, it was necessary to convert all recordings to a different format before beginning the analysis. Audio Interchange File (AIF) format was used as it can be read by all of the software tools. SoX 14.4.0 (http://sox.sourceforge.net/), an open source command line utility, was used to perform the format conversion. To efficiently convert all files, a MATLAB routine was created that executed an SoX conversion command for every recording. Using SoX, it was possible to maintain the same sampling rate and preserve data on all eight channels. After conversion was complete, several files were randomly tested to ensure that the original and converted files were identical. This was accomplished by comparing the time signals and spectrograms of both signals and verifying that all values were the same.

ATOM recordings were also stripped of all but Channels 1 and 2 for two reasons:

1. Large differences in sound levels among channels triggered a bug in DTDs. Channels 1 and 2 had similar sound levels.

2. Human analysts focused only on Channel 1 to maximize their effort since there was so much similarity in sounds recorded on the various channels. Single channel sound can be viewed with less interface latency.

To strip channels, a MATLAB routine was used with SoX commands that are similar to the ones described above. Removing the unused channels significantly decreased detector processing time and the time needed to load files for hand-browsing. Also, this pre-processing step had the additional benefit of greatly improving DTD performance.

Several software modifications were identified as ways to address the incompatibility issues:

1. XBAT improvement: "sound_read" function should be able to handle defective sound files more gracefully, at the very least reporting the name of the defective file before failing, and failing without hanging MATLAB.

2. XBAT improvement: "get_schedule_from_files" function should report the names of any sound files whose time stamps are closer together than sound file duration should allow and fail to set up a duty cycle table.

3. XBAT bug fix: "get_schedule_from_files" function should address the rounding bug. Because a MATLAB datenum is involved in the calculation, resolution is on the order of 0.1 milliseconds (ms). This sometimes results in a large number of superfluous phantom duty cycles to be included in the recording schedule table, which slows XBAT performance and produces errors in sound browser function. It also makes the resolution of the recording schedule produced by XBAT to be worse than the extended time stamp format introduced by the Bioacoustics Research Program hardware team.

4. XBAT improvement: Report real date and time in duty cycle recordings without significant performance degradation, even when there are hundreds of duty cycles.

5. XBAT improvement: Read ISO 8601 time stamps (<yyyymmdd>T<HHMMSS>), as well as a more precise extended time format.

6. Raven improvement: Read CAF-format sound files with more than two channels.

7. AENA Noise Analyzer improvement: read CAF-format sound files.

Two techniques were used to analyze the data for presence of target birds species and other biological signals. One technique involved hand browsing a randomly selected set of 32-sec sound frames, while the other relied on using automated species specific XBAT DTD presets. The methodology and results for each approach are described below.

Stratified Random Hand Browsing

A portion of the ATOM data from FPSLT were "hand browsed." Hand browsing involves looking, in real time, at the sound recordings and marking events of interest. Hand browsing has the advantage of potentially finding all signals of interest and avoiding the technical glitches sometimes encountered with automated detection. It was not possible (practical) to hand browse the full 199 hours of data, so to reduce the work load in an unbiased way, ten 32-sec sound frames from each hour of the overall recording were selected. In other words, roughly 5 min from within every 60-min interval were analyzed. A total of 1,928 32-sec–long frames that occurred over 35 nights between 06 Dec 2011 and 06 Jan 2012 and 1–3 Apr 2012 was reviewed. This was a three-step process:

1. Using the Raven Selection tool, a data analyst (Klingensmith) hand browsed each of the 1,928 randomly selected 32-sec frames and marked all of the biological signals (events) found in the recording.

2. An expert in identification of avian vocalizations and flight calls (Tessaglia-Hymes) reviewed the biological signals and classified them to species or taxonomic group when signal quality prevented species-level identification.

3. A flight call expert (Farnsworth) summarized the results and compared them to results from automated DTDs.

In many cases, low signal quality and/or presence of intense ambient noise prevented a positive, species-level identification. Three example spectrograms from Klingensmith's hand browsing appear below in Figure 70, Figure 71, and Figure 72 as screen captures from Raven. Following those three figures, a summary table of acoustic events from Farnsworth appears in Table 22. Figure 70 shows an example of a relatively quiet portion of the day 20 Dec 2011 (20111220) with no detected bird events, a different time of day as the two events logged in Table 22 on row 20111220. In contrast, Figure 71 displays a noisy portion of the day 10 Dec 2011 (20111210) with both higher low-frequency noise (likely wind) and occasional broadband impulsive noises (likely a rope or line hitting something repeatedly due to the wind). This day logged no detections as shown in row 20111210 in Table 22. Figure 72 shows a bird call event against a quiet environment, found by both hand browsing and the preset as shown in row 062911 under day 20120403 in Table 22.
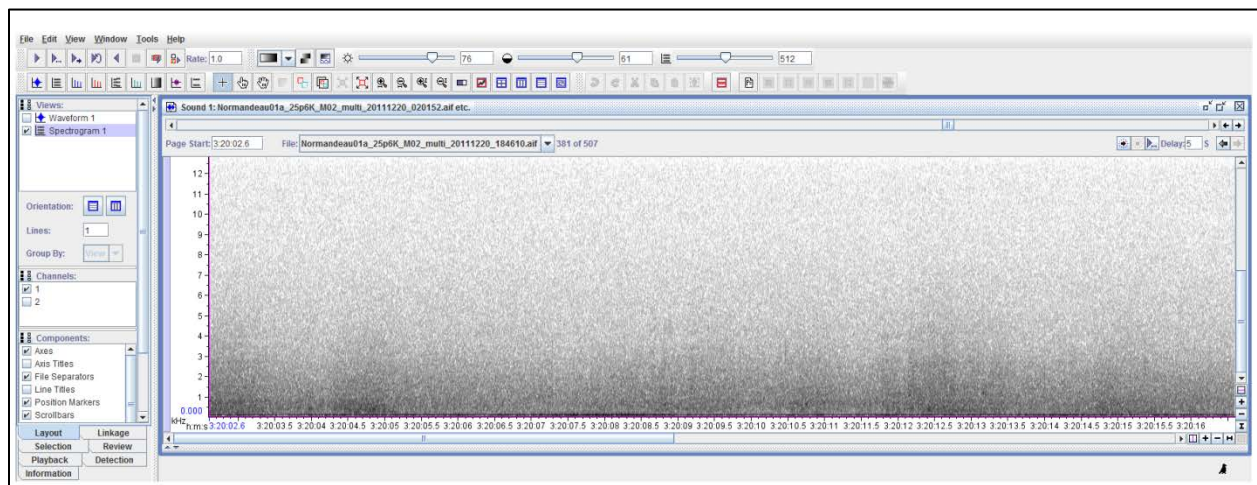
Figure 70. An example spectrogram of quiet background noise with no bird calls from 20 Dec 2011. Note that at a different time that day, two detections occurred as shown in Table 22.
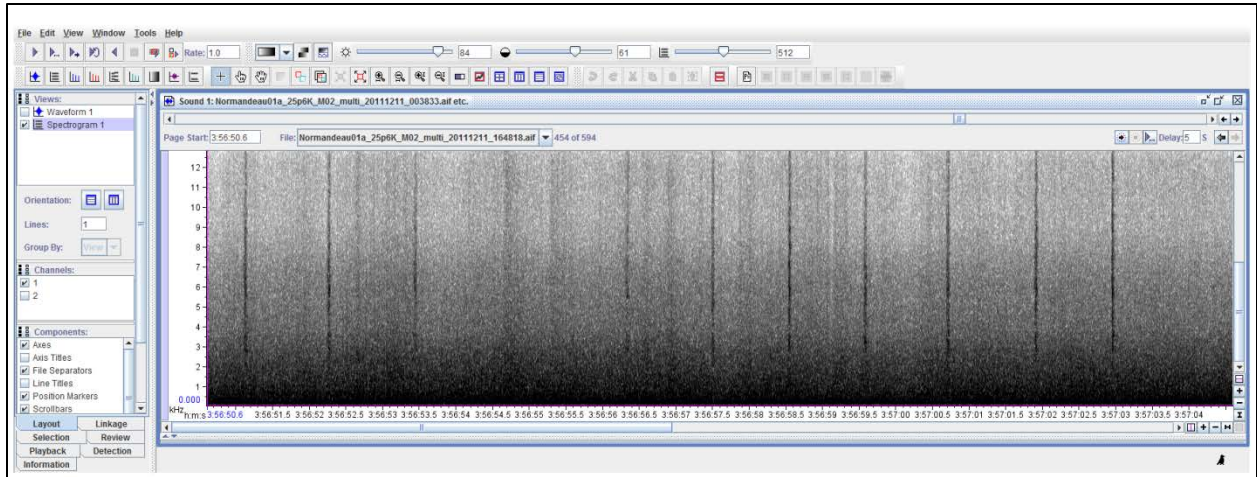
Figure 71. An example spectrogram of intense background noise with no bird calls from 10 Dec 2011. This date had no corresponding detections as reflected in the Table 22 summary.
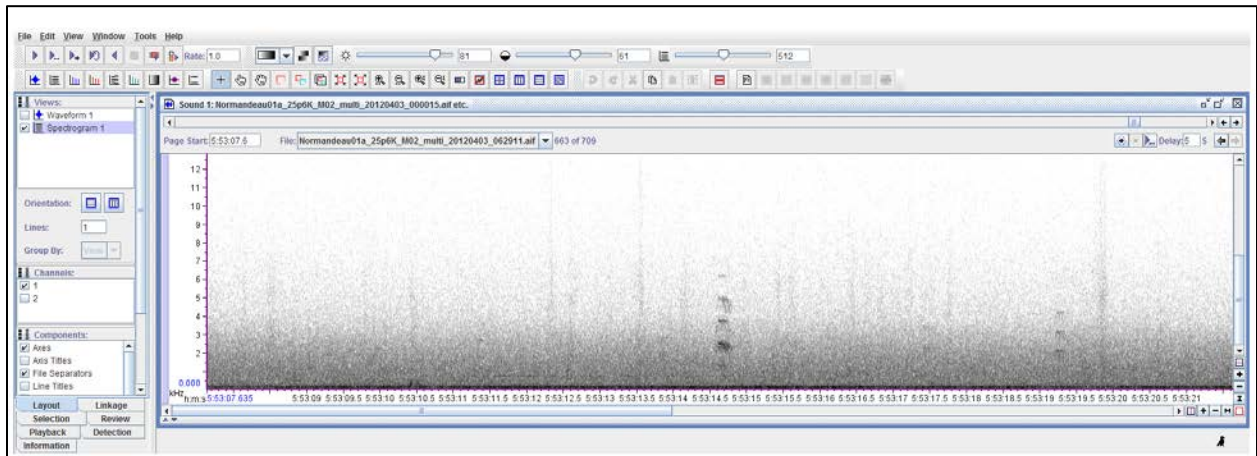
Figure 72. An example spectrogram of quiet background noise with bird calls detected both by hand browsing and by DTD preset as shown in Table 22, row 062911.

Table 22.

Summary of the human and preset detections from the FPSLT dataset showing details for one day (3 Apr 2012).

Labels	Overlapping Detections	Missed by Reviewer	XBAT Scores
Laridae	**4**		**4**
20111219	1		1
20111220	2		2
20111222	1		1
20120403			
054215			
Human			
Sternidae	**18**	**4**	**22**
20111207			
20111208	2		2
20111209	1		1
20111210			
20111214	1		1
20111215	3		3
20111216	2		2
20111217			
20111218			
20111220	2		2
20111222			
20111223			
20111224			
20120403	7	4	11
004636			
Human			
011742	1		1
Human	1		
REKN15a			1
015550			
Human			
060618	3		3
Human	3		
PIPL2a			1
PIPL3a			1
REKN15a			1
062319		1	1
Human			
REKN15a		1	1
062615			

Labels	Overlapping Detections	Missed by Reviewer	XBAT Scores
Human			
062911	1		1
Human	1		
REKN15a			1
063724			
Human			
064647	1	3	4
Human	1		
REKN9a			1
ROST6a		3	3
064757	1		1
Human	1		
REKN15a			1
Unknown			

Automated Data Template Detection

Given that the FPSLT data were collected during the winter months outside of the migration period, it is not surprising to find that automated DTD searches did not find target species in any of the recordings. Due to the absence of "target DTD species," only 0.1% of all detections from the hand browsed samples were represented by the top ten high scoring events found by DTD. Overall, 2.25% of detections flagged by DTDs overlapped with those found by human analysts. None of these were target species. DTDs did, however, detect 18 instances of sternid vocalizations, an appropriate confusion species (family) for the target species DTDs. The Piping Plover and Red Knot DTDs found four instances of larid vocalizations that were also found by human analysts despite no gulls on the list of likely confusion species for the plover and the knot. Only one event found by analysts was among the 10 highest scoring events found by DTD. This highlights the challenge of applying DTD in noise-rich environments. Of note, however, were four call detections from DTD in the random data set that human reviewers missed. This suggests that DTD can be quite effective in flagging events when noise thresholds are low. Future success with DTD technology will rely on better management and understanding of the noise environment. Furthermore, there were inherent problems in the FPSLT ATOM data that prevented the effective use of DTDs.

The process of creating the species specific DTD presets and the difficulties encountered with using DTDs on the ATOM data from FPSLT is described below.

SoundXT Preset Creation for the Five Target Species

SoundXT presets for each target species were automatically created from SoundXT's template ranking algorithm. These presets were created by inputting the truth log for each species into SoundXT, then creating a preset from the subset of calls that were found to represent the variation of the entire dataset. The SoundXT preset for American Redstart originally contained 81 exemplars, but the size was limited to 15 exemplars to minimize detector computation time. Table 23 shows the properties of the automatically created SoundXT presets. Spectrograms of

the templates that compose each SoundXT preset are shown in Figure 73. Each of these templates is a sound clip that was input to the tool and automatically added to the preset.

Performance characteristics of the SoundXT presets are shown in Figure 74 and Figure 75. The detector threshold refers to a cutoff parameter of the automated DTD (data template detector). Figure 74 and Figure 75 show the true positive rate for a given threshold setting of the DTD.

Figure 74 shows the true positive rate, or the number of flight calls correctly detected, as a function of the detector threshold. In order to obtain these performance measures, the SoundXT presets were run on the Macaulay Library recordings for each species. Because the Macaulay Library files had been "truthed" by flight call experts, this was a reliable method for measuring true detections. Figure 75 shows the number of false detections per hour as a function of detector threshold. These plots were created by running the SoundXT presets on the ATOM FPSLT data.

Table 23.

SoundXT preset properties for each of five target species.

Template Name	Alpha Code	Number of Templates	Mean Bandwidth (kHz)	Mean Center Frequency (kHz)	Mean Time Duration (ms)
American Redstart	AMRE	15	2.48	7.03	93
Piping Plover	PIPL	6	1.54	1.97	358
Red Knot	REKN	9	1.61	1.34	211
Roseate Tern	ROST	13	1.99	2.86	284
Swainson's Thrush	SWTH	8	4.76	3.12	423

a) American Redstart

b) Piping Plover

c) Red Knot

d) Roseate Tern

e) Swainson's Thrush
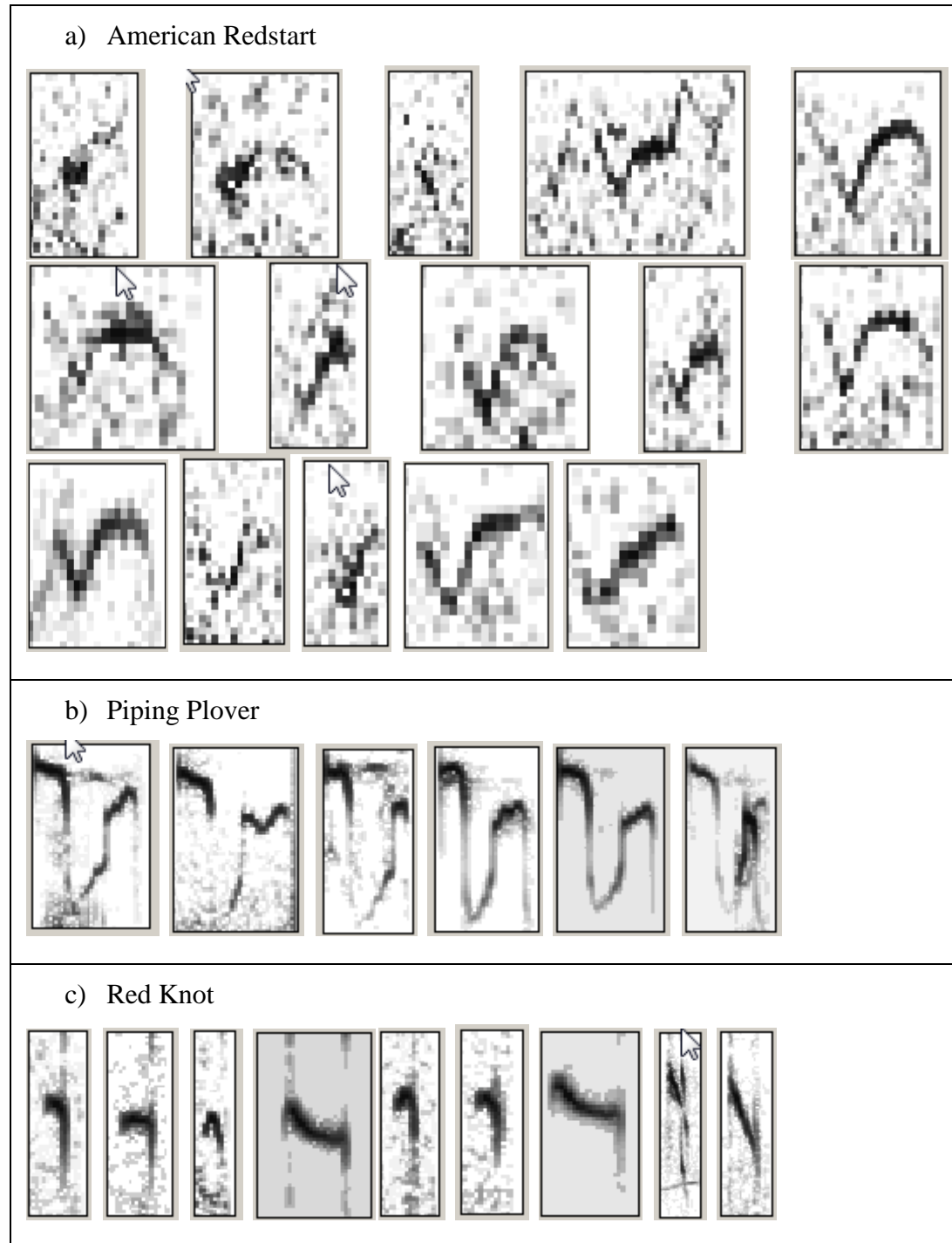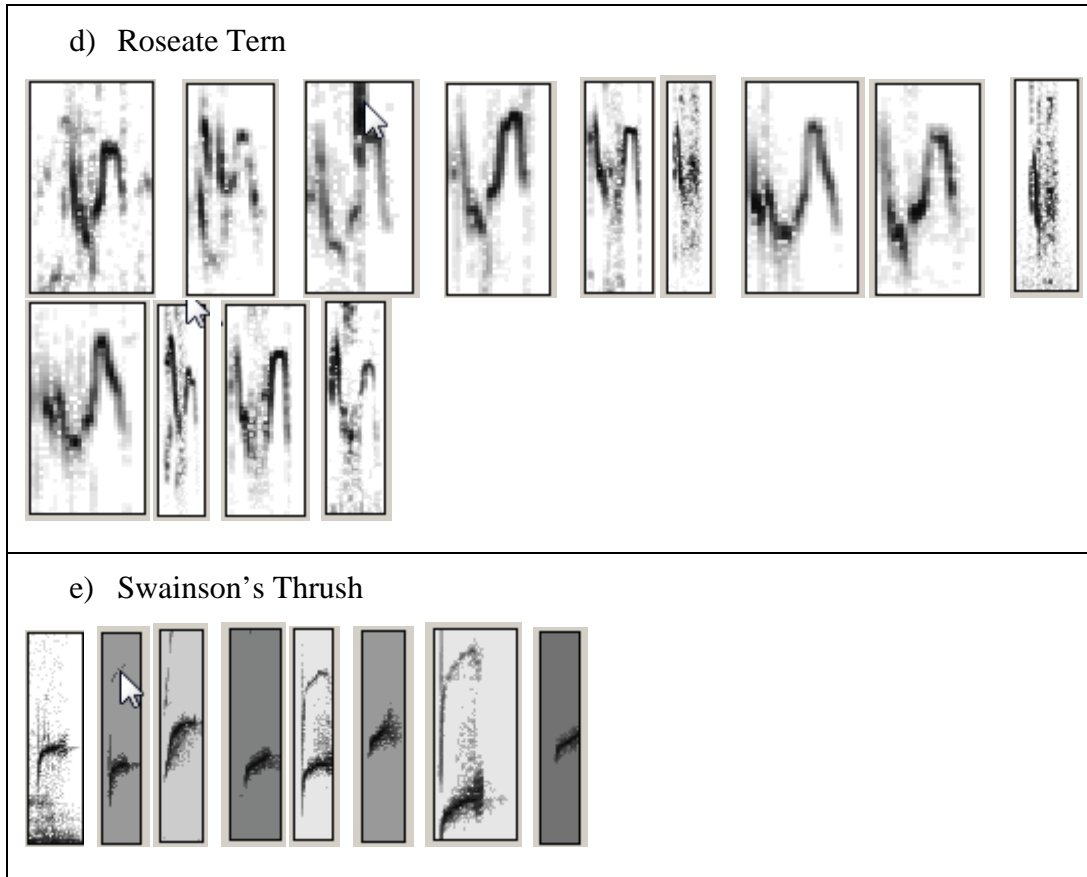
Figure 73. Spectrograms of SoundXT preset templates for five target species.
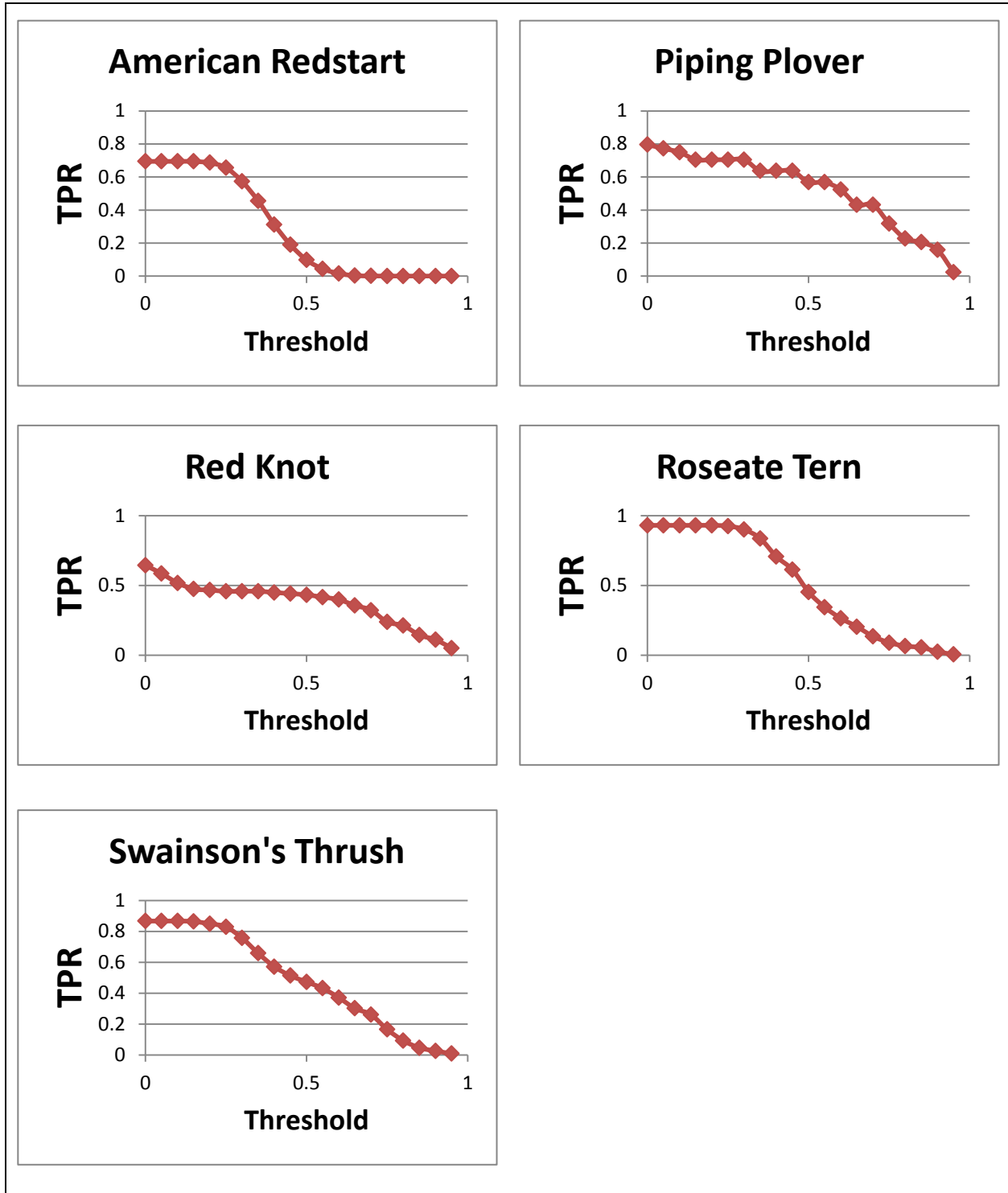
Figure 74. Plots of the number of flight calls correctly detected versus detector threshold for each SoundXT preset.
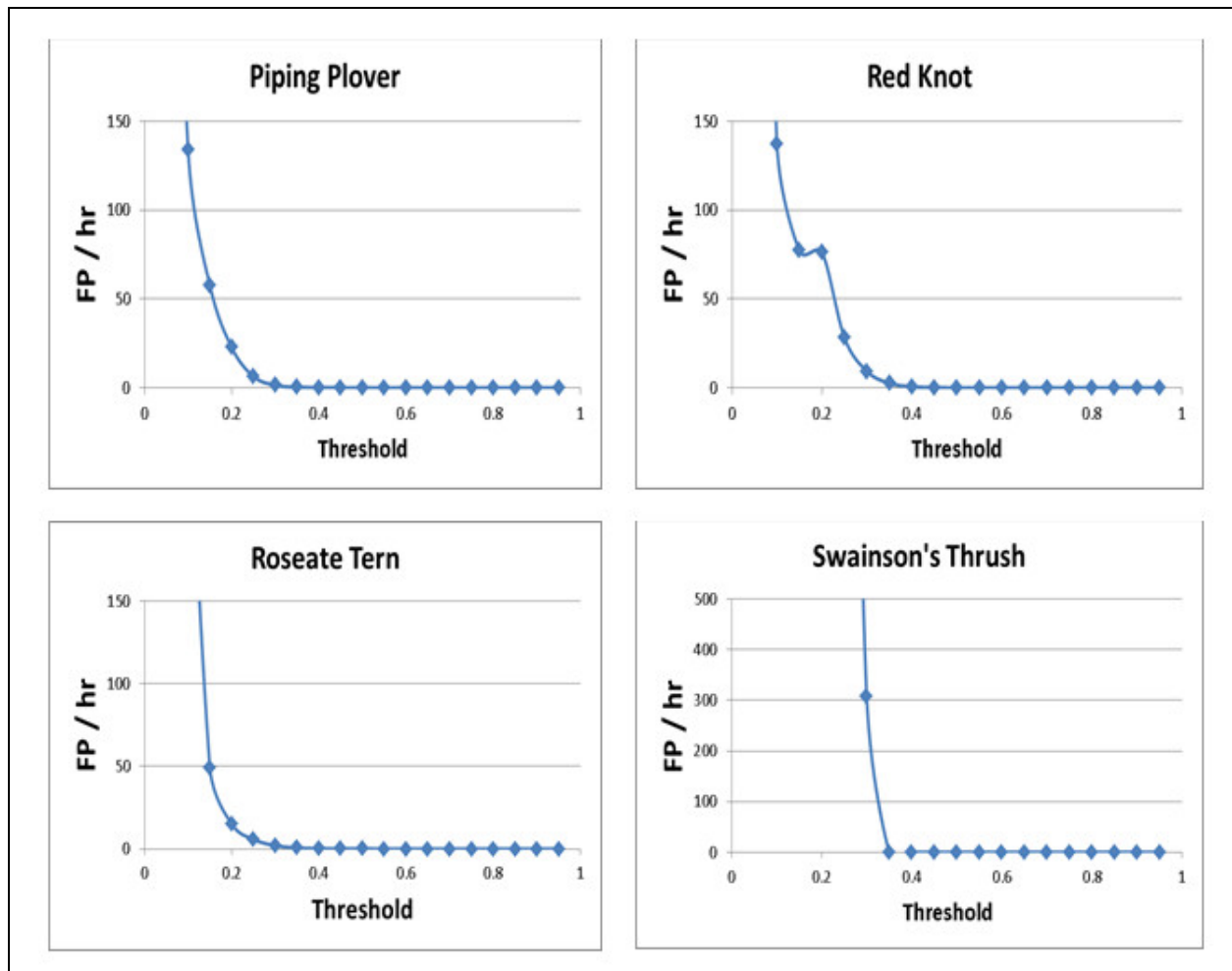
Figure 75. Plots of the number of false positives (FP) per hour versus detector threshold for each SoundXT preset.

Hand-built Presets for Four of the Five Target Species

Hand-built presets were created for American Redstart, Piping Plover, Red Knot, and Roseate Tern. These presets were created by hand browsing truth logs and selecting exemplars that appeared to represent typical flight call structure. When hand building presets, research analysts create potential presets, run trial detections on segments of sound files, and then modify presets as needed. Analysts aim to keep the number of templates in each preset small to avoid impairing detector speed. Table 24 lists properties of the hand-built presets for four target species.

Figure 76 contains spectrograms of the templates that are contained in each hand-built DTD preset. When building presets by hand, analysts have the option to only use a portion of a flight call as a template rather than an entire call. This is advantageous in cases where flight calls have stereotyped segments with high power because spectrogram correlation scores can be increased when using only these segments and omitting surrounding noise. Figure 77 and Figure 78 show performance characteristics of the hand-built presets, which were calculated using the method described above.

Table 24.

Hand-built preset properties for four of the five target species.

Template Name	Alpha Code	Number of Templates	Mean Bandwidth (kHz)	Mean Center Frequency (kHz)	Mean Time Duration (ms)
American Redstart	AMRE	10	1.73	6.62	55
Piping Plover	PIPL	7	0.698	2.49	328
Red Knot	REKN	9	1.22	1.79	138
Roseate Tern	ROST	7	2.08	3.04	248

a) American Redstart

b) Piping Plover

c) Red Knot

d) Roseate Tern
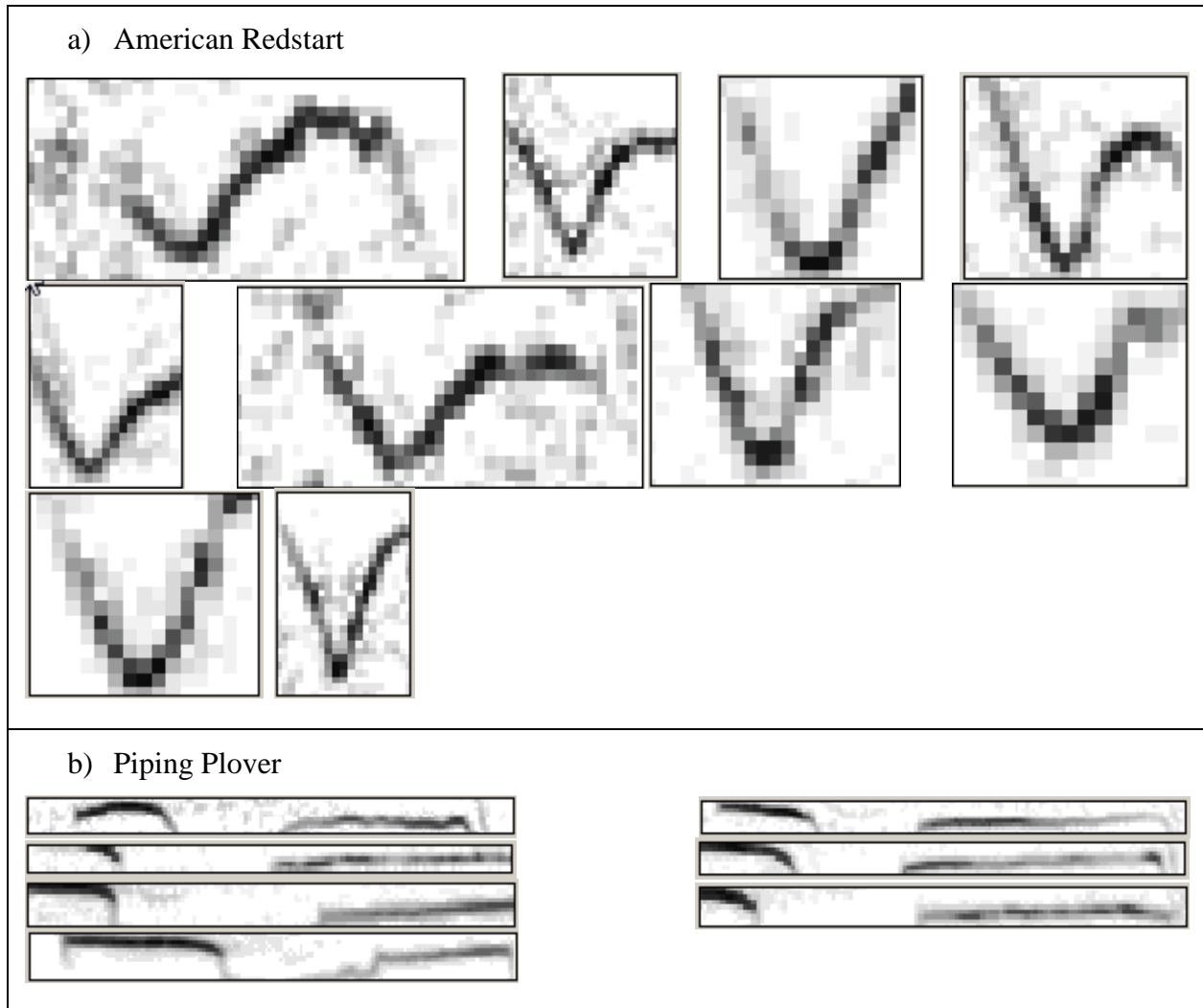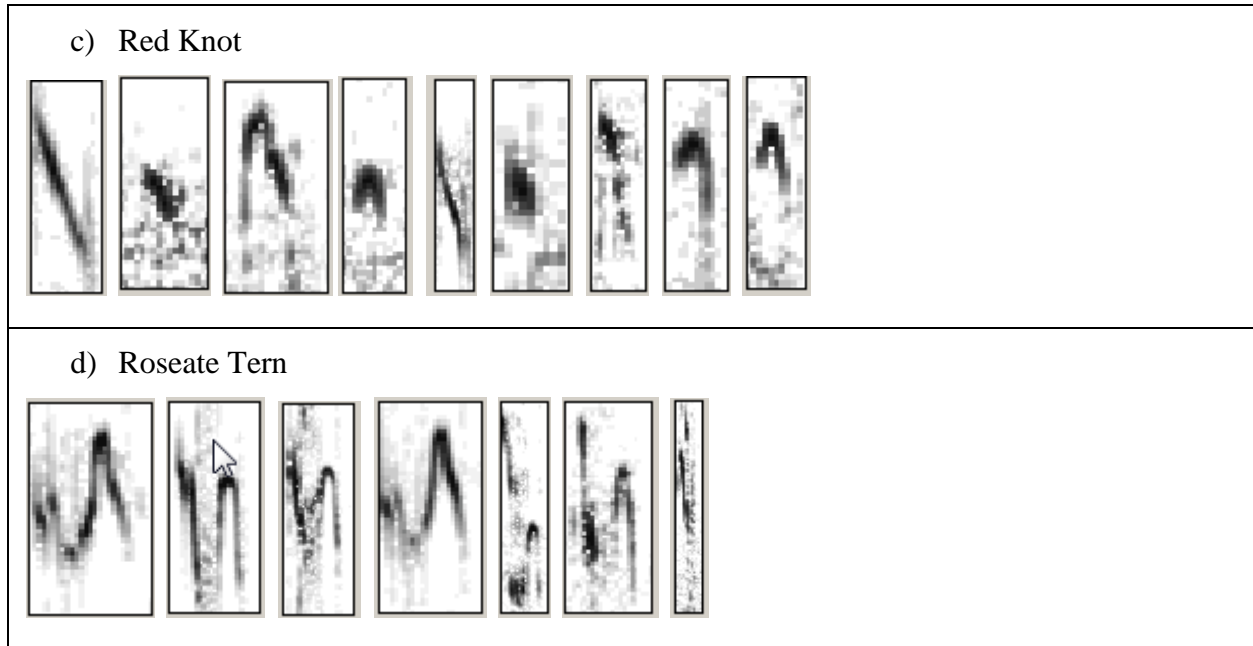
Figure 76. Spectrograms of hand-built preset templates.
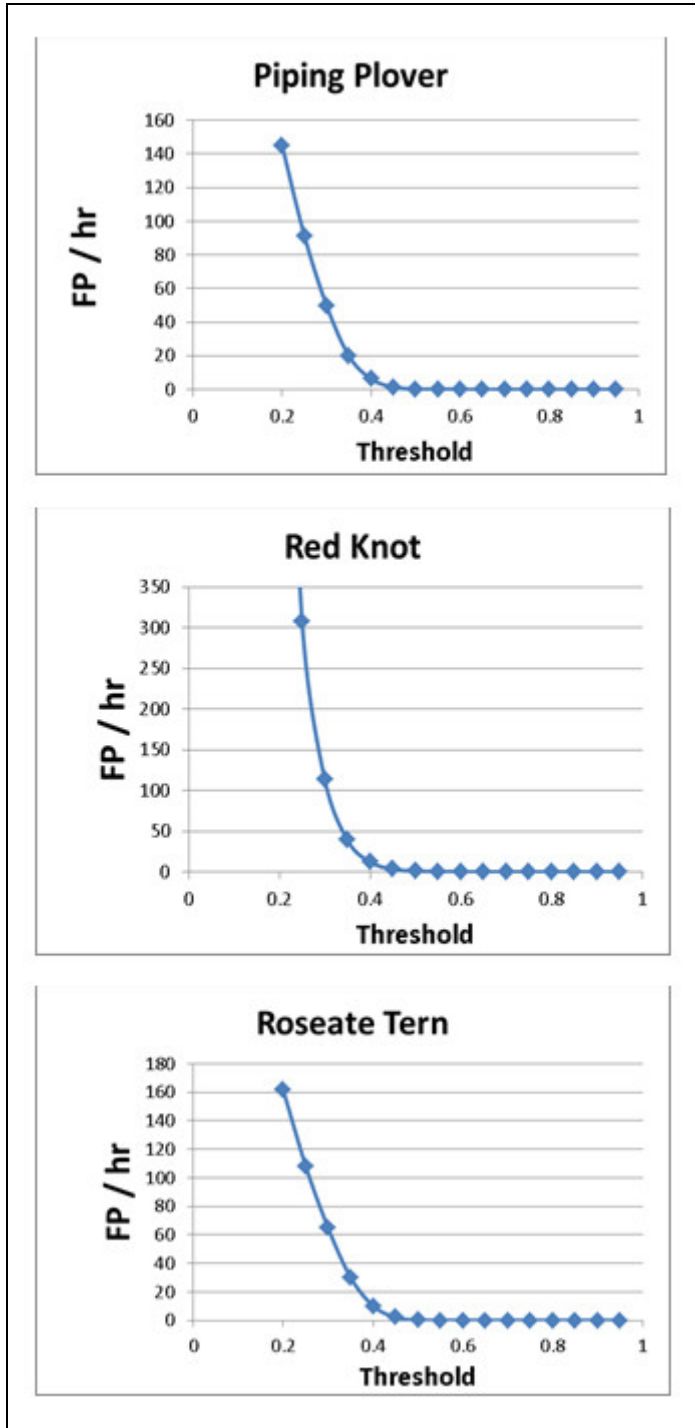
Figure 77. Plots of the false positive rate (FPR) versus
detector threshold for each hand-built
preset.
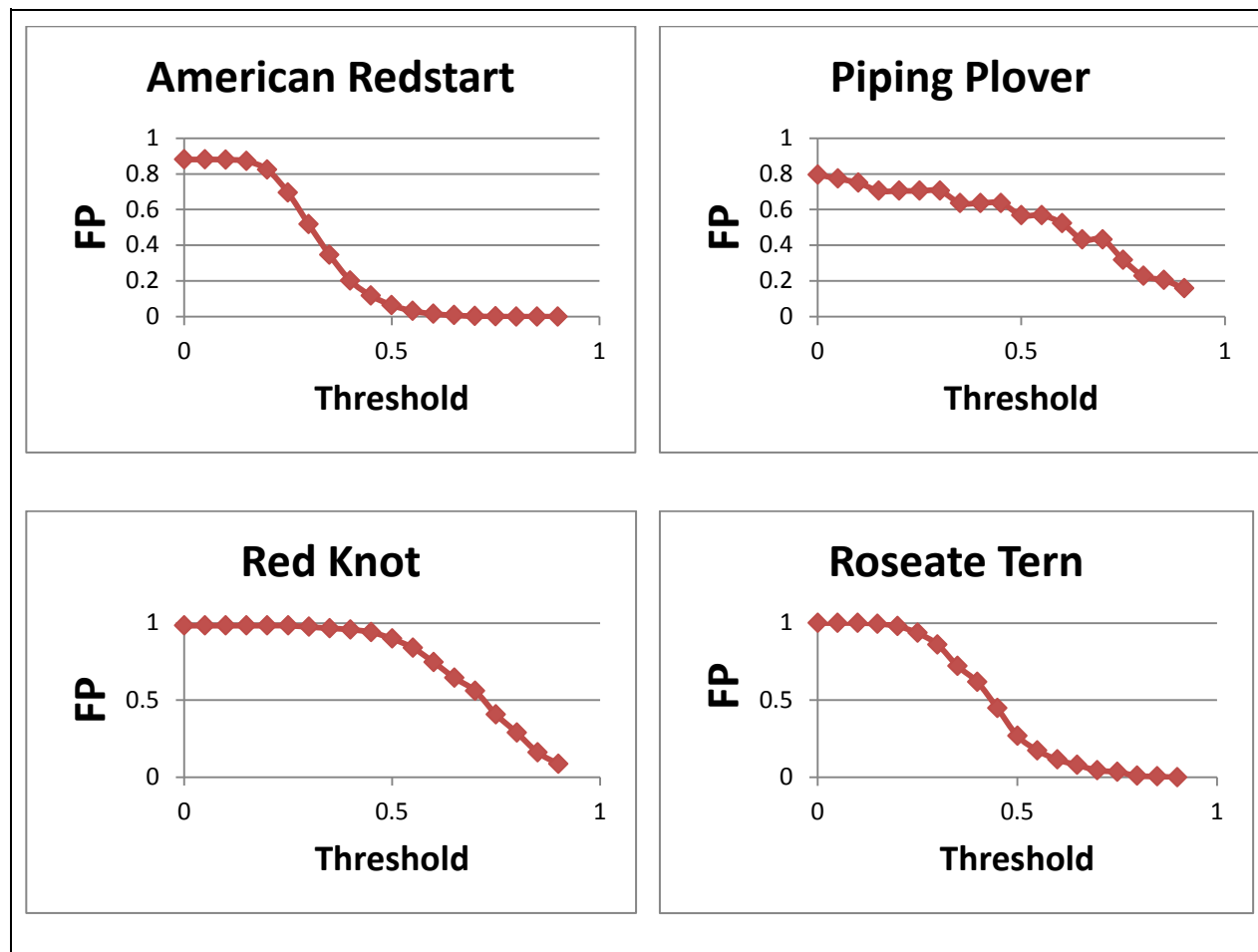
Figure 78. Plots of the number of false positives (FP) per hour versus detector threshold for each hand-built preset.

Challenges: XBAT Data Template Detector Issues

While using XBAT's DTD with the presets described above, the program often calculated correlation scores greater than 1.0 when comparing a spectrogram of an exemplar template to a spectrogram of a field recording. Correlations scores should be between -1 and 1. These incorrect correlation scores were caused by running the detector on sounds that had segments of extremely low power. The FPSLT recordings contained multiple periods of low power because several channels did not have microphones connected and therefore contain low power random noise. There were also periods of silence in the field recordings due to duty-cycling and occasional power outages. It was possible to delete the unused channels from the sound files but not the segments of silence. Unfortunately, these segments resulted in multiple false detections in the FPSLT dataset, meaning that detection algorithms had to be modified to process these data.

The XBAT DTD functions by correlating spectrograms of exemplars with spectrograms of small clips of the main sound file. This is repeated until the exemplar spectrogram has been correlated with sound file spectrogram at all possible time lags. When XBAT performs spectrogram correlation, the result is a vector of correlation scores in the range of [-1-1]. Each entry in this

vector describes how well the spectrogram matrices are correlated at the corresponding lag. The correlation vector is then normalized, and the vector peaks are located. If these peaks are above the user-selected threshold (a value between 0 and 1), then an XBAT event is flagged at the corresponding time in the sound file.

Upon running the DTD on the FPSLT data, XBAT returned many erroneous detections that occurred in areas of the spectrogram containing no noticeable flight calls or peaks in power (see Figure 79). Most often these detections were on channels that were not connected to microphones or they occurred when recorder power was cut. Despite the low power values within the boundaries of these events, the detector correlation scores often greatly exceeded 1 (see Figure 80), frequently falling in the range of 500 to 10,000. Because the data template detector had not previously been used on recordings with segments of silence or unconnected channels, this error had never before been observed in XBAT.

These impossibly high scores were clearly inaccurate and the precise source of the problem must be identified in the XBAT software. Multiple test runs revealed that the problem only occurred when sound files contained segments of very low power. After discovering that low power segments elicited incorrect scores, the spectrogram correlation algorithm was examined in order to determine why this occurs and to pinpoint where the error is located.

On the recordings made from 03 Apr (beginning of SR-02) through Dec 2012 (end of SR-05), two analyses of migrant songbirds were focused on: (1) describing the passage of migrant songbirds during the recording period and (2) exploring patterns of avian activity at the recording site.
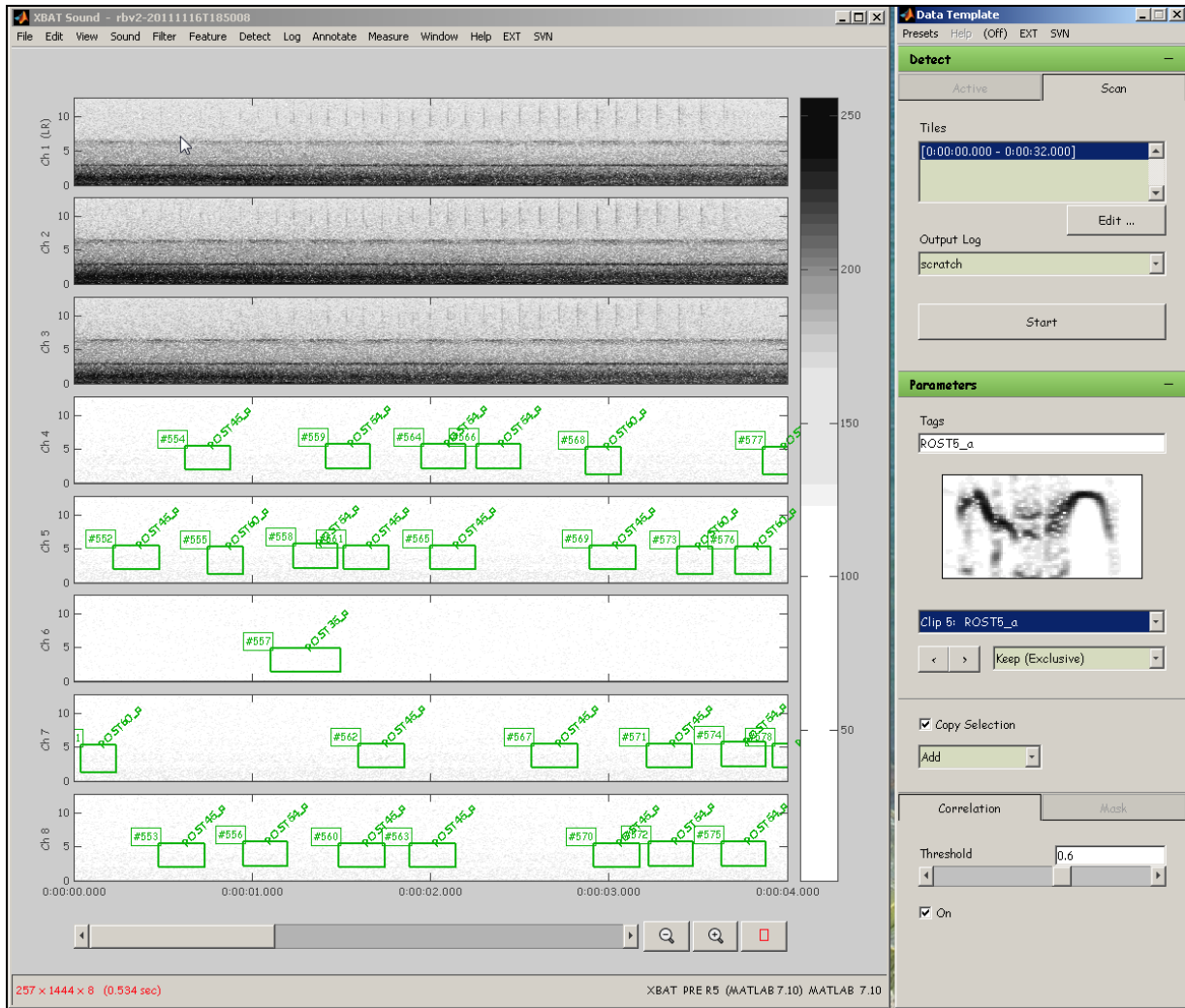
Figure 79. An XBAT sound window and the user interface for the DTD showing green boxes where the detector found events.
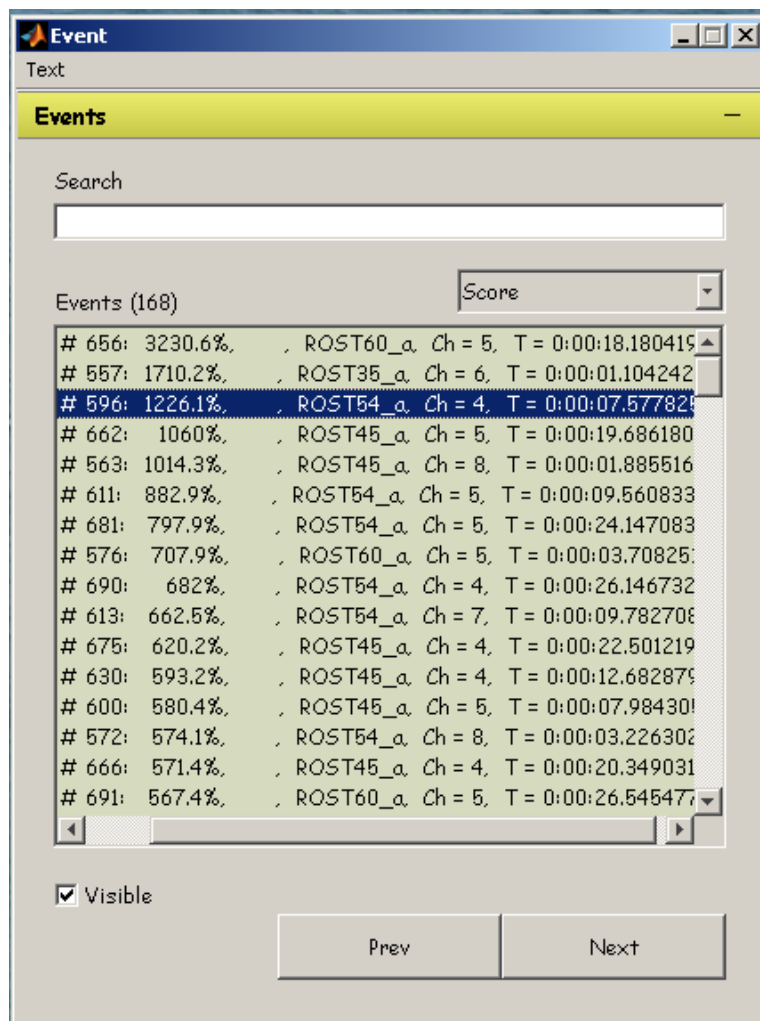
Figure 80. The XBAT event palette listing all events found
by the DTD. The correlation score is printed
immediately after the event number.

Nocturnal Flight Call Analysis

Nocturnal flight calls (NFCs) are species-specific vocalizations, either frequency-modulated or
pure, of up to several syllables that generally are in the 1–11 kHz frequency band and 50–300 ms
in duration. These calls are the primary vocalizations given by many species of birds during
long, sustained flights characteristic of nocturnal migration (Evans and O'Brien 2002). Flight
calls are distinct from songs and, more importantly, they are distinct from other types of short
calls such as "chip" notes and alarm calls. For a complete overview of NFCs, see Farnsworth
(2005).

Raven Pro Sound Analysis Software v.1.5 (Bioacoustics Research Program 2013) was used to
process and analyze the sound recordings using two different Band Limited Energy Detectors to
detect possible NFCs in two discrete frequency ranges: a high range encompassing 6000–11000
Hz to capture sparrows and warbler calls and a lower range between 2250–3750 Hz to capture

thrushes, shorebirds, and other species (Table 25; see Evans 1994; Evans and Rosenberg 2000; and Farnsworth et al. 2004 for reasoning behind two frequency ranges).

Table 25.

Band Limited Energy Detector parameters used to detect potential nocturnal flight calls in high- and low-frequency bands.

Parameters		High Band	Low Band
Target Signal Parameters			
Frequency	Minimum (Hz)	6000	2250
	Maximum (Hz)	11000	3750
Duration	Minimum (ms)	21.25	30
	Maximum (ms)	501	500
Separation	Minimum (ms)	27	20
Signal-to-Noise Ratio Parameters			
Occupancy	Minimum (%)	20	20
	SNR Threshold (dB)	1.0	2.5
Noise Power Estimation			
	Block Size (ms)	1002	1000
	Hop Size (ms)	250	250
	Percentile	50	50

In previous projects automated detection algorithms that were designed to detect NFCs while limiting the number of false positives were used, allowing efficient processing of large datasets. The natural downside is that such a process necessarily limited the number of true detections, often capturing only the most pristinely recorded calls and missing fainter or more distant calls. Implementation of a Random Forest (RF) model allows the use of more permissive detectors, thereby capturing more true positives. Previous, more-restrictive detectors were altered by decreasing the SNR parameters with additional, small changes made to Target Signal parameters and Noise Power estimations. The detector trials were done on single night recordings that had been hand browsed to identify all night flight calls. Detection results were compared to the truth tables, allowing meaningful evaluation of detector performance.

To further improve efficiency in reviewing the high number of false detections, an RF model (Liaw and Wiener 2002) was used to rank the likelihood a given detection was an actual flight call. The high-band and low-band models included in the R package flightcallr, which are assembled from data at 13 terrestrial deployment locations, were used. The scores from these models were used to rank the probability a detection was a true call or a false positive.

The RF model reliably ranks flight calls highly compared to clutter and noise that are also detected, and for this reason all ranked detections (which number in the millions) are not evaluated. The variability in recording quality (which impacts the score assigned by the model) precludes use of a specific score as a cut-off as the variability in the number of detections precludes use of a specific number of detections to review. To ensure that no pockets of calling activity were missed, an analyst reviewed no fewer than 10,000 (preferably 20,000) events. If no flight calls were found in at least 100 of the next-ranked candidates, there were likely no identifiable calls below that score. As an added precaution, several thousand additional lower ranked detections were spot-checked to determine if there were low-ranked calls mixed in with the clutter and noise. In no cases did this additional review reveal any calls.

Based on previous work, review of the top 1% of the top-ranking detections, as ranked by the RF model, sufficiently captures the vast majority of true positives. In this analysis, acoustic analysts reviewed the top 1% of the ranked detections, which encompasses tens of thousands of candidate calls, confirming each as true calls or noise. All true calls were annotated to the most specific taxonomic level possible. Classification was dependent on the quality of the recorded call coupled with the intricacies of flight call identification, specifically the potential confusion between similar looking and sounding species. Calls were identified to the lowest taxonomic level possible based on the spectrographic and audible information. For example, the flight calls of Yellow Warbler and Blackpoll Warbler can be difficult to separate with certainty, in which case they are reported at the genus level, *Setophaga* sp. See Appendix 3 for a list of species and higher-order taxonomic groupings used in this report.

Activity Analysis

The second focus of the analysis was to determine if there were any discernible patterns in avian activity at the recording site. One challenging aspect of reviewing the candidate NFC detections was the sheer number of false detections due to presence of terns and gulls. When present, their vocalizations often obscured the spectrogram so completely it was nearly impossible to visualize any other calls. Based on this observation, a sampling regime was designed that yielded valuable information regarding patterns in activity with the assumption that periods of high vocalization counts equate to periods of high numbers of birds or increased activity of birds. To determine where periods of high activity occurred, an analyst evaluated two randomly selected 32-sec sound files per recorded clock hour and assigned each block one of four possible categories (Table 26).

Table 26.

Definitions of annotations to describe contents of randomly selected blocks throughout the deployment.

Annotation*	Definition
NFC	At least one possible flight call present in the block, but no other avian calls
OtherAvian	At least one non-flight call is present in the block, but no true flight calls are present
NFC & OtherAvian	At least one possible flight call is present in the block, along with at least one non-flight call
Not of Interest	No avian calls of any kind appear in the block

* If OtherAvian was included in an annotation, the analyst made an assessment about the level of activity during the block of sound.

Only complete sound file blocks were used (32-sec duration) as shorter files were corrupt and unreadable by the sound analysis software. Each block was assigned to a clock hour based on the start time of the sound file. A MATLAB script randomly selected two blocks from the pool of available blocks in each clock hour (even if the hour was missing some of the expected sound files) and wrote them to an XBAT log, which was converted to a Raven selection table for analyst review. In cases where there were two or fewer sound files in an hour, all available sound files for that hour were used. Where sound files contained non-flight call vocalizations (OtherAvian annotation), the analyst subjectively determined whether the extent of calling amounted to high vocal activity or not. Examples of high vocal activity (high activity of birds) included spectrograms filled with numerous calls that reveal multiple birds calling repeatedly in the area (Figure 81, A and B). Calls appear as stacked, dark lines of variable duration; their intensity (dark or faint) indicates how well the call was recorded. Spectrogram A (top) shows relatively faint calls that appear blurred and run together, indicating multiple individuals that are some distance away from the microphone. Spectrogram B (bottom) also shows overlapping, distant terns but also darker calls from closer, also vocally active, terns.
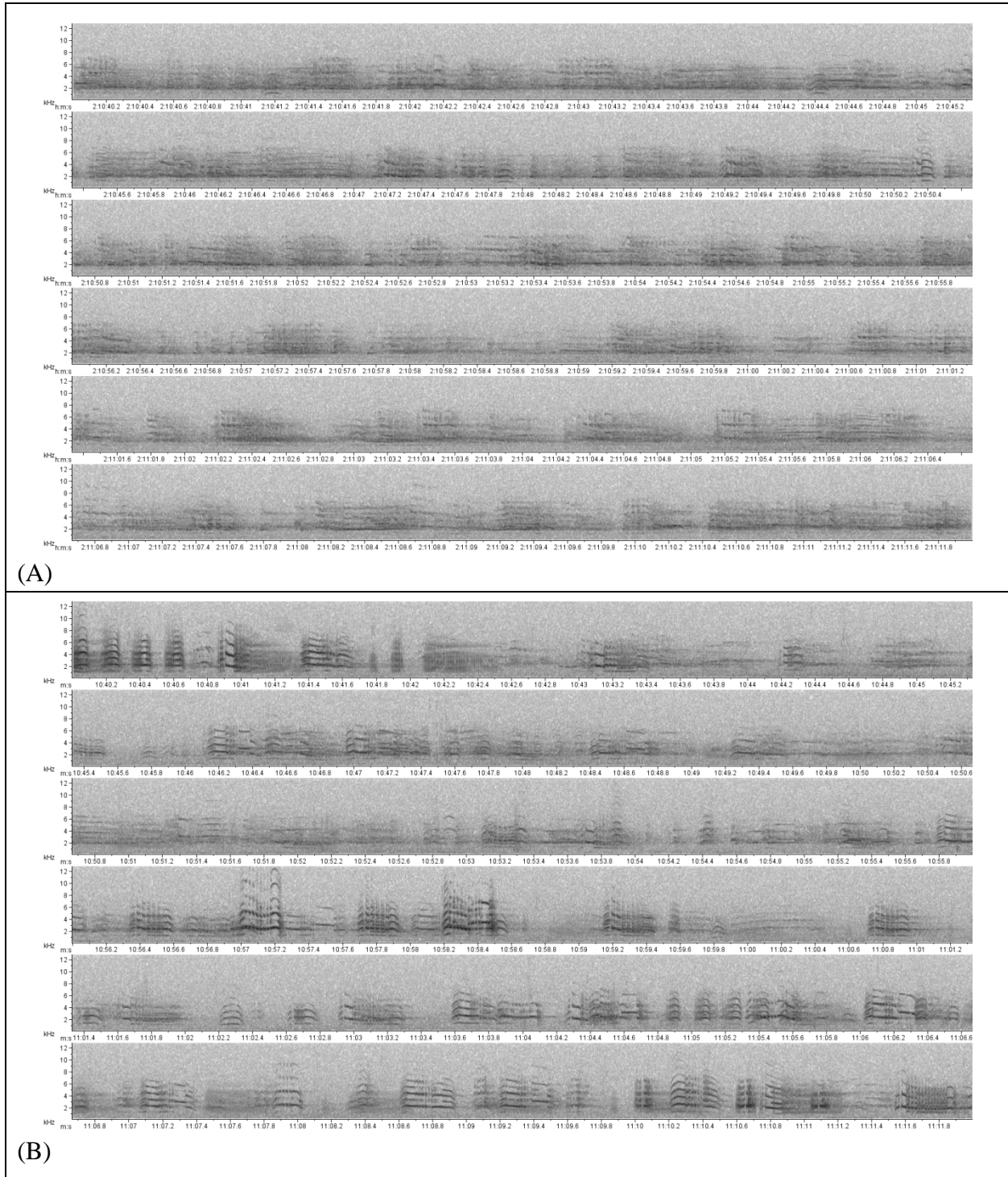
Figure 81. Two examples of high vocal activity at FPSLT showing high rates of calling and multiple individuals overlapping calls.

Examples of low activity included a single or small number of calls (Figure 82, A and B), indicating presence at the recording site was limited. As above, calls appear as stacked, dark

lines of variable duration; their intensity (dark or faint) indicates how well the call was recorded. Spectrogram A (top) shows three calls, likely given by a single tern; Spectrogram B (bottom) shows a similar scenario with only one identifiable call.
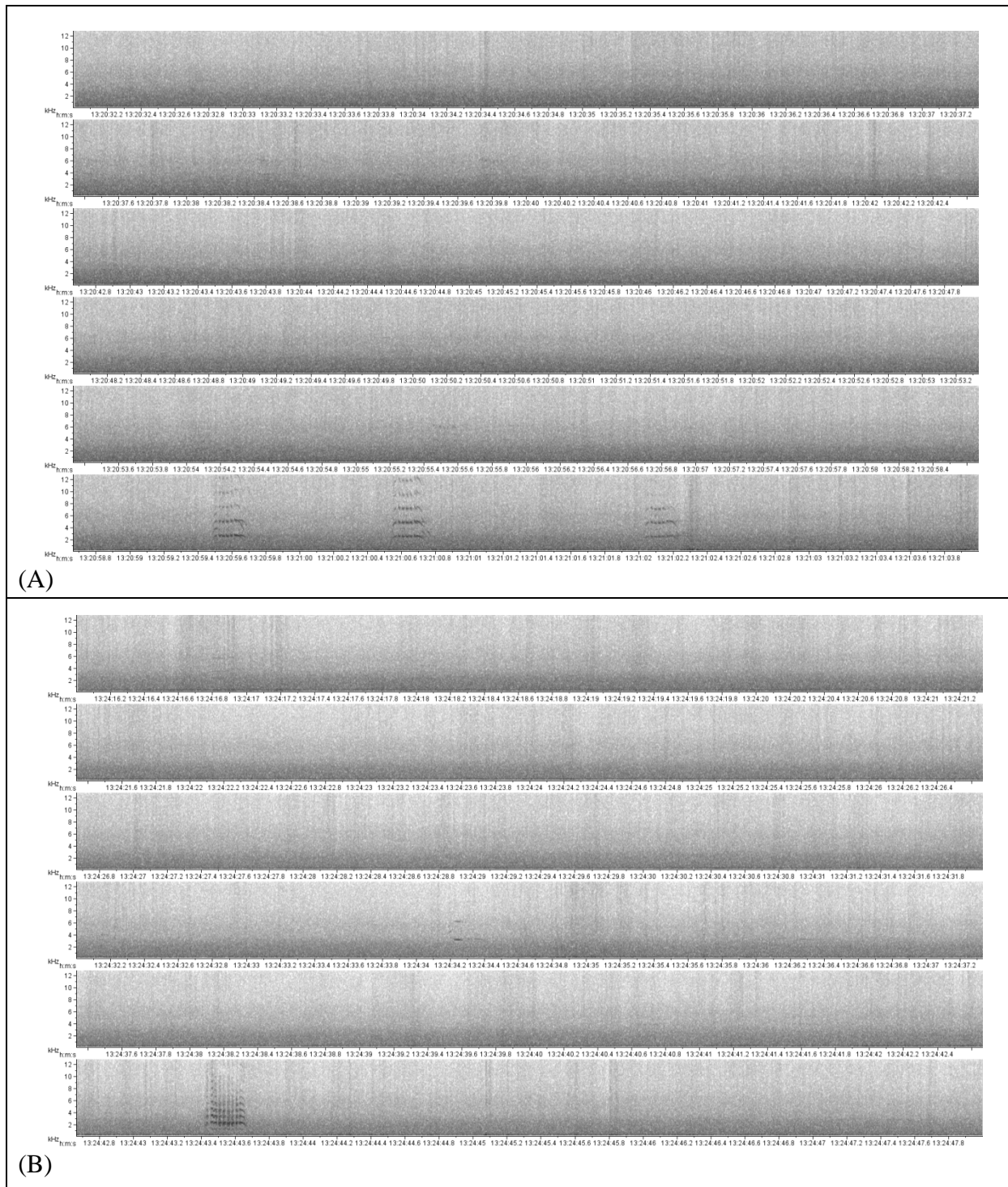
Figure 82. Two examples of low vocal activity at FPSLT showing periods of limited calling but with at least a single bird present.

All periods that were marked as high activity were evaluated to determine species composition. Given the complexity of many of the high-activity blocks no attempt to quantify the number of birds, nor the frequency that each species showed throughout the deployment, was made but instead a species list of each new species as it appeared in a block of high vocal activity was maintained. Species were identified to the most specific taxonomic group possible, ideally to the species level, although in many cases only the sub-family level, either Larinae for an unidentified gull species or Sterninae for an unidentified tern species, was possible.

Still focusing on NFCs, a summary of these acoustic data was provided by CLO containing data on the species or taxonomic group, date, time, and season. This dataset was the result of the acoustic analysis and species identification performed on the data as described above. The acoustic detector operational time across the daytime, nighttime, and the whole day was totaled to calculate the percentage of operational hours as a proportion of the total amount of day, night, and total 24-hr period. Percent operational time was used to correct observed abundance to account for times that the acoustic detectors were not running. Estimated corrected abundance for acoustic analysis was calculated according to the following:

$$A_c = \frac{A_o}{O_t} \qquad \text{(Eq. 6)}$$

where A_c is the corrected abundance, A_o is the abundance observed, and O_t is the observational time the acoustic detector was running. Abundance corrections were only performed on a monthly basis because that was the only timeframe where adequate sample sizes were available. Where possible, the corrected estimates of acoustic calls are presented in the figures and tables and those instances are noted accordingly. Other acoustic summaries by taxa and species are also presented.

7.2.2 Thermographic Analysis

Automated and preliminary manual review was completed on all data collected by the ATOM system on FPSLT between 6 Dec 2011 and 28 Oct 2012 consisting of 2816.86 hrs of video gathered on 174 days. Approximately 55% of the recording hours were during the day (1548.52 hrs) and 45% were during the night (1268.34 hrs) based on monthly sunrise and sunset times (Table 27, Figure 83). The system was functional until 18 Feb 2013, but the data management process for these remaining months of data could not be completed due to time constraints.

Table 27.

Hours of operation per month for thermographic cameras on FPSLT between 6 Dec 2011 and 28 Oct 2012.

Month	Total Recording Hours	Diurnal Recording Hours	Nocturnal Recording Hours
Dec 2011	126.74	53.63	73.11
Jan 2012	11.92	3.00	8.92
Feb 2012	0.00	0.00	0.00

Month	Total Recording Hours	Diurnal Recording Hours	Nocturnal Recording Hours
Mar 2012	0.00	0.00	0.00
Apr 2012	490.41	254.59	235.83
May 2012	284.83	164.87	119.96
Jun 2012	583.29	350.72	232.57
Jul 2012	147.89	90.22	57.67
Aug 2012	171.17	106.51	64.66
Sep 2012	558.28	304.63	253.65
Oct 2012	442.33	220.35	221.98
Total	2816.86	1548.52	1268.34
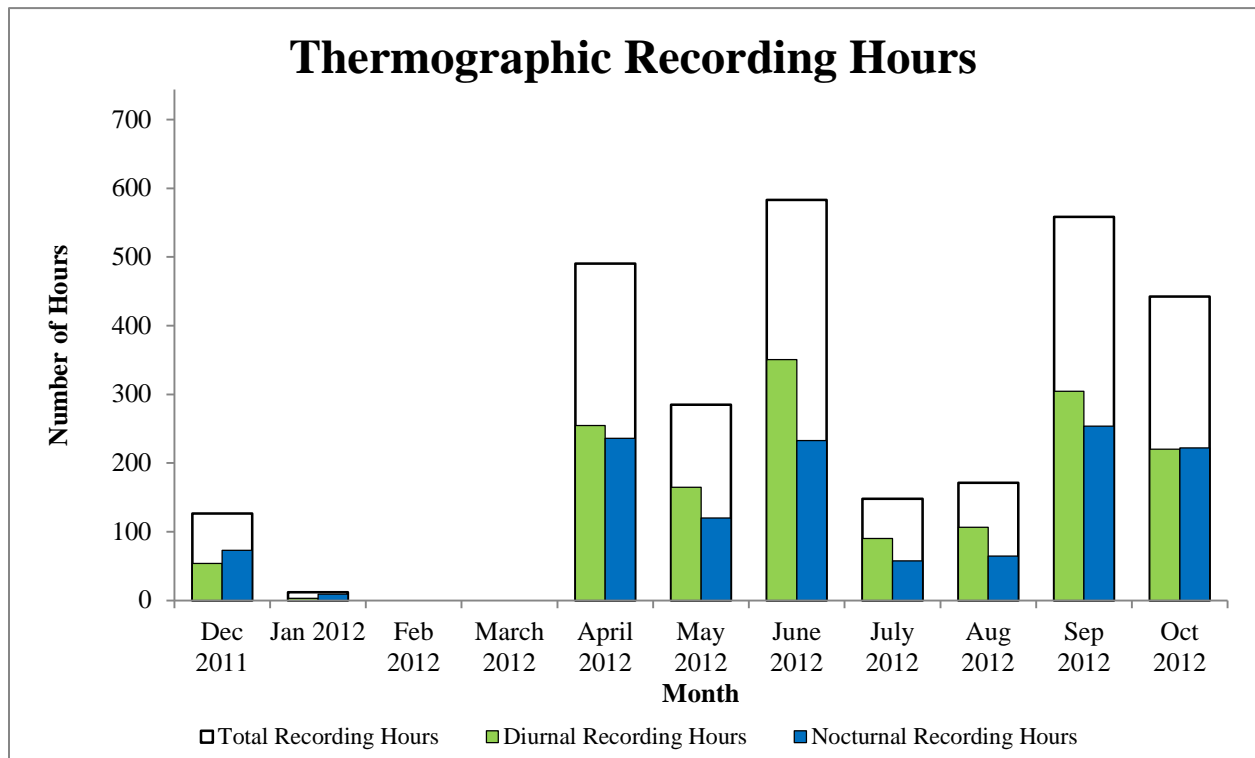
Figure 83. Hours of operation per month for thermographic cameras on FPSLT between 6 Dec 2011 and 28 Oct 2012.

Data were processed through the target detection program SwisTrack (see Section 2.2 for program details), which produced 10,065 video segments, or tracks, of potential targets. Birds were visible in 1,763 of the video segments. However, 237 tracks were following the flight path of a previous bird (e.g., a bird circling above the cameras in and out of the field of view) and 34 were not following the flight path of the bird correctly. These 34 were recorded as false positives

(clouds) since the altitude and measurements calculated by the software would not be accurate. Taking these two factors into consideration, 1,492 individual birds were detected flying over the thermal cameras at FPSLT. The remaining tracks were passing clouds, insects, or airplanes (see Table 28).

Table 28.

Number of tracks targeted by SwisTrack and analyzed in Analyst Workbench.

Month	Total Bird	Diurnal Bird	Nocturnal Bird	Repeated Bird	Cloud (Empty)	Insect or Plane	Repeated Insect or Plane	Total
Dec 2011	50	38	12	1	431	5	0	487
Jan 2012	1	1	0	0	52	2	1	56
Apr 2012	539	389	150	52	2353	107	1	3052
May 2012	109	96	13	8	1031	23	0	1171
Jun 2012	231	216	15	150	1595	181	0	2157
Jul 2012	4	4	0	0	125	362	0	491
Aug 2012	252	227	25	11	590	69	2	924
Sep 2012	211	203	8	10	783	134	4	1142
Oct 2012	95	71	24	5	274	209	2	585
Total	1492	1245	247	237	7234	1092	10	10065

The auto target detection algorithm used by SwisTrack was modified after Jul 2012 data had been analyzed. All data from Dec 2011 to Jul 2012 was reprocessed and reanalyzed. The results were then compared to ascertain the level of improvement. The new algorithm outperformed the original and was able to greatly increase the number of tracks with potential targets. The improved algorithm tracked the same birds as the original, except for one, and was able to track 589 additional birds (see Table 29 and Table 30 for details).

Table 29.

Number of tracks targeted by the original algorithm used by SwisTrack and analyzed in Analyst Workbench.

Month	Original Algorithm				
	Total Bird	**Repeated Bird**	**Cloud (Empty)**	**Insect or Airplane**	**Total**
Dec 2011	21	0	127	2	150
Jan 2012	0	0	8	0	8
Apr 2012	205	10	254	3	472
May 2012	40	2	96	1	139
Jun 2012	77	11	155	8	251
Jul 2012	2	0	12	26	40
Total	345	23	652	40	1060

Table 30.

Number of tracks targeted by the modified algorithm used by SwisTrack and analyzed in Analyst Workbench.

Month	Modified Algorithm					
	Total Bird	**Repeated Bird**	**Cloud (Empty)**	**Insect or Airplane**	**Repeated Insect or Airplane**	**Total**
Dec 2011	50	1	431	5	0	487
Jan 2012	1	0	52	2	1	56
Apr 2012	539	52	2353	107	1	3052
May 2012	109	8	1031	23	0	1171
Jun 2012	231	150	1595	181	0	2157
Jul 2012	4	0	125	362	0	491
Total	934	211	5556	680	2	7383

Raw video segments were reviewed to help develop a more successful detection algorithm and monitor its overall effectiveness. Portions of video from each month were randomly selected to equal 10% of monthly recording hours available for Dec 2011 through Oct 2012, totaling 281.72 hrs. The birds found in the constant video stream were compared to the birds detected by SwisTrack and matched via timestamps and visual confirmation. Monthly success rates of bird detection ranged from below 15% to over 60%. Overall, SwisTrack detected 38.45% of the birds present in the selected video streams. During review of the tracks, it became evident that

SwisTrack was quite often missing birds when multiple birds were flying within the camera's view at the same or overlapping times. A count was recorded when these birds not detected by SwisTrack could be seen via another bird's track. For the 10% of selected hours, a total of 246 non-tracked birds could be seen with other tracked birds.

Data from SwisTrack were reviewed and cleaned to ensure they were entered and formatted correctly for data analysis purposes. All birds flying at an altitude of less than 10 m were removed to minimize the number of birds using the platform as a roost. SwisTrack data were corrected for both detection ability and survey time. Detection ability was determined by reviewing 10% of the images manually for targets and comparing this number with what was detected from SwisTrack. Success values are calculated on a monthly basis. Survey time was corrected by assuming the same number of targets occurred during times when the thermographic camera was not running as when it was running. Corrections for survey time were performed for day, night, and overall. Corrected abundance was calculated by summing the number of birds across each month and dividing by the SwisTrack correction for the given month and dividing by the percentage of the month that was surveyed. Corrected abundance was calculated according to the following:

$$A_c = \frac{\frac{A_o}{S_s}}{O_t} \qquad \text{(Eq. 7)}$$

where A_c is the corrected abundance, A_o is the abundance observed, S_s is the SwisTrack success, and O_t is the observational time. Abundance corrections were only performed on a monthly basis because that was the only timeframe where adequate sample sizes were available. In addition to evaluating abundance data from SwisTrack analyses, flight altitude, flight bearing, and flight velocity were also examined by season. Means and 95% confidence intervals are presented for flight velocity and flight altitude. Weather variables including wind speed and wind direction were also evaluated with respect to their influence on abundance, flight altitude, and flight direction. Separate results for passerines and non-passerines for flight altitude, bearing, and velocity are also presented. Passerines were determined by considering birds <20 cm in size as passerines and birds >30 cm were considered non-passerines. Birds between 20 and 30 cm were not included because this size category overlaps with some passerine and some Laridae species.

7.2.3 Ultrasound Analysis

The full spectrum ultrasound acoustic data collected by the ATOM system at FPSLT from 6 Dec 2011 through 28 May 2012 were completely analyzed. This consisted of 2,653.22 hrs of recording from 131 days on which the system was functioning. Approximately 54% of the recording hours were during the day (1,429.21 hrs) and 46% were during the night (1,224.01 hrs) based on monthly sunrise and sunset times (Figure 84). These data were analyzed using automated and manual processes that were developed by Normandeau's bat biologists for use with the ReBAT® system. In the automated process (automated target detection), SCAN'R© filtering software (Binary Acoustic Technology, Tucson, AZ) was used to remove extraneous noise files. This program recognizes a potential bat pass event and produces a 1.7-sec duration ".wav" file any time at least two consecutive potential bat echolocation calls are recorded. SCAN'R© uses the ultrasound spectrographic patterns of bat calls to recognize potential bat calls

(Binary Acoustic Technology 2010). The SCAN'R©-passed files were run through the additional ReBAT.com filter to remove noise files not captured by SCAN'R©. Additionally, a subset of the files removed by the ReBAT.com filter was manually reviewed for QA/QC.
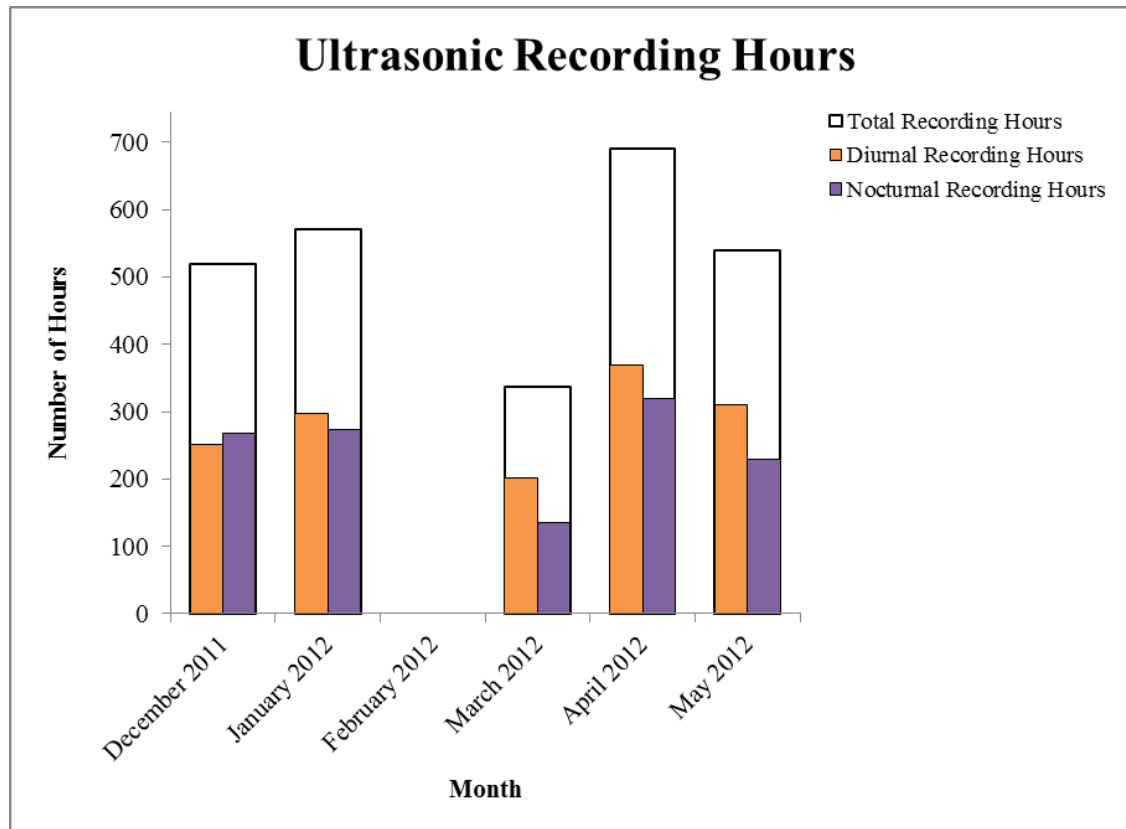
Figure 84. Hours of operation per month for ultrasonic microphones from initial deployment on 6 Dec 2011 until its last known functional date 28 May 2012.

8 Results from the Frying Pan Shoals Light Tower

8.1 Thermographic Results

SwisTrack analyses show that the majority of bird detections occurred in the daylight hours, primarily between 6 AM and 6 PM; much lower activity was detected at night (Figure 85). This same trend in daytime activity occurred consistently throughout the year with twice as many daytime detections as nighttime detections occurring in all seasons (Figure 86). Over the course of the year, abundance peaked in Apr and Aug with lower abundance reported during other months (Figure 87). Hourly abundance varied by season with peak spring abundance between 6 and 10 AM and peak fall abundance between 10 AM and 2 PM (Figure 86). Migration behavior in Apr shows higher than usual nocturnal activity, although diurnal activity was consistently higher through all months (Figure 87). Analyzed on a monthly basis, higher abundance was recorded in Apr than any other month (Figure 88).
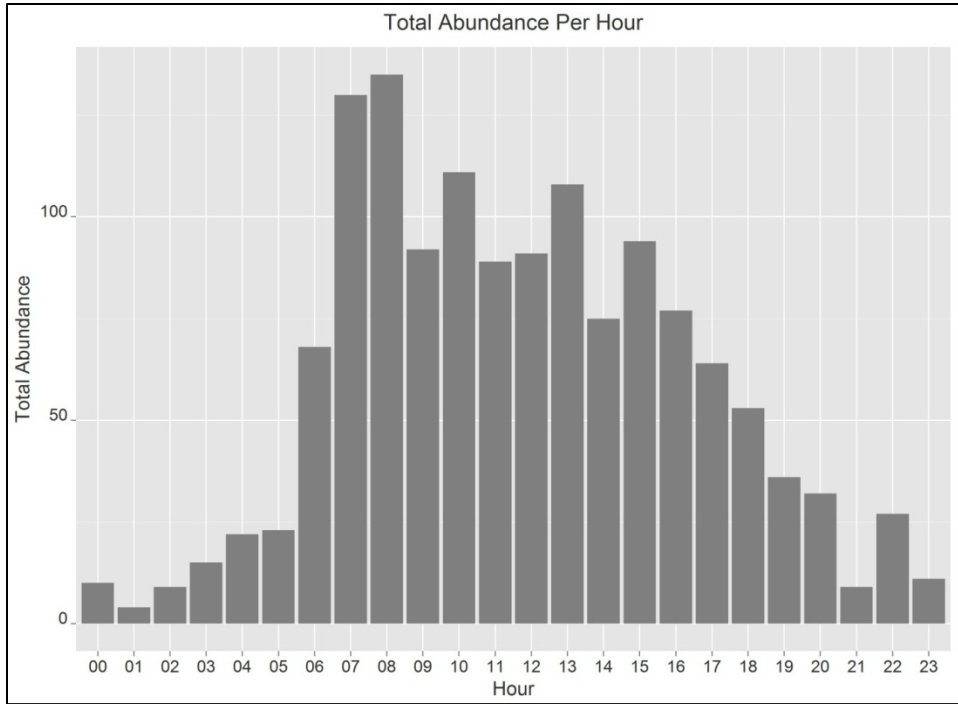
Figure 85. Total bird abundance across all species combined for all months
on an hourly basis.
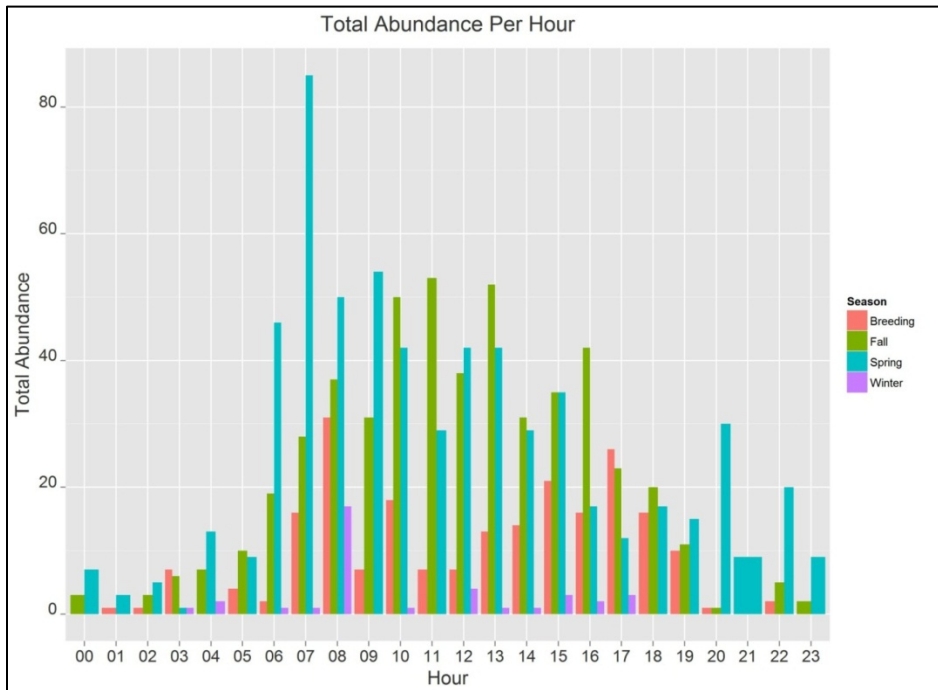
Figure 86. Total bird abundance across all species by season on an hourly
basis.
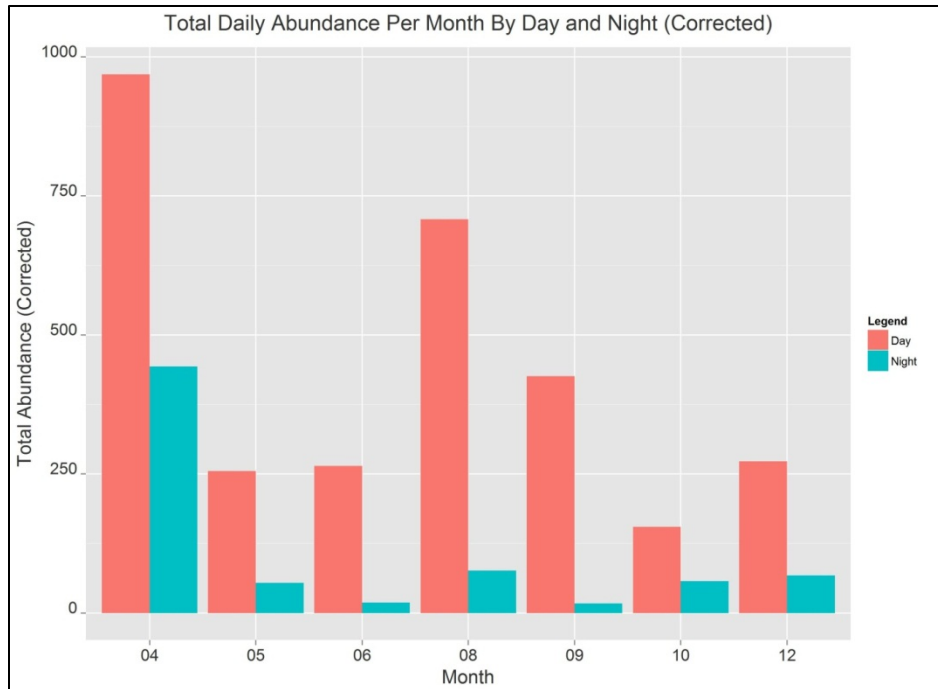
Figure 87. Total corrected bird abundance across all species on a monthly basis by day and night. Corrected abundance accounts for the success of the SwisTrack detection algorithm and the amount of time the system was running as a percentage of the total duration of the study.
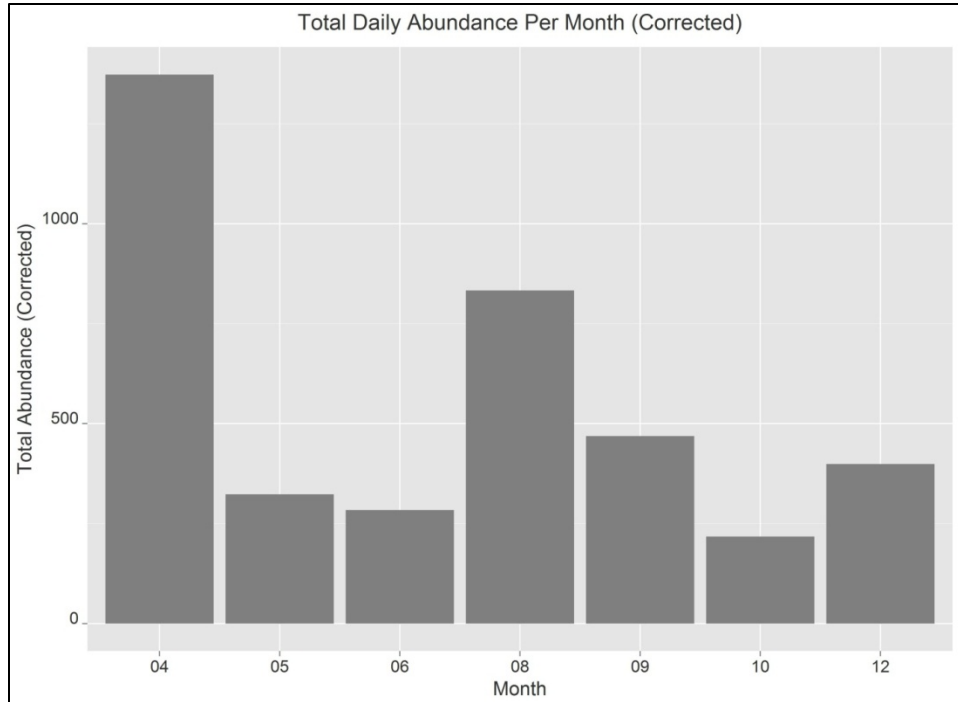
Figure 88.   Total corrected bird abundance across all species on a monthly
basis. Corrected abundance accounts for the success of the
SwisTrack detection algorithm and the amount of time the
system was running as a percentage of the total duration of the
study.

Flight altitude was consistent throughout the day with slightly higher altitudes being detected in
the early evening, though the variation around these estimates is high (Figure 89). Throughout
the year, flight altitude was lowest during the summer months of Jul and Aug and highest during
the spring and fall; although, those differences were not significant (Figure 90). There was no
significant difference in flight altitude during the spring when analyzed on an hourly basis
(Figure 91). During the breeding season, slightly higher altitude was observed near sunrise
(Figure 92). There was no significant difference in flight altitude during the fall when analyzed
on an hourly basis (Figure 93). Winter data were sparse for flight altitude (Figure 94).
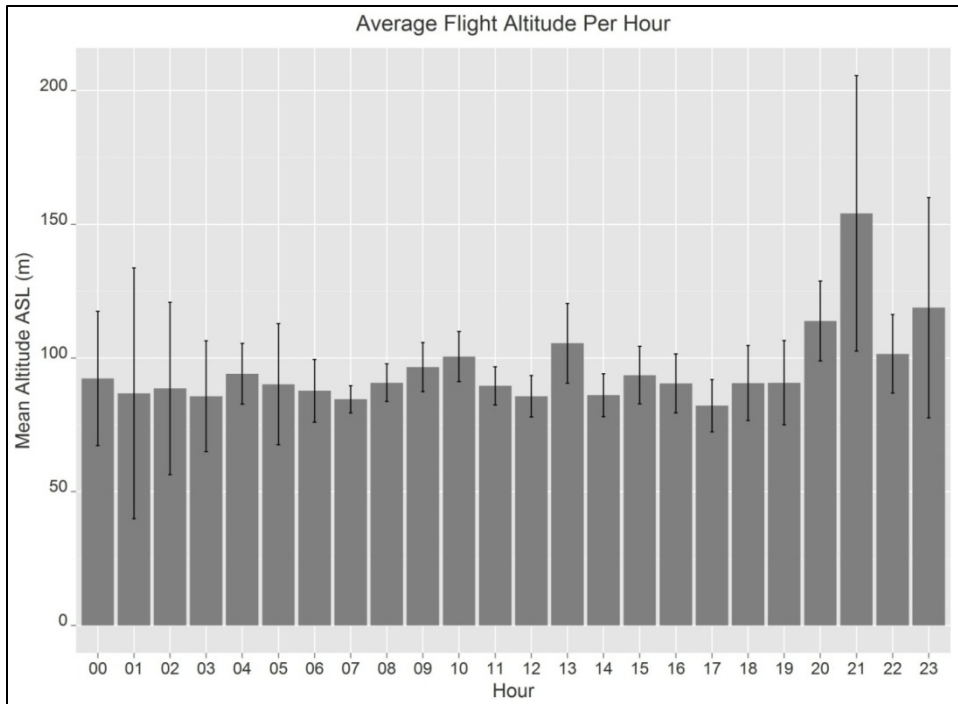
Figure 89. Mean (95% confidence intervals) flight altitude across all seasons and species on an hourly basis.
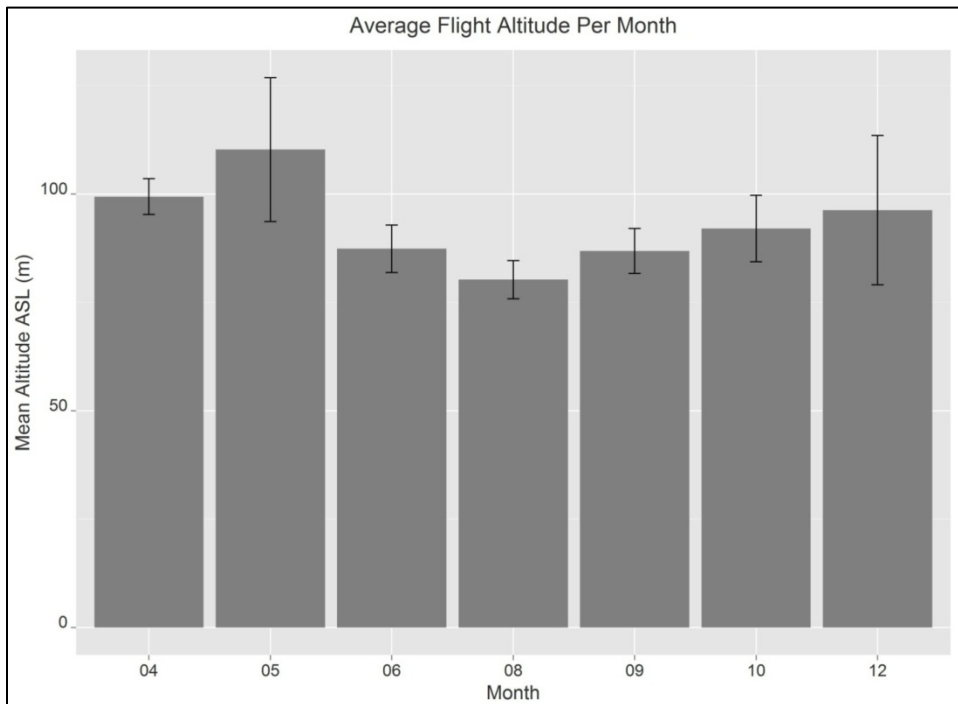
Figure 90. Mean (95% confidence intervals) flight altitude across all seasons and species on a monthly basis.
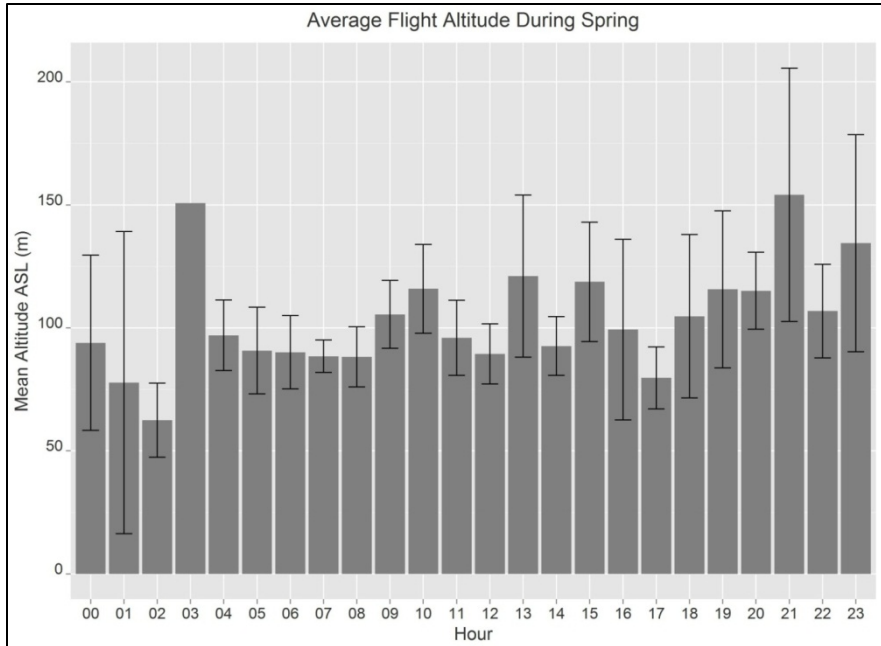
Figure 91. Mean (95% confidence intervals) flight altitude across all
species during spring on an hourly basis. Lack of
confidence intervals at a particular time indicates that
there was only one observation at that time.
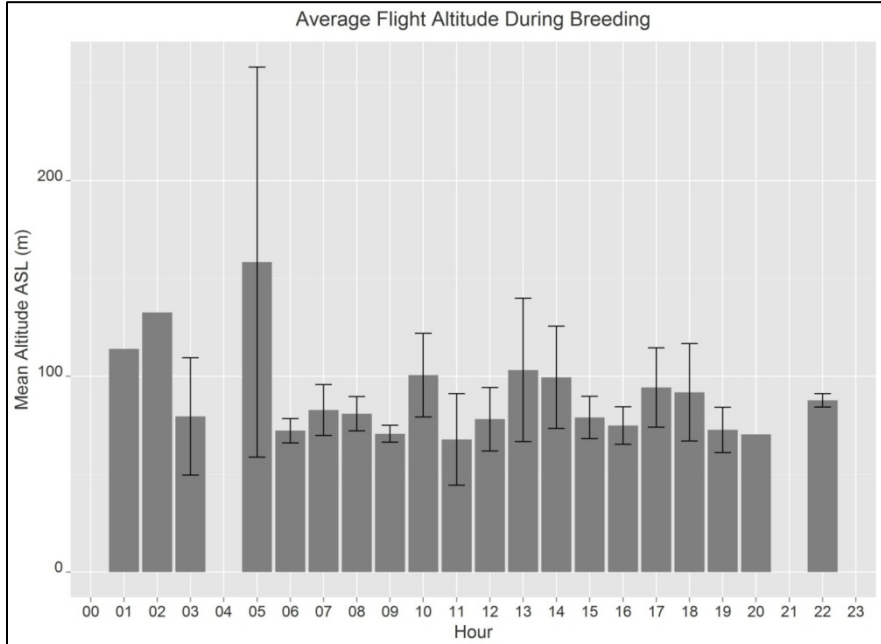
Figure 92. Mean (95% confidence intervals) flight altitude across all
species during the breeding season on an hourly basis.
Lack of confidence intervals at a particular time indicates
that there was only one observation at that time.
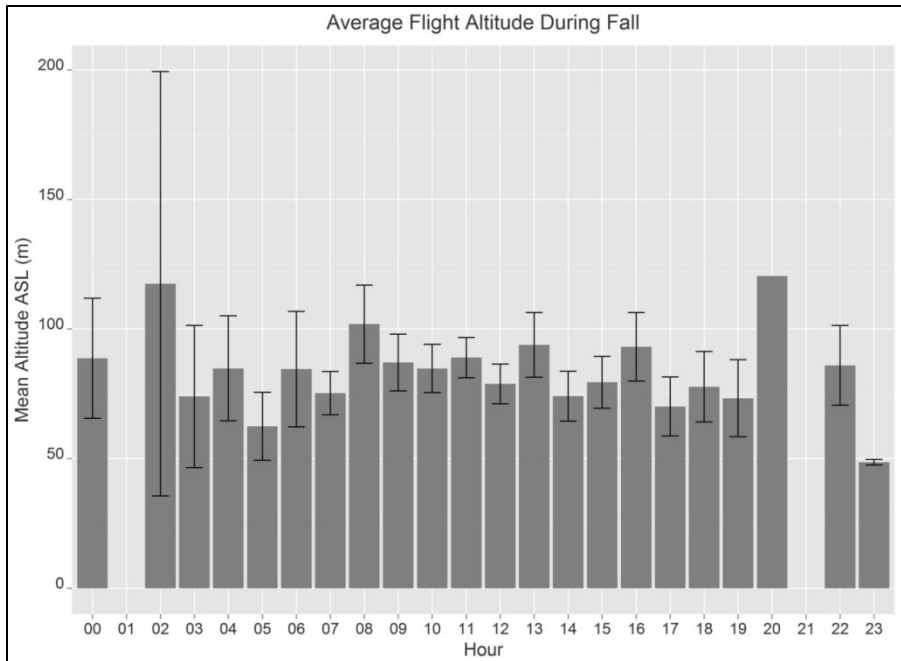
Figure 93. Mean (95% confidence intervals) flight altitude across all species during fall on an hourly basis. Lack of confidence intervals at a particular time indicates that there was only one observation at that time.
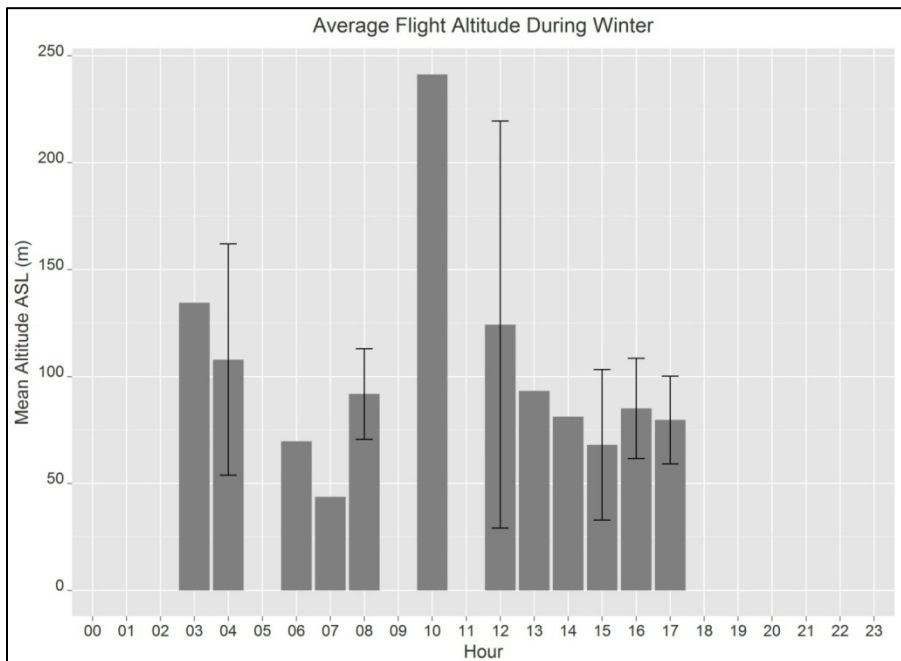
Figure 94. Mean (95% confidence intervals) flight altitude across all species during winter on an hourly basis. Lack of confidence intervals at a particular time indicates that there was only one observation at that time.

Comparing flight heights of passerines to non-passerines showed that passerine flight altitudes were higher than non-passerines; the non-passerines had higher maximum recorded flight height (Figure 95 and Figure 96).
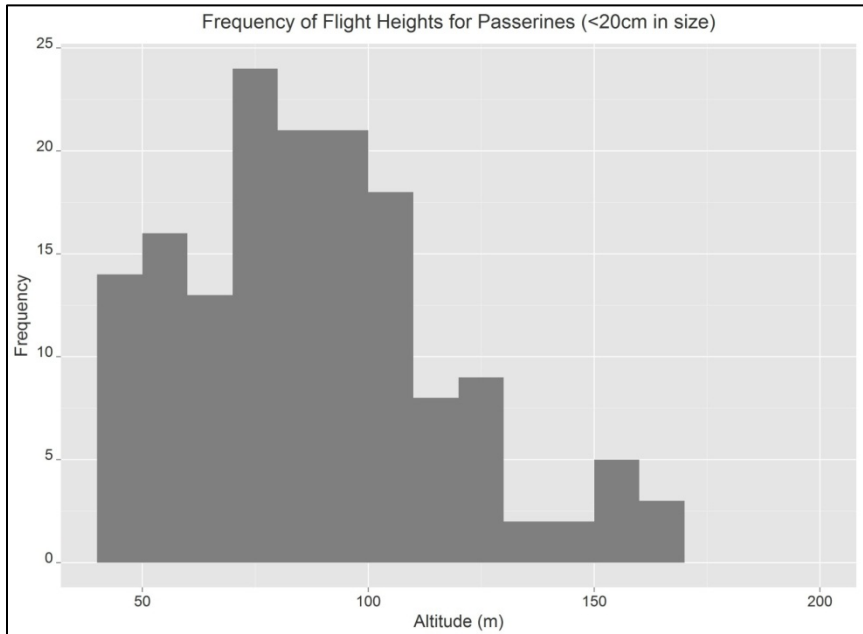
Figure 95. Frequency of various flight heights recorded for passerines recorded throughout the study duration.
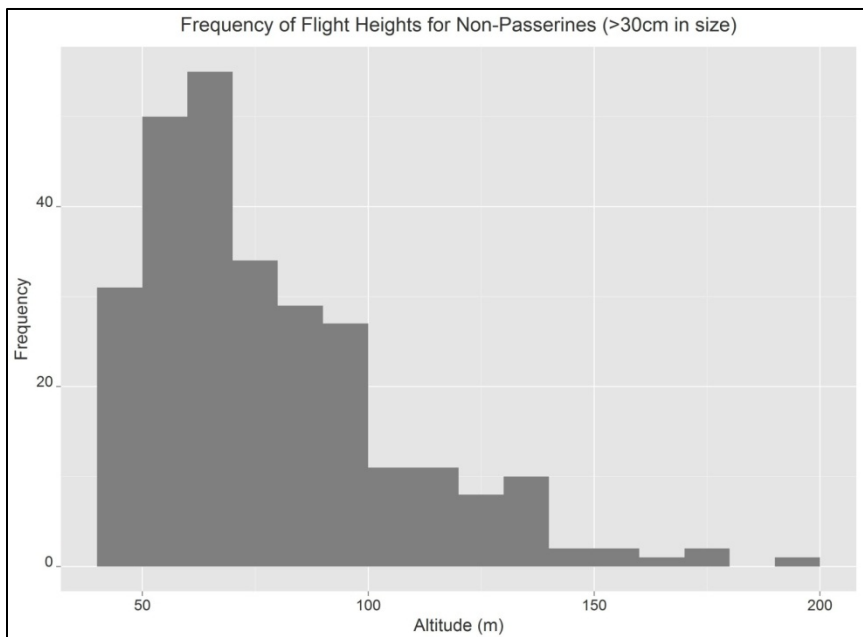
Figure 96. Frequency of various flight heights recorded for non-passerines recorded throughout the study duration.

Seasonal differences in flight bearing were observed for passerines, but similar trends were not evident with non-passerines. Passerines showed strong tendencies to fly to the south and southeast during the fall and to the northwest during the spring (Figure 97). Flight bearings for non-passerines did not mirror these trends and no discernable patterns were evident (Figure 98).

Flight velocities were fairly consistent throughout the day with moderately slower speeds were detected during the early evening hours (Figure 99). Flight velocities among months were similar and not significantly different among one another (Figure 100).
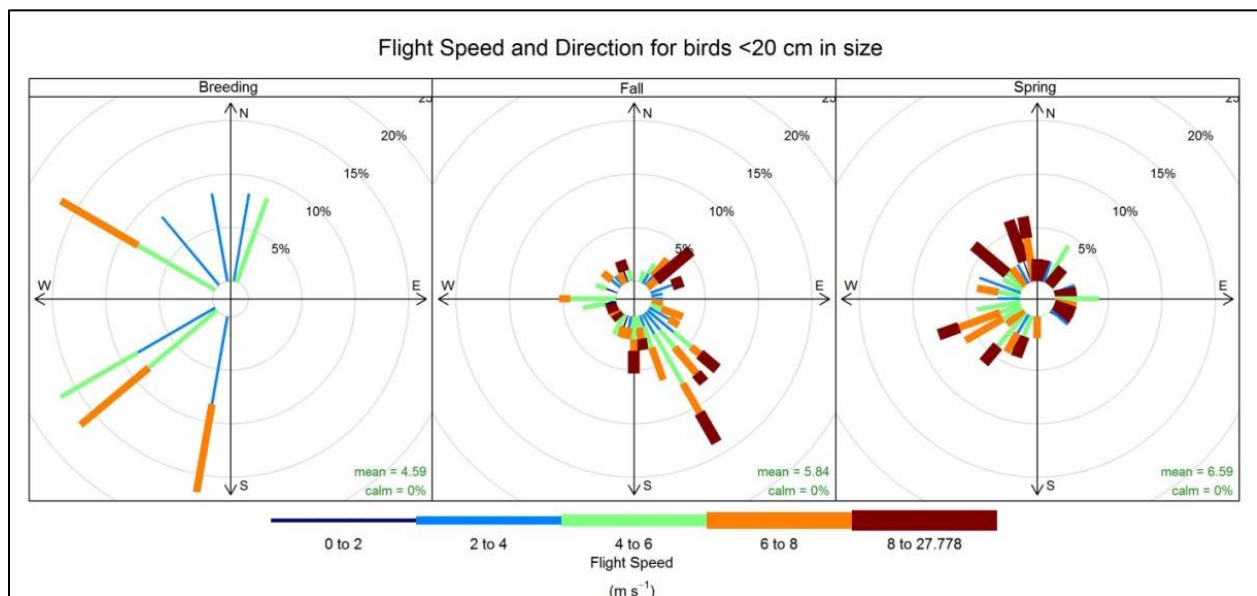
Figure 97. Seasonal variation in bearing and wind speed for passerines recorded throughout the duration of the study. Longer bars indicate higher frequency in each given direction.
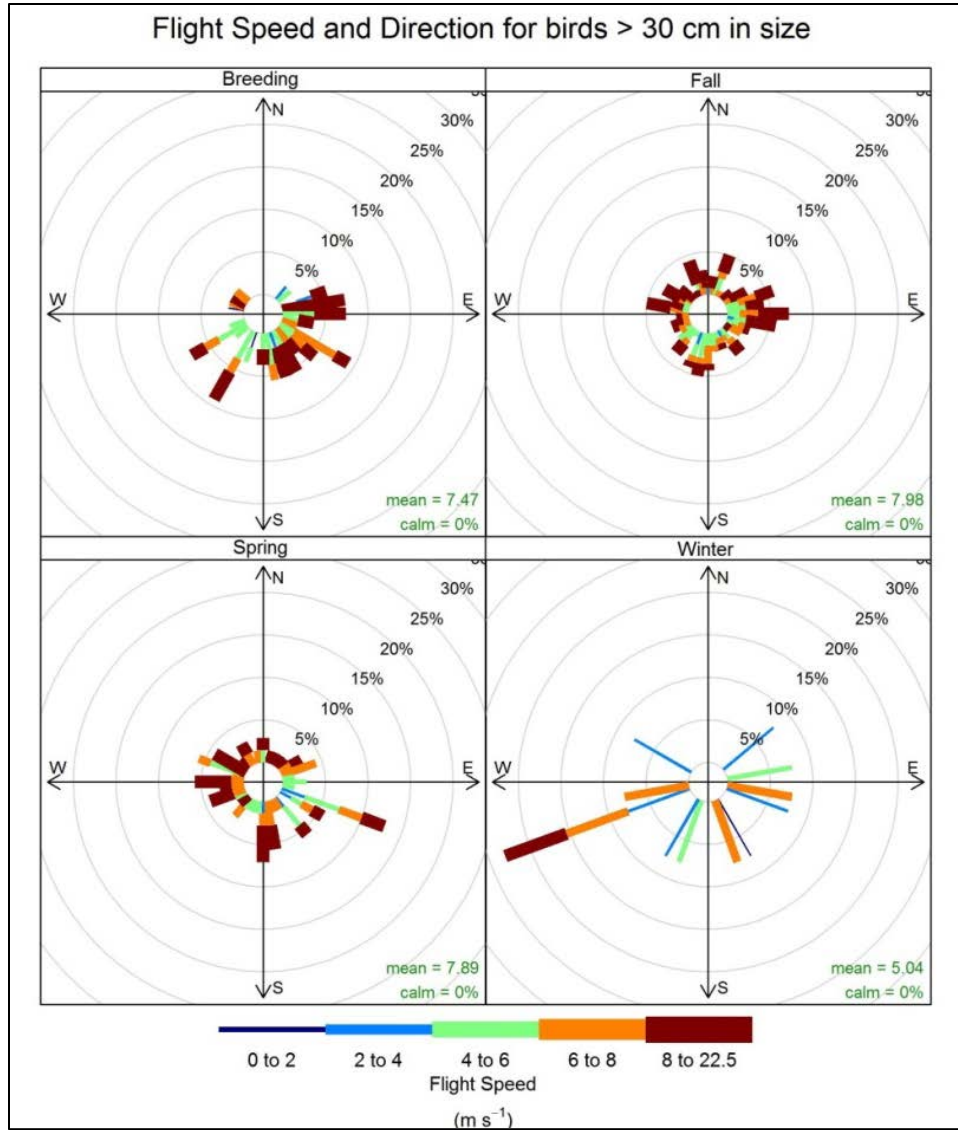
Figure 98. Seasonal variation in bearing and wind speed for non-passerines recorded throughout the duration of the study. Longer bars indicate higher frequency in each given direction.
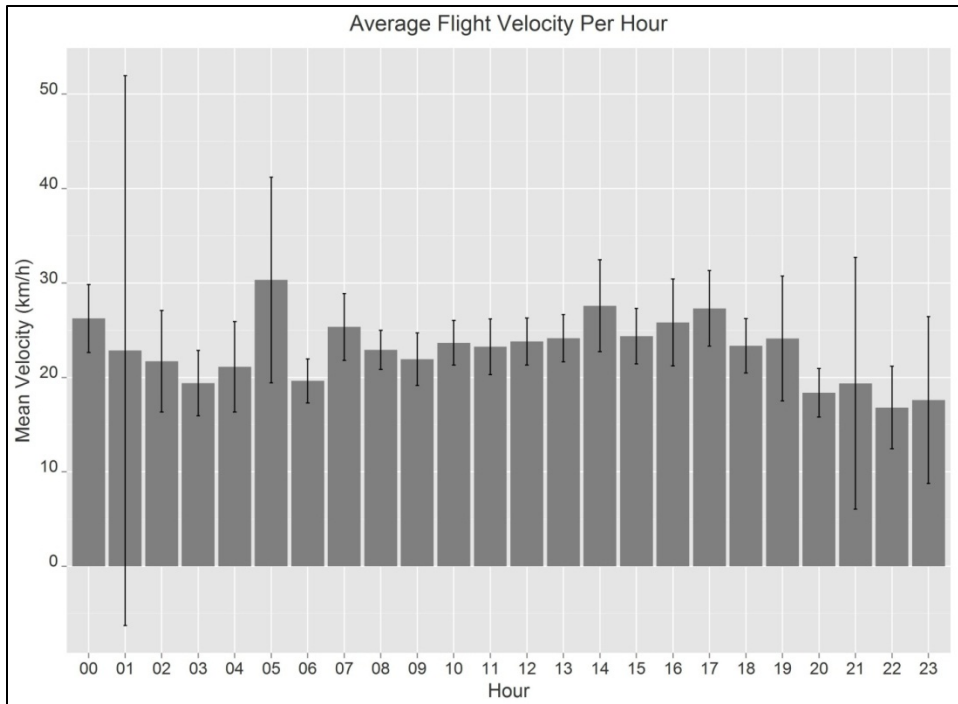
Figure 99. Mean (95% confidence intervals) flight velocity across all months and species on an hourly basis.
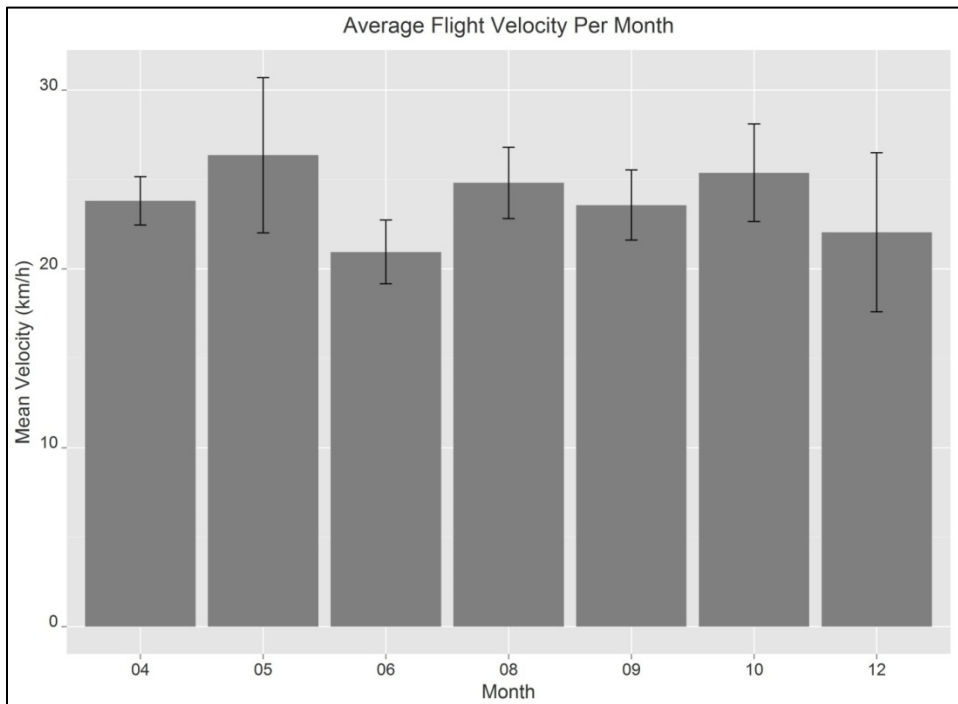
Figure 100. Mean (95% confidence intervals) flight velocity across all species on a monthly basis.

Weather variables had varying influence on bird abundance, flight altitude, and flight direction. Birds occurred consistently through the range of wind speeds up until around 10 km/hr when abundance declined sharply (Figure 101). Wind speed did not appear to have any effect on the altitude at which birds fly (Figure 102). There was some relationship between wind direction and flight direction with more birds flying into or against the wind; fewer birds were observed flying across the wind direction (Figure 103). There was little relationship between wind speed and flight speed with consistent flight speeds being reported across the range of wind speeds (Figure 104). A measure of humidity was used as a surrogate for visibility as lower visibility normally occurs (rain and fog) as the humidity increases and approaches 100%. Flight altitude did not appear to be heavily influenced by relative humidity (Figure 105).
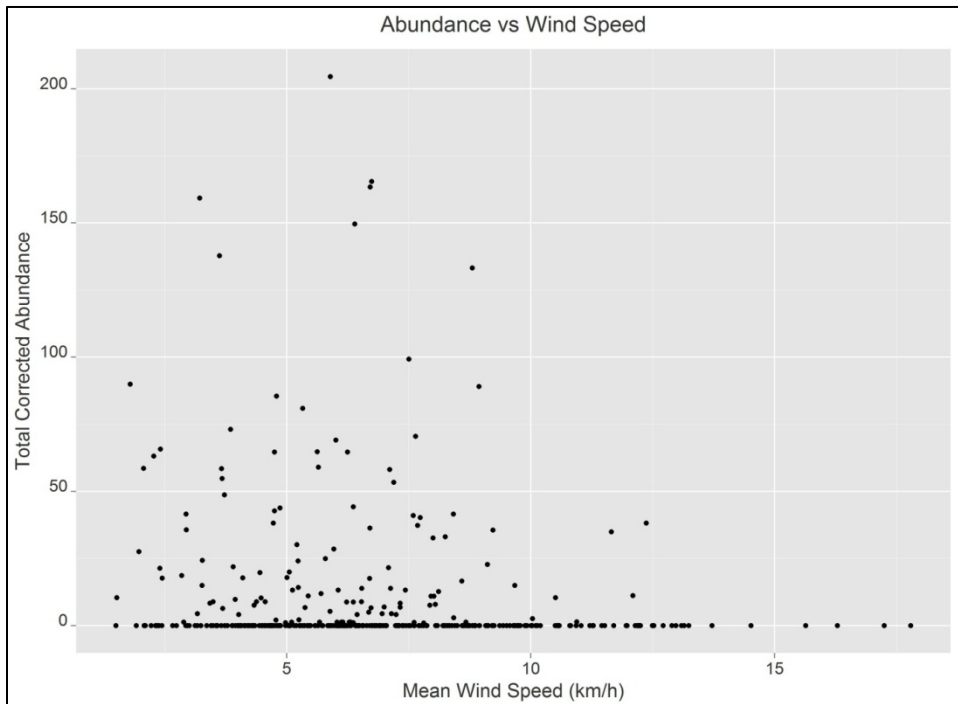
Figure 101. Mean wind speed versus total corrected bird abundance for birds detected with the SwisTrack system.
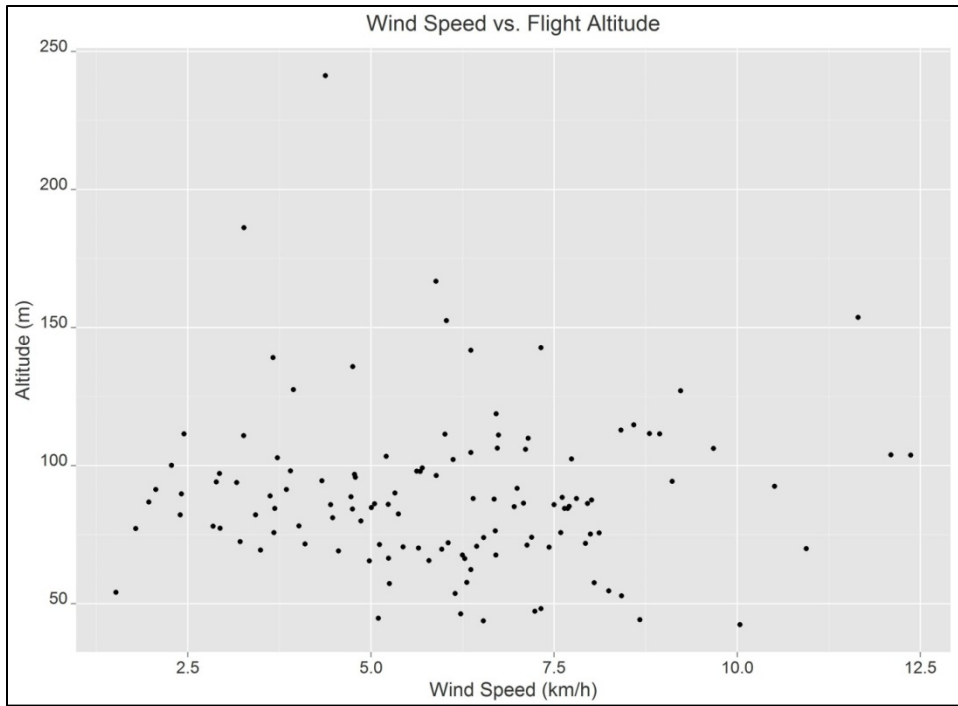
Figure 102. Mean wind speed versus mean flight altitude for birds detected with the SwisTrack system.
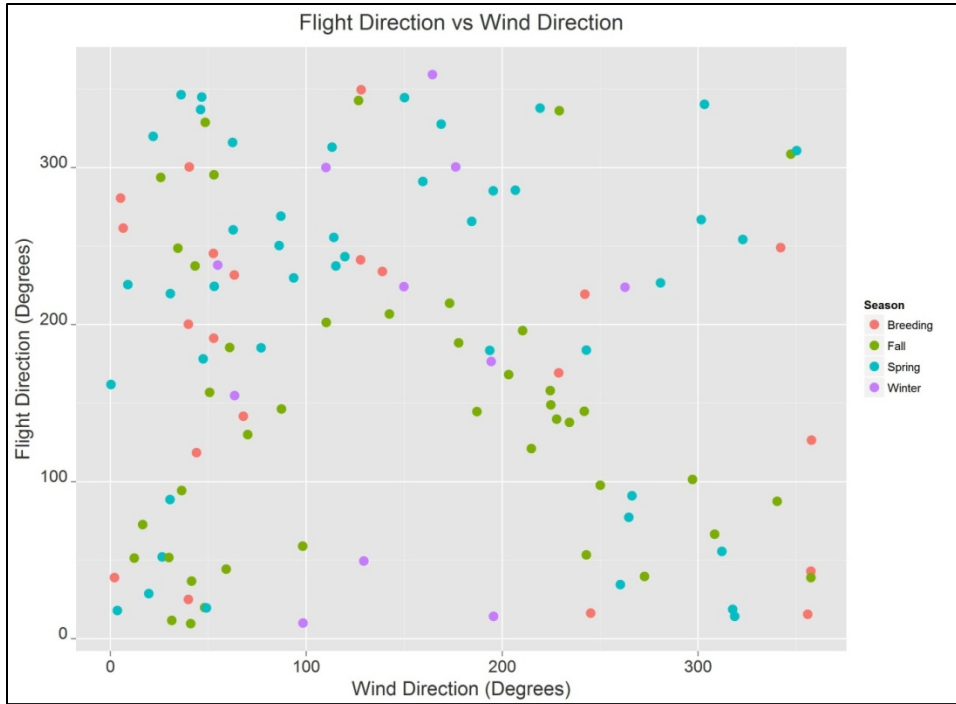
Figure 103.   Mean wind direction versus mean flight direction for birds
detected with the SwisTrack system for each season. Mean
directions were calculated using circular statistics. Note
that the wind direction in this figure is the direction to
which the wind is blowing rather than the direction of
origin to allow simple correlation with bird direction
information.
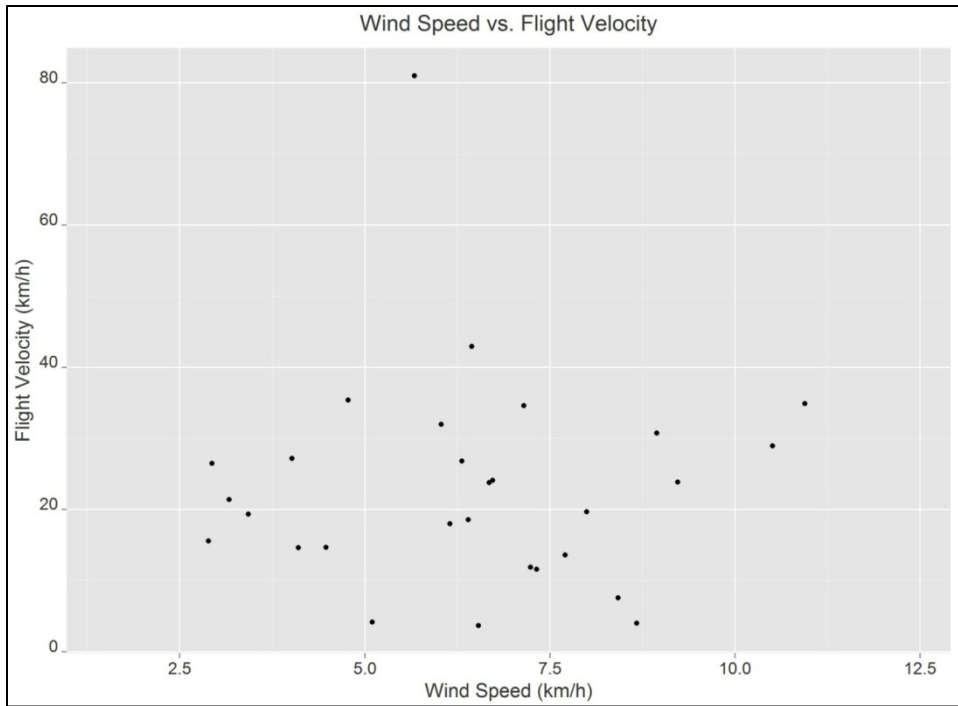
Figure 104. Mean wind speed versus flight velocity across all species and
months in the study.
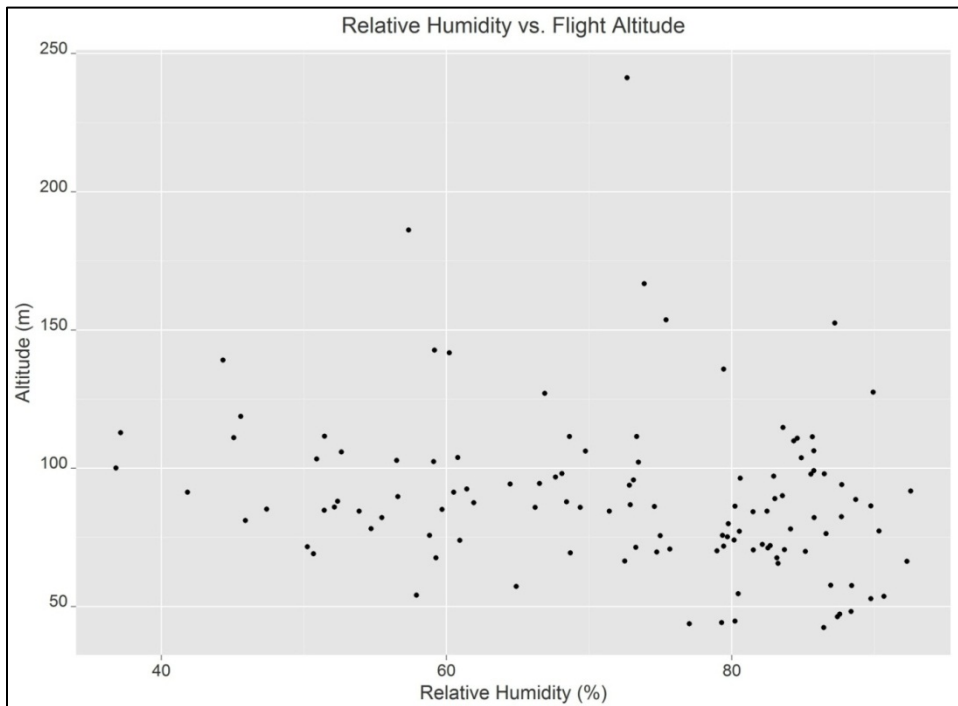
Figure 105.   Mean relative humidity versus flight altitude across all
species and months in the study.

8.2 Acoustic Results

Recordings were successfully made on 153 different dates starting on 03 Apr 2012 and ending in Feb 2013. The small number of files from 2013 was reviewed, but as they only captured human voices and personnel in the vicinity of the recording device, they are not part of the results or discussion. Results are presented until the final recording from 2012, which occurred on 12 Dec 2012.

8.2.1 Nocturnal Flight Call Analysis

These calls are not necessarily calls that occurred at night. As described in the methods, they are species-specific vocalizations, either frequency modulated or pure, of up to several syllables that generally are in the 1–11 kHz frequency band and 50–300 ms in duration. These calls are the primary vocalizations given by many species of birds during long, sustained flights, characteristic of nocturnal migration (Evans and O'Brien 2002). Automated detectors returned 125,213,655 potential candidates for such calls. After applying the generic RF model, nearly 200,000 detections were evaluated in both the high and low frequency bands through human review, of which 2,640 were avian flight calls (Table 31). Many more of these calls were in the high frequency band than in the low. This is primarily a function of recording quality and the potential for masking noise in the low frequency band rather than a function of some biologically relevant pattern or process, per se.

Table 31.

Raw detections and performance of the Random Forest model.*

Sound Retrieval	Detections		Top-Ranked Calls Reviewed		Total Calls (Frequency Band)		Total (All Flight Calls)
	High	Low	High	Low	High	Low	
SR-02	40,082,256	17,735,398	24,649	19,011	199	8	207
SR-03	15,800,396	7,666,902	27,102	21,000	0	0	0
SR-04	17,839,329	6,908,012	11,036	28,685	2,057	342	2,399
SR-05	12,971,758	6,209,590	35,440	18,424	14	20	34
Total	86,693,719	38,519,902	98,227	87,120	2,270	370	2,640

* Raw detections in each focal frequency band (high [6000–11000 Hz] and low [2250–3750 Hz]) are presented separately, as are the number of ranked calls that were reviewed by an analyst and the total number of flight calls identified.

A total of 2,640 calls was recorded from 39 different taxonomic units in the files analyzed, representing at least 33 different species (Table 32). Fall call counts outnumbered spring call counts by more than one order of magnitude (Figure 106). The species composition reflects a reasonable expectation in that many trans-Atlantic migrants that winter in the Caribbean and northern South America, including Amazonia, are present. These include, for example, Cape May and Black-throated Blue Warblers, species known to winter primarily in the Caribbean and

presumed to migrate mostly across the northwestern North Atlantic; these also include species like Gray-cheeked Thrush, Blackpoll Warbler, and Bobolink, species known to winter east of the Andes in South America. The species list also includes a number of unexpected species, such as American Pipit, Chipping Sparrow, and Dark-eyed Junco. Though they are migratory species, it is likely they were displaced offshore because they typically do not migrate to locations that would require an offshore passage.

Table 32.

Call counts of all species identified by nocturnal flight call analyses during the full deployment (03 Apr–12 Dec 2012).

Species Common Name	Spring	Breeding	Fall	Winter	Grand Total
Royal Tern	1	0	0	0	1
Least Bittern	0	0	1	0	1
Green Heron	0	0	7	0	7
Veery	0	0	14	0	14
Gray-cheeked Thrush	0	0	81	0	81
Swainson's Thrush	0	0	114	0	114
Hermit Thrush	0	0	0	20	20
Wood Thrush	1	0	4	0	5
American Pipit	0	0	0	5	5
Ovenbird	13	0	76	0	89
Northern Waterthrush	0	0	9	0	9
Black-and-white Warbler	0	0	33	0	33
Prothonotary Warbler	1	0	0	0	1
Common Yellowthroat	12	0	21	0	33
American Redstart	0	0	69	0	69
Cape May Warbler	0	0	476	0	476
Northern Parula	3	0	209	0	212
Magnolia Warbler	0	0	6	0	6
Bay-breasted Warbler	0	0	14	0	14
Blackburnian Warbler	0	0	4	0	4
Yellow Warbler	2	0	2	0	4
Chestnut-sided Warbler	0	0	2	0	2
Blackpoll Warbler	16	0	32	0	48
Black-throated Blue Warbler	1	0	54	0	55
Palm Warbler	1	0	324	0	325
Yellow-rumped Warbler	7	0	196	0	203
Canada Warbler	2	0	0	0	2

Species Common Name	Spring	Breeding	Fall	Winter	Grand Total
Chipping Sparrow	18	0	0	0	18
Savannah Sparrow	0	0	10	0	10
White-throated Sparrow	24	0	1	0	25
Dark-eyed Junco	1	0	0	0	1
Blue Grosbeak	0	0	1	0	1
Indigo Bunting	30	0	9	0	39
Bobolink	0	0	11	0	11
Genus Level Identifications					
Catharus sp.	0	0	29	0	29
Setophaga sp.	18	0	134	0	152
Family Level Identifications					
Parulidae sp.	4	0	20	2	26
Emberizidae sp.	0	0	3	0	3
Order Level Identifications					
Passeriformes	43	3	431	7	484
Class Level Identifications					
Aves	6	1	1	0	8
Grand Total	**204**	**4**	**2,398**	**34**	**2,640**
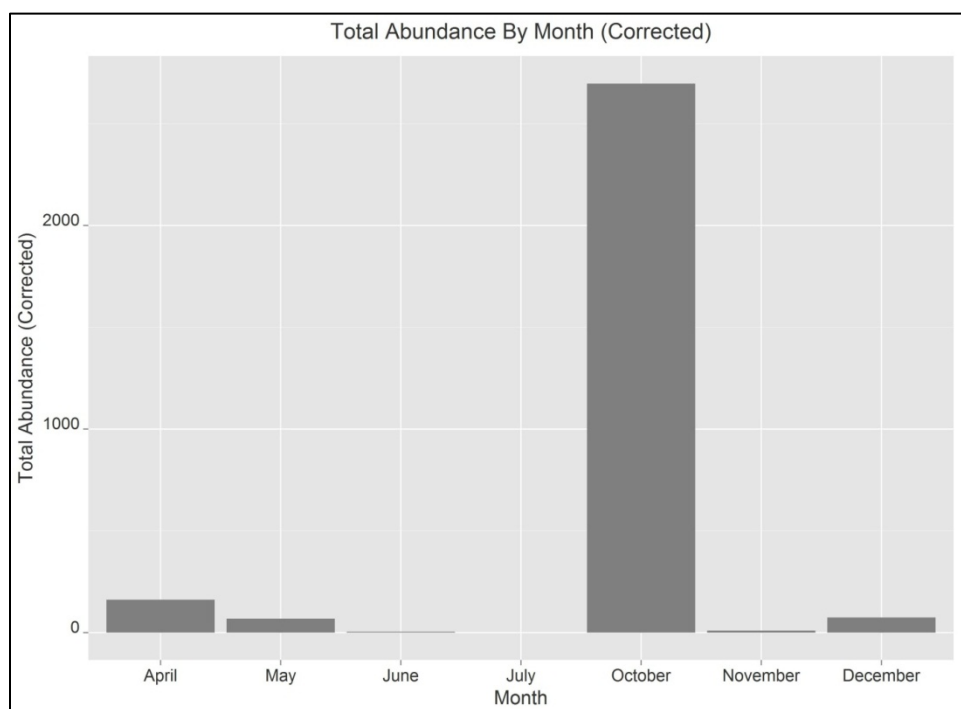
Figure 106.   Total corrected number of nocturnal flight call counts throughout the duration of the study.

Despite the lack of continuous nightly and seasonal coverage, an expected pattern can be seen of peaks for call count activity that is probably real rather than a function of skewed analysis and sampling distribution. Substantially greater call counts occur during periods of major migratory movements for many species in late Apr to mid-May and from late Sep to late Oct. These periods are characterized by the arrivals and departures of many species in eastern North America, so the presence of numerous calls of these species offshore presumably reflects the magnitude and extent of these movements.

The largest number of calls was recorded in the full deployment during the local 5–6 AM window (Figure 107). This pattern was not consistent across seasons with variation showing extreme differences among hours and among seasons. Spring season showed peak call counts in the local 1–2 PM window, whereas fall migration showed the largest number of calls recorded during the local 5–6 AM window (Figure 108). This pattern may reflect an important aspect of migration biology and the departure from stopover areas. Migrants typically depart from their stopover habitat during sunset and civil twilight 30–45 min after sunset. Points of origin for spring migrants over the platform in spring presumably originated from the Florida Peninsula, Caribbean, and South America, and in fall departures primarily originated from the mid-Atlantic and New England coasts. The patterns presumably reflect the arrival of these migrants to the air space above the platform in the time it takes to fly from their initial points of departure. In theory, future comprehensive analyses could identify potential sources for migrants passing the platform and the offshore area of interest with the addition of information about prevailing and local weather conditions as well as some calculations about basic attributes of bird migration speeds.
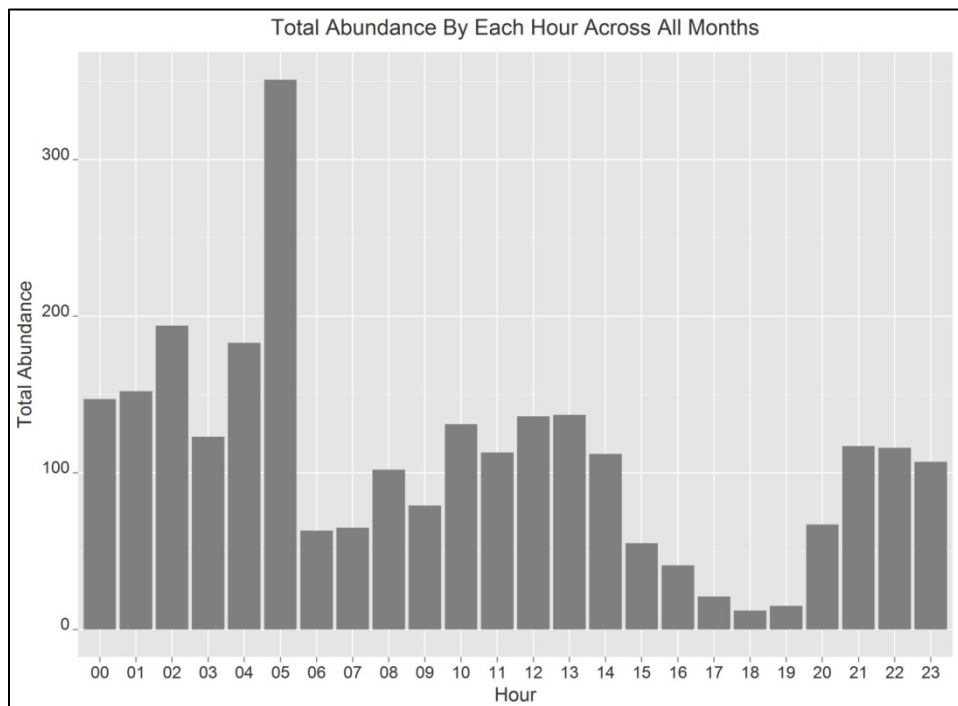
Figure 107.   Call counts by clock hour of all species recorded across the
full deployment.
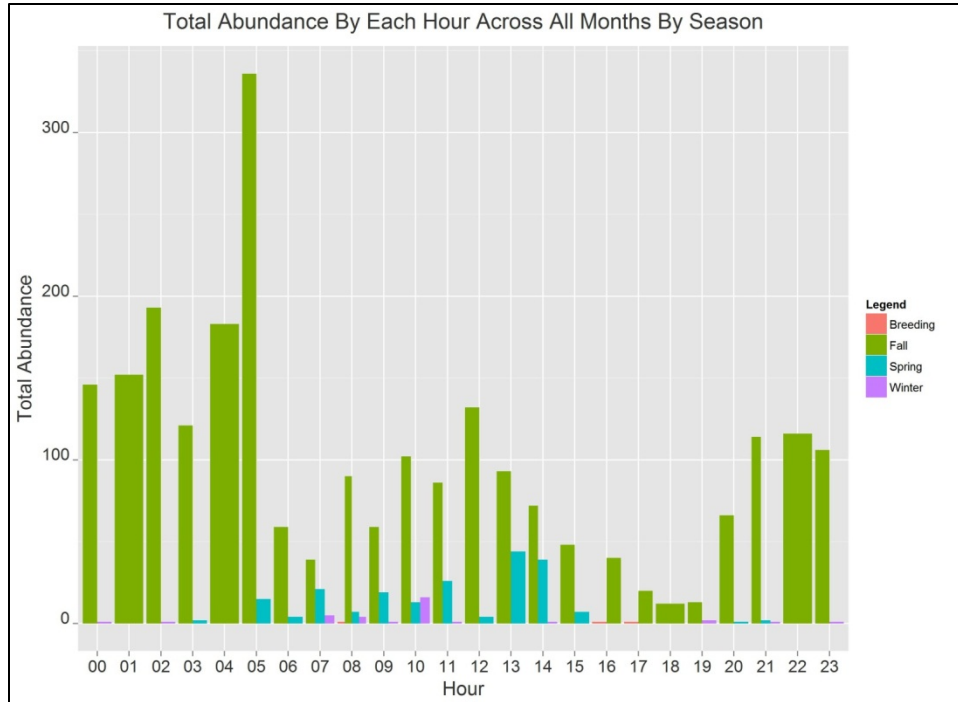
Figure 108.   Call counts by clock hour of all species presented by season.

Total abundance of activity correlates to wind speed as was also found in the thermographic data
with most activity occurring during wind speeds of less than 10 km/hr (Figure 109). Notable
were high counts of several species, such as Cape May Warbler, Northern Parula, Palm Warbler,
Yellow-rumped Warbler, and Swainson's Thrush (Figure 110). This species group represents a
mix of different migrant strategies, and it highlights the importance of this type of monitoring
offshore. Cape May Warbler is a typical trans-Atlantic migrant that breeds in the boreal forests
and winters in the Caribbean. Many Palm Warblers and some Northern Parulas probably employ
the same strategy, although from different destinations, and occur primarily during the fall with
some small numbers recorded in the spring. Yellow-rumped Warblers may be doing something
different, either displaced migrants with non-Caribbean destinations and origins, rather from the
mainland. Moreover, Swainson's Thrush is a primarily Central American and western
Amazonian and Andean wintering species, so their presence off the coast, while not unexpected,
is of interest in terms of strategic decisions that birds make. Calls from all 5 of these species
peaked in Oct with a much smaller number being recorded during other months, if at all (Figure
111 through Figure 115).
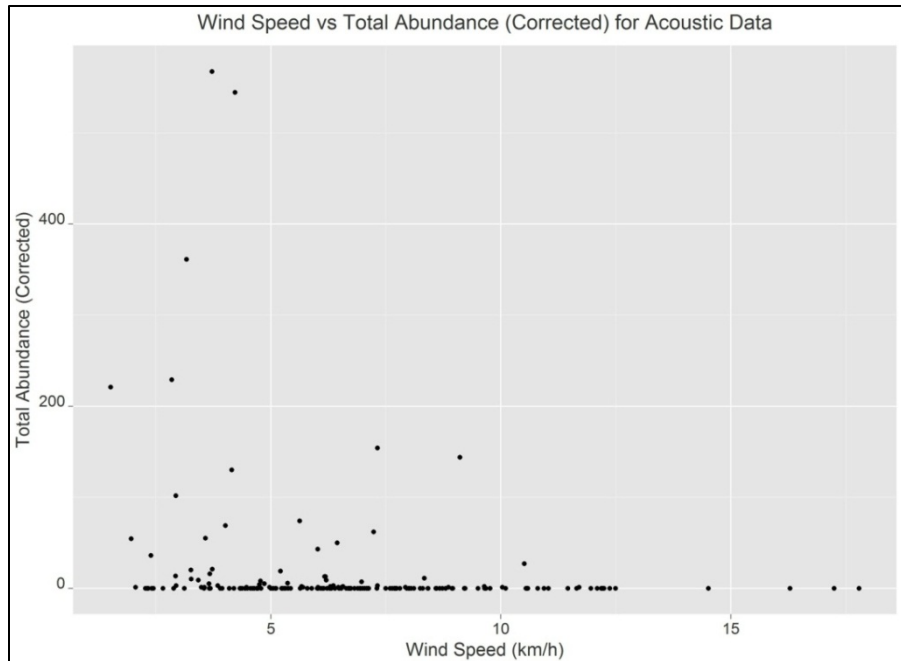
Figure 109.   Mean wind speed versus total corrected bird abundance for birds detected by nocturnal flight call analysis.
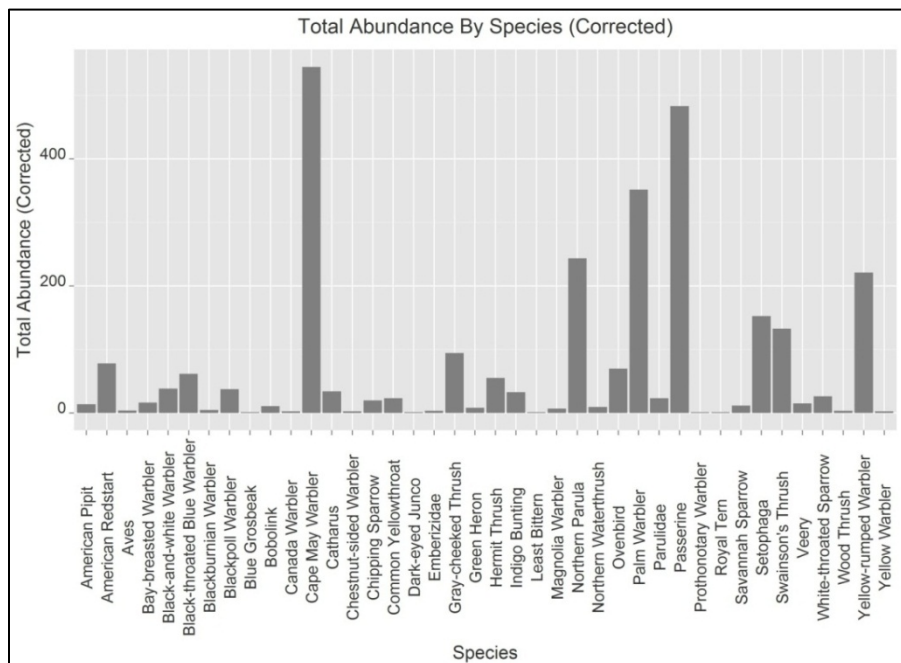
Figure 110.   Total number of nocturnal counts by species across the duration of the study. When calls could not be identified to the species level, the most precise taxa-level classification was assigned.
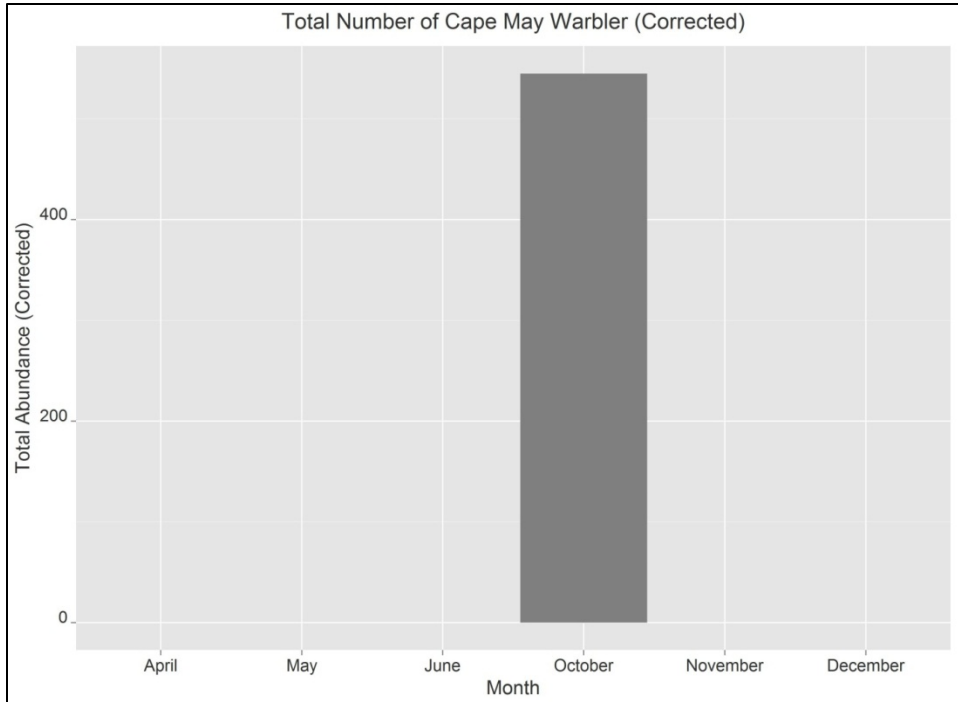
Figure 111.   Total number of Cape May Warbler calls by month across
the duration of the study.
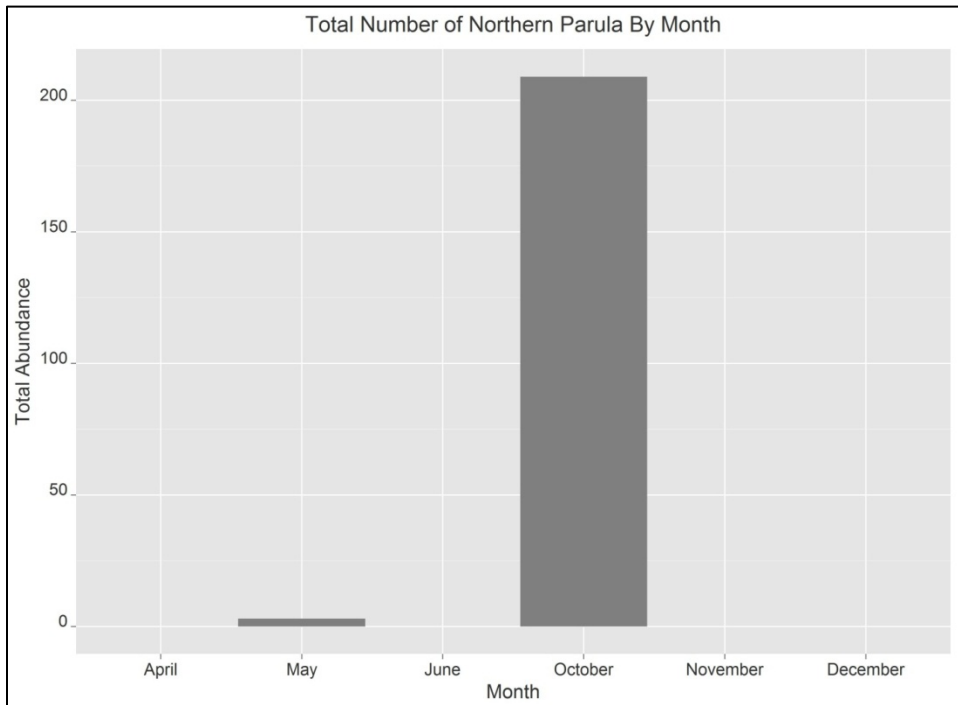
Figure 112.   Total number of Northern Parula calls by month across the
duration of the study.
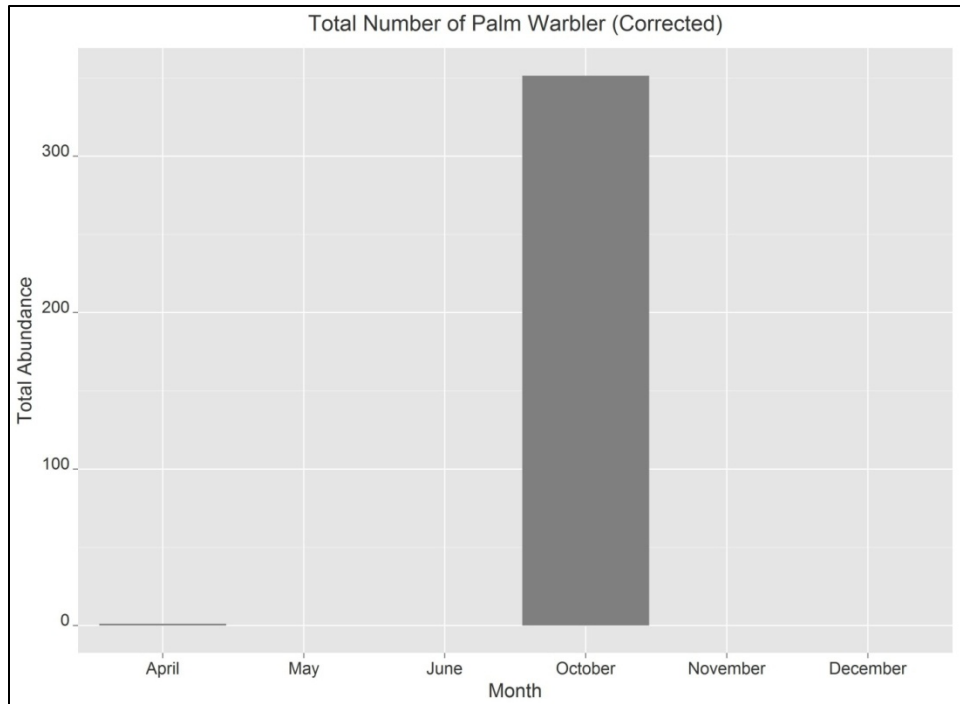
Figure 113.   Total number of Palm Warbler calls by month across the duration of the study.
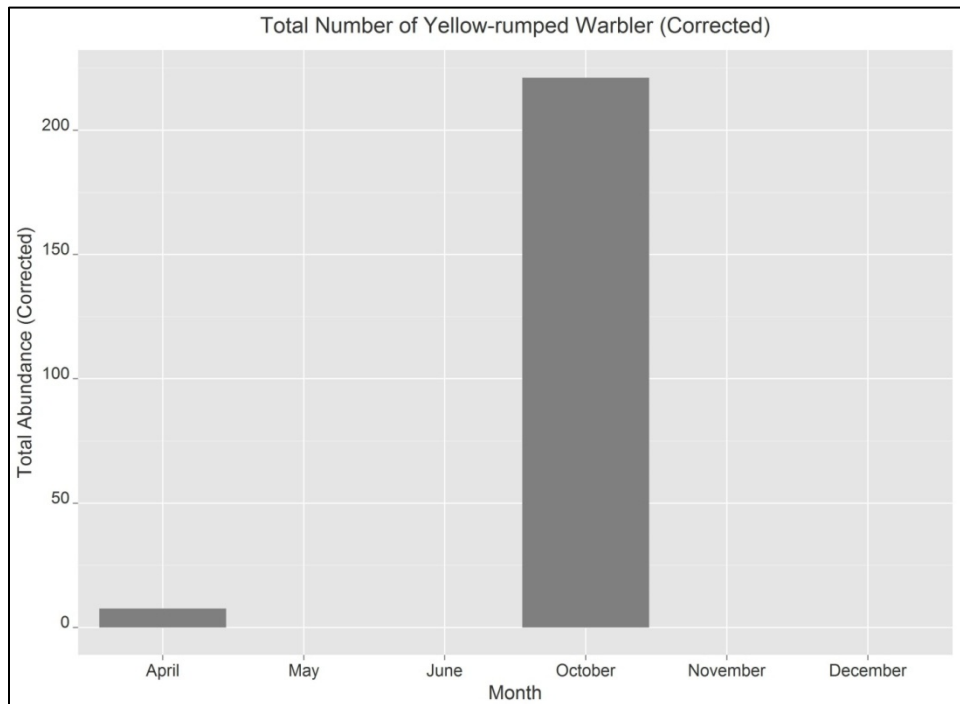
Figure 114.   Total number of Yellow-rumped Warbler calls by month across the duration of the study.
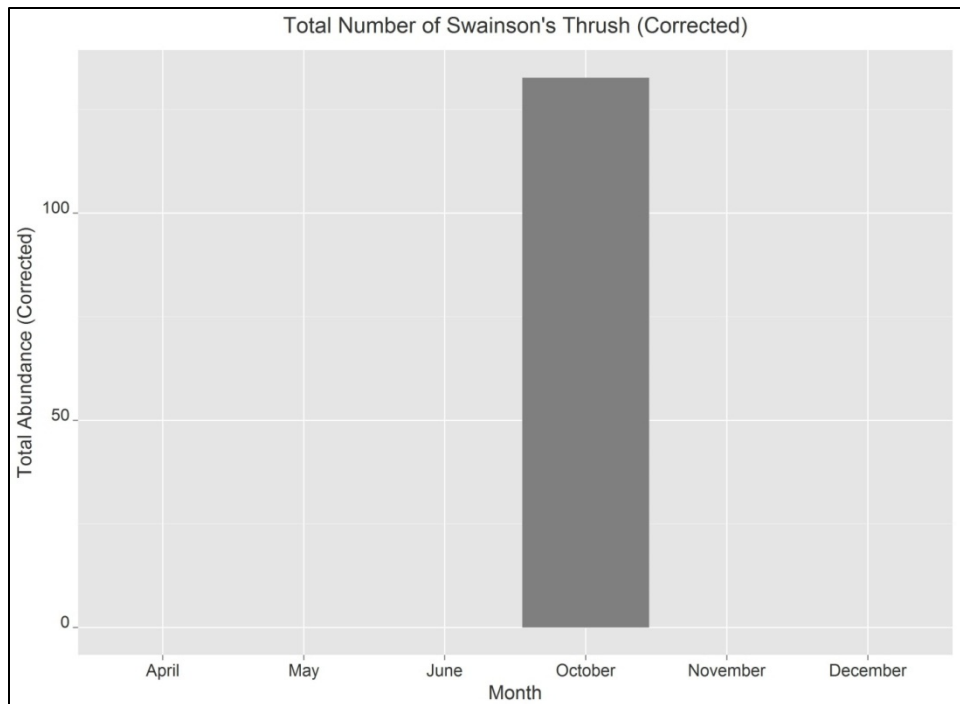
Figure 115.   Total number of Swainson's Thrush calls by month across
               the duration of the study.

Spring recordings highlight a period from mid-to-late Apr through mid-May when migration is heaviest (Table 33). The largest numbers of calls in Apr correspond to earlier migrating species like Ovenbirds, Indigo Buntings, and White-throated Sparrows. Blackpoll Warbler and other *Setophaga* species are more characteristic of later season migration in May.

Table 33.

The five nights with highest calling during the spring migration period occurred in mid- and late April, except for one active night in mid-May.

Species Common Name	18 Apr	19 Apr	21 Apr	29 Apr	17 May	Grand Total
Royal Tern	0	0	1	0	0	1
Ovenbird	0	13	0	0	0	13
Common Yellowthroat	0	0	0	0	4	4
Blackpoll Warbler	0	0	0	1	15	16
Yellow-rumped Warbler	5	0	0	0	0	5
Chipping Sparrow	0	0	18	0	0	18
White-throated Sparrow	0	0	0	23	0	23
Dark-eyed Junco	0	0	1	0	0	1
Indigo Bunting	7	23	0	0	0	30

Species Common Name	18 Apr	19 Apr	21 Apr	29 Apr	17 May	Grand Total
Genus Level Identifications						
Setophaga sp.	0	0	0	1	16	17
Family Level Identifications						
Parulidae sp.	3	0	0	1	0	4
Order Level Identifications						
Passeriformes	1	38	0	1	1	41
Class Level Identifications						
Aves	0	0	0	1	0	1
Grand Total	**16**	**74**	**20**	**28**	**36**	**174**

Fall patterns reflect a greater diversity of migrants, in particular during the early-to-mid Oct window when many species are migrating offshore and advancing toward several (at least) distinct destinations (Table 34). Some highlights of this period include largest movements of the Caribbean-wintering migrant Palm and Cape May Warblers as well as the presence of South American wintering migrant Blackpoll Warbler and Bobolink. Note that these species probably travel more easterly routes over the Atlantic and recordings represent the westernmost individuals departing from the U.S. coastlines farthest to the South. The patterns of peak density during fall migration correspond with tail winds (Figure 116), but data were sparse for spring migration as no data were collected in Mar. Therefore it is difficult to conclude that spring migration was with or without accompanying tail winds, but using the existing data, patterns affecting migration are not evident.

Table 34.

The five nights with highest calling occurred in early- and mid-October.

Species Common Name	04 Oct	05 Oct	06 Oct	07 Oct	11 Oct	17 Oct	Grand Total
Green Heron	2	2	0	0	0	1	5
Veery	3	3	0	5	0	0	11
Gray-cheeked Thrush	3	3	2	33	2	25	68
Swainson's Thrush	11	21	7	27	2	29	97
Wood Thrush	1	1	0	1	0	0	3
Ovenbird	8	20	3	12	7	1	51
Northern Waterthrush	0	3	0	1	1	0	5
Black-and-white Warbler	1	6	4	3	1	13	28
Common Yellowthroat	2	6	1	1	4	0	14
American Redstart	20	15	9	0	0	4	48
Cape May Warbler	32	199	11	87	57	25	411

Species Common Name	04 Oct	05 Oct	06 Oct	07 Oct	11 Oct	17 Oct	Grand Total
Northern Parula	7	32	8	21	22	19	109
Magnolia Warbler	0	2	0	0	3	0	5
Bay-breasted Warbler	0	6	0	0	0	0	6
Blackburnian Warbler	0	1	0	0	0	0	1
Yellow Warbler	0	1	0	1	0	0	2
Chestnut-sided Warbler	1	1	0	0	0	0	2
Blackpoll Warbler	0	4	0	7	5	0	16
Black-throated Blue Warbler	7	15	14	3	7	0	46
Palm Warbler	69	66	106	27	7	16	291
Yellow-rumped Warbler	6	16	6	5	6	98	137
Savannah Sparrow	0	2	0	0	0	3	5
Blue Grosbeak	1	0	0	0	0	0	1
Indigo Bunting	1	2	1	0	0	0	4
Bobolink	6	0	2	1	0	0	9
Genus Level Identifications							
Catharus sp.	4	7	1	10	0	2	24
Setophaga sp.	6	25	2	18	9	0	60
Family Level Identifications							
Parulidae sp.	1	3	0	2	1	4	11
Emberizidae sp.	0	2	0	0	0	0	2
Order Level Identifications							
Passeriformes	37	80	44	65	20	80	326
Grand Total	**229**	**544**	**221**	**330**	**154**	**320**	**1,798**
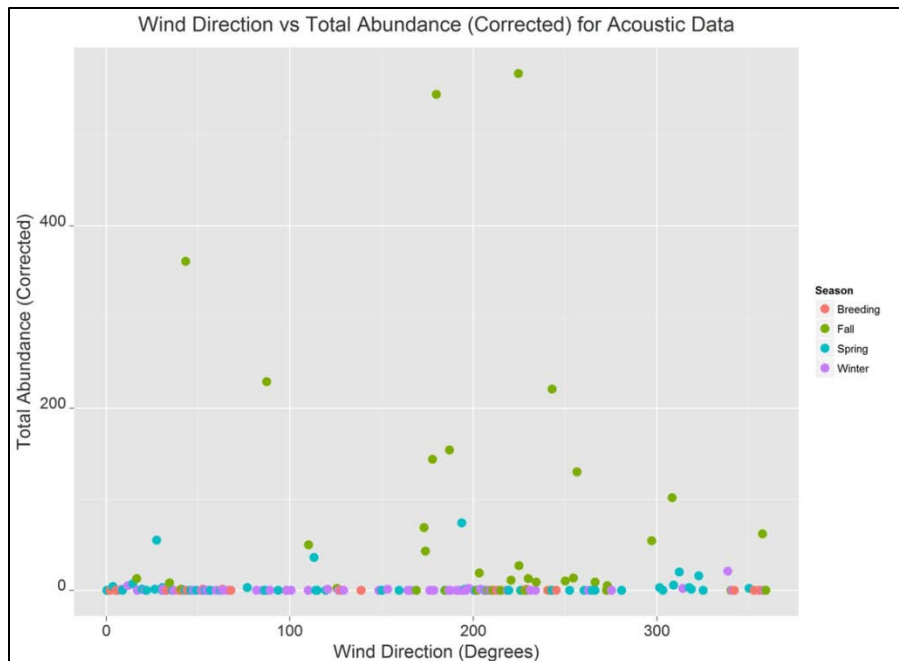
Figure 116. Mean wind direction versus mean density for birds detected in acoustic data for each season. Mean directions were calculated using circular statistics. Note that the wind direction in this figure is the direction to which the wind is blowing rather than the direction of origin, to allow simple correlation with bird direction information.

8.2.2 Activity Analysis

Using all data, not just the nocturnal flight activity sound files, eight species were identified that were the primary components of the calling during the high activity periods. Table 35 shows the species composition. In addition, numerous instances of unidentified gulls and terns were found, identified only to family because the sound quality was insufficient for specific identification or because distant, overlapping, and otherwise masked calls made species-level identification impossible. The gulls and terns are primarily species that are either resident or regular during most of the year at or near the platform, sometimes using it to feed and roost. Because these species tend to aggregate, it is no surprise that their presence in the acoustic dataset marked periods of high activity with hundreds and thousands of vocalizations.

Although some of the blocks with high vocal activity (multiple birds calling at the same time) align with periods when migrant activity was high, there is not particularly good agreement between these high activity periods and high passerine calling periods. This suggests that high activity periods may be a useful way to target periods of acoustic interest, but that these periods may or may not be times when large numbers of migrant calls are occurring. High vocal activity peaked during the daylight hours and this trend was consistent across seasons (Figure 117 through Figure 120). There were no periods of high activity recorded during the winter season, 01 Nov–12 Dec.

Table 35.

Species identified in sound files of high activity.

Common Name	Scientific Name	Species Code
Species Level Identifications		
Laughing Gull	*Leucophaeus atricilla*	LAGU
Ring-billed Gull	*Larus delawarensis*	RBGU
Herring Gull	*Larus argentatus*	HEGU
Common Tern	*Sterna hirundo*	COTE
Forster's Tern	*Sterna forsteri*	FOTE
Royal Tern	*Thalasseus maximus*	ROYT
Sandwich Tern	*Thalasseus sandvicensis*	SATE
White-throated Sparrow	*Zonotrichia albicollis*	WTSP
Sub-family Level Identifications		
Larinae sp.		
Sterninae sp.		
Class Level Identifications		
Aves		
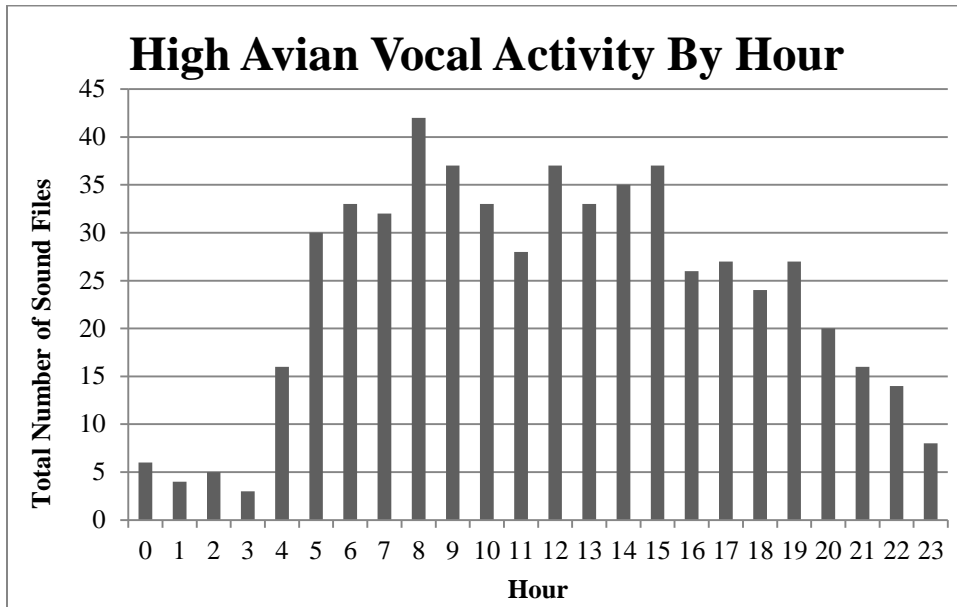
Figure 117.   Number of high-activity sound files per clock hour
calculated across the entire deployment period (03 Apr–12
Dec 2012).
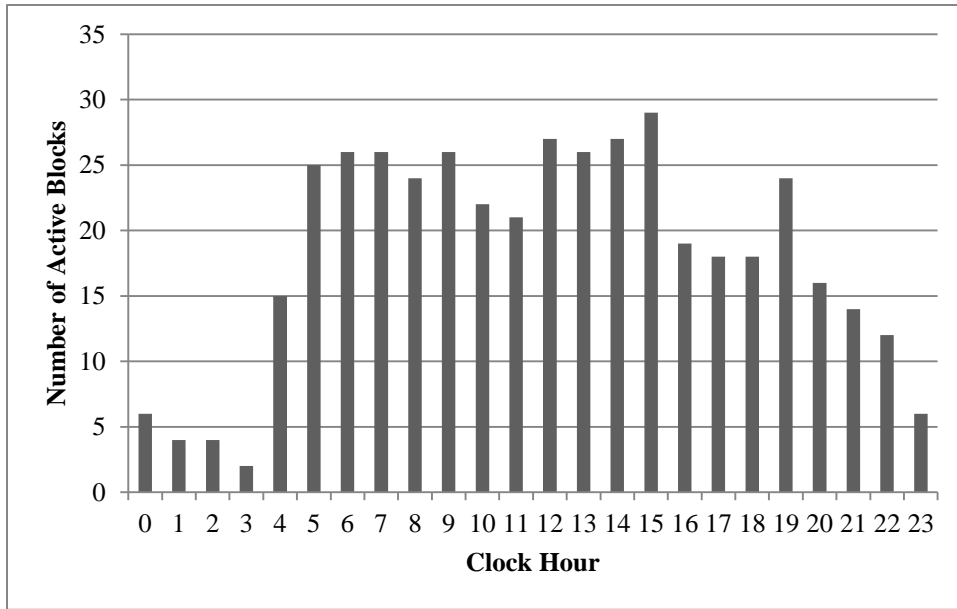
Figure 118. Number of high-activity sound files per clock hour calculated across the spring migration (03 Apr–31 May 2012), indicating the presence of multiple birds around the clock during this period.
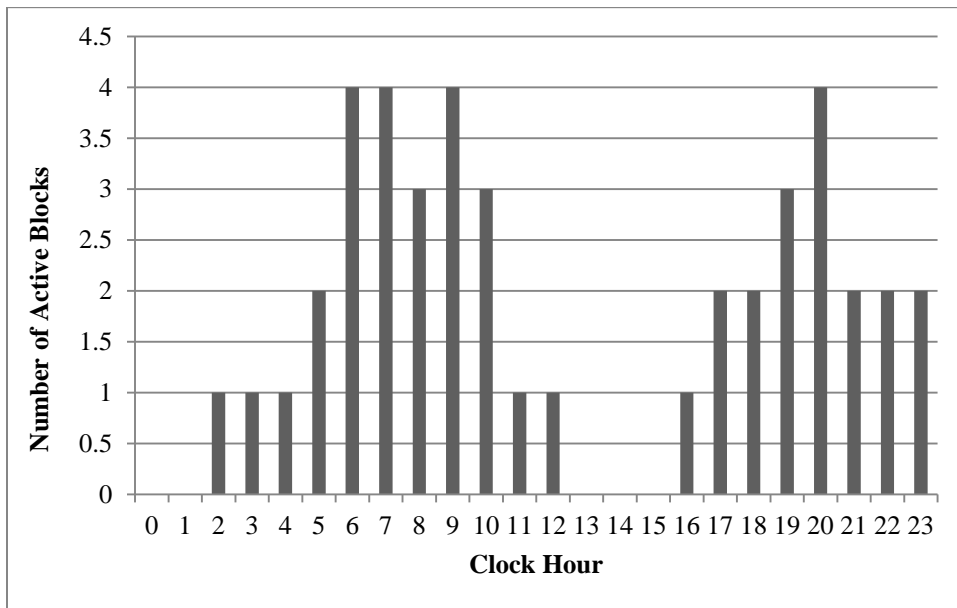
Figure 119. Number of high-activity sound files per clock hour calculated across the breeding season (01 Jun–15 Jul). Although there are far fewer periods of high vocal activity during this period, birds appear to still be present, at least in some degree, around the clock.
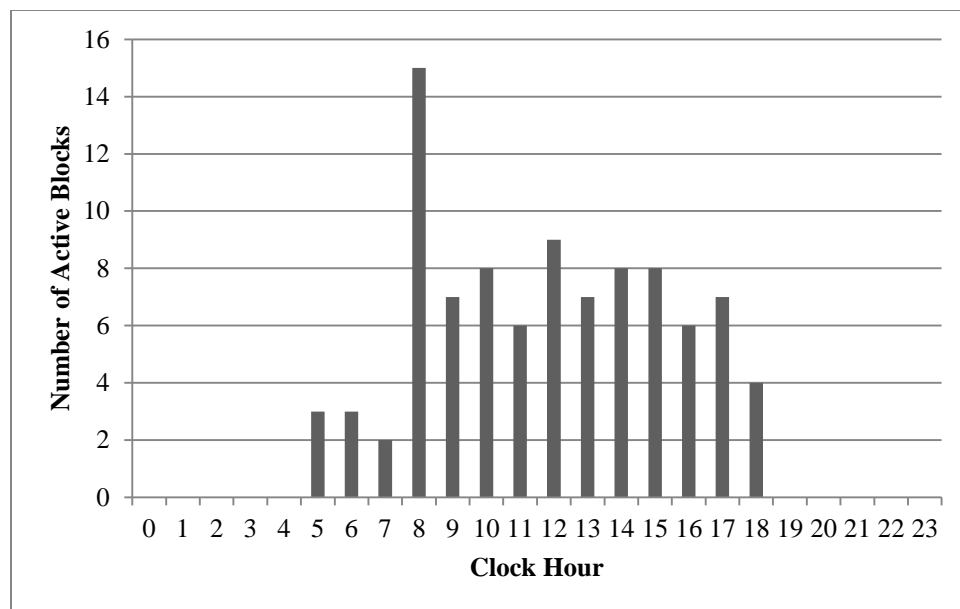
Figure 120.   Number of high-activity sound files per clock hour
              calculated during fall migration (16 Jul–31 Oct). Active
              periods during the fall migration appear to be concentrated
              during the diurnal hours, differing from the other seasons.

8.3 Combined Thermographic and Acoustic Results

Combined thermographic and acoustic species-specific data collected show Yellow-rumped
Warbler with flight altitudes of 103.9 m and 46.3 m (n=2) and Laridae with flight altitudes
ranging from 49.1 m to 193.9 m, mean 87.43 m (n=35) (Table 36).

Table 36.

Combined thermal and acoustic data matches.

Type	Date	Time	Taxa	Altitude	Decimal Bearing	Compass Bearing
Acoustic	4/5/2012	06:52:00	Laridae			
Thermo	4/5/2012	06:52:05	Bird	51.4	172.9	SSE
Acoustic	4/7/2012	10:21:00	Laridae			
Thermo	4/7/2012	10:21:05	Bird	119.3	12.5	NNE
Acoustic	4/12/2012	20:11:00	Laridae			
Thermo	4/12/2012	20:11:00	Bird	129.1	34.8	NNE
Acoustic	4/12/2012	20:17:00	Laridae			
Thermo	4/12/2012	20:16:59	Bird	90.5	279	WNW
Acoustic	4/12/2012	22:15:00	Laridae			

Type	Date	Time	Taxa	Altitude	Decimal Bearing	Compass Bearing
Thermo	4/12/2012	22:15:02	Bird	147.6	351.7	NNW
Acoustic	4/12/2012	22:21:00	Laridae			
Thermo	4/12/2012	22:21:00	Bird	94.2	132.4	ESE
Acoustic	4/12/2012	22:33:00	Laridae			
Thermo	4/12/2012	22:33:05	Bird	118.7	317.6	NNW
Acoustic	4/13/2012	12:03:00	Laridae			
Thermo	4/13/2012	12:03:02	Bird	91.2	36.8	NNE
Acoustic	4/13/2012	12:03:00	Laridae			
Thermo	4/13/2012	12:03:03	Bird	97.6	30.5	NNE
Acoustic	4/13/2012	14:22:00	Laridae			
Thermo	4/13/2012	14:22:01	Bird	193.9	77	ENE
Acoustic	4/13/2012	16:51:00	Laridae			
Thermo	4/13/2012	16:51:04	Bird	78.7	340.6	NNW
Acoustic	4/13/2012	16:51:00	Laridae			
Thermo	4/13/2012	16:51:05	Bird	94.2	45.9	ENE
Acoustic	4/18/2012	09:34:00	Laridae			
Thermo	4/18/2012	09:34:05	Bird	80.4	301	WNW
Acoustic	4/19/2012	07:06:00	Laridae			
Thermo	4/19/2012	07:06:01	Bird	78.9	190.5	SSW
Acoustic	4/19/2012	07:06:00	Laridae			
Thermo	4/19/2012	07:06:02	Bird	84.2	195.6	SSW
Acoustic	4/25/2012	09:35:00	Laridae			
Thermo	4/25/2012	09:35:01	Bird	73.3	192.7	SSW
Acoustic	5/11/2012	07:16:00	Laridae			
Thermo	5/11/2012	07:16:02	Bird	77.1	328.9	NNW
Acoustic	5/13/2012	10:31:00	Laridae			
Thermo	5/13/2012	10:31:05	Bird	93.3	71	ENE
Acoustic	5/17/2012	18:22:00	Laridae			
Thermo	5/17/2012	18:21:55	Bird	69.2	93.4	ESE
Acoustic	5/17/2012	18:22:00	Laridae			
Thermo	5/17/2012	18:22:05	Bird	76.3	185.9	SSW
Acoustic	5/27/2012	09:49:00	Laridae			
Thermo	5/27/2012	09:49:04	Bird	49.7	106.5	ESE

Type	Date	Time	Taxa	Altitude	Decimal Bearing	Compass Bearing
Acoustic	5/27/2012	12:29:00	Laridae			
Thermo	5/27/2012	12:28:58	Bird	62	98.9	ESE
Acoustic	6/2/2012	07:27:00	Laridae			
Thermo	6/2/2012	07:26:55	Bird	83.2	N/A	N/A
Acoustic	6/2/2012	07:29:00	Laridae			
Thermo	6/2/2012	07:29:04	Bird	83.9	N/A	N/A
Acoustic	6/2/2012	07:29:00	Laridae			
Thermo	6/2/2012	07:29:04	Bird	83.9	N/A	N/A
Acoustic	6/2/2012	08:43:00	Laridae			
Thermo	6/2/2012	08:43:03	Bird	54.8	N/A	N/A
Acoustic	6/2/2012	08:43:00	Laridae			
Thermo	6/2/2012	08:43:03	Bird	54.3	N/A	N/A
Acoustic	6/2/2012	17:21:00	Laridae			
Thermo	6/2/2012	17:20:56	Bird	65.7	312.7	WNW
Acoustic	6/2/2012	19:38:00	Laridae			
Thermo	6/2/2012	19:38:05	Bird	N/A	N/A	N/A
Acoustic	6/6/2012	17:02:00	Laridae			
Thermo	6/6/2012	17:02:01	Bird	49.1	271.3	WNW
Acoustic	6/8/2012	15:18:00	Laridae			
Thermo	6/8/2012	15:18:02	Bird	53.3	207.9	SSW
Acoustic	6/8/2012	15:18:00	Laridae			
Thermo	6/8/2012	15:18:02	Bird	56.4	204.7	SSW
Acoustic	6/11/2012	10:17:00	Laridae			
Thermo	6/11/2012	10:17:03	Bird	88.4	21.2	NNE
Acoustic	6/20/2012	10:40:00	Laridae			
Thermo	6/20/2012	10:40:02	Bird	174.6	72.4	ENE
Acoustic	6/21/2012	07:04:00	Laridae			
Thermo	6/21/2012	07:04:05	Bird	74.4	242.4	WSW
Acoustic	10/17/2012	11:40:36	YRWA			
Thermo	10/17/2012	11:40:33	Bird	46.3	311.7	WNW
Acoustic	10/17/2012	11:42:46	YRWA			
Thermo	10/17/2012	11:42:44	Bird	103.9	148.9	SSE

8.4 Ultrasound Results

The ultrasonic microphone recorded a total of 261,584 files while deployed at the FPSLT. Due to the harsh marine environment, the microphone became damaged and stopped working after May 2012 and all files after that date were unusable.

None of the reviewed files from the FPSLT data contained bat calls, validating their removal by the filter. Ultrasound spectrograms from all "bat" files were then manually reviewed by an expert bat biologist who is qualified to identify all species of North American bats on the basis of their ultrasound spectrograms. This manual review process is performed using Normandeau's ReBAT.com user interface software. In this process, any .wav files containing potential bat vocalizations that require detailed analysis are subsequently analyzed by an expert biologist using SonoBat™ (SonoBat 3.0, Arcata, CA) acoustic analysis software, which contains spectrogram visualization tools and bat call reference libraries that analysts use to ascribe any recorded bat calls to species or species group. In the complete review of ATOM ultrasound data from 6 Dec 2011 through 28 May 2012 from the FPSLT deployment, no bat calls were discovered.

8.5 Discussion

Results show a clear pattern of migrant occurrence in the offshore environment with Apr and Oct showing peak density with combined acoustic and thermographic data. However, a paucity of data from Mar means that a potentially important month for bird activity was under-surveyed. Peak in fall density of migrating birds occurred during periods of north to northwest winds (i.e., with a tail wind).

Most birds appear to fly higher in the evenings with an estimated flight height increase of 1.8 times from 8 PM to 12 AM than at all other times of day. Flight altitude seems unaffected by wind speed. Instead, both acoustic and thermographic data show that there is more bird activity during wind speeds of less than 10 km/hr, but with no discernable alteration in altitude.

Flight direction is affected by wind speed and direction with data showing birds have a slight inclination to fly into head wind, although some flew with tail wind but few flew with cross winds. Flight bearing in passerines showed seasonal differences, but similar trends were not evident with non-passerines. Passerines showed strong tendencies to fly to the south and southeast during the fall and to the northwest during the spring. Mean flight direction during Apr was 286º (NW) and in Oct was 151º (SSE). Flight bearings for non-passerines did not mirror these trends and no discernable patterns were evident.

Although flight velocity is not available for every bird, velocity data are consistent throughout the year, as well as throughout the day, with an average velocity of 23 km/hr.

A number of seabird species, including gulls, terns, and frigatebirds, were expected to occur during the offshore deployment and were duly identified by ATOM. The dataset of land bird species identified by ATOM is a significant contribution to filling gaps in knowledge about these migrants and includes herons, bitterns, and many passerines. Not all species vocalize in the offshore environment. Thermographic data are also able to identify those species that have key

morphological characteristics and that don't vocalize. For example, the occurrence of a frigatebird was recorded in thermographic data. Flight altitude for this individual was 44.2 m above sea level. This bird was attracted to the tower and circled several times.

The system is designed to survey birds and bats within the rotor swept area of a turbine, consequently most flight altitude data are within this detection area. Acoustic data also fill information gaps on small birds flying higher than 150 m that might otherwise be missed by thermographic technology due to the decay in detection over distance for small birds. One approach to addressing the decreased detections at longer distances is to incorporate distance sampling methodology and creating a detection function to estimate loss in detectability over distances (Buckland et al. 1993). The detection function predicts a range of detection probabilities at various distances then detection probabilities are used to account for birds/bats present but not detected. Regardless if distance sampling is used or not, information from these two detection methods provides new data on peak migration times for both vocal and silent species.

Bats, though known from other studies to occur at offshore locations (e.g., Pelletier and Peterson 2013; Pelletier et al. 2013; Mackiewicz and Backus 1956; Carter 1950), were not found at FPSLT from within the ultrasonic or thermographic data. However, no data were gathered in Feb and the microphone had ceased functioning at the end of May 2012. Bats are most likely to be found offshore during the fall migration period when inclement weather forces them off their normal migration paths (e.g., Mackiewicz and Backus 1956; Carter 1950). Although bats have been encountered this far offshore and away from any terrestrial habitat, data show that it is unlikely that they occur at remote stations like FPSLT with any regularity. They are more likely to be found near offshore islets and outcrops with some semblance of roosting and/or foraging habitat suitable to the migratory species.

Although an original goal was that ATOM would give species-specific information on flight altitude, velocity, and bearing, sufficient data were not collected that could match many species level identifications with all detectors. Increased system reliability should augment the amount of data that could be matched, and longer deployment would gather more data from all sensors. However, species specific data collected show Yellow-rumped Warbler with flight altitudes of 103.9 m and 46.3 m (n=2) and Laridae with flight altitudes ranging from 49.1 m to 193.9 m, mean 87.43 m (n=35).

The data collected in this study are invaluable for attempting to clarify the movements of birds and bats, particularly offshore migrants, and assessing the potential risk that these species might face. The results presented in this report are evidence of remarkable progress in the use of acoustic and thermographic monitoring to understand the ecology of large-scale migrations and their implications for conservation. Particularly novel is the dataset itself, the first of its kind from the offshore environment in the western Atlantic Ocean.

9   Lessons Learned

The objective of this study was to test and operate acoustic and thermographic detectors on offshore structures to detect bird species by call and to estimate bird numbers based on a

combination of call rates and thermographic video. An additional goal of this study was to assess similar information for bats using ultrasound recordings and thermographic video. The study was successful in being able to deploy such a system and collect the intended data but not as consistently or continuously as was originally conceived.

It was known and planned for that an offshore deployment would be a challenging study environment but in retrospect there would have been more consistent and continuous data had the system not been 29 mi offshore. In the proposal, it was assumed that the first deployment was going to be 3 to 10 mi offshore. But when ATOM needed to be installed to meet project timelines, FPSLT was the only location available to install the system. Normandeau and BOEM contacted every potential agency and private company that had or was planning on having a platform in the AOCS but none were able to cooperate/collaborate for this study during that time period. This study was the first of its kind with the ATOM system being deployed offshore. Being on FPSLT made it more costly and limited the ability to access the system, which increased system down-time, delayed repairs, and increased the cost of deploying and maintaining the system. While the location was a significant challenge for the first ATOM deployment, the study did collect some new information on bird and bat use in the offshore environment. It also brought to light some physical, hardware, and software changes that are needed for future successful data collection.

The marine environment was especially harsh on the exposed acoustic and ultrasonic microphones. While this was expected, microphone elements failed more than expected. Going forward new microphone covers have been identified but future studies should plan for periodic microphone replacement and acoustic data quality should be monitored for degradation over time.

Waterproofing and wind mitigation were also an issue. While all the enclosed equipment was designed to be tightly sealed, the battery box, for example, had water in it on a couple of occasions and strapping down the battery box lid to secure it during high winds was ineffective. Subsequently "Lock-tite" substance and locking hardware were implemented to prevent equipment damage. Similarly, corrosion affected the wiper arm assembly of the cameras and caused water to seep into the controller box. This was addressed with a new design that has been implemented in new installations. Rain would pool and seep into the lens cleaner reservoir and dilute the mixture. A new reservoir system was being investigated and tested towards the end of the project.

The biggest cause of inconsistent data collection was the data storage computer. A separate data storage computer was built to hold all the thermal video data. The ATOM system was originally designed to store the data uncompressed because of concerns that compressing the data might impact the ability to identify targets and concerns over the power needed to compress the data. As a result, a 90 TB data storage computer was built that enabled individual storage drives to be turned on and off as they were filled. This kept the power draw down and also enabled 100% of the video to be stored. Custom software and hardware was developed for this purpose. Unfortunately, the data storage computer had consistent issues throughout the study with Normandeau staff remotely having to try to keep that computer working. By the time the project was over, Normandeau had come up with an alternative design that included compressing and

storing the data on a single 1TB SSD (solid state drive), which holds almost a year's worth of data. Normandeau was able to compare the compressed data to raw data using the thermal analysis software developed for the project and found that the compressed data did not impact the ability to identify targets. Compressing the data and storing it on the SSD eliminates the need for the separate data storage computer and it also reduces the power draw, significantly improving system reliability. In addition, for locations not requiring satellite communications such as those with reasonably good cellular access, it is practical to upload all audio and video data in real time so data can be analyzed in a more timely manner.

With many bird detections happening during daylight hours, the use of an ambient light system to record birds, in tandem with a thermographic camera has been considered. This could potentially have the advantage of allowing some species ID using image data alone. However, in periods of bad weather with rain or other poor visibility conditions, this system would still fail to reach identification level consistently. Also, the current advantage of stereo thermographic cameras for gathering accurate flight altitude data would be complicated by using one thermographic and one ambient light camera, with the requirement of either similar specifications, or the development of complex compensatory software. Integrating an ambient light camera with two thermographic cameras has also been discussed. Costs for the ATOM system are already such that the benefits of adding an ambient light camera could be considered to be outweighed by the additional costs. However, the development team has considered looking into a much higher specification thermographic camera with a wider field of view and finer resolution.

When the project was conceived, it was assumed that the offshore wind developers would have to install meteorological platforms to collect wind data but it appears that sodar technology on buoys is becoming more of an option. Consequently platforms may not be as prevalent. Looking forward, bird and bat data collection will most likely need to be collected from buoys rather than platforms. As result of this project Normandeau has subsequently modified the ATOM system to work on a buoy. Buoy deployments will enable ATOM systems to be deployed in more locations and at lower costs.

BOEM funded a study that developed technology that can monitor flying vertebrates in the ocean. That technology can be used to collect long term data sets on the species or taxa, passage rates, height, speed, and direction of targets flying within the potential rotor swept zone of a wind turbine. This information can be used to assess preconstruction risk and the technology can also be installed on wind turbines to monitor avoidance and collision of birds and bats.

10 Literature Cited

Adams, A. M., M. K. Jantzen, and R. M. Hamilton. 2011. Bat detector comparison with synthetic playback and free-flying bats. North American Society for Bat Research 41st Annual Meeting, Toronto, Ontario.

Arnett, E. B., J. P. Hayes, and M. M. P. Huso. 2006. An evaluation of the use of acoustic monitoring to predict bat fatality at a proposed wind facility in south-central Pennsylvania. An annual report submitted to the Bats and Wind Energy Cooperative. Bat Conservation International. Austin, Texas, USA.

Atlas, M. 2011. MRI Atlas of the Human Brain, vol. 2011.

Baird, J., and I. C. T. Nisbet. 1960. Northward fall migration on the Atlantic coast and its relation to offshore drift. *Auk* 77: 119–149.

Baker, R. H. 1947. Observations on the birds of the North Atlantic. *Auk* 64: 245–259.

Ballard, D. H., and C. M. Brown. 1982. *Computer Vision.* Englewood Cliffs, New Jersey: Prentice Hall International Inc.

Barclay, R. M. R., E. F. Baerwald, and J. C. Gruver. 2007. Variation in bat and bird fatalities at wind energy facilities: Assessing the effects of rotor size and tower height. *Canadian Journal of Zoology* 85(3): 381–387.

Bioacoustics Research Program. 2013. Raven Pro: Interactive Sound Analysis Software (Version 1.5) [Computer software]. Ithaca, NY: The Cornell Lab of Ornithology. Available from http://www.birds.cornell.edu/raven.

Brown, J. C. 1896. The American crossbill at sea. Auk 13: 176.

Buckland, S.T., Anderson, D.R., Burnham, K.P. and Laake, J.L. 1993. Distance Sampling: Estimating Abundance if Biological Populations. Chapman and Hall, London. 446pp

Burnham, K. P., and D. R. Anderson. 2002. Model selection and multimodel inference: A practical information-theoretic approach. Second edition. Springer-Verlag, New York, New York, USA.

Butler, A. W. 1926. Landbirds at sea. *Auk* 43: 103.

Carter, T. D. 1950. On the migration of the red bat, *Lasiurus borealis borealis*. *Journal of Mammalogy* 31: 349–350.

Charif, R. A., K. A. Cortopassi, H. K. Figueroa, J. W. Fitzpatrick, K. M. Fristrup, M. Lammertink, M. D. Luneau, Jr., M. E. Powers, and K. V. Rosenberg. Letter to Science. 2 September 2005: 1489.

Cooke, W. W. 1904. Distribution and migration of North American warblers. U.S. Dept. Agriculture, Division of Biological Survey Bulletin 18. 142 pp.

Dalgaard, P. 2008. Introductory Statistics with R. Second Edition. Springer, New York, New York, USA.

Duda, R. O., P. E. Hart, and D. G. Stork. 2001. Pattern Classification. United States of America, John Wiley and Sons.

Dugan, P. J., A. N. Rice, I. R. Urazghildiiev, and C. W. Clark. 2010a. North Atlantic Right Whale acoustic signal processing, Part I: Comparison of machine learning recognition algorithms. Applications and Technology Conference (LISAT), 2010 Long Island Systems, pp. 1.

Dugan, P. J., A. N. Rice, I. R. Urazghildiiev, and C. W. Clark. 2010b. North Atlantic Right Whale acoustic signal processing, Part II: Improved decision architecture for auto-detection using multi-classifier combination methodology. Applications and Technology Conference (LISAT), 2010 Long Island Systems, pp. 1.

Erbe, C., and A. R. King. 2008. Automatic detection of marine mammals using information entropy. *J. Acoust. Soc. Am.* 124(5): 2833–2840.

Evans, W. R., and M. O'Brien. 2002. Flight Calls of Migratory Birds, *Eastern North American Landbirds*. Old Bird, Inc. [CD-ROM]

Evans, W. R. 1994. Nocturnal flight call of Bicknell's Thrush. *Wilson Bulletin* 106: 55–61.

Evans, W. R., and K. V. Rosenberg. 2000. Acoustic monitoring of night-migrating birds: A progress report. *In* R. Bonney, D. N. Pashley, R. J. Cooper, and L. Niles, eds., Strategies of Bird Conservation: The Partners in Flight Planning Process. Proceedings of the 3rd Partners in Flight Workshop; 1995 October 1–5; Cape May, NJ. Proceedings RMRS-P-16. Ogden, UT: U.S. Department of Agriculture, Forest Service, Rocky Mountain Research Station.

Farnsworth, A. 2005. Flight calls and their value for future ornithological studies and conservation research. *Auk* 122(3): 733–746.

Farnsworth, A., and R. W. Russell. 2007. Monitoring flight calls of migrating birds from an oil platform in the northern Gulf of Mexico. *Journal of Field Ornithology* 78: 279–289. doi: 10.1111/j.1557-9263.2007.00115.x

Farnsworth, A., S. A. Gauthreaux, and D. van Blaricom. 2004. A comparison of nocturnal call counts of migrating birds and reflectivity measurements on Doppler radar. *Journal of Avian Biology* 35: 365–369.

Fiedler, J. K. 2004. Assessment of Bat Mortality and Activity at Buffalo Mountain Windfarm, Eastern Tennessee. M.S. Thesis. University of Tennessee, Knoxville.

Figueroa, H. K. 2005. XBAT v5. Cornell University Bioacoustics Research Program, Ithaca, NY. http://xbat.org/.

Fitzpatrick, J. W., M. Lammertink, M. D. Luneau, Jr., T. W. Gallagher, B. R. Harrison, G. M. Sparling, K. V. Rosenberg, R. W. Rohrbaugh, E. C. H. Swarthout, P. H. Wrege, S. B. Swarthout, M. S. Dantzker, R. A. Charif, T. R. Barksdale, J. V. Remsen, Jr., S. D. Simon, and D. Zollner. 2005. Ivory-billed Woodpecker (*Campephilus principalis*) Persists in Continental North America. *Science* 308(5727): 1460–1462.

Ghose, K., T. K. Horiuchi, P. S. Krishnaprasad, and C. F. Moss. 2006. Echolocating bats use a nearly time-optimal strategy to intercept prey. *PLoS Biol* 4(5): e108. DOI: 10.1371/journal.pbio.0040108.

Gordon, M. S. 1955. Summer ecology of oceanic birds off southern New England. *Auk* 72: 138–147.

Grayce, R. I. 1950. Bird transects on the North Atlantic. *Wilson Bulletin* 62: 32–35.

Helmuth, W. T. 1920. Extracts from notes made while in naval service. *Auk* 37: 255–261.

Johnson, J. B., J. E. Gates, and N. P. Zegre. 2011. Monitoring seasonal bat activity on a coastal barrier island in Maryland, USA. *Environmental Monitoring and Assessment* 173: 685–699.

Kerns, J., W. P. Erickson, and E. B. Arnett. 2005. Bat and bird fatality at wind energy facilities in Pennsylvania and West Virginia. Pages 24–95 *in* E. B. Arnett, ed., Relationships between bats and wind turbines in Pennsylvania and West Virginia: An assessment of bat fatality search protocols, patterns of fatality, and behavioral interactions with wind turbines. A final report submitted to the Bats and Wind Energy Cooperative. Bat Conservation International, Austin, Texas, USA.

Kunz, T. H., E. B. Arnett, B. M. Cooper, W. P. Erickson, R. P. Larkin, T. Mabee, M. L. Morrison, M. D. Strickland, and J. M. Szewczak. 2007. Assessing impacts of wind-energy development on nocturnally active birds and bats: A guidance document. *Journal of Wildlife Management* 71: 2449–2486.

Kunz, T. H., S. A. Gauthreaux, Jr., N. I. Hristov, J. W. Horn, G. Jones, E. K. V. Kalko, R. P. Larkin, G. F. McCracken, S. W. Swartz, R. B. Srygley, R. Dudley, J. K. Westbrook, and M. Wikelski. 2008. Aeroecology: Probing and modeling the aerosphere. *Integrative and Comparative Biology* 48: 1–11. doi:10.1093/icb/icn037

Lampert, T. A., and S. E. M. O'Keefe. 2011. A detailed investigation into low-level feature detection in spectrogram images. *Pattern Recognit* 44(9): 2076–2092.

Lanzone, M., E. DeLeon, L. Grove, and A. Farnsworth. 2009. Revealing undocumented or poorly known flight calls of warblers (Parulidae) using a novel method of recording birds in captivity. *Auk* 126: 511–519.

Lee, D. S., and J. Booth, Jr. 1979. Seasonal distribution of offshore and pelagic birds in North Carolina waters. *American Birds* 33: 715–721.

Liaw, A., and M. Wiener. 2002. Classification and Regression by randomForest. *R News 2*(3): 18–22.

Lincoln, F. C. 1935. The migration of North American birds. U.S. Department of Agriculture, Circular 363. Washington, D.C.

Lincoln, F. C., S. R. Peterson, and J. L. Zimmerman. 1998. Migration of birds. Circular 16 (Version 02APR2002). U.S. Fish and Wildlife Service, Washington, D.C.

Mackiewicz, J., and R. H. Backus. 1956. Oceanic records of *Lasionycteris noctivagans* and *Lasiurus borealis*. *Journal of Mammalogy* 37: 442–443.

Mathworks. 2011. MATLAB. vol. Parallel Computing Toolbox.

Mellinger, D. K., and C. W. Clark. 2000. Recognizing transient low-frequency whale sounds by spectrogram correlation. *J. Acoust. Soc. Am.* 107(6): 3518–3529.

Mills, H. 2000. Geographically distributed acoustical monitoring of migrating birds. *J. Acoust. Soc. of Am.* 108(5): 2582.

Moore, H. B. 1951. The seasonal distribution of oceanic birds in the western North Atlantic. *Bulletin of Marine Science for the Gulf and Caribbean* 1: 1–14.

Murphy, R. C. 1915. A note on the migration at sea of shore birds and swallow. *Auk* 32(2): 236.

Nichols, J. T. 1913. Notes on offshore birds. *Auk* 30: 505–511

O'Connell, A. F., B. Gardner, A. T. Gilbert, and K. Laurent. 2009. Compendium of Avian Occurrence Information for the Continental Shelf Waters along the Atlantic Coast of the United States, Final Report (Database Section, Seabirds). Prepared by the USGS Patuxent Wildlife Research Center, Beltsville, MD. U.S. Department of the Interior, Geological Survey, and Bureau of Ocean Energy Management Headquarters, OCS Study BOEM 2012-076.

O'Connell, A., C. S. Spiegel, and S. Johnson. 2011. Compendium of Avian Occurrence Information for the Continental Shelf Waters along the Atlantic Coast of the United States, Final Report (Database Section, Shorebirds). Prepared by the U.S. Fish and Wildlife Service, Hadley, MD, for the USGS Patuxent Wildlife Research Center, Beltsville, MD. U.S. Department of the Interior, Geological Survey, and Bureau of Ocean Energy Management Headquarters, OCS Study BOEM 2012-076.

Palmer, R. S., ed. 1962. Handbook of North American Birds. Volume 1. Yale University Press, New Haven, Connecticut.

Parks, S. E., I. Urazghildiiev, and C. W. Clark. 2009. Variability in ambient noise levels and call parameters of North Atlantic right whales in three habitat areas. *J. Acoust. Soc. Am.* 125(2): 1230–1239.

Paton, P., K. Winiarski, C. Trocki, and S. McWilliams. 2010. Spatial distribution, abundance, and flight ecology of birds in nearshore and offshore waters of Rhode Island. Interim technical report for the Rhode Island Ocean Special Area Management Plan 2010. University of Rhode Island.

Payne, P. M., L. A. Seltzer, and A. R. Knowlton. 1984. Distribution and density of cetaceans, marine turtles and seabirds in the shelf waters of the Northeastern United States, June 1980–December 1983, based on shipboard observations. Final report to the National Marine Fisheries Service Northeast Fish. Sci. Cent. in fulfillment of contract NA-81-FA-C-023. Manomet Bird Observatory, Manomet, MA. 246 pp.

Pelletier, S. K., K. Omland, K. S. Watrous, T. S. Peterson. 2013. Information Synthesis on the Potential for Bat Interactions with Offshore Wind Facilities – Final Report. U.S. Dept of the Interior, Bureau of Ocean Energy Management, Headquarters, Herndon, VA. OCS Study BOEM 2013-01163. 119 pp.

Pelletier, S. K., and T. S. Peterson. 2013. Wind power and bats offshore: What are the risks? A current understanding of offshore bat activity. Oral presentation at American Wind Energy Association Offshore WindPower 2013. Providence, Rhode Island. October 2013.

Penard, T. E. 1926. Warblers at sea. *Auk* 43: 276–277.

Porat, B. 1997. A Course in Digital Signal Processing. United States: John Wiley and Sons, Inc.

Powers, K. D. 1982. A comparison of two methods of counting birds at sea. *Journal of Field Ornithology* 53: 209–222.

Powers, K. D. 1983. Pelagic distributions of marine birds off the northeastern United States. NOAA Technical Memorandum NMFS-F/ NEC-27. U.S. Department of Commerce, Washington D.C. 202 pp.

Powers, K. D., G. L. Pittman, and S. J. Fitch. 1980. Distribution of marine birds on the mid- and North Atlantic U.S. outer continental shelf. U.S. Dept. of Energy, Washington, D.C.

Ramaswamy, B., G. R. Potty, and J. H. Miller. 2001. A marine mammal acoustic detection and localization algorithm using spectrogram image correlation. OCEANS, 2001. MTS/IEEE Conference and Exhibition, pp. 2354.

R Development Core Team. 2009. R: A Language and Environment for Statistical Computing. R Foundation for Statistical Computing. Vienna, Austria. http://www.R-project.org

R Development Core Team. 2012. R: A Language and Environment for Statistical Computing. R Foundation for Statistical Computing, Vienna, Austria. ISBN 3-900051-07-0, URL http://www.R-project.org/.

Scholander, S. I. 1955. Land birds over the western North Atlantic. *Auk* 72(3): 225–239.

South FL Birding. 2013. http://southfloridabirding.com/

Tasker, M. L., P. H. Jones, T. Dixon, and B. F. Blake. 1984. Counting seabirds at sea from ships: A review of methods employed and a suggestion for a standardized approach. *Auk* 101: 567–577.

Tjandranegara, E. 2005. Distance Estimation Algorithm for Stereo Pair Images. ECE Technical Reports. Paper 64.

Urazghildiiev, I. R., C. W. Clark, and T. Krein. 2008. Detection and recognition of North Atlantic right whale contact calls in the presence of ambient noise. *Canadian Acoustics* 36: 111–117.

Urazghildiiev, I. R., and C. W. Clark. 2007a. Acoustic detection of North Atlantic right whale contact calls using spectrogram-based statistics. *J. Acoust. Soc. Am.* 122(2): 769–776.

Urazghildiiev, I. R., and C. W. Clark. 2007b. Detection performances of experienced human operators compared to a likelihood ratio based detector. *J. Acoust. Soc. Am.* 122(1): 200–204.

Urick, R. J. 1996. Principals of Underwater Sound. USA: McGraw Hill.

Van Gelder, R. G., and D. B. Wingate. 1961. The taxonomy and status of bats in Bermuda. *American Museum Novitates* 2029: 1–9.

Venables, L. S. V. 1938. Birds seen in two winter transects of the North Atlantic. *British Birds* 31: 295–296.

Venables, L. S. V. 1939. Birds seen on an autumn and a spring Atlantic crossing. *British Birds* 33: 152–154.

Wallace, R., and R. Wigh. 2007. Pelagic birds of the southern South Atlantic Bight. *North American Birds* 61: 198–207.

Wiley, R. H. 1959. Birds observed during two Atlantic crossings. *Wilson Bulletin* 71: 364–370.

Winiarski, K., P. Paton, S. McWilliams, and D. Miller. 2012. Rhode Island Ocean Special Area Management Plan: Studies investigating the spatial distribution and abundance of marine birds in nearshore and offshore waters of Rhode Island. University of Rhode Island.

Zimmer, W. M. X. 2011. Passive Acoustic Monitoring for Cetaceans. United States, New York: University Press.

11 Appendices

Appendix 1: Full List of Component Parts for the ATOM System

- Control box
    - Portwell WADE-8067 mainboard
    - MOXA EDS-G308-T ethernet switch
    - EDT PCIe-4 dv-c link Camera Link capture card
    - 2 FLIR Tau 320 thermographic cameras
    - ph8 PowerControlBoard (custom)
    - M2-ATX-HV power supply
    - AR125-EXT ultrasonic microphone digitizer board
- Audio computer: National Instruments cRIO-9014
- Weather station: Columbia Weather Systems MicroServer
- Storage computer
    - Portwell PEB-2737 mainboard
    - Arduino Mega2560 microcontroller with custom signal distribution shield
- Microphone Array
    - Components:
        - Brüel & Kjaer 4198 Outdoor weatherproof microphone and preamp assembly for acoustic
        - SensComp Series 9000 Piezoelectirc transducer for ultrasonic

Appendix 2. Descriptions of Bird Call Samples Used by Cornell Lab of Ornithology in Testing of Preliminary Acoustic Monitoring Program (AMP) System

Swainson's Thrush Migration—California

Project Description	Swainson's Thrush (*Catharus ustulatus*) is commonly found breeding in northern spruce-fir forests across northern North America, whereas birds breeding in California occur in riparian areas along the western slope of the Sierra Nevada. Anecdotal reports during fall migration indicate small numbers migrate along the Pacific Coast in southern California while many more are observed from the Channel Islands in the California Bight. Conducting a season-long monitoring program is logistically challenging and costly. We used autonomous recording units (ARUs) to record flight calls to document and quantify this largely unseen offshore movement. ARUs can be deployed for months at a time, surveying on a rigorous schedule regardless of environmental conditions. This project aims to (1) record periods of migration to capture Swainson's Thrush flight calls; (2) determine the window of migration and identify peak migratory periods; (3) characterize the hours of peak migration each night; and (4) begin to quantify the numbers of birds passing over the California Bight.

Site Descriptions	Signal Peak
Lat-Long	33.470039 -119.038286
	Signal Peak is located on the south side of Santa Barbara Island (Channel Islands National Park, Santa Barbara County, California). The vegetation is primarily grassland with scattered cholla (*Cylindropuntia fulgida)* and Giant Coreposis (*Coreopsis gigantea*). The elevation makes it attractive to record migrations flying over the island, though the exposed nature of the peak will result in possible wind contamination. Recordings were made starting at the end of local civil twilight and ending at the beginning of civil twilight the next morning. A second recording was started at the beginning of civil twilight and ended two hours later. http://www.nps.gov/chis/index.htm

Site Descriptions	North Peak
Lat-Long	33.479808 -119.037503
	North Peak is located on the north side of Santa Barbara Island (Channel Islands National Park, Santa Barbara County, California). The vegetation is primarily grassland with scattered cholla (*Cylindropuntia fulgida)* and Giant Coreposis (*Coreopsis gigantea*). The microphone was placed near a large

patch of vegetation frequently used by migrants seeking shelter on the island; this site is sheltered from the western winds. Recordings were made starting at the end of local civil twilight and ending at the beginning of civil twilight the next morning. A second recording was started at the beginning of civil twilight and ended two hours later. http://www.nps.gov/chis/index.htm, Radar Comparison - Southern Tier New York

Nocturnal Migration

Project Description	This project is part of a larger pilot study that allows us to compare migratory patterns of birds that migrate at night. To generate patterns of call counts, which can be compared with radar reflectivities and subsequent morning's birding observations reported to eBird, we deployed four autonomous recording units at various distances from the Binghamton WSR-88D radar site (Johnson City, Broome County, New York). This study is at the forefront of a promising new line of research to combine radar, acoustic, and observational data that will help us model and understand relationships among these data sources, and eventually aid in making precise inferences about migration magnitude and composition.
Site Descriptions	Finch Hollow Nature Center
Lat-Long	42.160378 -75.983142
	Located 5.3 km south of the Binghamton WSR-88D radar site (Johnson City, Broome County, New York). Finch Hollow is a mixture of wetland (including pond), wooded and open field habitats. The recording unit was deployed in the most open area identified, which was a descent into to a field located southwest of the pond. We made stereo recordings using a Wildlife Acoustics Nocturnal Flight Call microphone to record to the left channel and a parabola microphone designed by the Bioacoustics Research Program at the Cornell Lab of Ornithology recording to the right channel. Recordings were made starting at the end of local civil twilight and ending at the beginning of civil twilight the next morning.
Site Descriptions	STK
Lat-Long	42.346306 -76.299092
	Private residence located between Shindagin Hollow and Potato Hill State Forests (Caroline, Tompkins County), 31 km northwest of the Binghamton WSR-88D radar site (Johnson City, Broome County, New York). The recording unit was placed in an open field bounded by areas of deciduous forest. We made stereo recordings using a Wildlife Acoustics Nocturnal Flight Call microphone to record to the left channel and a parabola microphone

designed by the Bioacoustics Research Program at the Cornell Lab of Ornithology recording to the right channel. Recordings were made starting at the end of local civil twilight and ending at the beginning of civil twilight the next morning.

Site Descriptions	Thrush Migration—Colombia
Lat-Long	42.346306 -76.299092

Two recording stations were set up in northeastern Colombia as a pilot test to monitor the arrival of thrushes on their fall migration. The equipment was shipped to Nick Bayly <www.selva.org.co> who deployed the units near existing banding stations in the Sierra Nevada de Santa Marta National Park, Magdalena, Colombia.

Site Descriptions	Quebrada Valencia
Lat-Long	11.2376 -73.80048

We made single-channel recordings using a Wildlife Acoustics Nocturnal Flight Call microphone to record to the left channel; recordings were made starting at the end of local civil twilight and ending at the beginning of civil twilight the next morning. Unit deployed by Nick Bayly, colleague from Selva < www.selva.org.co> near a banding station in the Sierra Nevada de Santa Marta National Park, Magdalena, Colombia).

Site Descriptions	Local Sites - Finger Lakes Region New York
Lat-Long	Multiple Sites

An ongoing project to monitor nocturnal migration at various local sites in the region surrounding the Cornell Lab of Ornithology. For the past four fall migration seasons we have deployed a variable number of recording units at a variety of locations, including local parks, nature centers, private land and residences, schools, and even Schoelkopf stadium on the Cornell University campus.

Site Descriptions	Danby School
Lat-Long	42.3591 -76.4911

We deployed a recording unit and microphone 14 km south/southwest of the Cornell Lab of Ornithology (Ithaca, Tompkins County, New York) at the

Ithaca City School District (unoccupied) school in Danby (Tompkins County, New York). The microphone was placed on the school's roof to minimize disturbance and to reduce the effect of ambient biological (insects, amphibians) and mechanical (cars) sounds. We made single-channel recordings using a "pod-style" microphone designed by the Bioacoustics Research Program at the Cornell Lab of Ornithology recording to the left channel. Recordings were made starting at the end of local civil twilight and ending at the beginning of civil twilight the next morning.

Site Descriptions	Danby—Marsh Road
Lat-Long	42.3628 -76.4376

We deployed a recording unit and microphone on private land 13 km south/southeast of the Cornell Lab of Ornithology (Ithaca, Tompkins County, New York) in the town of Danby (Tompkins County, New York). The microphone was mounted on a stake approximately 1 meter off the ground and does include ambient biological (insects, amphibians) and mechanical (cars) sounds. We made single-channel recordings using a "pod-style" microphone designed by the Bioacoustics Research Program at the Cornell Lab of Ornithology recording to the left channel. Recordings were made starting at the end of local civil twilight and ending at the beginning of civil twilight the next morning.

Appendix 3. Distinct Species Identified during the Study, their Scientific Names, and their Species Codes, along with Higher-Level Taxonomic Groups Used Throughout the Report

Species Common Name	Scientific Name	Species Code
Species Level Identifications		
Laughing Gull	*Leucophaeus atricilla*	LAGU
Ring-billed Gull	*Larus delawarensis*	RBGU
Herring Gull	*Larus argentatus*	HEGU
Common Tern	*Sterna hirundo*	COTE
Forster's Tern	*Sterna forsteri*	FOTE
Royal Tern	*Thalasseus maximus*	ROYT
Sandwich Tern	*Thalasseus sandvicensis*	SATE
Least Bittern	*Ixobrychus exilis*	LEBI
Green Heron	*Butorides virescens*	GRHE
Veery	*Catharus fuscescens*	VEER
Gray-cheeked Thrush	*Catharus minimus*	GCTH
Swainson's Thrush	*Catharus ustulatus*	SWTH
Hermit Thrush	*Catharus guttatus*	HETH
Wood Thrush	*Hylocichla mustelina*	WOTH
American Pipit	*Anthus rubescens*	AMPI
Ovenbird	*Seiurus aurocapilla*	OVEN
Northern Waterthrush	*Parkesia noveboracensis*	NOWA
Black-and-white Warbler	*Mniotilta varia*	BAWW
Prothonotary Warbler	*Protonotaria citrea*	PROW
Common Yellowthroat	*Geothlypis trichas*	COYE
American Redstart	*Setophaga ruticilla*	AMRE
Cape May Warbler	*Setophaga tigrina*	CMWA
Northern Parula	*Setophaga americana*	NOPA
Magnolia Warbler	*Setophaga magnolia*	MAWA
Bay-breasted Warbler	*Setophaga castanea*	BBWA
Blackburnian Warbler	*Setophaga fusca*	BLBW
Yellow Warbler	*Setophaga petechia*	YEWA
Chestnut-sided Warbler	*Setophaga pensylvanica*	CSWA
Blackpoll Warbler	*Setophaga striata*	BLPW

Species Common Name	Scientific Name	Species Code
Black-throated Blue Warbler	*Setophaga caerulescens*	BTBW
Palm Warbler	*Setophaga palmarum*	PAWA
Yellow-rumped Warbler	*Setophaga coronata*	YRWA
Canada Warbler	*Cardellina canadensis*	CAWA
Chipping Sparrow	*Spizella passerina*	CHSP
Savannah Sparrow	*Passerculus sandwichensis*	SAVS
White-throated Sparrow	*Zonotrichia albicollis*	WTSP
Dark-eyed Junco	*Junco hyemalis*	DEJU
Blue Grosbeak	*Passerina caerulea*	BLGR
Indigo Bunting	*Passerina cyanea*	INBU
Bobolink	*Dolichonyx oryzivorus*	BOBO
Genus Level Identifications		
Catharus sp.		
Setophaga sp.		
Sub-family Level Identifications		
Larinae sp.		
Sterninae sp.		
Family Level Identifications		
Parulidae sp.		
Emberizidae sp.		
Order Level Identifications		
Passeriformes		
Class Level Identifications		
Aves		

The Department of the Interior Mission

As the Nation's principal conservation agency, the Department of the Interior has responsibility for most of our nationally owned public lands and natural resources. This includes fostering the sound use of our land and water resources, protecting our fish, wildlife and biological diversity; preserving the environmental and cultural values of our national parks and historical places; and providing for the enjoyment of life through outdoor recreation. The Department assesses our energy and mineral resources and works to ensure that their development is in the best interests of all our people by encouraging stewardship and citizen participation in their care. The Department also has a major responsibility for American Indian reservation communities and for people who live in island communities.

The Bureau of Ocean Energy Management

The Bureau of Ocean Energy Management (BOEM) works to manage the exploration and development of the nation's offshore resources in a way that appropriately balances economic development, energy independence, and environmental protection through oil and gas leases, renewable energy development and environmental reviews and studies.

www.boem.gov